To the Graduate Council:

I am submitting herewith a thesis written by Arnooparp Charmikorn entitled "An Investigation of Percolation Kinetics." I recommend that it be accepted in partial fulfillment of the requirements for the degree of Master of Science, with a major in Chemical Engineering.

Stanley H. Jury, Major Professor

We have read this thesis and recommend its acceptance:

Accepted for the Council:

Vice Chancellor
Graduate Studies and Research

A

Thesis
79
.C434
cop.2

AN INVESTIGATION OF PERCOLATION KINETICS

A Thesis

Presented for the

Master of Science

Degree

The University of Tennessee, Knoxville

Arnooparp Charmikorn

August 1979

1396872

ACKNOWLEDGEMENTS

The author wishes to express his appreciation to the National Science Foundation for the support given to this work during the past two years.

The author especially wishes to thank his advisor, Dr. S. H. Jury, without whose invaluable guidance and help this work would have been almost impossible to accomplish.

Appreciation is also expressed to the machine shop staff under the direction of Mr. H. B. Thompson and to the electronics shop staff under Mr. T. A. Long for their efforts in maintaining the equipment used in this project.

The author also wishes to thank Dr. H. F. Johnson, Head of the Department of Chemical, Metallurgical and Polymer Engineering, and the entire faculty and staff in the department.

ABSTRACT

The kinetic mechanisms of adsorptive drying were studied. The gas temperature and concentration expiration curves were determined for moist air and the two desiccants, activated alumina (Alcoa F-1) and Linde molecular sieve 4-A under adiabatic fixed bed conditions. Three different granule sizes, two different flow rates, one bed diameter, two different bed lengths, and two different feed gas concentrations were studied.

Models of kinetic mechanisms were devised and incorporated into a computerized numerical analysis program along with previously determined sorption therms, diffusivity relations, and heat transfer coefficient correlations. The models included the bipore concept and surface/internal release of heat of adsorption among others. The program was repeatedly executed with parameter adjustments in between until coincidence was obtained between theorectical and experimental results.

During the course of parameter adjustments, it was found that the total diffusivity, D, the heat of adsorption, λ, the mass transfer film coefficient, k_G, and the coefficient of heat transfer by radiation, h_R, had to be multiplied by 2.4, 1.27, 3.0, and 0.5 for Linde molecular sieve 4-A, and 3.0, 1.4, 3.0, and 0.5 for activated alumina, respectively. These multiplications are justified in the thesis.

In the computer program, the diffusion equations were expressed in terms of partial pressure and temperature instead of concentration and temperature which gave a remarkable advantage in the finite difference

calculation of mass transfer at the interface. The finite difference scheme of Crank and Nicolson was used due to the shortcomings of the Douglas method discussed in the thesis. A variable increment size was used in the granule to increase the speed of calculation. The explicit nature speeded calculations because iterative loops were eliminated.

TABLE OF CONTENTS

CHAPTER		PAGE
I.	INTRODUCTION	1
II.	HISTORICAL REVIEW OF PERCOLATION STUDIES	4
III.	THEORY AND NUMERICAL PROCEDURES	23
IV.	DIFFUSION ROUTINES	65
	Activated Alumina Diffusion Parameters	65
	Linde Molecular Sieve-4A Diffusion Parameters	72
V.	PROGRAM DEVELOPMENT	75
VI.	EXPERIMENTAL EQUIPMENT AND PROCEDURE	88
VII.	COMPARISON OF EXPERIMENTAL AND CALCULATED RESULTS	96
VIII.	DISCUSSION OF RESULTS AND CONCLUSIONS	121
LIST OF REFERENCES		128
APPENDICES		141
A.	PREPARATION OF SAMPLES	142
B.	MECHANICAL-OIL DIFFUSION PUMP AND VACUUM CONTROLLER	152
C.	CALIBRATION CHARTS OF WET TEST METER AND LAMINAR FLOWRATORS	158
D.	TABLES OF ORIGINAL EXPERIMENTAL DATA AND CONVERSION TO RATIOC	163
E.	TABLES OF COMPUTER RESULTS	206
F.	COMPUTER PROGRAM FOR LMS-4A AND ACTIVATED ALUMINA	244
VITA		260

LIST OF TABLES

TABLE		PAGE
I.	Summary of Numerical Analysis of Single Solute Gas-Solid Adsorption System	22
II.	Summary of Sorption Therms for the Five Desiccants	66
III.	Permeabilities and Diffusivities	68
IV.	Design of Experimental Run	95
V.	Conditions of Each LMS-4A Experimental Run	97
VI.	Conditions of Each Activated Alumina Experimental Run	98
VII.	Input Data of Each LMS-4A Computer Run	118
VIII.	Input Data of Each Activated Alumina Computer Run	119
IX.	Parameters and Adjusted Parameter Values That Produced Best Fits of Experimental Data	120
X.	Physical Properties of the Adsorbent Sample	144
XI.	Experimental Results of LMS-4A Run No. 1 (LMSX-1)	165
XII.	Experimental Results of LMS-4A Run No. 1N (LMSX-1N)	166
XIII.	Experimental Results of LMS-4A Run No. 2 (LMSX-2)	167
XIV.	Experimental Results of LMS-4A Run No. 3 (LMSX-3)	168
XV.	Experimental Results of LMS-4A Run No. 4 (LMSX-4)	175
XVI.	Experimental Results of LMS-4A Run No. 5 (LMSX-5)	176
XVII.	Experimental Results of LMS-4A Run No. 6 (LMSX-6)	177
XVIII.	Experimental Results of Activated Alumina Run No. 1 (ACTX-1)	178
XIX.	Experimental Results of Activated Alumina Run No. 2 (ACTX-2)	182
XX.	Experimental Results of Activated Alumina Run No. 3 (ACTX-3)	188

TABLE		PAGE
XXI.	Experimental Results of Activated Alumina Run No. 4 (ACTX-4)	194
XXII.	Experimental Results of Activated Alumina Run No. 5 (ACTX-5)	198
XXIII.	Experimental Results of Activated Alumina Run No. 6 (ACTX-6)	201
XXIV.	Computer Results of LMS-4A Run No. 1 (LMSC-1)	207
XXV.	Computer Results of LMS-4A Run No. 2 (LMSC-2)	208
XXVI.	Computer Results of LMS-4A Run No. 3 (LMSC-3)	209
XXVII.	Computer Results of LMS-4A Run No. 4 (LMSC-4)	213
XXVIII.	Computer Results of LMS-4A Run No. 5 (LMSC-5)	214
XXIX.	Computer Results of LMS-4A Run No. 6 (LMSC-6)	215
XXX.	Computer Results of LMS-4A Run No. 7 (LMSC-7)	216
XXXI.	Computer Results of LMS-4A Run No. 8 (LMSC-8)	217
XXXII.	Computer Results of LMS-4A Run No. 9 (LMSC-9)	218
XXXIII.	Computer Results of LMS-4A Run No. 10 (LMSC-10)	219
XXXIV.	Computer Results of LMS-4A Run No. 11 (LMSC-11)	220
XXXV.	Computer Results of LMS-4A Run No. 12 (LMSC-12)	221
XXXVI.	Computer Results of Activated Alumina Run No. 1 (ACTC-1)	222
XXXVII.	Computer Results of Activated Alumina Run No. 2 (ACTC-2)	224
XXXVIII.	Computer Results of Activated Alumina Run No. 3 (ACTC-3)	227
XXXIX.	Computer Results of Activated Alumina Run No. 4 (ACTC-4)	230
XL.	Computer Results of Activated Alumina Run No. 5 (ACTC-5)	232

TABLE		PAGE
XLI.	Computer Results of Activated Alumina Run No. 6 (ACTC-6)	234
XLII.	Computer Results of Activated Alumina Run No. 7 (ACTC-7)	237
XLIII.	Computer Results of Activated Alumina Run No. 8 (ACTC-8)	239
XLIV.	Computer Results of Activated Alumina Run No. 9 (ACTC-9)	241
XLV.	Computer Results of Activated Alumina Run No. 10 (ACTC-10)	242
XLVI.	The Complete Fortran IV Program of Activated Alumina . .	245
XLVII.	The Input Data and Diffusion Parameter Calculations of LMS-4A Program	257

LIST OF FIGURES

FIGURE		PAGE
1.	The Granule with Bipore Model	25
2.	The Granule Segments	25
3.	Differential Bed Model of Heat and Mass Transfer	26
4.	Stagewise Bed Model of Heat and Mass Transfer	30
5.	Interface between Δr and Δs inside the Granule	40
6.	Linear Interpolation of $U(t,r-(\Delta x)_2)$ and $U(t,r-(\Delta x)_2/2)$ . .	41
7.	Flow Chart of Program Development	76
8.	Flow Chart of the Earlier Computer Program	81
9.	Flow Chart of the Intermediate Computer Program	84
10.	Flow Chart of the Present Computer Program	85
11.	The Experimental Fixed Bed	90
12.	The Effect of a Change in D(K) on the Fit of LMS-4A Experimental Data Run No. 1	100
13.	The Combined Effect of Changes in D(K) and YLAMDA, and D(K), YLAMDA, and HR on the Fit of LMS-4A Experimental Data Run No. 1	101
14.	The Combined Effect of Changes in D(K), YLAMDA, HR, CAYG, and EF on the Fit of LMS-4A Experimental Data Run No. 1 . .	102
15.	The Combined Effect of Changes in D(K), YLAMDA, HR, CAYG, and SI on the Fit of LMS-4A Experimental Data Run No. 1 . .	103
16.	The Effect of Changes in SIG on the Fit of Activated Alumina Experimental Data Run No. 1	104
17.	The Effect of Changes in EF1 on the Fit of Activated Alumina Experimental Data Run No. 1	105
18.	Comparison of Experimental Data and Best Fit of LMS-4A Run No. 1	106

FIGURE PAGE

19. Comparison of Experimental Data and Best Fit of LMS-4A Run No. 2 107

20. Comparison of Experimental Data and Best Fit of LMS-4A Run No. 3 108

21. Comparison of Experimental Data and Best Fit of LMS-4A Run No. 4 109

22. Comparison of Experimental Data and Best Fit of LMS-4A Run No. 5 110

23. Comparison of Experimental Data and Best Fit of LMS-4A Run No. 6 111

24. Comparison of Experimental Data and Best Fit of Activated Alumina Run No. 1 112

25. Comparison of Experimental Data and Best Fit of Activated Alumina Run No. 2 113

26. Comparison of Experimental Data and Best Fit of Activated Alumina Run No. 3 114

27. Comparison of Experimental Data and Best Fit of Activated Alumina Run No. 4 115

28. Comparison of Experimental Data and Best Fit of Activated Alumina Run No. 5 116

29. Comparison of Experimental Data and Best Fit of Activated Alumina Run No. 6 117

30. Schematic Diagram of the Vacuum Control System 154

31. Calibration Curve of Wet Test Meter No. 63115 at 78°F . . . 159

32. Calibration Curve of Laminar Flowrator No. A for Low Air Supply at 78°F 160

33. Calibration Curve of Laminar Flowrator No. C for Intermediate Air Supply at 78°F 161

34. Calibration Curve of Laminar Flowrator No. D for High Air Supply at 78°F 162

LIST OF SYMBOLS

a_v	Granule-gas phase interfacial area per unit volume of bed, ft^2/ft^3 bed
AAP(t)	Convenience parameter defined in Eq. (152), lbmoles-ft/lb-hr
AP	Convenience parameter defined in Eq. (122), $lbmoles/ft^3$
A2	= k/h, convenience parameter, ft
A3	Convenience parameter defined in Eq. (177), dimensionless
A4	Convenience parameter defined in Eq. (201), hr/ft^2
A7	Convenience parameter defined in Eq. (202), Btu/hr ft^2°R
A8	Convenience parameter defined in Eq. (203), Btu/lbmole of water
A9	Convenience parameter defined in Eq. (204), dimensionless
BBP(t)	Convenience parameter defined in Eq. (153), lbmoles-ft/lb-hr
BE(K)	Parameter in Thomas algorithms, dimensionless
BETA	$= 2(DELX2)^2/(\alpha \cdot \Delta t)$, convenience parameter, dimensionless
BB6	Convenience parameter defined in Eq. (123), $lbmoles/ft^3$
B1	$= 1-\lambda\ EF \cdot \sigma \cdot TE(K)/k$, convenience parameter, dimensionless
B2	$= \sigma \cdot \lambda \cdot EF \cdot DP \cdot PE(K)/(\rho \cdot C_p \cdot \tau_I \cdot D(K))$, convenience parameter, dimensionless
C	Sorbate concentration in granule, $lbmoles/ft^3$
C*	Granule sorbate concentration at r = R, $lbmoles/ft^3$
C_c	Sorbate concentration of continuous phase, $lbmoles/ft^3$

CCP(t)	Convenience parameter defined in Eq. (154), lbmoles-ft/lb-hr
C_d	Average concentration in the microsphere of dispersed phase, lbmoles/ft^3
CF	Correction factor defined in Eq. (187), dimensionless
C_G	Gas phase sorbate concentration, lbmoles/ft^3
C_G^*	C_G measured at granule-gas interface, lbmoles/ft^3
C_p	Granule specific heat, Btu/lbmole °R
C_{PG}	Gas phase heat capacity, Btu/lbmole °R
C_{PT}	Heat capacity of polystyrene tube, Btu/lb °R
CQ	= $J^*(I+1,t_2)$ in Eq. (189), lbmoles/ft^{2}hr
CR	Combined emissivity and view factor parameter, dimensionless
CW	Parameter in heat transfer film coefficient from gas phase to polystyrene tube wall, dimensionless
d_I	Inside diameter of polystyrene tube, ft
d_o	Outside diameter of polystyrene tube, ft
D	Total diffusivity, ft^2/hr
DB1	Convenience parameter defined in Eq. (115), ft^3/lbmole
DB2	Convenience parameter defined in Eq. (116), dimensionless
DB3	Convenience parameter defined in Eq. (117), dimensionless
DC1	Convenience parameter defined in Eq. (266) and Eq. (263), Consistent units
D_d	Total diffusivity of the microsphere of dispersed phase, ft^2/hr

DE	Parameter in Thomas algorithms, dimensionless
DELUT(K)	= $UT(t_2,K)-UT(t_1,K)$, convenience parameter, dimensionless
DELX1	= $(\Delta x)_1$, length of small increment next to $(\Delta x)_2$ inside granule, ft
DELX2	= $(\Delta x)_2$, length of small increment near surface of granule, ft
DEN	Convenience parameter defined in Eq. (160), lbmoles-ft/lb-hr
DIN	Convenience parameter defined in Eq. (161), lbmoles-ft/lb-hr
DIVP	Convenience parameter defined in Eq. (169), lbmoles-ft/lb-hr
DLPSAT	Convenience parameter defined in Eq. (277), consistent units
D_o	Ordinary diffusivity, ft^2/hr
D_p	Average particle diameter, ft
DP	= P_F-P_I, convenience parameter, lb/ft^2
DSUM	Convenience parameter defined in Eq. (278), consistent units
DUM	Convenience parameter defined in Eq. (293) and Eq. (294), dimensionless
DX	= $(\Delta x)_2/(\Delta x)_1$, convenience parameter, dimensionless
EF	Fraction of heat of adsorption released internally, dimensionless
EF1	Fraction defined by $EF1 \cdot D/R^2 = D_d/R_d^2$, dimensionless

EPA	Convenience parameter defined in Eq. (258), consistent units
G(I+1,t)	= v(I+1,t) ρ_G(I+1,t), gas phase molar flux in bed, lbmoles/ft^{2}hr
GE(K)	Parameter in Thomas algorithms, dimensionless
h	Gas phase heat transfer film coefficient, Btu/hr ft^2°R
h_R	Coefficient of heat transfer by radiation from tube wall, Btu/hr ft^2°R
h_W	Heat transfer film coefficient from gas phase to polystyrene tube wall, Btu/hr ft^2°R
J*	Mass transfer flux at granule-gas interface, lbmoles/ft^2 hr
J_c	Mass transfer flux in granule at position r, lbmoles/ ft^2 hr
J_T	Thermal flux in granule at position r, Btu/ft^2 hr
k	Granule thermal conductivity, Btu/hr ft°R
k_G	Gas phase mass transfer film coefficient, ft/hr
$\bar{k}_G$	Gas phase thermal conductivity, Btu/hr ft°R
K	Index parameter for radial increment, dimensionless
NA	Number of Δs that was subdivided to Δr, dimensionless
N_{pr}	Prandtl number, dimensionless
NR	Number of Δr in each Δs, dimensionless
N_{Re}	Reynolds number, dimensionless
NS	Number of increment of r, dimensionless
P	Partial pressure of water inside the granule, lb/ft^2
P_c	Partial pressure of water in continuous phase, lb/ft^2

$\overline{P}_c$ = $(P_c-P_I)/DP$, normalized partial pressure of continuous phase, dimensionless

P_d Partial pressure of water in dispersed phase, lb/ft^2

PE = $D(\partial C/\partial P)_\tau$, total permeability, lbmoles-ft/lb-hr

P_F Feed gas partial pressure, lb/ft^2

PHID = $15 \cdot D_d \cdot \Delta t/R_d^2 = 15 \cdot EF1 \cdot D(K) \cdot \Delta t/R^2$, convenience parameter, dimensionless

PHID1 Convenience parameter defined in Eq. (162), dimensionless

P_I Initial equilibrium partial pressure of gas in bed, lb/ft^2

P_s Vapor pressure of pure water, lb/ft^2

P_T Total pressure, lb/ft^2

P7 Convenience parameter defined in Eq. (118), $ft^3/lbmole$

P8 Convenience parameter defined in Eq. (119), $lbmoles/ft^3$

P9 Convenience parameter defined in Eq. (121), dimensionless

P10 Convenience parameter defined in Eq. (120), dimensionless

QA Convenience parameter defined in Eq. (38), dimensionless

QB Convenience parameter defined in Eq. (39), dimensionless

Q3 Convenience parameter defined in Eq. (175), $lbmoles/ft^2hr$

Q4 Convenience parameter defined in Eq. (176), $lbmoles/ft^2hr$

Q5 Convenience parameter defined in Eq. (183), dimensionless

Q6 Convenience parameter defined in Eq. (192), dimensionless

r Radial distance from center of granule, ft

Δr Length of each increment in Δs, ft

R Average radius of granule, ft

$\overline{R}$ Gas law constant, lb-ft/lbmole°R

R_d	Average radius of the microsphere of dispersed phase, ft
RN	= YT-1, convenience parameter, dimensionless
R_2, R_{AI}	Peripheral radius of polystyrene tube and aluminum casing, respectively, ft
R_{SI}, R_{SO}	Radius of inner and outer radiation shields, respectively, ft
Δs	Length of each increment in r, ft
SDX	Convenience parameter defined in Eq. (146), dimensionless
SDX2	Convenience parameter defined in Eq. (147), dimensionless
SUM	Convenience parameter defined in Eq. (259), consistent units
t	Time, hr
TA	$= (\tau_A-\tau_I)/\tau_I$, normalized ambient temperature, dimensionless
TC	$= \tau$, °C
TD	Convenience parameter defined in Eq. (260), consistent units
TE	$\propto(\partial C/\partial\tau)_p$, lbmoles/hr ft°R
TG(I+1,t)	$= (\tau_G(I+1,t)-\tau_I)/\tau_I$, normalized gas phase temperature in bed, dimensionless
TW(I+1,t)	$= (\tau_W(I+1,t)-\tau_I)/\tau_I$, normalized temperature of polystyrene tube wall, dimensionless
UP	$= (r/R)((P-P_I)/DP)$, normalized partial pressure of granule, dimensionless
UPD	$= (r/R)((P_d-P_I)/DP)$, normalized partial pressure of dispersed phase, dimensionless

UT	$= (r/R)((\tau-\tau_I)/\tau_I)$, normalized granule temperature, dimensionless
v	Gas phase intersticial velocity, ft/hr
V21,V22,V23	Parameter in gas phase heat transfer film coefficient, dimensionless
W	Water content in granule, lb H_2O/lb dry granule
WO	Convenience parameter defined in Eq. (209), lbmoles/hr $ft^2{}^\circ R$
WO1	Convenience parameter defined in Eq. (217), dimensionless
WO2	Convenience parameter defined in Eq. (205), dimensionless
WO3	Convenience parameter defined in Eq. (206), hr/ft
WO4	Convenience parameter defined in Eq. (207), dimensionless
WO5	Convenience parameter defined in Eq. (225), dimensionless
WO6	$= TE(K) \cdot D(K)/(PE(K) \cdot \alpha)$, convenience parameter, dimensionless
WO7	Convenience parameter defined in Eq. (152), Btu/lbmole of water
W1	Convenience parameter defined in Eq. (210), lbmoles/hr $ft^2{}^\circ R$
W2	Convenience parameter defined in Eq. (211), lbmoles/hr $ft^2{}^\circ R$
W3	Convenience parameter defined in Eq. (235), consistent units
W4	Convenience parameter defined in Eq. (236), consistent units

W5	Convenience parameter defined in Eq. (234), consistent units
W6	Convenience parameter defined in Eq. (237), consistent units
W7 (= Q3)	Convenience parameter defined in Eq. (243), lbmoles/ft^2 hr
W8 (= Q4)	Convenience parameter defined in Eq. (244), lbmoles/ft^2hr
W9	Convenience parameter defined in Eq. (242), lbmoles/ft^2 hr°R
W10	Convenience parameter defined in Eq. (250), consistent units
W11	Convenience parameter defined in Eq. (251), consistent units
W12	Convenience parameter defined in Eq. (293), consistent units
W13	Convenience parameter defined in Eq. (169), consistent units
W14	Convenience parameter defined in Eq. (254), consistent units
WW1	Convenience parameter defined in Eq. (226), lb/ft^2°R
WW2	Convenience parameter defined in Eq. (227), lb/ft^2
WW3	Convenience parameter defined in Eq. (228), lb-hr/lbmole
WW4	Convenience parameter defined in Eq. (229), dimensionless
X	Partial pressure-temperature coordinate, consistent units
Y	= C_G/ρ_G, gas phase mole fraction in bed, dimensionless
YT	= NS•NR, convenience parameter, dimensionless
YY	= RN/YT, convenience parameter, dimensionless

z	Measure of length along bed, ft
ZA	Convenience parameter defined in Eq. (262), dimensionless
ZB	Convenience parameter defined in Eq. (263), dimensionless
α	$= k/\rho C_p$, thermal diffusivity of granule, ft^2/hr
β	Interpolation parameter, dimensionless
$\overline{\beta}$	Reciprocal of the maximum possible sorbate concentration due to adsorption ($1/C_{SAT}$ or $1/C^*$), ft^3 of adsorbent/ lbmole H_2O
γ	$= 4d_I h_W \Delta t/[\rho_T C_{PT}(d_o^2-d_I^2)]$, convenience parameter, dimensionless
γ_R	$= 4d_O h_R \Delta t/(\rho_T C_{PT}(d_o^2-d_I^2)]$, convenience parameter, dimensionless
δ	Thermal diffusivity, lbmoles/ft^3°R
θ	Coefficient in finite difference, dimensionless
ϵ	Bed void fraction, ft^3 void/ft^3 bed
$\epsilon_1,\epsilon_2,\epsilon_3,\epsilon_4$	Emissivity of polystyrene tube, inner and outer radiation shields and aluminum casing, respectively, dimensionless
λ	Heat of adsorption of granule, Btu/lbmole of water adsorbed
ρ	Granule density, lbmole/ft^3
ρ_G	Gas phase density, lbmole/ft^3
ρ_T	Density of polystyrene tube, lb/ft^3
σ	Fraction of continuous phase in granule, dimensionless
τ	Granule temperature at r and t, °R
τ^*	Granule-gas interfacial temperature, °R

τ_A Ambient temperature, °R

τ_c Temperature of continuous phase, °R

$\bar{\tau}_c$ = $(\tau_c-\tau_I)/\tau_I$, normalized temperature of granule, dimensionless

τ_d Temperature of dispersed phase, °R

τ_I Initial equilibrium temperature of granule and gas in bed, °R

τ_F Feed gas temperature, °R

τ_G Gas phase temperature, °R

τ_W Temperature of polystyrene tube wall, °R

CHAPTER I

INTRODUCTION

Stationary beds of granular desiccants have been and are being used to dry gases in the chemical industry, the food processing industry, the petroleum industry, in wind tunnel research, space research, the drying of oxygen for use at high altitudes, air-conditioning in space capsules, and in the preparation of isotope gases for separation by gaseous diffusion among a host of other applications. This drying operation is a transient diffusional operation of chemical engineering belonging to a group generally referred to as the "percolation" operations. The latter include fixed bed ion exchange, heat recuperation, certain types of chromatography, ion exclusion, fixed bed sorption in general.

During the course of evolution of the percolation operation the advantages of a scientific understanding of the diffusional mechanisms involved became apparent as is evidenced by the literature starting with Anzelius (8) in 1926. A significant volume of research has been and is being done in this area. However, due to the complex nature of these processes, only approximate models have been proposed and solved. Typical simplifying assumptions are linear sorption equilibrium isotherms, isothermal operation, constant linear velocity, constant intraparticle diffusivity, and others. For obvious reasons the literature on the percolation operation is permeated with the ordinary diffusivity, D_o. The way in which D_o depends on concentration and

temperature is generally disregarded in much of the literature. The same is true for thermal diffusion and its contribution to the sorptive kinetic mechanism. It is well known that an adsorption and thermal wave pass up through a percolator and that in the region of these wave fronts temperatures up to about 248°F have been measured with a feed gas temperature of 70°F. Thus thermal diffusion can have a very pronounced effect on the course of sorption and the sorption waves.

In past engineering designs of sorption equipment, it has been assumed that thermal diffusion does not exist. So-called "constant mean values" of ordinary diffusivities have also been used as a basis for design. These numbers are generally guesstimated to be oversized so that the design is on the "safe side," i.e., it is an overdesign. This, of course, is not the most economical design. It is intended that this research will shed light on this state of affairs in such a way as to provide the computer programs that give the best coincidence between experiment and theory.

In recent years several computer programs have been devised for analyzing and/or designing fixed bed sorption operation (15,25,32,72, 104,105,115) and in Dr. Jury's case (72) the program is even equipped to take into account the thermal as well as the ordinary diffusion coefficient and the way in which these vary with sorbate concentration and temperature. The state of this part of the art has until recently been much further advanced than has been the case for the diffusion coefficients in sorbent solids and other matters related to sorptive kinetic mechanisms.

Past research in the department has covered the sorption therms, diffusivities, and recuperative properties of desiccant beds (12,23,61, 69,70,74,75,79,80,86,87,94,96,101,114,132,133,157).

These results now make it possible to computerize a precision data analysis scheme for studying percolation kinetic mechanisms. For this purpose it is necessary to conduct in the laboratory a set of percolation runs and then to follow up with a computerized analysis in which a search is made for coincidence between the experimental and theoretical results. This then is the purpose of this thesis. The practical benefits should be obvious.

The five adsorbents—i.e., activated alumina, Linde molecular sieve 4-A, Florite, Drierite, and silica gel—have been the subjects of the past research program in the department. Here just two of these—i.e., activated alumina and Linde molecular sieve 4-A—are of concern.

CHAPTER II

HISTORICAL REVIEW OF PERCOLATION STUDIES

Active interest in the development of understanding the percolation operations began about 1926. Since that time, various investigators have tried to analyze these processes, first analytically and more recently numerically. The following is a summary of these efforts.

The work of Anzelius (8) is generally regarded as the beginning of modern day percolation research. In 1926 he treated the basic heat recuperation mathematically and obtained an analytical solution for the case of uniform initial gas and bed temperature with gas film controlling. A year later, in 1927, Nusselt (125) developed the analytical solution for the case of nonuniform initial bed temperature.

In 1929, Schumann (145) used more assumptions to simplify Anzelius's solutions and reduced the results to a standard, dimensionless chart. The assumptions involved are: (1) there are no thermal temperature gradients in the solid, (2) the axial conduction in the fluid and in the solid may be neglected, (3) the thermal parameters are independent of temperature effects, (4) the rate of heat transfer between gas and solid is proportional to the average temperature difference, (5) all volume changes due to temperature may be neglected, (6) the bed is adiabatic, (7) the temperature of the gas is uniform over cross section of the bed, and (8) the initial gas and bed temperatures are uniform. He found that actually evaluating his solution entailed a rather large amount of computation which was in fact practically

impossible except for very small values of dimensionless time and bed length. His model still received much attention because of its impact in the prediction of breakthrough curves in fixed adsorbers and thermal regenerators. It was first used by Furnas (45,46,47) in 1930 and 1932 in determining the coefficient of heat transfer between a flowing gas and a bed of granular particles. He used graphical integration to evaluate Schumann's solution and extended the range of dimensionless time and bed length parameters. Lowan (106), Saunders and Ford (143), and Mondt (119) also used this approach in obtaining the heat transfer film coefficient by matching the experimental and theoretical curves by eye. However, these curves do not allow easy interpolation of intermediate values of the dimensionless bed length parameter.

In 1928, Ponndorf and Knipping (134) reported experimental results involving gas drying in silica gel and charcoal beds as a parallel work of the analytical solutions by Anzelius (8), Nusselt (125), Schumann (145), and Furnas (45,46,47). Derr (41) reported his experimental results in 1938 about drying of air by activated alumina. Similar experimental results were reported by Ahlberg (3) in 1939, and by Amero, Moore, and Capell (5) in 1947 on silica gel and Florite, respectively. However, no discussion was presented of the dynamic relation between heat recuperation and sorption in stationary beds.

Smith (147) in 1934 and Binnie and Poole (13) in 1937, studied the cross flow heat exchanger problem and obtained a double power series solution which can also be applied to the heat recuperation and adsorption problems.

In 1939, Wicke (158,159) reported on analytical solution for the drying of gases by porous solids. In 1943, Gamson, Thodos, and Hougen (48) presented a review of heat, mass, and momentum transfer in the flowing of gases through granular solids. Several years later, in 1946, Grossman (54) solved the transient heat transfer problem by finite difference methods where he included an arbitrary initial temperature distribution and heat of reaction. A year later, Brinkley (19) extended Anzelius's work to include the case where the solid generated heat. His expressions are obtained for the temperatures of solid and fluid as functions of position and time, and he assumed that the heat source function is a linear function of the temperature of the solid with coefficients independent of position and time. A year later in 1947, Hougen and Marshall (60) studied isothermal adsorption in granular beds where the mass transfer across the film is controlling which is analogous to the heat transfer problem handled by Anzelius (8) and Schumann (145). A linear equilibrium relationship between fluid and adsorbate concentration was assumed, and the adsorbate content of the gas present in the bed at any instant was neglected in comparison to total adsorbate passed through in a cycle. A number of graphical methods and analytical studies have also appeared in that decade (37,59).

In 1952, Jury and Licht (83,84) developed a generalized analytical solution, besides Wicke (158,159) and Eagleton and Bliss (43), which included the above case and two additional cases of intragranular diffusion controlling and activated diffusion controlling. They concluded in this study that the idealized theories were applicable to

longer beds. That same year, Rosen (138) reported a theoretical investigation of the transient mass transfer behavior of a fixed bed. The system was a bed of spherical particles of uniform radius, through which a fluid flows with a constant linear velocity and constant density. Other assumptions to linearize the system were constant film coefficient, constant internal diffusion coefficient, and a linear adsorption isotherm. The heat of adsorption was not considered. Thus, the solution was obtained by utilizing Laplace transform for the effluent fluid concentration as a function of time and bed length. A simplified approximation to the exact solution was also presented in which the effect of the film coefficient was not considered as a rate controlling step. Two years later, Rosen (139) evaluated the integals in this problem numerically in terms of dimensionless time, bed length, and film resistance parameters. Also in 1952 Kasten, Lapidus, and Amundson (89) presented a solution for the transient behavior of an isothermal adsorption bed. However, the use of their derived equations for heat and mass transfer was limited because of the restrictive assumption of a linear adsorption isotherm. In 1956 Amundson (6) developed analytical solutions for non-adiabatic heat transfer in fixed beds taking into account heat generation. Axial mixing was also assumed but he did not consider intraparticle diffusion. Instead he assumed the major resistance to heat transfer was in the gas film at the particle surface.

In 1954, Hubard (62) presented equilibrium data for silica gel-water vapor. Carmen and Haul (24) presented the constant-volume method of measuring the diffusion coefficients of a gas or a liquid

solution into a solid. In 1956, Acrivos (1) developed the one-dimensional model for isothermal fixed bed operation in which the adsorption isotherm is either linear or Langmuir type. He solved both heat and mass transfer with chemical reaction numerically. In 1960, Acrivos (2) pointed out that in the models the mass transfer resistance around and within the particles can be replaced by an axial diffusion term, because the existance of the mass transfer resistance will result in an axial dispersion.

In 1957, Sanlaville (142) published his pioneering work on simultaneous heat and mass transfer during air drying in fixed beds of activated alumina. The results indicated that heat transfer alone controlled the overall speed of sorption. On this basis he formulated equations and concluded that these solutions agreed well with experimental data. However, his work was restricted to shallow beds. At the same time, Jury (69) demonstrated mathematically that an assumption regarding the rate equation for isothermal bed operation which had been made by Eagleton and Bliss (43) was applicable only to the longer times. Reilly (135) obtained solutions to the transient heat transfer problem in the form of Fourier series, allowing for variation in arbitrary initial solid temperature distribution and arbitrary inlet gas temperature. In 1958 Kota and Aoki (98) reported their study of adiabatic adsorption of Kaken gel desiccant, which is produced by gelation on desiccant clay from Na-Silicate solutions. Emphasis was placed on measuring effluent temperature of stationary beds rather than developing the theory. Vermeulen (152), in 1958, and

Granville (52), in 1964, reviewed the methods for gas separation or purification by adsorption.

As an extended application of the mass transfer zone, Treybal (151), in 1955, and Nutter and Burnett (126,127), in 1963 and 1966, reported their studies on the fixed bed drying of air using Molecular Sieves. Between 1963 to 1965, Masamune and Smith (110,111,112) solved transient mass transfer from a flowing fluid to a fixed bed of particles mathematically for the conditions where either external diffusion, intraparticle diffusion, or surface adsorption processes control the rate. Gupta and Thodos (55), in 1962, and Bradshaw and Myer (17), in 1963, made separate investigations on simultaneous heat and mass transfer in fixed and fluidized beds. Gupta and Thodos (55) correlated available literature data to yield a relationship between the Colburn j-factor modulus and a modified Reynolds number. Bradshaw and Myers (17) showed that the log-mean driving force was satisfactory for evaluating heat and mass transfer coefficients provided the ratio of inlet to outlet driving force was not large. Also in 1962, Leavitt (102) presented an analysis of non-isothermal adsorption for cases where the mass transfer zone is stable. He assumed that no heat is transferred through the bed wall. His treatment was broad enough to cover cases where there is a significant change in the superficial gas velocity as the adsorption proceeds in the transfer zone. Gould (51), in 1961; Ross and Olivier (140), in 1964; and Deitz (40), in 1965, reported the theoretical and experimental aspects of physical chemistry of adsorption.

In 1964, Bowen (21) has outlined an approach to the problem of prediction for isothermal fixed bed adsorption with nonlinear isotherm. He confined the mathematical analysis to the low concentration end of the adsorption zone of activated alumina-water vapor system. Getty and Armstrong (50) reported air drying over activated alumina at 1 atm. under dynamic adiabatic conditions. His equations are easy to use, but the procedure has not been widely applied because the dynamic data for the specific system must be collected to develop the correlation.

In 1965, Major, Sollami, and Kammermeyer (108) investigated the carbon dioxide removal from air by activated carbon and Linde Molecular Sieve. Tien and Thodos (150) extended their earlier work on kinetics for systems having nonlinear isotherm. They used the computer to produce concentration-bed length-time relationships of isothermal fixed bed adsorption. Amundson, Aris, and Swanson (7) applied the simple wave theory to the problem of adiabatic adsorption and desorption in a fixed bed. In 1966, Chao and Hoelscher (31) reported the simultaneous axial dispersion and solid-fluid mass exchange in a packed bed adsorber. They used the Peclet number to characterize axial dispersion and impulse response technique to obtain the simultaneously values of the axial Peclet number. Leung and Quon (105) developed a model with a numerical solution for the transient behavior of a packed bed of uniform spheres. Although the existence of thermal gradients within the solid particles was considered, the effect of the varying gas velocity was neglected. Separate solutions for heat transfer and for mass transfer were obtained but no attempt was made to solve the simultaneous case. Bobcock, Green,

and Perry (10) reported theoretical studies of longitudinal dispersion mechanisms during steady flow. The equations obtained were applicable to both heat and mass transfer processes.

In 1967, Meyer and Weber (115) extended Rosen's model (138,139) and obtained a numerical solution of the differential equations of adiabatic fixed bed adsorption. Their model incorporated heat and mass transfer resistances within and around the adsorbent particles of homogeneous uniform spherical size. The adsorption isotherms are not restricted to any special form, and the heat transfer between the bed and the wall is included as well as heat losses from the wall to the surroundings. There are several drawbacks in their model such as: many of the adsorbent beds cannot be adequately approximated as spherical particles of uniform size; the solid diffusion coefficients are unknown but the solution of the model is sensitive to the intraparticle diffusivity and requires a high accuracy of the diffusivity determination while only the magnitude of the transfer coefficient can be evaluated by matching the experimental data and the numerical solutions.

Carter's work (25), in 1966, and (26,27,28), in 1968, deals with isothermal and adiabatic air drying in fixed beds of activated alumina. He developed numerical solutions for the simultaneous heat and mass transfer case. Later in 1972, Carter (29) treated adsorption of CO_2 on Linde molecular sieve-4A. His program of numerical calculations gave results that closely agreed with experiment both adiabatic and isothermal cases. Handley and Heggs (56,57), in 1968 and 1969, investigated the heat transfer mechanism in regular shaped packing and proposed a

computer program which employed a numerical solution of the Schumann's model (145). However, variation of the gas velocity down the bed was not considered. Another limitation of this study was that the evaluated correlation for heat transfer film coefficient applied only to spherical packing. In 1968, Y. Kim (96) fitted an analytical expression to the equilibrium sorption therm data of Mattern (113). An attempt to analyze percolation runs was hampered by problems associated with the debug of a digital computer analysis. Rimpel, Camp, Kostecki, and Canjar (137) presented the kinetics of physical adsorption of propane from helium on fixed bed of activated alumina at 30°C and at atmospheric pressure. They found that the internal diffusion appeared to be by a pore diffusion rather than by a surface diffusion mechanism, and this rate can be best described by Fick's equation for unsteady state diffusion into a sphere.

In 1969, Lee and Weber (104) presented a mathematical model of isothermal adsorption of a single component in a fixed bed. Their model accounts for the diffusional resistance between the bulk gas and the surface of the adsorbent particles, and for the diffusional resistance within the particles. The adsorption reaction within the pores is assumed to be very rapid compared to these two rate controlling mechanisms. The model can be used for isotherms of any shape and for gaseous feeds of any concentration. The partial differential equations of the model were solved numerically. In 1970, Chi and Wasan (33) developed an experimental technique for isothermal and adiabatic dynamic adsorption desorption processes. The equations governing such

processes and the nonlinear equilibrium relations were simultaneously solved on the digital computer. Horng (61) presented nonlinear sorption equilibria for activated alumina and Linde molecular sieve-4A. Marcussen (109) developed the theoretical calculations of the mass transfer rates. His model included a nonlinear adsorption isotherm and simultaneous resistance to mass transfer in the pore system of the solid and in a film surrounding the particle. A comparison between the numerical solutions to the model and experiments of activated alumina-water vapor system allows a determination of both the effective diffusion coefficient in the pore and the gas film resistance as a function of gas velocity which are $3.6 \times 10^{-6} m^2/sec$ and $0.85 \times Re^{-0.5}$, respectively.

In 1971 Jury (72) published his numerical analysis scheme for the solution of systems of mixed partial differential equations associated with simultaneous heat and mass transfer in packed beds of sorbent granules. The model treats the general adiabatic percolator and allows for variations in gas velocity and in physical properties with temperature and concentration. In addition, his numerical analysis is free of instability problems. At that time his method involved implicit techniques and proved satisfactory when used in a simulated experimental run. Kondis and Dranoff (97) presented a numerical analysis of nonisothermal sorption of Ethane by Linde molecular sieve-4A in batch system. The diffusivity was assumed to be a function of temperature and adsorbed gas concentration. Lee and Chi (103) developed analytical solutions for Acrivos (1,2) and Vermeulen (152) models for irreversible nonlinear isotherm.

In 1972, Jefferson (68) developed simplified single parameter models which under certain conditions were used to predict breakthrough curves in packed adsorbent and thermal regenerator beds. Garg and Ruthven (49) employed a numerical analysis of isothermal adsorption of a single component from a dilute gas mixture on Linde molecular sieves. They assumed constant linear velocity, a Langmuir isotherm, and solid phase diffusion controlling. The ordinary diffusivity was expressed as a function of temperature and concentration. In 1973, E. K. Kim (94) reported the ordinary diffusion coefficient of Florite, activated alumina, Linde molecular sieve-4A, Drierite, and silica gel. In 1974, Berbano (12) treated the heat recuperation problem numerically. His analysis was noteworthy because of its stability, efficiency, and the explicit techniques used. He considered both intragranular heat conduction and variable gas velocity along the bed. Also in 1974, Weber and Chakravorti (155) reviewed several models for mass transfer in isothermal fixed beds and presented a numerical solution for the general case of a pore model with gas film resistance.

Pollock (132), in 1976, continued E. K. Kim's studies of diffusion of adsorbing gases in porous sorbent solids by various combinations of free diffusion, Knudsen diffusion, surface diffusion, interstitial diffusion, and grain boundary diffusion. Both ordinary and thermal diffusion were investigated using the thermodynamics of irreversible processes to derive the general flux equations so-called total permeability and total diffusivity. His research also produced a new approach to numerical integration which views the definite integral in

terms of steady state flux instead of the conventional area interpretation. He also developed a method for calculating the maximum temperature which can occur in a fixed bed sorption column without first producing the solution to the percolation problem. Isosteric heats of adsorption were also investigated, and a logarithmic dependence of the differential heat of adsorption on loading was found. Also in 1976, Braener (18) used the fundamental thermodynamic and statistical thermodynamics equations to derive adsorption equations for fixed bed adsorption on heterogeneous surface adsorbents under the basis of Langmuir models. His method involves the calculation of distribution functions of adsorption energy, which were estimated from the integral equation for the adsorption isotherm. For calculation of the adsorption isotherm and the surface pressure, he used a Taylor series in the kernel of the integral equation for different pressure ranges and for any distribution function of the adsorption energy. Schestopalov, Kisarov, and Fisher (146) presented an algorithm for the calculation of adsorption-desorption processes in a fixed bed of a sorbent. It involves calculation of inner diffusion as a function of granule saturation, mass transfer as a function of adsorption space saturation and the working layer length. Dropping the functional dependence of the internal diffusion coefficient on radius causes a decrease of the accuracy of the dynamic characteristic calculations, but the authors considered the results still acceptable for practical purposes. Crittenden (38) presented the mathematical model of fixed bed adsorption for single and multicomponent adsorbates. Thomas (149) presented the

mechanism of gas fixation on a zeolite. Henrion (58), Rhodin and Adams (136), and Gregg and Sing (53) reviewed the adsorption of gases and solids. Astakhov, Romankov, and Lukin (9), and Ostrovskii (128) presented fixed bed adsorption isotherms of various conditions and adsorbents.

In 1977, Carter and Husain (30) developed a new simplified model that considers the rate of adsorption by the granules to be proportional to the concentration difference $(w_s - \bar{w})$ so that:

$$\rho_b(d\bar{w}/dt) = \alpha \cdot a \cdot \rho_g \cdot D_e(w_s - \bar{w})/b$$

in which ρ_b and ρ_g are, respectively, the bed and granule densities (kg/m^3), $\bar{w}$ and w_s are, respectively, the average and surface adsorbate concentration on the adsorbent (kg/kg), t is time (hr), a is external area of granules per unit volume of bed (m^2/m^3), D_e is the effective adsorbed phase solid diffusion coefficient (m^2/sec), and b is the mean radius of the adsorbent granules (m). α is a constant to compensate for the loss in driving force using the above equation, which is found to be 5.0. This rate equation is based on one derived by Jury (70) as a "long time" approximation to internal diffusion. The calculation method was non-iterative and used an implicit Crank-Nicholson finite difference substitution in the partial differential equations. The KDF9 digital computer time can be reduced approximately 13 times when compared to the numerical solution of the equations for the solid diffusion model and approximately 26 times when compared to the numerical solution of the equations for the pore diffusion model. Their

simplified methods have considerable potential in practice of making rapid and accurate assessments of the performance of deep beds of adsorbents having a nonlinear isotherm and operating under isothermal conditions. The theoretical results using this simplified rate model showed excellent agreement with the experimental values on the adsorption of carbon dioxide from a flow of dry helium gas on fixed bed of 4A molecular sieve granules. Also in 1977, Von Rosenberg, Chambers, and Swan (154) published a numerical solution of surface controlled fixed bed adsorption. A simple numerical method was developed which can be described by equations of the form

$$- B_1\{u(\partial c/\partial x)+(\partial c/\partial t)\} = B_2(\partial w/\partial t) = f(c,w)$$

where c is the concentration of sorbate in the fluid, w is the concentration of sorbate on the solid, x is the length in the direction of flow, t is the time, u is the fluid velocity, B_1 is the capacity of the fluid for sorbate, B_2 is the capacity of the solid for sorbate, and f(c,w) is a function which describes the rate of adsorption. Breakthrough curves calculated by this method agree with experimental curves for the adsorption of carbon dioxide from a stream of nitrogen by molecular sieve. The computation time can be decreased by a modification which allows the time increment to be increased for a fixed length increment.

A number of researches on kinetics of adsorption were done in 1977 under various conditions, assumptions and models of adsorbents. Katawa and Ulin (90), and Zolotarev, Kataeva, and Ulin (160) presented

a numerical calculation and analysis of expiration curves for a fixed bed of biporous adsorbents in the case of a linear adsorption isotherm. The method described is based on a numerical inverse Laplace transformation within the changing interval 0.01-0.99 and the error in determining the expiration curves is less than 2%. The computer program is written in ALGOL language. The authors considered their program stable enough for calculating the expiration curves for various biporous adsorbent shapes at various diffusion relaxation time ratios. Miura and Hashimoto (118) presented analytical solutions for the breakthrough curves of fixed bed adsorbers under constant pattern and linear driving force approximations. Dubinin (42) presented a review of thermodynamics and osmotic theories of adsorption and of equilibrium and kinetics of gas and vapor adsorption on microporous adsorbents. S. G. Kim (95) reported a numerical solution of the equations describing adsorption in fixed bed columns. Both liquid film controlling and intraparticle diffusion controlling were assumed and the concentration distributions in the bed were estimated by numerical analysis under constant pattern conditions. The results were compared with the published experimental data and it was shown that for highly porous adsorbents, e.g., activated carbon, the method with the assumption of intraparticle diffusion controlling mechanism was a good approximation for concentration distributions. Nazarok and Kravetskii (122) and Nazarok, Ostrovskii, Kravetskii, and Khinkis (123) presented the kinetics of adsorption of readily adsorbable substances in batch systems with a Langmuir's isotherm. The numerical calculations of the

adsorption kinetics for spherical adsorbent granules were carried out under conditions of constant concentration of adsorbate. The calculations involve internal and gas film diffusion. Nam and Rhee (121) published an asymptotic solution and effective dispersion coefficient for a fixed bed adsorption system. Saveleva, Zamashkin, Savelev, and Dvoretskii (144) reported the possibility of separating vapor-air mixtures on carbon molecular sieves which were prepared from poorly-sintering and lean coal.

An analytical model of temperature breakthrough curves in heating or cooling a fixed bed column without and with adsorption or desorption was derived by Gerald, Radeke, and Gelbin (2) in 1977. Nagarev, Enikew, Shumyatskii, Torocheshnikov, and Ermakov (120) reported the thermal effects during drying of air on silica gel. Novak (124) presented a method for the study of interphase mass transfer at very low Reynolds number in packed beds. Ciembroniewicz and Schulz (36) presented diffusion coefficients of gases in porous solids. Their formula was derived for kinetics obtained at various intervals of adsorbate concentrations. Aleksashenko (4) derived an equation describing the internal diffusion coefficient in porous sorbents from nonlinear adsorption isotherm for particles of large dimensions. A number of articles concerning diffusion in adsorbents (11,16,20,34,35, 129,141,161,162,163) were published in that year.

In 1978 Keda, Fujino and Katoh (91) presented a numerical method, based on the cell model, to obtain breakthrough and temperature curves for nonisothermal, fixed bed adsorption column with nonlinear

equilibrium. The effects of the variables on heat and mass transfer were studied for solid phase mass transfer coefficient, overall heat transfer coefficient at column wall, length of bed or number of cells, and equilibrium isotherms. The bed performance based on the cell model approach gives essentially the same result as that based on the diffusion model approach when the cell has the same height as 1 particle diameter and the value of Reynolds number and Schmidt number is large enough. Also in 1978, McGreavy and Nussey (116) presented a theory of simultaneous heat and mass transfer in transient adsorption on solid particles in a fixed bed. The intraparticle transport arises from surface diffusion and the nonlinear adsorption isotherm, although other physical and operational parameters display parametric sensitivity effects with regard to predicted breakthrough curves. Volskchuk, Gorlov, Dubinin, Erasho, Zolotarev, and Ulin (153) presented the kinetics of adsorption in biporous adsorbents in case of a sharply convex adsorption isotherm. Maachi and Vergnaud (107) reported the adsorption of water vapor on molecular sieves type 4A and 3A. Lason, and Nodzenski (100) reported the adsorption of CO_2+Xe mixtures on alumina of various porosity as functions of total and relative pressures.

Jaroniec (64,65,66,67) worked on adsorption in multi-component gases.

The elegant kinetic mechanisms under consideration in this thesis and the need for high speed numerical computation suggest the utility of a table in which we can summarize the distinguishing features of past (and present even though premature at this point) numerical research.

These details were either omitted or discussed qualitatively in the above historical review because they are now summarized in Table I. It is quite obvious from the table that there is a very broad range of computational times involved when one considers the influence of increment size, implicit calculations involving repeated iteration and simple versus elegant kinetic mechanisms. Some researchers also had stability problems and these are not noted in the table. Some of the claims in the table are too broad as will become more and more obvious during the course of this thesis.

Table I. Summary of Numerical Analysis of Single Solute Gas-Solid Adsorption System.

Ref. No.	Solute	Type of Percolation		Kinetic Mechanisms							Increment Size			Prog. Impl./ Expl.
		Recup.	Ads.	Heat Transfer	Mass Transfer	Gas Film	Int. Diff.	Bipore	Heat Release Surf./Int.	Isotherm Linear/ Nonlinear	Δt sec	Δr in	Δz in	
1	Water-Vapor	No	Yes	Yes	Yes	Yes	No	No	*	Nonlinear	*	*	*	Impl.
105	Gases	Yes	No	Yes	No	No	Yes	No	Surf.	-	.05-5.0	R/15-R/5	.6-8.64	Impl.
25	Water-Vapor	No	Yes	Yes	Yes	Yes	Yes	No	Surf.	Linear	4.5	R/5	.04	Impl.
115	Methane	No	Yes	Yes	Yes	Yes	Yes	No	Int.	Nonlinear	.0072	R/8	3.75	Impl.
104	Methane	No	Yes	No	Yes	Yes	Yes	No	-	Nonlinear	*	*	*	Expl.
57	Hot-Air	Yes	No	Yes	No	No	Yes	No	Surf.	-	*	*	*	Impl.
109	Water-Vapor	No	Yes	No	Yes	Yes	Yes	No	-	Nonlinear	*	.0054	*	*
49	Gases	No	Yes	No	Yes	No	Yes	No	-	Nonlinear	*	*	*	Impl.
12	Hot-Air	Yes	No	Yes	No	Yes	Yes	No	Surf.	-	2.0	.0023	.0411	Impl.
30	CO_2	No	Yes	No	Yes	Yes	Yes	No	-	Nonlinear	*	*	*	Expl.
154	CO_2	No	Yes	No	Yes	Yes	Yes	No	-	Linear	*	*	*	*
Our	Water-Vapor	No	Yes	Yes	Yes	Yes	Yes	Yes	Both	Nonlinear	3.0, 12.0 Variable	R/20-R/224 Variable	4R Variable	Expl.

Note: * indicates unknown.

- indicates not being used or studied.

CHAPTER III

THEORY AND NUMERICAL PROCEDURES

The simultaneous heat and mass transport of percolation operations will be defined in terms of a system of mixed partial differential equations which are nonlinear. The sorption therm expressions, heat transfer film coefficient relations, and diffusion relationships including the new bipore model and surface/internal release of heat of adsorption will be assembled along with appropriate bed equations into a method for accounting for experimental results of fixed bed percolator runs. Second order interpolation followed by integration over an increment of the time or space variable will be used as a method for arriving at finite difference equations equivalent of the original partial differential equations of bed increments. Thomas algorithm will be used as a method to determine the partial pressure or temperature inside the granules.

In all the previous work it was assumed that all the heat of adsorption is liberated at the very surface of the granule. In the case of free and/or Knudsen diffusion into a granule some or all of the adsorption heat might be liberated inside of the granule at the point of adsorption. It is more beneficial to use a model that takes this effect into account. The fraction of heat of adsorption released internally, EF, and the fraction of heat of adsorption released at granule surface, 1-EF, will be included in the equations involved.

From attempts to fit activated alumina data it became necessary to adopt a bipore model. This model involves blind micropores which are shown in Figure 1. Figure 2 shows the segmental granule shown in Figure 1. For simplicity, the continuous phase fraction in the granule is σ, and the dispersed phase fraction is $1-\sigma$. The average concentration in the microsphere of the dispersed phase is C_d, the total diffusivity is D_d, and the radius of the microsphere is R_d. Since we do not have any information on D_d and R_d, we will assume a proportionally fraction EF1 which is defined as follows:

$$D_d/R_d^2 = EF1 \cdot D/R^2 \tag{1}$$

For simplicity, it has been assumed in writing the transport equations that:

1. The gas phase velocity profile in the bed is uniform across its cross-section.
2. The specific heat of the gas phase, C_{PG}, is constant. If it is not, it would be included in the appropriate derivatives of the equations in which it appears. Later this interpretation is limited to one Δt and C_{PG} then is allowed to vary from one Δt to the next.

A sketch of a packed bed section is shown in Figure 3.

The overall gas phase mass balance over a differential bed length, Δz is

$$\partial \rho_G/\partial t + \partial v \rho_G/\partial z = - \sigma a_v J^*/\varepsilon \tag{2}$$

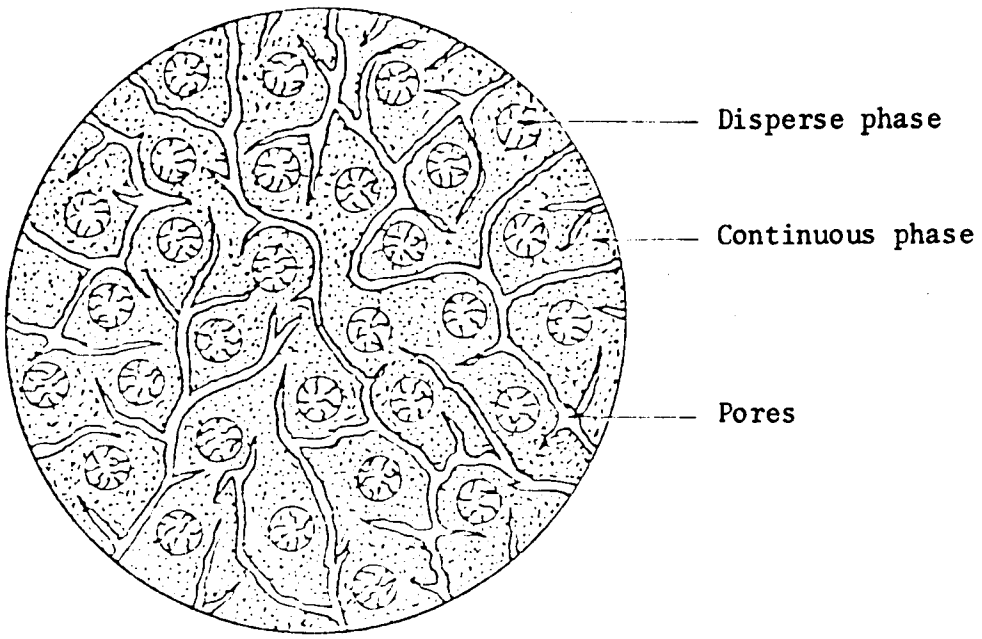


Figure 1. The Granule with Bipore Model.

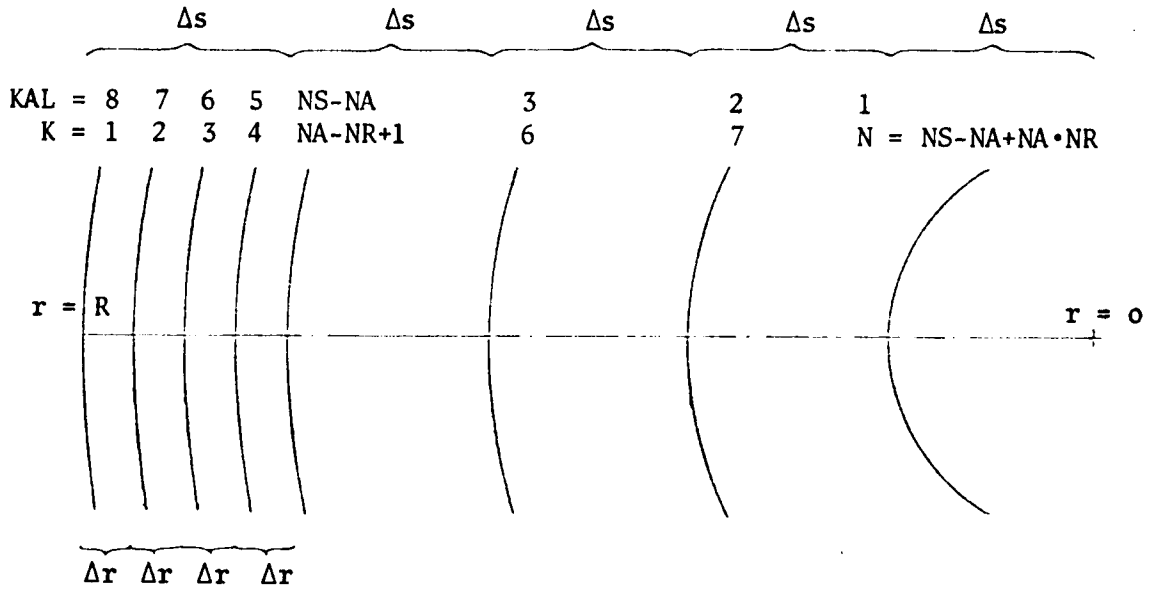


Figure 2. The Granule Segments.

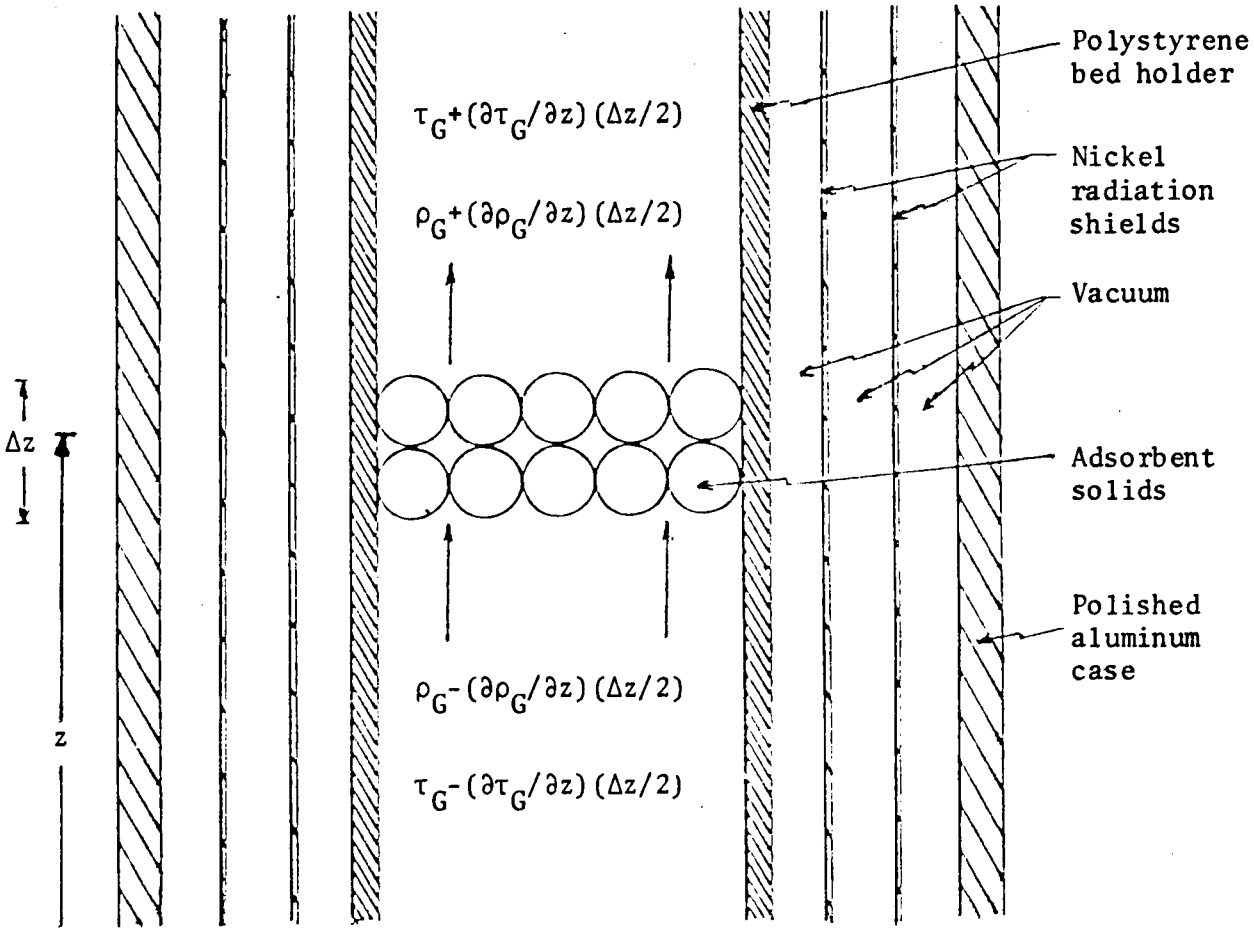


Figure 3. Differential Bed Model of Heat and Mass Transfer.

The solute gas mass balance is

$$\partial C_G/\partial t + \partial v C_G/\partial z = - \sigma a_v J^*/\varepsilon \tag{3}$$

The gas phase thermal balance is

$$\partial \rho_G \tau_G/\partial t + \partial v \rho_G \tau_G/\partial z = (h a_v/\varepsilon C_{PG})(\tau^* - \tau_G) - (4h_W/\varepsilon C_{PG} d_I)(\tau_G - \tau_W) - \sigma a_v \tau_G J^*/\varepsilon \tag{4}$$

The h in Eq. (4) was taken from Berbano's thesis (12) as a correlation which is

$$h = V21(\bar{k}_G/D_p)(N_{Re})^{V22}(N_{Pr})^{V23} \tag{5}$$

where V21 = 0.64152

V22 = 0.67160

V23 = 0.34685

and h_w was taken from the literature (14) which is

$$h_w = CW\ (\bar{k}_G/d_I)(N_{Re})^{0.83} \tag{6}$$

The convectional mass transfer rate equation is (based on the basics of diffusion) taken to be

$$J^* = k_G \rho_G (C_G - C_G^*)/(\rho_G - C_G) \tag{7}$$

The gas phase equation of state is (assuming ideal gas law behavior)

$$P_T = \rho_G \bar{R} \tau_G \tag{8}$$

For the drying of air the Lewis relation is applicable, i.e.

$$h = k_G C_{PG} \rho_G \tag{9}$$

In addition to the foregoing equations above, the initial and boundary conditions are specified such as

$$C_G(o,t) = \text{constant} \tag{10}$$

$$v(o,t) = \text{constant} \tag{11}$$

$$\tau_G(o,t) = \text{constant} \tag{12}$$

$$C_G(z,o) = \text{constant} \tag{13}$$

$$\tau_G(z,o) = \text{constant} \tag{14}$$

In addition to heat storage in the tube that contains the bed, see Figure 3, the radiation heat loss from the bed via the tube wall to the vacuum insulation was considered. A heat balance on an elemental section of the tube consequently yields

$$\partial\tau_w/\partial t = \{4h_W d_I/\rho_T C_{PT}(d_o^2-d_I^2)\}(\tau_G-\tau_w) - \{4h_R d_o/\rho_T C_{PT}(d_o^2-d_I^2)\}(\tau_w-\tau_A) \tag{15}$$

the initial condition is

$$\tau_w(z,o) = \tau_I \tag{16}$$

and the equation for h_R was taken from the texts (14,99) which is

$$h_R = 1.712 \times 10^{-9}\ CR(\tau_W^2+\tau_A^2)(\tau_W+\tau_A) \tag{17}$$

where

$$CR = 1/\{1/\varepsilon_1+(R_2/R_{SI})(1/\varepsilon_2-1)+(R_2/R_{SI})(1/\varepsilon_2)+(R_2/R_{so})(1/\varepsilon_3-1)$$
$$+(R_2/R_{so})(1/\varepsilon_3)+(R_2/R_{AI})(1/\varepsilon_4-1)\} \quad (18)$$

In developing the finite difference equivalents of the percolation equations, Jury's method of second order interpolation followed by integration (72) was used.

The gas phase thermal balance, Eq. (4), can be written for a finite bed length Δz, illustrated in Figure 4, in which the gas phase in each stage is assumed uniformily mixed. In this case we obtain

$$\partial\rho_G(I+1,t)\tau_G(I+1,t)/\partial t = (1/\Delta z)\{v(I,t)\rho_G(I,t)\tau_G(I,t)-v(I+1,t)$$
$$\rho_G(I+1,t)\tau_G(I+1,t)\}+(ha_v/\varepsilon C_{PG})$$
$$\{\tau^*(I+1,t)-\tau_G(I+1,t)\}-(4h_w/\varepsilon C_{PG}d_I)$$
$$\{\tau_G(I+1,t)-\tau_w(I+1,t)\}-(\sigma a_v/\varepsilon)\tau_G(I+1,t)$$
$$J^*(I+1,t) \quad (19)$$

where I refers to the bed increment prior to the current bed increment I+1 being computed.

If ideal gas behavior with constant pressure operation is assumed, i.e.

$$P/\overline{R} = \rho_G(I+1,t)\tau_G(I+1,t) = \text{constant} \quad (20)$$

then

$$\partial\rho_G(I+1,t)\tau_G(I+1,t)/\partial t = 0 \quad (21)$$

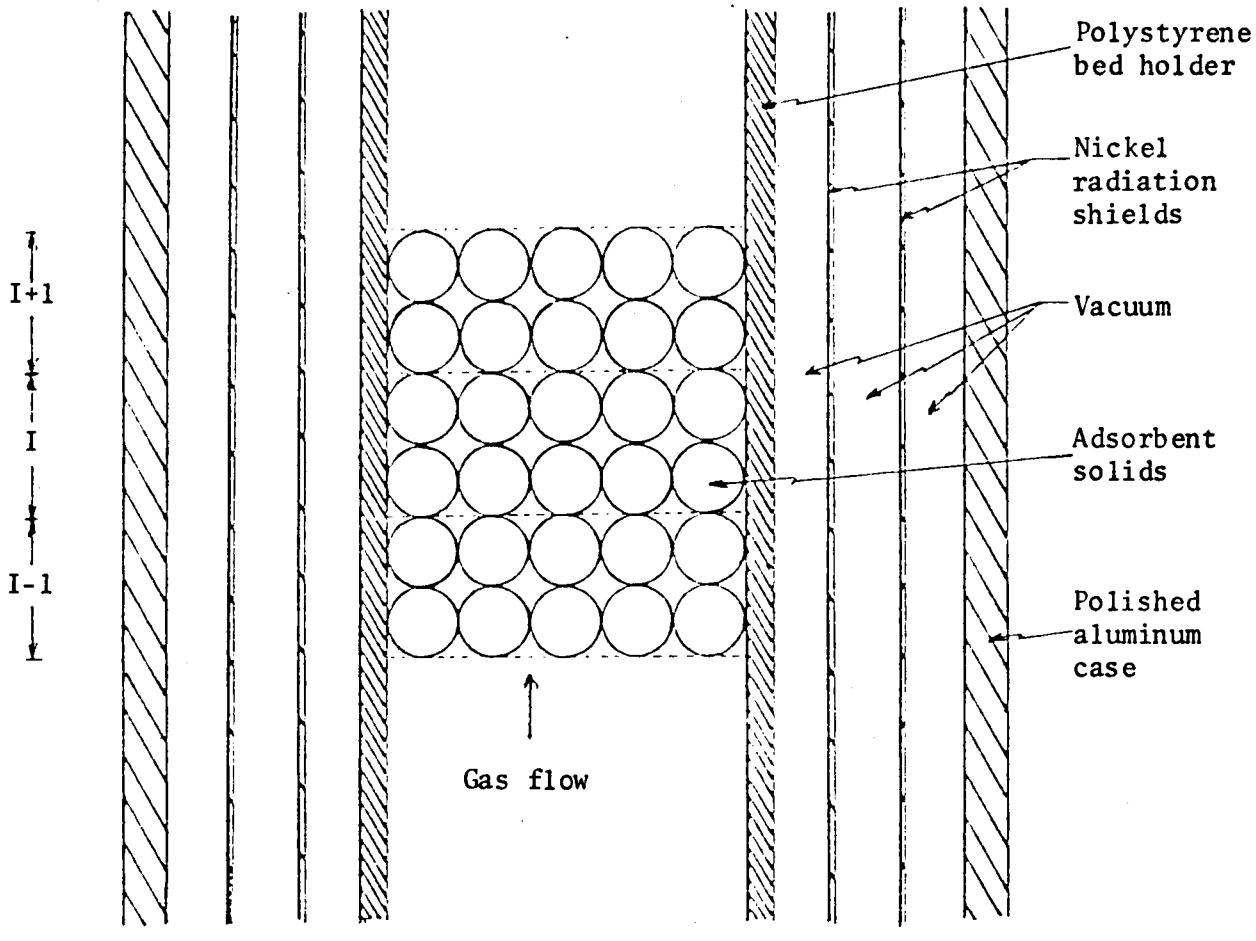


Figure 4. Stagewise Bed Model of Heat and Mass Transfer.

and, for purposes of scaling set

$$G(I+1,t) = v(I+1,t)\rho_G(I+1,t) \tag{22}$$

Then, Eq. (19) reduces to

$$G(I+1,t_2)\tau_G(I+1,t_2)-G(I,t_2)\tau_G(I,t_2) = (ha_v\Delta z/\varepsilon C_{PG})\{\tau^*(I+1,t_2) - \tau_G(I+1,t_2)\}-(4h_W\Delta z/\varepsilon C_{PG}d_I)\{\tau_G(I+1,t_2)-\tau_w(I+1,t_2)\} -(\sigma a_v\Delta z/\varepsilon)\{\tau_G(I+1,t_2)J^*(I+1,t_2)\} \tag{23}$$

where t_1 refers to the time prior to the current time t_2 being computed.

The overall gas phase mass balance, Eq. (2) is

$$\partial\rho_G(I+1,t)/\partial t = (1/\Delta z)\{v(I,t)\rho_G(I,t)-v(I+1,t)\rho_G(I+1,t)\} -(\sigma a_v/\varepsilon)J^*(I+1,t) \tag{24}$$

This can be integrated by second order interpolation and then integration, and multiplied by $\tau_G(I+1,t_2)$, i.e.

$$\rho_G(I+1,t_2)\tau_G(I+1,t_2)-\rho_G(I+1,t_1)\tau_G(I+1,t_2) = \beta(\Delta t/\Delta z)\{G(I,t_1)-G(I+1,t_1)-(\sigma a_v\Delta z/\varepsilon)J^*(I+1,t_1)\}\tau_G(I+1,t_2) +(1-\beta)(\Delta t/\Delta z)\{G(I,t_2)-G(I+1,t_2)-(\sigma a_v\Delta z/\varepsilon)J^*(I+1,t_2)\}\tau_G(I+1,t_2) \tag{25}$$

Eq. (23) and (25) may be manipulated into the form

$$P/\bar{R}-\rho_G(I+1,t_1)\tau_G(I+1,t_2)$$

$$= \beta(\Delta t/\Delta z)\{G(I,t_1)-G(I+1,t_1)-(\sigma a_v \Delta z/\varepsilon)J^*(I+1,t_1)\}\tau_G(I+1,t_2)$$

$$+(1-\beta)(\Delta t/\Delta z)[G(I,t_2)\tau_G(I+1,t_2)-G(I,t_2)\tau_G(I,t_2)-(ha_v\Delta z/\varepsilon C_{PG})$$

$$\{\tau^*(I+1,t_2)-\tau_G(I+1,t_2)\}+(4h_W\Delta z/\varepsilon C_{PG}d_I)\{\tau_G(I+1,t_2)-\tau_w(I+1,t_2)\}] \quad (26)$$

The heat balance for the elemental section of tube wall, Eq. (15) is

$$\partial\tau_W(I+1,t)/\partial t = \{4h_W d_I/\rho_T C_{PT}(d_o^2-d_I^2)\}\{\tau_G(I+1,t)-\tau_w(I+1,t)\}$$

$$-\{4h_R d_o/\rho_T C_{PT}(d_o^2-d_I^2)\}\{\tau_w(I+1,t)-\tau_A\} \quad (27)$$

Again second order interpolation followed by integration can be used, and Eq. (27) is then

$$\tau_W(I+1,t_2) = [\tau_W(I+1,t_1)$$

$$+\beta\{\gamma\tau_G(I+1,t_1)-(\gamma+\gamma_R)\tau_w(I+1,t_1)\}+(1-\beta)\gamma\tau_G(I+1,t_2)+\gamma_R\tau_A]/$$

$$\{1+(1-\beta)(\gamma+\gamma_R)\} \quad (28)$$

where

$$\gamma = 4d_I h_W \Delta t/\{\rho_T C_{PT}(d_o^2-d_I^2)\} \quad (29)$$

$$\gamma_R = 4d_o h_R \Delta t/\{\rho_T C_{PT}(d_o^2-d_I^2)\} \quad (30)$$

From the stability analysis (72), it was shown that computations are unconditionally stable if $\beta \leq 1/2$. So for convenience, we can set

$$\beta = 0 \quad (31)$$

and define the normalized temperatures

$$TG(I+1,t_2) = \{\tau_G(I+1,t_2)-\tau_I\}/\tau_I \tag{32}$$

$$TW(I+1,t_2) = \{\tau_W(I+1,t_2)-\tau_I\}/\tau_I \tag{33}$$

$$TA = (\tau_A-\tau_I)/\tau_I \tag{34}$$

$$UT(t_2,1) = \{\tau(t_2,1)-\tau_I\}/\tau_I \tag{35}$$

Finally, Eq. (28) is reduced to

$$TW(I+1,t_2) = \{TW(I+1,t_1)+\gamma\cdot TG(I+1,t_2)+\gamma_R\cdot TA\}/(1+\gamma+\gamma_R) \tag{36}$$

The $\tau_W(I+1,t_2)$ in Eq. (26) is eliminated by means of Eq. (28). The resulting equation produces a result solvable for $TG(I+1,t_2)$ via the simplifying relations (29)-(36) as follows

$$TG(I+1,t_2) = QB+QA\cdot UT(t_2,1) \tag{37}$$

where

$$QA = 1/[(\varepsilon C_{PG}/ha_v\Delta t)\{\rho_G(I+1,t_1)+(\Delta t/\Delta z)G(I,t_2)\}+1$$
$$+4h_W(1+\gamma_R)/\{ha_v d_I(1+\gamma+\gamma_R)\}] \tag{38}$$

$$QB = QA[(\varepsilon C_{PG}/ha_v\Delta t)\{P/\overline{R}\,\tau_I-\rho_G(I+1,t_1)+(\Delta t/\Delta z)G(I,t_2)TG(I,t_2)\}$$
$$+4h_W\{TW(I+1,t_1)+\gamma_R\cdot TA\}/\{ha_v d_I(1+\gamma+\gamma_R)\}] \tag{39}$$

Having $TG(I+1,t_2)$ in hand, we can calculate $\rho_G(I+1,t_2)$ from the gas law, i.e.

$$\rho_G(I+1,t_2) = P/\overline{R}\cdot\tau_G(I+1,t_2) \tag{40}$$

The $G(I+1,t_2)$ can be calculated from Eq. (23) and so on, thus

$$G(I+1,t_2) = [G(I,t_2)\{TG(I,t_2)+1\}+(ha_v\Delta z/\varepsilon C_{PG})\{UT(t_2,1)-TG(I+1,t_2)\}-(\sigma a_v\Delta z/\varepsilon)\{TG(I+1,t_2)+1\}J^*(I+1,t_2)] /\{TG(I+1,t_2)+1\} \quad (41)$$

The solute gas mass balance, Eq. (3), can be rearranged to

$$\partial C_G(I+1,t)/\partial t = (1/\Delta z)\{v(I,t)C_G(I,t)-v(I+1,t)C_G(I+1,t)\} -(\sigma a_v/\varepsilon)J^*(I+1,t) \quad (42)$$

If we define a mole fraction, Y, such that

$$Y = C_G/\rho_G = P/P_T \quad (43)$$

then, Eq. (42) can be rewritten as

$$\rho_G(I+1,t_2)Y(I+1,t_2)-\rho_G(I+1,t_1)Y(I+1,t_1) = \beta(\Delta t/\Delta z)\{G(I,t_1)Y(I,t_1)-G(I+1,t_1)Y(I+1,t_1)-(\sigma a_v\Delta z/\varepsilon) J^*(I+1,t_1)\}+(1-\beta)(\Delta t/\Delta z)\{G(I,t_2)Y(I,t_2)-G(I+1,t_2)Y(I+1,t_2) -(\sigma a_v\Delta z/\varepsilon)J^*(I+1,t_2)\} \quad (44)$$

For $\beta = 0$, Eq. (44) can be solved for $Y(I+1,t_2)$ as follow

$$Y(I+1,t_2) = \{(\Delta z/\Delta t)\rho_G(I+1,t_1)Y(I+1,t_1)+G(I,t_2)Y(I,t_2)-(\sigma a_v\Delta z/\varepsilon) J^*(I+1,t_2)\}/\{(\Delta z/\Delta t)\rho_G(I+1,t_2)+G(I+1,t_2)\} \quad (45)$$

The mass transfer rate equation, Eq. (7), is

$$J^*(I+1,t_2) = k_G\{\rho_G(I+1,t_2)Y(I+1,t_2)-C_G^*(I+1,t_2)\}/\{1-Y(I+1,t_2)\} \quad (46)$$

This can be solved for $C_G^*(I+1,t_2)$ thus

$$C_G^*(I+1,t_2) = \rho_G(I+1,t_2)Y(I+1,t_2)-\{1-Y(I+1,t_2)\}J^*(I+1,t_2)/k_G \quad (47)$$

The granule-gas interface thermal balance is

$$(1-EF)\lambda\sigma J^* = h(\tau^*-\tau_G)+k(\partial\tau/\partial r)_{r\,=\,R} \quad (48)$$

The granule-gas interface equilibrium relation in general is

$$C^* = C^*(P^*,\tau^*) \quad (49)$$

The granule equation for continuity of heat around the granule, as shown in Figure 1 (page 25), is

$$\partial\rho C_p\tau_c/\partial t = \partial J_T/\partial r+(2/r)J_T+\lambda EF\{\sigma(\partial C_c/\partial t)+(1-\sigma)(\partial C_d/\partial t)\} \quad (50)$$

where

$$J_T = k(\partial\tau_c/\partial r) \quad (51)$$

and $\tau_d \simeq \tau_c$ because thermal diffusivity, $\alpha = k/\rho C_p$ is large. Then J_T can be eliminated between Eq. (50) and (51), thus

$$\partial\tau_c/\partial t = \alpha\{\partial^2\tau_c/\partial r^2+(2/r)(\partial\tau_c/\partial r)\}$$
$$+(\lambda EF/\rho C_p)\{\sigma(\partial C_c/\partial t)+(1-\sigma)(\partial C_d/\partial t)\} \quad (52)$$

The continuous phase mass balance for an increment of granule shown in Figures 1 and 2 is

$$\partial C_c/\partial t = \{\partial J_c/\partial r+(2/r)J_c\}-\{(1-\sigma)/\sigma\}(\partial C_d/\partial t) \quad (53)$$

where if we include thermal as well as Fickian diffusion

$$J_c = D\{\partial C/\partial r+\delta(\partial \tau/\partial r)\} \tag{54}$$

and

$$\delta = -(\partial C/\partial \tau)_{J_c} = 0 \tag{55}$$

Since the sorption therm is

$$C = C(P,\tau) \tag{56}$$

and

$$dC = (\partial C/\partial P)_\tau dP+(\partial C/\partial \tau)_p d\tau \tag{57}$$

then

$$J_c = D(\partial C/\partial P)_\tau [\partial P/\partial r+(\partial \tau/\partial r)\{\delta+(\partial C/\partial \tau)_p\}/(\partial C/\partial P)_\tau] \tag{58}$$

Pollock (132) showed from his experiments that

$$\{\delta+(\partial C/\partial \tau)_p\}/(\partial C/\partial P)_\tau = 0 \tag{59}$$

So

$$J_C = D(\partial C/\partial P)_\tau(\partial P/\partial r) \tag{60}$$

and the term $D(\partial C/\partial P)_\tau$ is the so-called permeability, PE. The dispersed phase equation for continuity of mass is taken to be

$$\partial C_d/\partial t = (15\ D_d/R_d^2)(C-C_d) \tag{61}$$

This was taken from literature (70) and it is assumed to apply here because we do not have any information of the dispersed phase.

In addition to the above equations, we must also specify the initial and boundary conditions such as, for example

$$\{\partial\tau(r,t)/\partial r\}_{r=o} = 0 \tag{62}$$

$$\{\partial C(r,t)/\partial r\}_{r=o} = 0 \tag{63}$$

$$\tau(r,o) = \text{constant} \tag{64}$$

$$C(r,o) = \text{constant} \tag{65}$$

$$(J_c)_{r=R} = J^* \tag{66}$$

If we use the Euler chain rule

$$\partial C_d/\partial t = (\partial C/\partial P)_\tau(\partial P_d/\partial t)+(\partial C/\partial\tau)_P(\partial\tau_d/\partial t) \tag{67}$$

and

$$dC = (\partial C/\partial P)_\tau dP+(\partial C/\partial\tau)_P d\tau \tag{68}$$

or

$$\Delta C = (\partial C/\partial P)_\tau \Delta P+(\partial C/\partial\tau)_P \Delta\tau \tag{69}$$

or

$$C-C_d = (\partial C/\partial P)_\tau (P-P_d)+(\partial C/\partial\tau)_P(\tau-\tau_d) \tag{70}$$

If $\propto$ is large then $\tau_d \simeq \tau$, and the rate equation for dispersed phase, Eq. (61), may be written

$$\begin{aligned}\partial C_d/\partial t &= (\partial C/\partial P)_\tau(\partial P_d/\partial t)+(\partial C/\partial\tau)_P(\partial\tau/\partial t)\\ &= (15\ D_d/R_d^2)(\partial C/\partial P)_\tau(P-P_d)\end{aligned} \tag{71}$$

or

$$\partial P_d/\partial t = (15\ D_d/R_d^2)(P-P_d)-\{(\partial C/\partial\tau)_P/(\partial C/\partial P)_\tau\}(\partial\tau/\partial t) \tag{72}$$

If we define

$$TE = \propto(\partial C/\partial\tau)_P \tag{73}$$

$$DP = P_F - P_I \tag{74}$$

and adopt the normalized notations

$$UT = (r/R)\{(\tau-\tau_I)/\tau_I\} \tag{75}$$

$$UP = (r/R)\{(P-P_I)/DP\} \tag{76}$$

$$UPD = (r/R)\{(P_d-P_I)/DP\} \tag{77}$$

Eq. (72) can be written

$$\partial UPD/\partial t = (15\ D_d/R_d^2)(UP-UPD)-\{(TE\cdot D\cdot\tau_I)/(PE\cdot\alpha\cdot DP)\}(\partial UT/\partial t) \tag{78}$$

and the finite difference form used here is

$$UPD(t_2,K)-UPD(t_1,K) = (15\cdot D_d\cdot\Delta t/R_d^2)\{UP(t_2,K)-UPD(t_2,K)\} -\{(TE(K)\cdot D(K)\cdot\tau_I)/(PE(t_2,K)\cdot\alpha\cdot DP)\}\{UT(t_2,K)- UT(t_1,K)\} \tag{79}$$

For convenience we can define

$$PHID = 15\cdot D_d\cdot\Delta t/R_d^2 = 15\cdot EF1\cdot D(K)\cdot\Delta t/R^2 \tag{80}$$

$$DELUT(K) = UT(t_2,K)-UT(t_1,K) \tag{81}$$

$$WO6 = TE(K)\cdot D(K)/(PE(t_2,K)\cdot\alpha) \tag{82}$$

Eq. (79) can be solved for $UPD(t_2,K)$, thus

$$UPD(t_2,K) = \{UPD(t_1,K)+PHID\cdot UP(t_2,K)-WO6\cdot\tau_I\cdot DELUT(K)/DP\}/ (1+PHID) \tag{83}$$

To accommodate rapid changes at the surface of granule without drastic increases in N, where N is the total number of segments, we divide r into NS ΔS and then we subdivide NA of NS ΔS into NR Δr as shown in Figure 2 (page 25). At the interface let us define our model in such a way that the results will apply either side of the interface as shown in Figure 5.

Then for the granule thermal balance or mass balance, the $\partial^2 U(t,r)/\partial r^2$ term can be finite differenced using the central difference procedure in such a way that the Δr is positive thus

$$\partial^2 U(t,r)/\partial r^2 = \partial(\partial U/\partial r)/\partial r = \Delta(\Delta U/\Delta r)/\Delta r$$

$$= \Delta[\{U(t,r+(\Delta x)_2/2)-U(t,r-(\Delta x)_2/2)\}/ \{r+(\Delta x)_2/2-(r-(\Delta x)_2/2)\}]/\{r+(\Delta x)_2/2 -(r-(\Delta x)_2/2)\} \quad (84)$$

$$= \Delta\{U(t,r+(\Delta x)_2/2)-U(t,r-(\Delta x)_2/2)\}/(\Delta x)_2^2 \quad (85)$$

$$= [U(t,r+(\Delta x)_2)-U(t,r)-\{U(t,r)-U(t,r-(\Delta x)_2)\}]/ (\Delta x)_2^2 \quad (86)$$

Using linear interpolation as shown in Figure 6

$$U(t,r-(\Delta x)_2) = U(t,r)-\{(\Delta x)_2/(\Delta x)_1\}\{U(t,r)-U(t,r-(\Delta x)_1)\} \quad (87)$$

and then

$$\partial^2 U(t,r)/\partial r^2 = [U(t,r+(\Delta x)_2)-2\cdot U(t,r)+U(t,r)-\{(\Delta x)_2/(\Delta x)_1\} \{U(t,r)-U(t,r-(\Delta x)_1)\}]/(\Delta x)_2^2 \quad (88)$$

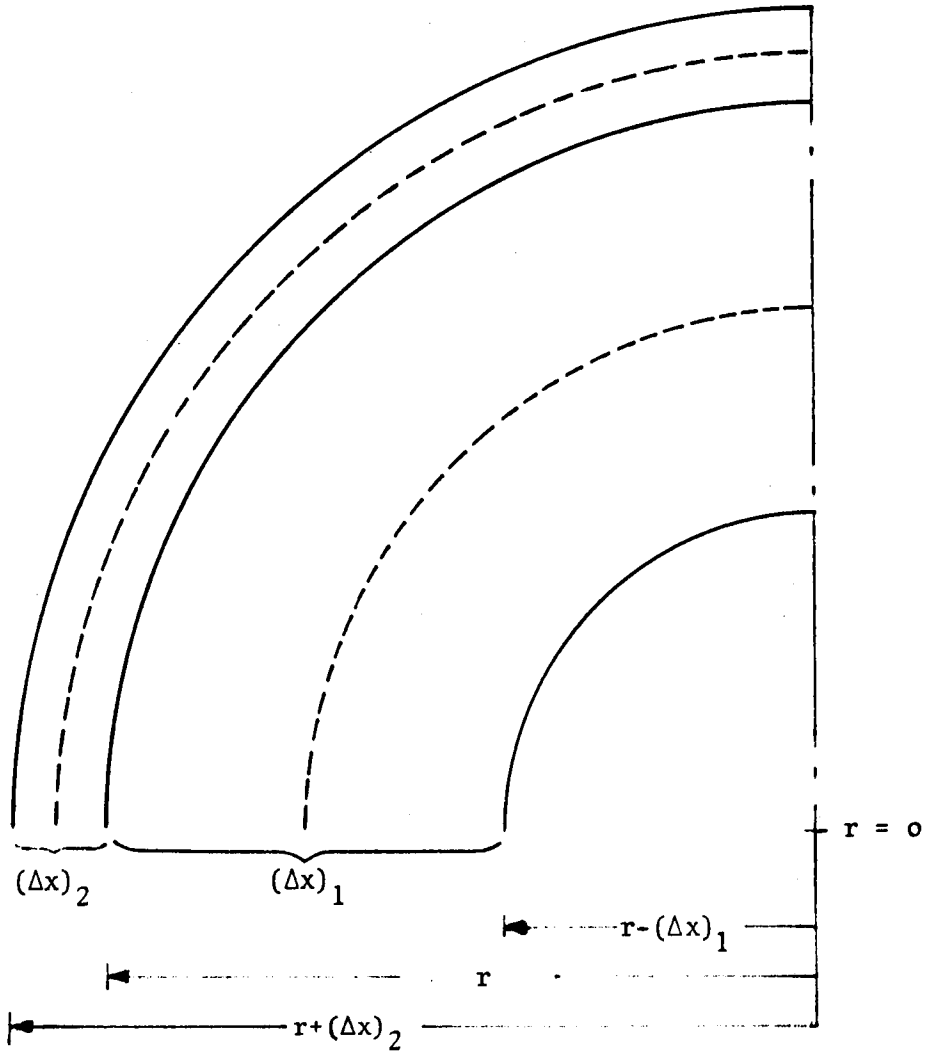


Figure 5. Interface between Δr and Δs inside the Granule.

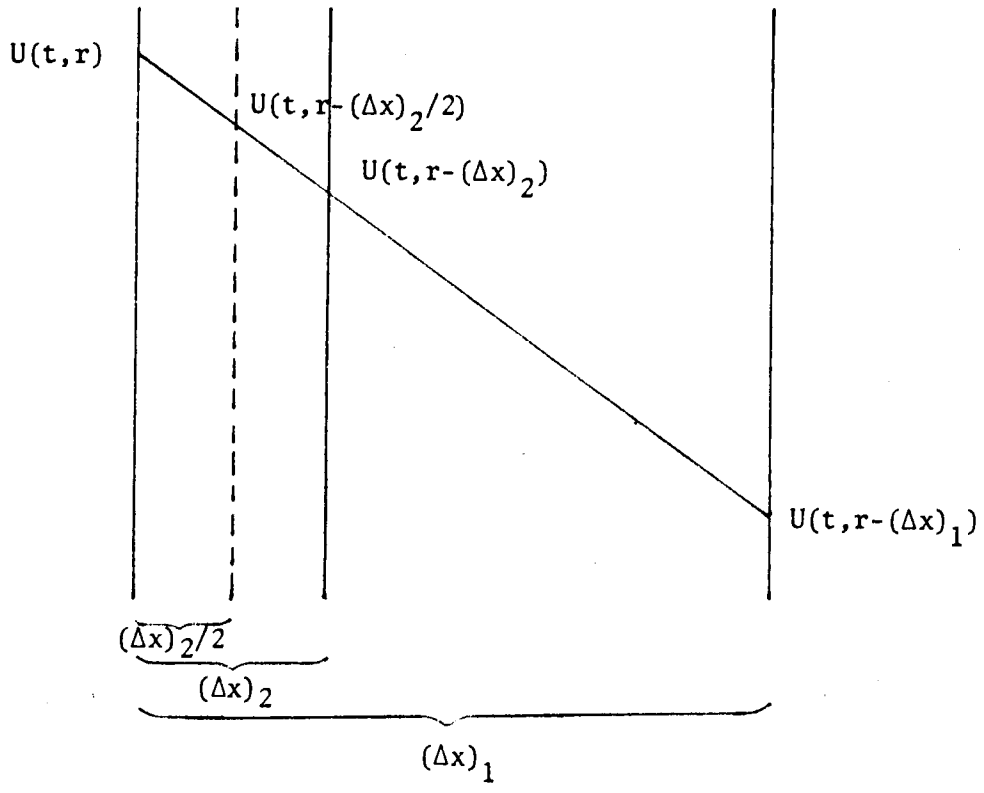


Figure 6. Linear Interpolation of $U(t,r-(\Delta x)_2)$ and $U(t,r-(\Delta x)_2/2)$.

$$= \{U(t,K-1)-(1+DX)\cdot U(t,K)+DX\cdot U(t,K+1)\}/(DELX2)^2 \quad (89)$$

where

$$DX = (\Delta x)_2/(\Delta x)_1 \quad (90)$$

$$DELX2 = (\Delta x)_2 \quad (91)$$

The equation in the form

$$\partial U(t_2,K)/\partial t = K\{\partial^2 U(t_2,K)/\partial r^2\} \quad (92)$$

where K is a constant, can be written into a general finite difference form for the diffusion equation. Thus

$$\begin{aligned} U(t_2,K)-U(t_1,K) = {} & \theta\{K\cdot\Delta t/(\Delta x)_2^2\}\{DX\cdot U(t_2,K+1)-(1+DX)\cdot U(t_2,K) \\ & +U(t_2,K-1)\}+(1-\theta)\{K\cdot\Delta t/(\Delta x)_2^2\}\{DX\cdot U(t_1,K+1) \\ & -(1+DX)\cdot U(t_1,K)+U(t_1,K-1)\} \end{aligned} \quad (93)$$

where

$\theta = 0$; Schmidt method; stable if $K\cdot\Delta t/(\Delta x)_2^2 \leq 1/2$

$\theta = 1$; Von Newmann method; stable for all $K\cdot\Delta t/(\Delta x)_2^2$

$\theta = 1/2$; Crank Nicolson method; stable for all $K\cdot\Delta t/(\Delta x)_2^2$

$\theta = 1/2-1/\{12\cdot(K\cdot\Delta t/(\Delta x)_2^2)\}$; Douglas method; stable for all $K\cdot\Delta t/(\Delta x)_2^2$

Eq. (52) may be written

$$\begin{aligned} \partial\tau_c/\partial t = {} & \alpha\{\partial^2\tau_c/\partial r^2+(2/r)(\partial\tau_c/\partial r)\}+\{\lambda\cdot EF/(\rho\cdot C_p)\} \\ & [\sigma\{(\partial C/\partial P)_\tau(\partial P_c/\partial t)+(\partial C/\partial\tau)_p(\partial\tau_c/\partial t)\} \\ & +(1-\sigma)(15\cdot EF1/R^2)PE(t_2,K)(P_c-P_d)] \end{aligned} \quad (94)$$

or

$$\{1-\lambda\cdot EF\cdot\sigma\cdot TE(K)/k\}(\partial UT/\partial t)$$

$$= \alpha(\partial^2 UT/\partial r^2)+\{\sigma\cdot\lambda\cdot EF\cdot DP/(\rho\cdot C_p\cdot\tau_I)\}\{PE(t_2,K)/D(K)\}$$

$$[\partial UP/\partial t+D(K)(15\cdot EF1/R^2)\{(1-\sigma)/\sigma\}\{UP(t_2,K)-UPD(t_2,K)\}] \quad (95)$$

If we define

$$B1 = 1-\lambda\cdot EF\cdot\sigma\cdot TE(K)/k \quad (96)$$

$$B2 = \{\sigma\cdot\lambda\cdot EF\cdot DP/(\rho\cdot C_p\cdot\tau_I)\}\{PE(t_2,K)/D(K)\} \quad (97)$$

The finite difference form of Eq. (95) becomes

$$B1\cdot\{UT(t_2,K)-UT(t_1,K)\}$$

$$= \theta\{\alpha\cdot\Delta t/(DELX2)^2\}\{DX\cdot UT(t_2,K+1)-(1+DX)\cdot UT(t_2,K)+U(t_2,K-1)\}$$

$$+(1-\theta)\{\alpha\cdot\Delta t/(DELX2)^2\}\{DX\cdot UT(t_1,K+1)-(1+DX)\cdot UT(t_1,K)+U(t_1,K-1)\}$$

$$+B2[UP(t_2,K)-UP(t_1,K)+PHID\{(1-\sigma)/\sigma\}\{UP(t_2,K)-UPD(t_2,K)\}] \quad (98)$$

If we define

$$BETA = 2\cdot(DELX2)^2/(\alpha\cdot\Delta t) \quad (99)$$

Eq. (98) can be rearranged to read

$$-(2\cdot\theta\cdot DX/BETA)\cdot UT(t_2,K+1)+\{B1+2\cdot\theta\cdot(1+DX)/BETA\}\cdot UT(t_2,K)$$

$$-(2\cdot\theta/BETA)\cdot UT(t_2,K-1) = DE \quad (100)$$

where

$$DE = \{2\cdot(1-\theta)\cdot DX/BETA\}\cdot UT(t_1,K+1)-\{2\cdot(1-\theta)\cdot(1+DX)/BETA-B1\}$$
$$\cdot UT(t_1,K)+\{2\cdot(1-\theta)/BETA\}\cdot UT(t_1,K-1)+B2\cdot[UP(t_2,K)-UP(t_1,K)$$
$$+PHID\cdot\{(1-\sigma)/\sigma\}\{UP(t_2,K)-UPD(t_2,K)\}] \tag{101}$$

The Thomas algorithm may be developed from Eq. (100) by first defining

$$UT(t_2,K-1) = BE(K-1)\cdot UT(t_2,K)+GE(K-1) \tag{102}$$

thus

$$-(2\cdot\theta\cdot DX/BETA)\cdot UT(t_2,K+1)+\{B1+2\cdot\theta\cdot(1+DX)/BETA-2\cdot\theta\cdot BE(K-1)/$$
$$BETA\}\cdot UT(t_2,K) = DE+2\cdot\theta\cdot GE(K-1)/BETA \tag{103}$$

Then

$$BE(K) = 2\cdot\theta\cdot DX/\{B1\cdot BETA+2\cdot\theta\cdot(1+DX)-2\cdot\theta\cdot BE(K-1)\} \tag{104}$$

$$GE(K) = \{DE\cdot BETA+2\cdot\theta\cdot GE(K-1)\}/\{B1\cdot BETA+2\cdot\theta\cdot(1+DX)$$
$$-2\cdot\theta\cdot BE(K-1)\} \tag{105}$$

These formulas can be applied anywhere in the granule by setting $(\Delta x)_2$ and $(\Delta x)_1$. If

$$\{K-(NA\cdot NR+1)\} < 0;\ (\Delta x)_2 = (\Delta x)_1 = \Delta r$$
$$= 0;\ (\Delta x)_2 = \Delta r \text{ and } (\Delta x)_1 = \Delta s$$
$$> 0;\ (\Delta x)_2 = (\Delta x)_1 = \Delta s$$

The granule-gas interface thermal balance, Eq. (48), is

$$(k/h\cdot\Delta r)\{UT(t_2,1)-(YT/RN)\cdot UT(t_2,2)\}$$

$$= TG(I+1,t_2)-UT(t_2,1)+\{(1-EF)\cdot\lambda\cdot\sigma/(h\cdot\tau_I)\}J^*(I+1,t_2) \quad (106)$$

If we define

$$YY = (YT-1)/YT = RN/YT \quad (107)$$

$$A2 = k/h \quad (108)$$

then

$$TG(I+1,t_2) = \{(A2/\Delta r)+1\}\cdot UT(t_2,1)-\{A2/(\Delta r\cdot YY)\}\cdot UT(t_2,2)$$

$$-\{(1-EF)\cdot\lambda\cdot\sigma/(h\cdot\tau_I)\}J^*(I+1,t_2) \quad (109)$$

By using Eq. (37), $TG(I+1,t_2)$ can be eliminated thus

$$UT(t_2,1) = [\{A2/(YY\cdot\Delta r)\}\cdot UT(t_2,2)+QB+\{(1-EF)\cdot\lambda\cdot\sigma/(h\cdot\tau_I)\}$$

$$J^*(I+1,t_2)]/(1+A2/\Delta r-QA) \quad (110)$$

By comparing this with Eq. (102), we see that

$$BE(1) = \{A2/(YY\cdot\Delta r)\}/(1+A2/\Delta r-QA) \quad (111)$$

$$GE(1) = [QB+\{(1-EF)\cdot\lambda\cdot\sigma/(h\cdot\tau_I)\}J^*(I+1,t_2)]/(1+A2/\Delta r-QA) \quad (112)$$

or

$$BE(1) = 1/\{(RN/YT)(DB1\cdot P8+1+DB2)\} \quad (113)$$

$$GE(1) = [DB1\cdot(AP+BB6)+DB3\cdot TW(I+1,t_1)\cdot h_w/h+\{\Delta r\cdot(1-EF)\cdot\lambda\cdot\sigma/$$

$$(k\cdot\tau_I)\}\cdot J^*(I+1,t_2)]/(DB1\cdot P8+1+DB2) \quad (114)$$

where

$$DB1 = P7 \cdot \Delta r / (A2 \cdot P9) \tag{115}$$

$$DB2 = (\gamma+1) \cdot h_W \cdot P10 \cdot \Delta r / (A2 \cdot P9 \cdot h) \tag{116}$$

$$DB3 = P10 \cdot \Delta r / (A2 \cdot P9) \tag{117}$$

$$P7 = \epsilon \cdot C_{PG} / (h \cdot a_v \cdot \Delta t) \tag{118}$$

$$P8 = \rho_G(I+1,t_1) + G(I,t_2)/(\Delta z/\Delta t) \tag{119}$$

$$P10 = 4/\{a_v \cdot d_I \cdot (1+\gamma+\gamma_R)\} \tag{120}$$

$$P9 = P7 \cdot P8 + 1 + P10 \cdot (\gamma+1) \cdot h_W/h \tag{121}$$

$$AP = P/(\bar{R} \cdot \tau_I) - \rho_G(I+1,t_1) \tag{122}$$

$$BB6 = G(I,t_2) \cdot TG(I,t_2)/(\Delta z/\Delta t) \tag{123}$$

also

$$QA = 1/P9 \tag{124}$$

$$QB = (P7/P9)(AP+BB6) + (P10/P9) \cdot TW(I+1,t_1) \cdot h_W/h \tag{125}$$

The continuous phase equation for continuity of mass, Eq. (53), is

$$\partial C_c/\partial t = \partial D(\partial C/\partial P)_\tau (\partial P_c/\partial r)/\partial r + (2/r) D(\partial C/\partial P)_\tau (\partial P_c/\partial r) - \{(1-\sigma)/\sigma\}(15 \cdot D_d/R_d^2)(\partial C/\partial P)_\tau (P-P_d) \tag{126}$$

If we define

$$\bar{P}_c = (P_c - P_I)/DP \tag{127}$$

$$\bar{P}_d = (P_d - P_I)/DP \tag{128}$$

$$\bar{\tau}_c = (\tau_c - \tau_I)/\tau_I \tag{129}$$

and use the Euler chain rule for the $\partial C_c/\partial t$, Eq. (126) becomes

$$(\partial C/\partial P)_\tau (\partial \bar{P}_c/\partial t) + (\partial C/\partial \tau)_p (\tau_I/DP)(\partial \bar{\tau}_c/\partial t)$$

$$= \{\partial D(\partial C/\partial P)_\tau (\partial \bar{P}_c/\partial r)/\partial r + (2/r)\cdot D\cdot(\partial C/\partial P)_\tau (\partial \bar{P}_c/\partial r)\}$$

$$-\{(1-\sigma)/\sigma\}(15\cdot D_d/R_d^2)(\partial C/\partial P)_\tau (\bar{P}_c - \bar{P}_d) \tag{130}$$

$$= (1/r^2)\{\partial D(\partial C/\partial P)_\tau r^2 (\partial \bar{P}_c/\partial r)/\partial r\}$$

$$-\{(1-\sigma)/\sigma\}(15\cdot D_d/R_d^2)(\partial C/\partial P)_\tau (\bar{P}_c - \bar{P}_d) \tag{131}$$

From the definition of UP, Eq. (76), we have

$$\bar{P}_c = (R/r)\cdot UP \tag{132}$$

Then

$$\partial \bar{P}_c/\partial r = R\{-(1/r^2)\cdot UP + (1/r)(\partial UP/\partial r)\} \tag{133}$$

$$(1/r^2)\{\partial D(\partial C/\partial P)_\tau r^2 (\partial \bar{P}_c/\partial r)/\partial r\}$$

$$= (1/r^2)\{\partial PE(t,r) r^2 (\partial \bar{P}_c/\partial r)/\partial r\} \tag{134}$$

$$= (R/r^2)[\partial PE(t,r)\{-UP(t,r) + r\partial UP(t,r)/\partial r\}/\partial r] \tag{135}$$

$$= (R/r)[(1/r)\{-\partial PE(t,r)UP(t,r)/\partial r + PE(t,r)\partial UP(t,r)/\partial r\}$$

$$+\partial PE(t,r)\{\partial UP(t,r)/\partial r\ /\partial r] \tag{136}$$

$$= (R/r)[\{-\Delta PE(t,r)UP(t,r) + PE(t,r)\Delta UP(t,r)\}/r\Delta r$$

$$+\Delta PE(t,r)\Delta UP(t,r)/(\Delta r)^2] \tag{137}$$

In implementing the central difference procedure we choose $r+(\Delta x)_2/2$ and $r-(\Delta x)_2/2$ because $(\Delta x)_2 \leq (\Delta x)_1$, and so the quantities $PE(t,r-(\Delta x)_2/2)$, $UP(t,r-(\Delta x)_2/2)$, $PE(t,r-(\Delta x)_2)$, and $UP(t,r-(\Delta x)_2)$ can be linearly interpolated in the $(\Delta x)_1$ interval, as shown in Figure 6, page 41.

$$\{UP(t,r)-UP(t,r-(\Delta x)_2/2)\}/\{(\Delta x)_2/2\} = \{UP(t,r) -UP(t,r-(\Delta x)_1)\}/(\Delta x)_1 \tag{138}$$

and

$$\{UP(t,r)-UP(t,r-(\Delta x)_2)\}/(\Delta x)_2 = \{UP(t,r)-UP(t,r-(\Delta x)_1)\}/(\Delta x)_1 \tag{139}$$

We can also linearly interpolate PE and write a similar pair of formulas. Thus

$$UP(t,r-(\Delta x)_2/2) = UP(t,r)-\{(\Delta x)_2/2(\Delta x)_1\}\{UP(t,r)- UP(t,r-(\Delta x)_1)\} \tag{140}$$

$$= [1-\{(\Delta x)_2/2(\Delta x)_1\}]\cdot UP(t,r)+\{(\Delta x)_2/2(\Delta x)_1\} \cdot UP(t,r-(\Delta x)_1) \tag{141}$$

$$UP(t,r-(\Delta x)_2) = [1-\{(\Delta x)_2/(\Delta x)_1\}]\cdot UP(t,r)+\{(\Delta x)_2/(\Delta x)_1\} \cdot UP(t,r-(\Delta x)_1) \tag{142}$$

$$PE(t,r-(\Delta x)_2/2) = [1-\{(\Delta x)_2/2(\Delta x)_1\}]\cdot PE(t,r)+\{(\Delta x)_2/2(\Delta x)_1\} \cdot PE(t,r-(\Delta x)_1) \tag{143}$$

$$PE(t,r-(\Delta x)_2) = [1-\{(\Delta x)_2/(\Delta x)_1\}]\cdot PE(t,r)+\{(\Delta x)_2/(\Delta x)_1\} \cdot PE(t,r-(\Delta x)_1) \tag{144}$$

Then Eq. (137) can be written

$$(1/r^2)\{\partial D(\partial C/\partial P)_\tau r^2(\partial \overline{P}_c/\partial r)/\partial r\}$$

$$= (R/r)\left[\left[-\{PE(t,r+(\Delta x)_2)+PE(t,r)\}\{UP(t,r+(\Delta x)_2)+UP(t,r)\}/\right.\right.$$

$$\{4r(\Delta x)_2\}+\left[\left[[1-\{(\Delta x)_2/2(\Delta x)_1\}]PE(t,r)+\{(\Delta x)_2/2(\Delta x)_1\}\right.\right.$$

$$PE(t,r-(\Delta x)_1)\left]\right] \left[\left[[1-\{(\Delta x)_2/2(\Delta x)_1\}]UP(t,r)+\{(\Delta x)_2/2(\Delta x)_1\}\right.\right.$$

$$UP(t,r-(\Delta x)_1)\left]\right] /\{r(\Delta x)_2\}+\{PE(t,r)/r(\Delta x)_2\}\left[\left[(1/2)\right.\right.$$

$$\{UP(t,r+(\Delta x)_2)+UP(t,r)\}-\left[[1-\{(\Delta x)_2/2(\Delta x)_1\}]UP(t,r)\right.$$

$$\left.+\{(\Delta x)_2/2\,(\Delta x)_1\}UP(t,r-(\Delta x)_1)\right]\left]\right] + \{PE(t,r+(\Delta x)_2)+PE(t,r)\}$$

$$\{UP(t,r+(\Delta x)_2)-UP(t,r)\}/\{2(\Delta x)_2{}^2\}-\left[\left[1-\{(\Delta x)_2/2(\Delta x)_1\}\right]\right.$$

$$PE(t,r)+\{(\Delta x)_2/2(\Delta x)_1\}\ PE(t,r-(\Delta x)_1)\left]\right]\left[\left[UP(t,r)-\left[[1-\right.\right.\right.$$

$$\left.\left.\{(\Delta x)_2/(\Delta x)_1\}]UP(t,r)-\{(\Delta x)_2/(\Delta x)_1\}UP(t,r-(\Delta x)_1)\right]\right]/(\Delta x)_2{}^2\left]\right] \tag{145}$$

If we define

$$SDX = 1-(\Delta x)_2/(\Delta x)_1 \tag{146}$$

$$SDX2 = 1-(\Delta x)_2/2(\Delta x)_1 \tag{147}$$

$$DELX1 = (\Delta x)_1 \tag{148}$$

$$DX2 = (\Delta x)_2/2(\Delta x)_1 \tag{149}$$

Eq. (145) can be written

$$(1/r^2)\{\partial D(\partial C/\partial P)_\tau r^2(\partial \bar{P}_c/\partial r)/\partial r\}$$

$$= (R/r)\Big[-\{PE(t,K-1)+PE(t,K)\}\{UP(t,K-1)+UP(t,K)\}/\{4r(\Delta x)_2\}$$

$$+\{SDX2\cdot PE(t,K)+DX2\cdot PE(t,K+1)\}\{SDX2\cdot UP(t,K)+DX2\cdot UP(t,K+1)\}/$$

$$\{r(\Delta x)_2\}+\{PE(t,K)/2r(\Delta x)_2\}\{UP(t,K-1)-SDX\cdot UP(t,K)-DX\cdot$$

$$UP(t,K+1)\}+\{PE(t,K-1)+PE(t,K)\}\{UP(t,K-1)-UP(t,K)\}/\{2(\Delta x)_2{}^2\}$$

$$-\{SDX2\cdot PE(t,K)+DX2\cdot PE(t,K+1)\}\cdot DX\cdot\{UP(t,K)-UP(t,K+1)\}/(\Delta x)_2{}^2\Big] \tag{150}$$

or

$$= \{R/r(\Delta x)_2{}^2\}\{AAP(t)\cdot UP(t,K+1)-BBP(t)\cdot UP(t,K)+CCP(t)\cdot UP(t,K-1)\} \tag{151}$$

where

$$AAP(t) = (DX2\cdot DELX2/r+DX)\{SDX2\cdot PE(t,K)+DX2\cdot PE(t,K+1)\}$$
$$-PE(t,K)\cdot DX\cdot DELX2/2r \tag{152}$$

$$BBP(t) = (DELX2/4r+1/2)\{PE(t,K-1)+PE(t,K)\}+(DX-DELX2\cdot SDX2/r)$$
$$\{SDX2\cdot PE(t,K)+DX2\cdot PE(t,K+1)\}+(SDX\cdot DELX2/2r)PE(t,K) \tag{153}$$

$$CCP(t) = (1/2-DELX2/4r)\{PE(t,K-1)+PE(t,K)\}+(DELX2/2r)PE(t,K) \tag{154}$$

If we assume

$$PE(t,K+1) = PE(t,K) = PE(t,K-1) \tag{155}$$

the coefficients reduce to

$$AAP(t) = DX\cdot PE(t,K) \tag{156}$$

$$BBP(t) = (1+DX)\cdot PE(t,K) \tag{157}$$

$$CCP(t) = PE(t,K) \tag{158}$$

and if we replace PE with α this is applicable to Eq. (95) as well.

The finite difference equivalent of Eq. (131) is

$$(\partial C/\partial P)_\tau\{UP(t_2,K)-UP(t_1,K)\}+(\partial C/\partial\tau)_p(\tau_I/DP)\{UT(t_2,K)-UT(t_1,K)\}$$

$$= \{\theta\cdot\Delta t/(\Delta x)_2^2\}\{AAP(t_2)\cdot UP(t_2,K+1)-BBP(t_2)\cdot UP(t_2,K)$$

$$+CCP(t_2)\cdot UP(t_2,K-1)\}+\{(1-\theta)\Delta t/(\Delta x)_2^2\}\{AAP(t_1)\cdot$$

$$UP(t_1,K+1)-BBP(t_1)\cdot UP(t_1,K)+CCP(t_1)\cdot UP(t_1,K-1)\}-\{(1-\sigma)/\sigma\}$$

$$(15\cdot EF1\cdot D(K)\cdot\Delta t/R^2)(\partial C/\partial P)_\tau\{UP(t_2,K)-UPD(t_2,K)\} \tag{159}$$

If we define

$$DEN = (\Delta x)_2^2\cdot PE(t_2,K)/\{\theta\cdot D(K)\cdot\Delta t\} \tag{160}$$

$$DIN = (\Delta x)_2^2\cdot PE(t_1,K)/\{(1-\theta)\cdot D(K)\cdot\Delta t\} \tag{161}$$

$$PHID1 = PHID/(1+PHID) \tag{162}$$

$$WO2 = (1-\sigma)/\sigma \tag{163}$$

Then Eq. (159) may be written as

$$\{UP(t_2,K)-UP(t_1,K)\}+WO6\cdot\tau_I\cdot DELUT(K)/DP$$

$$= (1/DEN)\{AAP(t_2)\cdot UP(t_2,K+1)-BBP(t_2)\cdot UP(t_2,K)+CCP(t_2)\cdot$$

$$UP(t_2,K-1)\}+(1/DIN)\{AAP(t_1)\cdot UP(t_1,K+1)-BBP(t_1)\cdot UP(t_1,K)$$

$$+CCP(t_1)\cdot UP(t_1,K-1)\}-WO2\cdot PHID1\{UP(t_2,K)-UPD(t_1K)$$

$$+WO6\cdot\tau_I\cdot DELUT(K)/DP\} \tag{164}$$

or

$$-AAP(t_2)\cdot UP(t_2,K+1)/DEN+\{1+BBP(t_2)/DEN+WO2\cdot PHID1\}\cdot UP(t_2,K)$$

$$-CCP(t_2)\cdot UP(t_2,K-1)/DEN = DE \tag{165}$$

where

$$DE = AAP(t_1)\cdot UP(t_1,K+1)-\{BBP(t_1)-DIN\}\cdot UP(t_1,K)+CCP(t_1)\cdot UP(t_1,K-1)$$

$$-\{WO6\cdot\tau_I\cdot DELUT(K)/DP\}(1+WO2\cdot PHID1)+WO2\cdot PHID1\cdot UPD(t_1,K) \tag{166}$$

Using the Thomas equation

$$UP(t_2,K-1) = BE(K-1)\cdot UP(t_2,K)+GE(K-1) \tag{167}$$

We can eliminate $UP(t_2,K-1)$ from Eq. (165), thus

$$DIVP\cdot UP(t_2,K) = AAP(t_2)\cdot UP(t_2,K+1)+DE\cdot DEN+CCP(t_2)\cdot GE(K-1) \tag{168}$$

where

$$DIVP = DEN+BBP(t_2)+DEN\cdot WO2\cdot PHID1 \tag{169}$$

and then by comparison with Eq. (102), we see that

$$BE(K) = AAP(t_2)/DIVP \tag{170}$$

$$GE(K) = \{DE\cdot DEN+CCP(t_2)\cdot GE(K-1)\}/DIVP \tag{171}$$

For Crank-Nicolson's method $\theta = 1/2$. The above equations can be used anywhere inside the granule by setting $(\Delta x)_2$ and $(\Delta x)_1$.

If

$$\{K-(NA\cdot NR+1)\} < 0;\ (\Delta x)_2 = (\Delta x)_1 = \Delta r$$

$$= 0;\ (\Delta x)_2 = \Delta r \text{ and } (\Delta x)_1 = \Delta s$$

$$> 0;\ (\Delta x)_2 = (\Delta x)_1 = \Delta s$$

Eq. (24) can be written ($\beta = 0$, as described by Eq. (31)).

$$(\Delta z/\Delta t)\rho_G(I+1,t_2)+G(I+1,t_2) = (\Delta z/\Delta t)\rho_G(I+1,t_1)+G(I,t_2) - (\sigma a_v \Delta z/\varepsilon)J^*(I+1,t_2) \quad (172)$$

and Eq. (45) can be written

$$Y(I+1,t_2)\{(\Delta z/\Delta t)\rho_G(I+1,t_2)+G(I+1,t_2)\} = (\Delta z/\Delta t)\rho_G(I+1,t_1)Y(I+1,t_1)+G(I,t_2)Y(I,t_2) - (\sigma a_v \Delta z/\varepsilon)J^*(I+1,t_2) \quad (173)$$

Eq. (173) can be replaced by Eq. (172), thus

$$Y(I+1,t_2)\{(\Delta z/\Delta t)\rho_G(I+1,t_1)+G(I,t_2)-(\sigma a_v \Delta z/\varepsilon)J^*(I+1,t_2)\} = (\Delta z/\Delta t)\rho_G(I+1,t_1)Y(I+1,t_1)+G(I,t_2)Y(I,t_2) - (\sigma a_v \Delta z/\varepsilon)J^*(I+1,t_2) \quad (174)$$

If we define

$$Q3 = (\Delta z/\Delta t)\rho_G(I+1,t_1)+G(I,t_2) \quad (175)$$

$$Q4 = (\Delta z/\Delta t)\rho_G(I+1,t_1)Y(I+1,t_1)+G(I,t_2)Y(I,t_2) \quad (176)$$

and $$A3 = \sigma a_v \Delta z/\varepsilon \quad (177)$$

Then

$$Y(I+1,t_2) = \{Q4-A3\cdot J^*(I+1,t_2)\}/\{Q3-A3\cdot J^*(I+1,t_2)\} \tag{178}$$

and

$$1-Y(I+1,t_2)=(Q3-Q4)/\{Q3-A3\cdot J^*(I+1,t_2)\} \tag{179}$$

Eq. (43) can be written

$$C_G^*(I+1,t_2) = \rho_G(I+1,t_2)\{DP\cdot UP(t_2,1)+P_I\}/P_T \tag{180}$$

If we replace Eq. (46) by Eq. (180), we have

$$J^*(I+1,t_2)\{1-Y(I+1,t_2)\}/\{k_G\rho_G(I+1,t_2)\}-Y(I+1,t_2)$$
$$= -(DP/P_T)\cdot UP(t_2,1)-P_I/P_T \tag{181}$$

or

$$\{Q5\cdot J^*(I+1,t_2)-Q4\}/\{A3\cdot J^*(I+1,t_2)-Q3\}$$
$$= (DP/P_T)\cdot UP(t_2,1)+P_I/P_T \tag{182}$$

where

$$Q5 = (Q3-Q4)/\{k_G\rho_G(I+1,t_2)\}+A3 \tag{183}$$

If we divide the left-hand side term of Eq. (182) mathematically, we will have

$$\{Q5\cdot J^*(I+1,t_2)-Q4\}/\{A3\cdot J^*(I+1,t_2)-Q3\}$$
$$= Q5/A3+\{(Q5\cdot Q3/A3-Q4)/A3\}/\{J^*(I+1,t_2)-Q3/A3\} \tag{184}$$

and we can approximate $1/\{J^*(I+1,t_2)-Q3/A3\}$ by

$$1/\{J^*(I+1,t_2)-Q3/A3\} = -A3/Q3-(A3/Q3)^2 J^*(I+1,t_2)$$

$$-(A3/Q3)^3\{J^*(I+1,t_2)\}^2- \ldots \ldots \quad (185)$$

$$= -A3/Q3\{1+CF(A3/Q3)J^*(I+1,t_2)\} \quad (186)$$

where

$$CF = [-1+1/\{1-(A3/Q3)J^*(I+1,t_2)\}]/\{(A3/Q3)J^*(I+1,t_2)\}$$

$$= 1/\{1-(A3/Q3)J^*(I+1,t_2)\} \quad (187)$$

Then Eq. (182) becomes

$$Q4/Q3-(CF/Q3)(Q5-Q4\cdot A3/Q3)J^*(I+1,t_2)$$

$$= (DP/P_T)\cdot UP(t_2,1)+P_I/P_T \quad (188)$$

or

$$J^*(I+1,t_2) = \{Q4-(Q3/P_T)(DP\cdot UP(t_2,1)+P_I)\}/\{CF(Q5-Q4\cdot A3/Q3)\} \quad (189)$$

Also, Eq. (60) can be written

$$J^*(I+1,t_2) = PE(t_2,1)(DP/\Delta r)\{UP(t_2,1)-YT\cdot UP(t_2,2)/RN\} \quad (190)$$

If we replace Eq. (188) by Eq. (190), we will have

$$Q6\{UP(t_2,1)-(YT/RN)UP(t_2,2)\}+(DP/P_T)UP(t_2,1) = Q4/Q3-P_I/P_T \quad (191)$$

where

$$Q6 = (CF/Q3)(Q5-Q4\cdot A3/Q3)(DP/\Delta r)PE(t_2,1) \quad (192)$$

or

$$UP(t_2,1) = \{Q6/(Q6+DP/P_T)\}(YN/RN)UP(t_2,2)$$

$$+\{(Q4/Q3)-(P_I/P_T)\}/\{Q6+DP/P_T\} \quad (193)$$

So that

$$BE(1) = (Q6 \cdot YT)/\{RN(Q6+DP/P_T)\} \tag{194}$$

$$GE(1) = (Q4/Q3-P_I/P_T)/(Q6+DP/P_T) \tag{195}$$

In the program $J^*(I+1,t_2)$ in Eq. (189) is called CQ and in Eq. (190) is called YJST.

Dr. Jury developed the following long-time calculation equations in order to speed the program up for large values of time. He defined the larger value of time limitation by the dimensionless relation

$$D \cdot t/R^2 \geq 0.101 \tag{196}$$

The details of this relation can be read from literature (70).

The continuous phase thermal accumulation rate is

$$\partial\tau_c/\partial t = (15 \cdot \alpha/R^2)(\tau^*-\tau_c)+\{3 \cdot \sigma \cdot EF \cdot \lambda/(\rho \cdot C_p \cdot R)\}J^* \tag{197}$$

which can be finite differenced to

$$\tau_c(I+1,t_2) = [\tau_c(I+1,t_1)+15 \cdot \alpha \cdot \Delta t \cdot \tau^*(I+1,t_2)/R^2+\{3 \cdot \sigma \cdot EF \cdot \lambda \cdot \Delta t/(\rho \cdot C_p \cdot R)\}J^*(I+1,t_2)]/(1+15 \cdot \alpha \cdot \Delta t/R^2) \tag{198}$$

The gas film heat transfer equation is

$$\sigma(1-EF)\lambda J^* = h(\tau^*-\tau_G)+(5 \cdot \alpha \cdot \rho \cdot C_p/R)(\tau^*-\tau_c) \tag{199}$$

We can eliminate τ_c of Eq. (199) by using Eq. (198) thus

$$\sigma(1-EF)\lambda J^*(I+1,t_2) = -h\cdot\tau_G(I+1,t_2)+\{h+(5\cdot\alpha\cdot\rho\cdot C_p/R)/(1+15\cdot\alpha\cdot\Delta t/R^2)\}\tau^*(I+1,t_2)-\{(5\cdot\alpha\cdot\rho\cdot C_p/R)/(1+15\cdot\alpha\cdot\Delta t/R^2)\}\tau_c(I+1,t_1)-\{(15\cdot\alpha\cdot\Delta t/R^2)/(1+15\cdot\alpha\cdot\Delta t/R^2)\}\cdot\sigma\cdot EF\cdot\lambda\cdot J^*(I+1,t_2) \quad (200)$$

If we define

$$A4 = 15\cdot\Delta t/R^2 \quad (201)$$

$$A7 = 5\cdot\alpha\cdot\rho\cdot C_p/R \quad (202)$$

$$A8 = (1-EF)\lambda \quad (203)$$

$$A9 = A4\cdot\alpha \quad (204)$$

$$WO2 = (1-\sigma)/\sigma \quad (205)$$

$$WO3 = 3\cdot\Delta t/R \quad (206)$$

$$WO4 = 1+A9 \quad (207)$$

$$WO7 = \sigma(A8+A9\cdot\lambda\cdot EF/WO4) \quad (208)$$

$$WO = h/WO7 \quad (209)$$

$$W1 = (h+A7/WO4)/WO7 \quad (210)$$

$$W2 = \{A7\cdot\tau_c(I+1,t_1)/WO4\}/WO7 \quad (211)$$

Eq. (200) can be written

$$J^*(I+1,t_2) = W1\cdot\tau^*(I+1,t_2)-WO\cdot\tau_G(I+1,t_2)-W2 \quad (212)$$

The granule continuous phase mass balance is

$$\partial C_c/\partial t = (15\cdot D/R^2)(\partial C/\partial P)_\tau(P_c^*-P_c)-\{(1-\sigma)/\sigma\}(\partial C_d/\partial t) \quad (213)$$

The dispersed phase material balance Eq. (71) can be used to eliminate $\partial C_d/\partial t$ from Eq. (213) and the result can be written in pressure/temperature form thus

$$(\partial C/\partial P)_\tau(\partial P_c/\partial t)+(\partial C/\partial \tau)_p(\partial \tau_c/\partial t) = (15\cdot D/R^2)(\partial C/\partial P)_\tau(P^*-P_c)-\{(1-\sigma)/\sigma\}(15\cdot D_d/R_d^2)(\partial C/\partial P)_\tau(P_c-P_d) \quad (214)$$

Eq. (197) can be used to eliminate $\partial \tau_c/\partial t$ thus

$$\partial P_c/\partial t = -(\partial C/\partial \tau)_p/(\partial C/\partial P)_\tau[(15\cdot\alpha/R^2)(\tau^*-\tau_c)+\{3\cdot\sigma\cdot EF\cdot\lambda/(\rho\cdot C_p\cdot R)\}J^*]+(15\cdot D/R^2)(P^*-P_c)-\{(1-\sigma)/\sigma\}(15\cdot D_d/R_d^2)(P_c-P_d) \quad (215)$$

The finite difference form of this equation is

$$P_c(I+1,t_2) = P_c(I+1,t_1)-WO6[A9\{\tau^*(I+1,t_2)-\tau_c(I+1,t_2)\}-\{\sigma\cdot EF\cdot\lambda\cdot WO3/(\rho\cdot C_p)\}J^*(I+1,t_2)]+A4\cdot D(1)\{P^*(I+1,t_2)-P_c(I+1,t_2)\}-WO2\cdot WO1\{P_c(I+1,t_2)-P_d(I+1,t_2)\} \quad (216)$$

where

$$WO1 = 15\cdot D_d\cdot\Delta t/R_d^2 \quad (217)$$

$$WO6 = (\partial C/\partial \tau)_p/(\partial C/\partial P)_\tau = TE\cdot D/(PE\cdot\alpha) \quad (218)$$

Eq. (71) may be written

$$(\partial C/\partial P)_\tau(\partial P_d/\partial t)+(\partial C/\partial \tau)_p(\partial \tau_d/\partial t) = (15\cdot D_d/R_d^2)(\partial C/\partial P)_\tau(P_c-P_d) \quad (219)$$

and we can use Eq. (197) to eliminate $\partial\tau_d/\partial t$ which is equal to $\partial\tau_c/\partial t$ thus

$$\partial P_d/\partial t = -(\partial C/\partial\tau)_P/(\partial C/\partial P)_\tau[(15\cdot\alpha/R^2)(\tau^*-\tau_c)+\{3\cdot\sigma\cdot EF\cdot\lambda/(\rho\cdot C_p\cdot R)\}J^*]+(15\cdot D_d/R_d^2)(P_c-P_d) \tag{220}$$

The finite difference equivalent of this is

$$P_d(I+1,t_2) = \Big[\Big[P_d(I+1,t_1)+WO1\cdot P_c(I+1,t_2)-WO6[A9\{\tau^*(I+1,t_2)-\tau_c(I+1,t_2)\}+\{\sigma\cdot EF\cdot\lambda\cdot WO3/(\rho\cdot C_p)\}J^*(I+1,t_2)]\Big]\Big]/(1+WO1) \tag{221}$$

This can be used to eliminate $P_d(I+1,t_2)$ in Eq. (216) thus

$$\{1+A4\cdot D(1)\cdot WWO\}P_c(I+1,t_2) = P_c(I+1,t_1)+WWO\cdot P_d(I+1,t_1)+A4\cdot D(1)\cdot P^*(I+1,t_2) -\{\sigma\cdot EF\cdot\lambda\cdot WO3\cdot WO6\cdot(1+WWO)/(\rho\cdot C_p)\}J^*(I+1,t_2) -WO6\cdot A9(1+WWO)\{\tau^*(I+1,t_2)-\tau_c(I+1,t_2)\} \tag{222}$$

where

$$WWO = WO2\cdot WO1/(1+WO1) \tag{223}$$

Eq. (198) can be used to eliminate $\tau_c(I+1,t_2)$ from Eq. (222) thus

$$\{1+A4\cdot D(1)+WWO\}P_c(I+1,t_2) = P_c(I+1,t_1)+WWO\cdot P_d(I+1,t_1)+A4\cdot D(1)\cdot P^*(I+1,t_2)-\{\sigma\cdot EF\cdot\lambda\cdot WO3\cdot WO6\cdot(1+WWO)/(\rho\cdot C_p\cdot WO4)\}J^*(I+1,t_2)-\{WO6\cdot A9\cdot(1+WWO)/WO4\}\tau^*(I+1,t_2)+\{WO6\cdot A9\cdot(1+WWO)/WO4\}\tau_c(I+1,t_1) \tag{224}$$

If we define

$$WO5 = 1+A4 \cdot D(1)+WWO \tag{225}$$

$$WW1 = WO6 \cdot A9 \cdot (1+WWO)/(WO4 \cdot WO5) \tag{226}$$

$$WW2 = [P_c(I+1,t_1)+WWO \cdot P_d(I+1,t_1)+\{WO6 \cdot A9 \cdot (1+WWO)/WO4\}$$

$$\tau_c(I+1,t_1)]/WO5 \tag{227}$$

$$WW3 = \sigma \cdot EF \cdot \lambda \cdot WO3 \cdot WO6 \cdot (1+WWO)/(\rho \cdot C_p \cdot WO4 \cdot WO5) \tag{228}$$

$$WW4 = A4 \cdot D(1)/WO5 \tag{229}$$

then

$$P_c(I+1,t_2) = WW4 \cdot P^*(I+1,t_2)-WW1 \cdot \tau^*(I+1,t_2)+WW2-WW3 \cdot J^*(I+1,t_2) \tag{230}$$

The granule continuous phase mass balance may be written

$$\partial C_c/\partial t = (3/R)J^*-\{(1-\sigma)/\sigma\}(\partial C_d/\partial t) \tag{231}$$

When compared with Eq. (213), we have

$$J^*(I+1,t_2) = (5 \cdot D/R)(\partial C/\partial P)_\tau \{P^*(I+1,t_2)-P_c(I+1,t_2)\} \tag{232}$$

We can eliminate $P_c(I+1,t_2)$ by using Eq. (230) thus

$$[R/\{5 \cdot D(1)\}-(\partial C/\partial P)_\tau WW3]J^*(I+1,t_2)$$

$$= (\partial C/\partial P)_\tau (1-WW4)P^*(I+1,t_2)+(\partial C/\partial P)_\tau \cdot WW1 \cdot \tau^*(I+1,t_2)$$

$$-(\partial C/\partial P)_\tau WW2 \tag{233}$$

If we define

$$W5 = R/\{5 \cdot D(1)\} - (\partial C/\partial P)_{\tau} WW3 \tag{234}$$

$$W3 = (\partial C/\partial P)_{\tau}(1-WW4)/W5 \tag{235}$$

$$W4 = (\partial C/\partial P)_{\tau} WW1/W5 \tag{236}$$

$$W6 = (\partial C/\partial P)_{\tau} WW2/W5 \tag{237}$$

Then

$$J^*(I+1,t_2) = W3 \cdot P^*(I+1,t_2) + W4 \cdot \tau^*(I+1,t_2) - W6 \tag{238}$$

Eq. (37) can be written

$$\tau^*(I+1,t_2) = \{\tau_G(I+1,t_2) - \tau_I(1+QB-QA)\}/QA \tag{239}$$

which can be used to eliminate $\tau^*(I+1,t_2)$ from Eq. (238) thus

$$J^*(I+1,t_2) = W3 \cdot P^*(I+1,t_2) + W4\{\tau_G(I+1,t_2) - \tau_I(1+QB-QA)\}/QA - W6 \tag{240}$$

Also, $\tau^*(I+1,t_2)$ in Eq. (151) can be eliminated by Eq. (239) thus

$$J^*(I+1,t_2) = (W1/QA-WO)\tau_G(I+1,t_2) - W9 \tag{241}$$

where

$$W9 = W2 + W1 \cdot \tau_I \cdot (1+QB-QA)/QA \tag{242}$$

If we set

$$W7 = Q3 = (\Delta z/\Delta t)\rho_G(I+1,t_1) + G(I,t_2) \tag{243}$$

$$W8 = Q4 = (\Delta z/\Delta t)\rho_G(I+1,t_1)Y(I+1,t_1)+G(I,t_2)Y(I,t_2) \quad (244)$$

Then Eq. (178) can be written

$$Y(I+1,t_2) = \{W8-A3\cdot J^*(I+1,t_2)\}/\{W7-A3\cdot J^*(I+1,t_2)\} \quad (245)$$

We can use ideal gas law, $P_T = \rho_G \bar{R}\tau_G$, to eliminate $\rho_G(I+1,t_2)$ from Eq. (46) thus

$$P^*(I+1,t_2) = P_T[Y(I+1,t_2)-\{\bar{R}/(k_G P_T)\}\tau_G(I+1,t_2)\{1-Y(I+1,t_2)\}$$
$$J^*(I+1,t_2)] \quad (246)$$

which can be used to eliminate $P^*(I+1,t_2)$ from Eq. (240) thus

$$J^*(I+1,t_2) = W3\cdot P_T[Y(I+1,t_2)-\{\bar{R}/(k_G P_T)\}\tau_G(I+1,t_2)\{1-Y(I+1,t_2)\}$$
$$J^*(I+1,t_2)]+(W4/QA)\cdot\tau_G(I+1,t_2)-W6-W4\cdot\tau_I\cdot$$
$$(1+QB-QA)/QA \quad (247)$$

From this we can eliminate $\tau_G(I+1,t_2)$ by using Eq. (241) thus

$$J^*(I+1,t_2) = W3\cdot P_T\cdot Y(I+1,t_2)-W6-W4\cdot\tau_I\cdot(1+QB-QA)/QA+[W4/QA$$
$$-(\bar{R}\cdot W3/k_G)\{1-Y(I+1,t_2)\}J^*(I+1,t_2)][\{J^*(I+1,t_2)$$
$$+W9\}/(W1/QA-WO)] \quad (248)$$

Also we can eliminate $Y(I+1,t_2)$ by using Eq. (245), thus

$$J^*(I+1,t_2) = W3\cdot P_T\cdot[\{W8-A3\cdot J^*(I+1,t_2)\}/\{W7-A3\cdot J^*(I+1,t_2)\}]$$
$$-W6-W4\cdot\tau_I\cdot(1+QB-QA)/QA+(W4/QA)[\{J^*(I+1,t_2)$$

$$+W9\}/(W1/QA-WO)] + (\bar{R}\cdot W3/k_G)J^*(I+1,t_2)$$

$$[\{J^*(I+1,t_2)+W9\}/(W1/QA-WO)][(-W7+W8)/$$

$$\{W7-A3\cdot J^*(I+1,t_2)\}] \tag{249}$$

If we define

$$W10 = W4\cdot W9/\{(W1/QA-WO)QA\}-W6-W4\cdot\tau_I\cdot(1+QB-QA)/QA \tag{250}$$

$$W11 = (\bar{R}\cdot W3/k_G)(W8-W7)/(W1/QA-WO) \tag{251}$$

$$W12 = W14/(W1-QA\cdot WO) \tag{252}$$

$$W13 = \{W7+(P_T\cdot W3+W10)\cdot A3-W9\cdot W11-W7\cdot W12\}/[2\cdot\{W11 + (1-W12)\cdot A3\}] \tag{253}$$

$$W14 = (W3\cdot P_T\cdot W8+W10\cdot W7)/[\{W11+(1-W12)\cdot A3\}(W13)^2] \tag{254}$$

Then

$$J^*(I+1,t_2) = W13\{1-(1-W14)^{1/2}\} \tag{255}$$

This completes the theory and its extensions along with the pertinent finite differencing operations leading to the writing of a Fortran algorithm for the simultaneous solution of the equations involved.

The additional limiting conditions not already discussed are rather obvious. It is necessary for example to describe the initial state of the bed and gas contained therein, i.e., the initial concentrations and temperatures must be specified. The concentration, temperature, and

flow rate of the inlet gas must be specified. The UP and UT variables must be set equal to zero at the center of the granule. At the gas-granule interface the temperatures and partial pressures must be equal and the heat and mass flow rates in the two phases at the interface must match up.

The diffusion routines remain to be developed and this is done in the following chapter.

CHAPTER IV

DIFFUSION ROUTINES

From the theory presented in the previous chapter it should be obvious that D(K), PE(t_2,K), and TE(K) must be calculated and these in turn require the calculation of $(\partial C/\partial P)_\tau$ and $(\partial C/\partial \tau)_p$ from the sorption therm. For this purpose we have assembled in Tables II and III all the earlier pertinent research results obtained here at The University of Tennessee, Knoxville. These results are taken from various theses and other references (77,78,79,80,85,86,87,88). We will be concerned here only with the results for activated alumina and Linde molecular sieve-4A.

Activated Alumina Diffusion Parameters

In the case of activated alumina

$$X = (P/P_s)^{\tau/AE} \tag{256}$$

and it is necessary to have an analytical expression for P_s. The one given in the steam table (92) for 32°F and above is

$$P_s = \{220.88/(1.01325 \times 14.696 \times 144)\}\exp(EPA) \tag{257}$$

where

$$EPA = 10^{-2}(374.136-TC)SUM/(TC+273.15) \tag{258}$$

Table II. Summary of Sorption Therms for the Five Desiccants.

Desiccant (Model)	Sorption Therm Equations $W = W(X),\ X = X(P,\tau)$	Sorption Therm Constants
Activated Alumina	$W = \left(\frac{A \cdot B \cdot X}{1-X}\right)\left(\frac{1-(n+1)X^{n}+n \cdot X^{n+1}}{1+(B-1)X-B \cdot X^{n+1}}\right)$ $X = (P/P_s)^{\tau/AE}$	A = 0.0443 B = 4.3676 n = 11.0238 AE = 741.9829,°K
Florite	$W = \left(\frac{A \cdot B \cdot X}{1-X}\right)\left(\frac{1-(n+1)X^{n}+n \cdot X^{n+1}}{1+(B-1)X-B \cdot X^{n+1}}\right)$ $X = (P/P_s)^{\tau/AE}$	A·B = 0.03615 B = 2.777 n = 12.0 AE = (2000/1.8),°K
Silica Gel	$W = \frac{A \cdot B \cdot X}{1+B \cdot X} + \frac{C \cdot D \cdot X^{n}}{1+D \cdot X^{n}}$ $X = (P/P_s)^{\tau/AE}$	A·B = 2.0 C·D = 10.15 B = 13.33 D = 46.7 n = 3.3 AE = (500/1.8),°K
Drierite	$W \cdot 100 = \frac{A \cdot B \cdot X}{1+B \cdot X} + \frac{C \cdot V1 \cdot X}{1+V1 \cdot X} + \frac{E \cdot V2 \cdot X}{1+V2 \cdot X}$ $X = (P/\tau^{1/2})e^{AE/\tau}\{10^{-7}/25.4(1.8)^{1/2}\}$	V1 = 0.5D[1+ERF{G1(X-XR1)}] V2 = 0.5F[1+ERF{G2(X-XR2)}] A = 0.34 F = 0.0028 B = 15.0 G1 = 5.26 C = 4.80 G2 = 0.005 D = 3.90 XR1 = 1.70 E = 3.85 XR2 = 260.0 AE = (13720/1.8),°K

Table II (continued)

Desiccant (Model)	Sorption Therm Equations $W = W(X),\ X = X(P,\tau)$	Sorption Therm Constants	
LMS-4A	$W = \frac{A \cdot B \cdot X}{1+B \cdot X} + \frac{C \cdot D \cdot X}{1+D \cdot X}$	A = 0.1579	C = 0.0479
		B = 6.371D-9	D = 3.095D-11
	$X = (P/\tau^{1/2})e^{AE/\tau}$	AE = 7509,°K	

Table III. Permeabilities and Diffusivities.

Desiccant (Model)	Total Permeability PE, lbmoles-ft/lb-hr	Total Diffusivity D, ft^2/hr
Activated Alumina	$\frac{C(\tau)\bar{\beta}C^3}{P} + \frac{A(\tau)(1-\bar{\beta}C)}{B(\tau)-\alpha_{AB}P/P_T}$	$C(\tau)\bar{\beta}C^2 \frac{\partial \ln P}{\partial \ln C} + \frac{A(\tau)(1-\bar{\beta}C)}{B(\tau)-\alpha_{AB}P/P_T} \frac{\partial P}{\partial C}$
	$A(\tau) = AA \cdot (\tau)^{1/2}$ $B(\tau) = BB \cdot \tau + 1$ $C(\tau) = CC \cdot (\tau)^{1/2} \cdot e^{-EE/\tau}$	AA = 3.015D-11 BB = 3.918D-2 CC = 10582.0 EE = 5980.2 $\bar{\beta} = 42.3577$ $\alpha_{AB} = 0.2114$
Florite	$\frac{C(\tau)\bar{\beta}C^3}{P} + A(\tau)(1-\bar{\beta}C)$	$C(\tau)\bar{\beta}C^2 \frac{\partial \ln P}{\partial \ln C} + A(\tau)(1-\bar{\beta}C) \frac{\partial P}{\partial C}$
	$A(\tau) = AK/(\tau)^{1/2}$ $C(\tau) = CC \cdot (\tau)^{1/2} \cdot e^{-EE/\tau}$	AK = 2.4988D-9 CC = 4.3289D-5 EE = 6558.1 $\bar{\beta} = 144.85$
Silica Gel	$\frac{C(\tau)\bar{\beta}C^2}{P} + \frac{A(\tau)(1-\bar{\beta}C)}{B(\tau)-\alpha_{AB}P/P_T}$	$C(\tau)\bar{\beta}C \frac{\partial \ln P}{\partial \ln C} + \frac{A(\tau)(1-\bar{\beta}C)}{B(\tau)-\alpha_{AB}P/P_T} \frac{\partial P}{\partial C}$
	$A(\tau) = AA \cdot (\tau)^{1/2}$ $B(\tau) = BB \cdot \tau + 1$ $C(\tau) = CC \cdot (\tau)^{1/2} \cdot e^{-EE/\tau}$	AA = 2.0D-10 BB = 3.8D-10 CC = 676.45 EE = 6818.3 $\bar{\beta} = 41.96$ $\alpha_{AB} = 0.2114$

Table III (continued)

Desiccant (Model)	Total Permeability PE, lbmoles-ft/lb-hr	Total Diffusivity D, ft^2/hr
Drierite	$\frac{C(\tau)(1-\bar{\beta}C)C}{P} + A(\tau)$	$C(\tau)(1-\bar{\beta}C)\frac{\partial \ln P}{\partial \ln C} + A(\tau)\frac{\partial P}{\partial C}$
	$A(\tau) = AA/(\tau)^{1/2}$	AA = 1.1460D-8 $\quad \bar{\beta} = 112.0$
	$C(\tau) = CC \cdot e^{-EE/\tau}$	CC = 78.990 EE = 7203.0
LMS-4A	$\frac{C(\tau)(1-\bar{\beta}C)C}{P} + A(\tau)$	$C(\tau)(1-\bar{\beta}C)\frac{\partial \ln P}{\partial \ln C} + A(\tau)\frac{\partial P}{\partial C}$
	$A(\tau) = AA/(\tau)^{1/2}$	AA = 1.7062D-8 $\quad \bar{\beta} = 65.1$
	$C(\tau) = CC \cdot e^{-EE/\tau}$	CC = 9.5088 EE = 6994.0

$$SUM = -741.9242-29.721(TD)-11.55286(TD)^2-0.8685635(TD)^3 +0.1094098(TD)^4+0.439993(TD)^5+0.2520658(TD)^6 +0.05218684(TD)^7 \quad (259)$$

$$TD = 0.65-0.01(TC) \quad (260)$$

$$TC = \tau/1.8-273.161111111111 \quad (261)$$

If we define

$$ZA = 1-(n+1)X^n+nX^{n+1} \quad (262)$$

$$ZB = 1+(B-1)X-BX^{n+1} \quad (263)$$

Then

$$W = \{A\cdot B\cdot X/(1-X)\}(ZA/ZB) \quad (264)$$

and

$$\partial W/\partial X=[A\cdot B/\{(1-X)ZB\}][ZA/(1-X)+n(n+1)X^n(X-1) -\{X\cdot ZA(B-1-B(n+1)X^n)\}/ZB] \quad (265)$$

Let

$$DC1 = \partial C/\partial X = (\rho/18.01534)(\partial W/\partial X) \quad (266)$$

then

$$\partial P/\partial C = AE\cdot P/(DC1\cdot\tau\cdot X) \quad (267)$$

and

$$\partial \ln P/\partial \ln C = C\cdot AE\cdot P/(P\cdot DC1\cdot\tau\cdot X) \quad (268)$$

From Table III, we can write

$$PE = CC \cdot \tau^{1/2} \cdot e^{-EE/\tau} \cdot \bar{\beta} \cdot C^3 / P + \{AA \cdot \tau^{1/2} \cdot (1 - \bar{\beta} \cdot C)\} / (BB \cdot \tau + 1 - \alpha_{AB} \cdot P/P_T) \quad (269)$$

$$D = PE \cdot AE \cdot P / (DC1 \cdot \tau \cdot X) \quad (270)$$

All the parameters in Table III have to be changed from metric units to English units such as

AA = 1.952347015D-9	$lbmoles\text{-}ft/hr \cdot lb \cdot {}^\circ R^{1/2}$
BB = 2.176666667D-2	$1/{}^\circ R$
CC = 489.5788676	$(ft^3 adsorbent)^2/lbmole \cdot hr \cdot ft \cdot {}^\circ R^{1/2}$
EE = 10764.36	$^\circ R$
$\bar{\beta}$ = 0.6785017209	$ft^3 adsorbent/lbmole$
α = 0.2114	dimensionless
AE = 1335.56922	$^\circ R$

From the definition of TE, Eq. (73), we can write

$$TE = \alpha \cdot DC1 \cdot (\partial X/\partial \tau)_P \quad (271)$$

We can take logarithm of Eq. (256) thus

$$\ln X = (\tau/AE)(\ln P - \ln P_s) \quad (272)$$

and the derivative form of Eq. (272) is

$$(1/X)(\partial X/\partial \tau)_P = \{(\ln P/P_s)/AE\} - (\tau/AE)(d\ln P_s/d\tau) \quad (273)$$

We can take logarithm of Eq. (257), thus

$$\ln P_s = \ln\{220.88/(1.01325 \times 14.696 \times 144)\}+0.01(374.136 -TC)SUM/(TC+273.15) \quad (274)$$

and the derivative form of Eq. (274) is

$$d\ln P_s/d\tau = \{-0.01/(TC+273.15)^2 \times 1.8\}(374.136+273.15)SUM +\{0.01/(TC+273.15)\}(374.136-TC)(dSUM/dT) \quad (275)$$

Also

$$dSUM/d\tau = (-0.01/1.8)\{-29.721-2(11.55286)(TD)-3(0.8685635)(TD)^2+4(0.1094098\ (TD)^3+5(0.439993)(TD)^4+6(0.2520685)(TD)^5+7(0.05218684)(TD)^6\} \quad (276)$$

If we define

$$DLPSAT = -d\ln P_s/d\tau \quad (277)$$

and

$$DSUM = dSUM/d\tau \quad (278)$$

Then

$$TE = -\alpha \cdot DC1 \cdot X\{\ln(P_s/P)+\tau \cdot DLPSAT\}/AE \quad (279)$$

Linde Molecular Sieve-4A Diffusion Parameters

From Table II (page 66) we have

$$X = P \cdot e^{AE/\tau}/\tau^{1/2} \quad (280)$$

$$W = A \cdot B \cdot X/(1+B \cdot X)+C \cdot D \cdot X/(1+D \cdot X) \tag{281}$$

Then

$$\partial W/\partial X = A \cdot B/(1+B \cdot X)^2+C \cdot D/(1+D \cdot X)^2 \tag{282}$$

Let

$$DC1 = \partial C/\partial X = (\rho/18.01534)(\partial W/\partial X) \tag{283}$$

then

$$\partial P/\partial C = P/(DC1 \cdot X) \tag{284}$$

and

$$\partial \ln P/\partial \ln C = C/(DC1 \cdot X) \tag{285}$$

From Table III (page 67), we can write

$$PE = CC \cdot e^{-EE/\tau} \cdot (1-\overline{\beta} \cdot C)C/P+AA/\tau^{1/2} \tag{286}$$

and

$$D = PE \cdot P/(DC1 \cdot X) \tag{287}$$

All the parameters in Table III have to be changed from metric units to English units such as

B	= 3.069699154D-9	$ft^2 \cdot {}^\circ R^{1/2}/lb$
D	= 1.491244527D-11	$ft^2 \cdot {}^\circ R^{1/2}/lb$
AA	= 1.988713121D-6	$lbmoles \cdot ft \cdot {}^\circ R^{1/2}/lb \cdot hr$
CC	= 36.84667369	ft^3adsorbent/hr·ft
EE	= 12589.2	°R

$\overline{\beta}$ = 1.042796517 $ft^3/lbmole$

AE = 13516.2 °R

We can take logarithm of Eq. (280), thus

$$\ln X = \ln P + AE/\tau - (1/2)\ln\tau \tag{288}$$

and the derivative form of Eq. (288) is

$$(1/X)(\partial X/\partial\tau)_p = -AE/\tau^2 - 1/(2\cdot\tau) \tag{289}$$

Then, TE from Eq. (271) can be written

$$TE = -\alpha\cdot DC1\cdot X\cdot(0.5+AE/\tau)/\tau \tag{290}$$

In all of the previous calculations the temperature, τ, and the partial pressure, P, are calculated from the reduced temperature, UT, and the reduced partial pressure, UP, thus

$$\tau = \{DUM\cdot UT(t_1,K)+1\}\tau_I \tag{291}$$

and

$$P = DUM\cdot UP(t_1,K)\cdot DP+P_I \tag{292}$$

where

$$DUM = NS/(N-K+1) \quad \text{when } K \geq NR\cdot NA+1 \tag{293}$$

or

$$DUM = NS/\{NS-NA+(NR\cdot NA-K+1)/NR\} \quad \text{when } K < NR\cdot NA+1 \tag{294}$$

CHAPTER V

PROGRAM DEVELOPMENT

In any development, extending over a decade or more, the course of events tends to become blurred with time and notebooks become so voluminous that it is a major chore to retrace footsteps of these events. Thus it was felt that an account should be included in this thesis in such a way that it is concise and understandable. Another requirement of such an account is that it take on the form of charts and not require reading of a lot of textual material in order to comprehend the overall picture of the development.

It should also be pointed out here that numerous graduate students, laboratory assistants from both the electronics shop and the machine shop, and part-time or full-time employees were involved and most of them have their own records of account, usually in the form of notebooks, and this also contributes to the difficulty of retracing at some later date exactly the course of events that transpired at any particular time in the development.

The overall objectives in this development were to increase the computational speed to its maximum and to put into the program all the kinetic details envisioned to satisfy the requirement of satisfactory fit of the experimental data.

Dr. Jury started the program development on March 16, 1967. This and subsequent phases of this development are shown in the form of a flow chart in Figure 7.

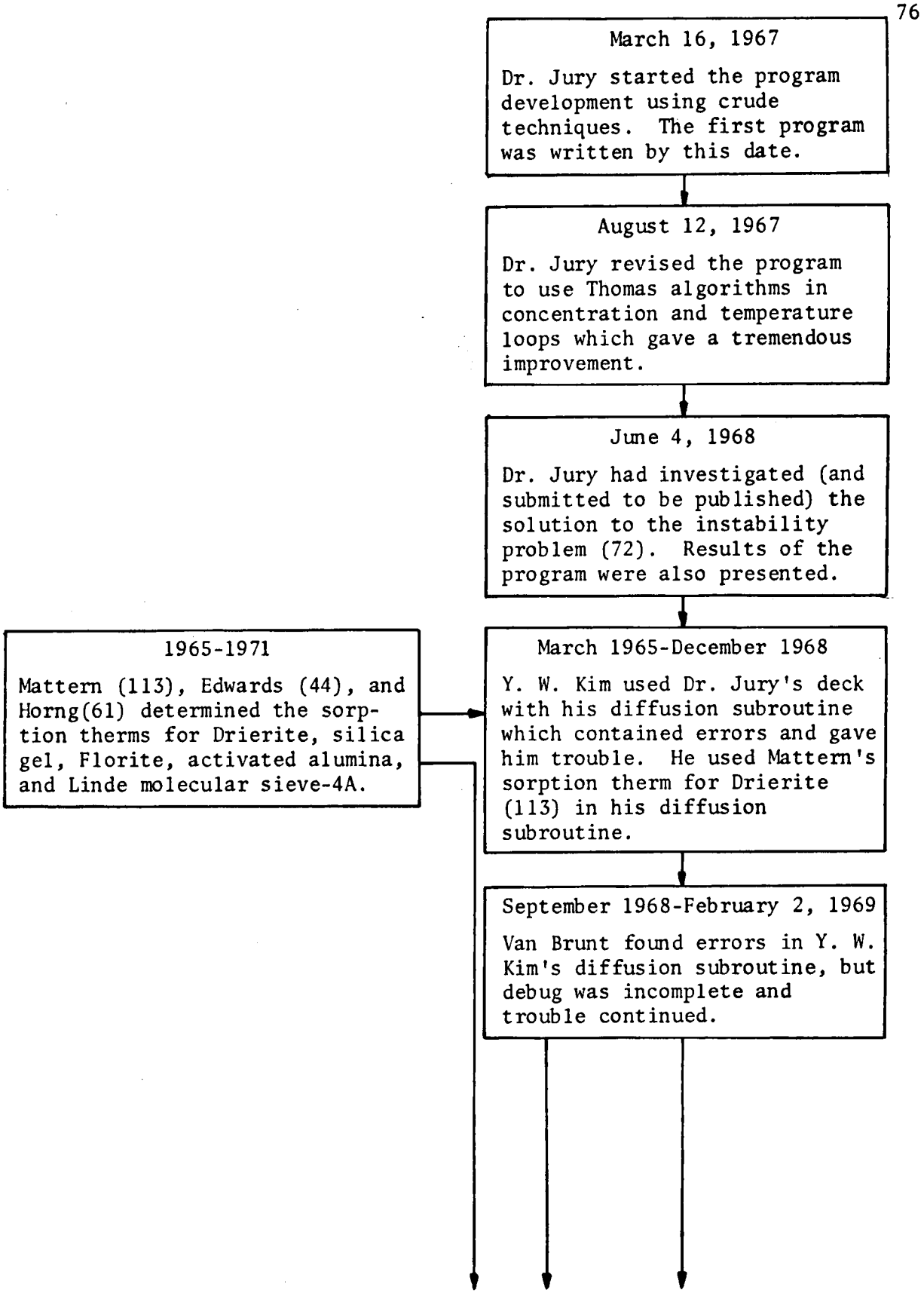


Figure 7. Flow Chart of Program Development.

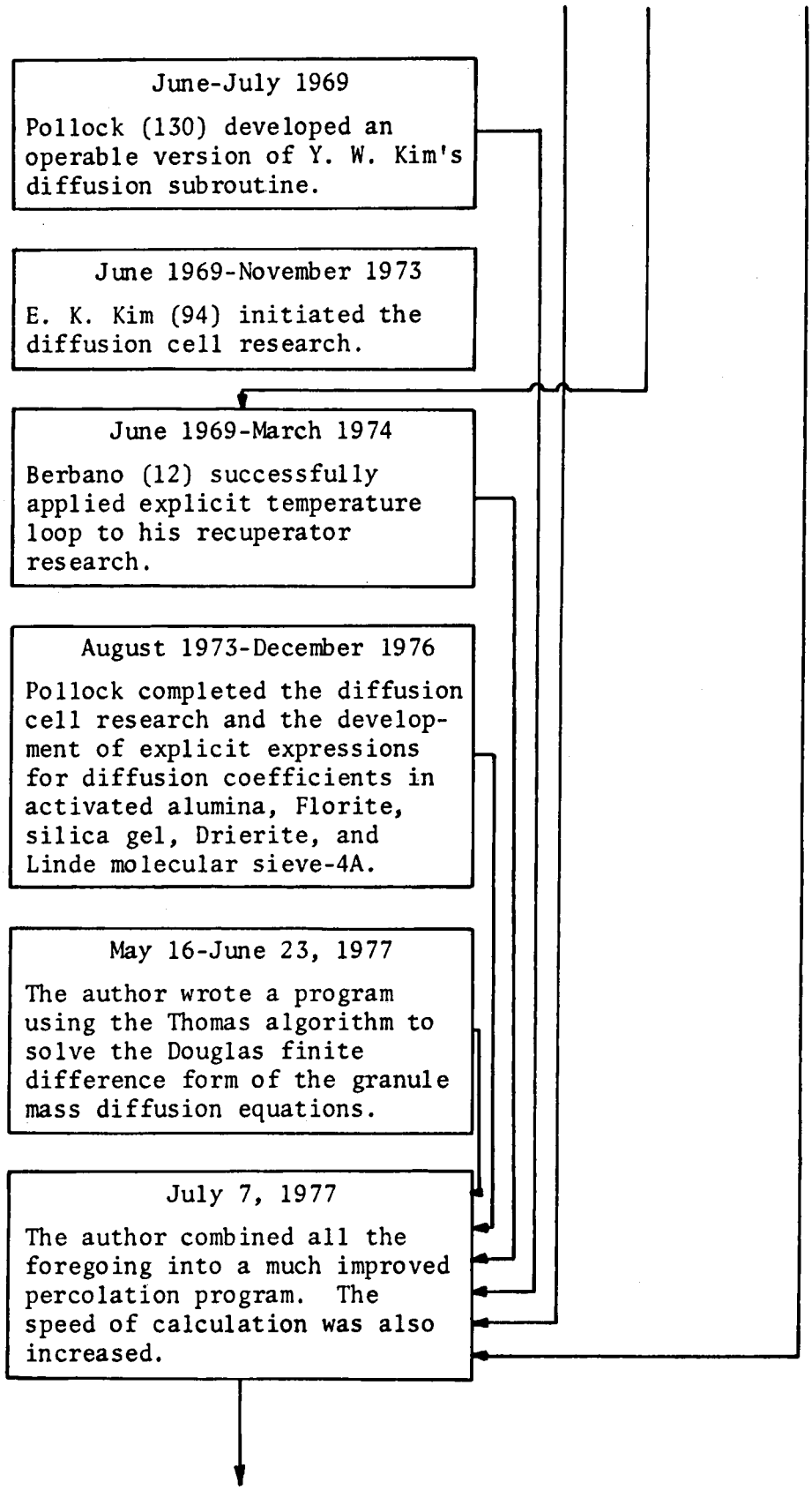


Figure 7 (continued)

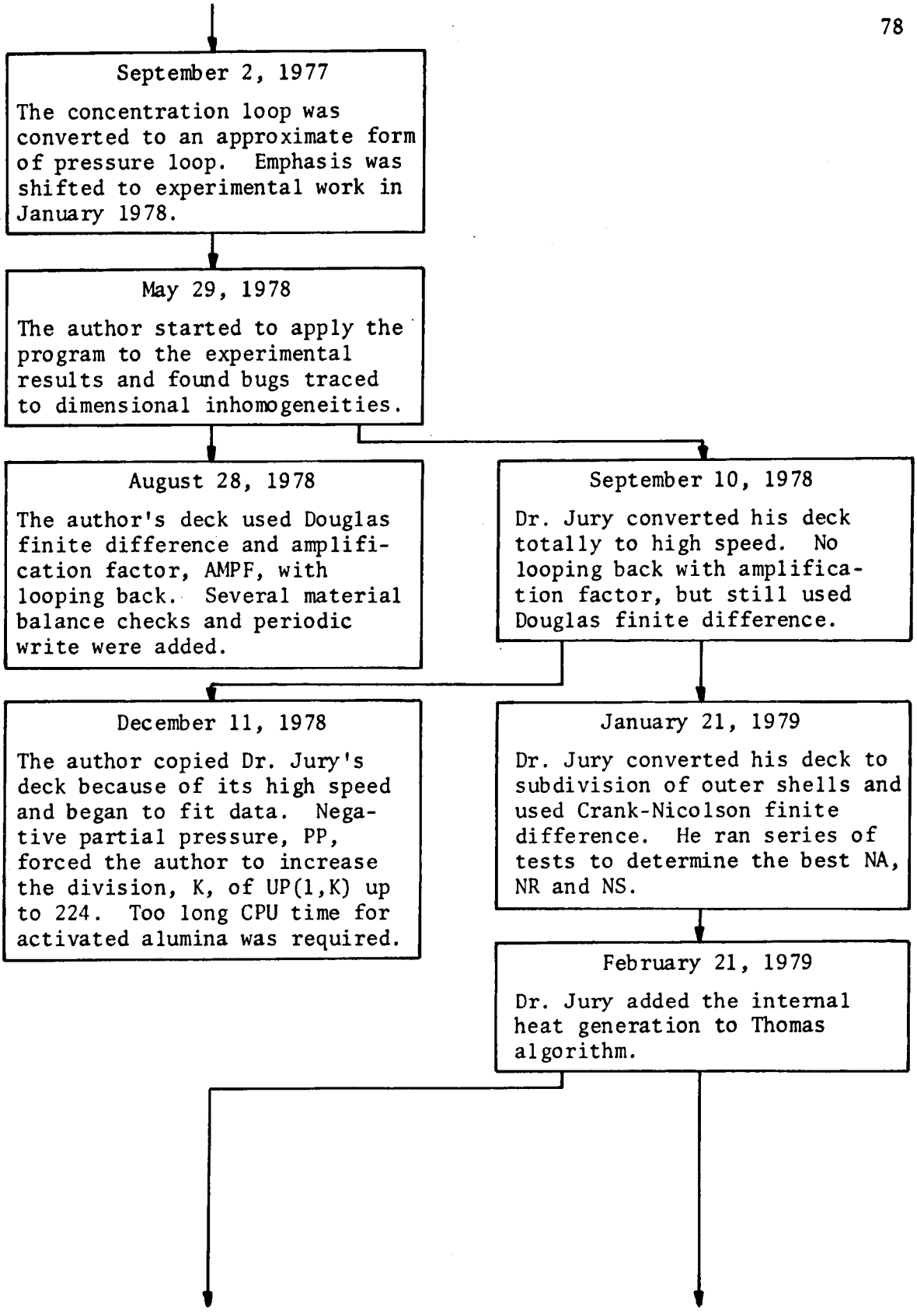


Figure 7 (continued)

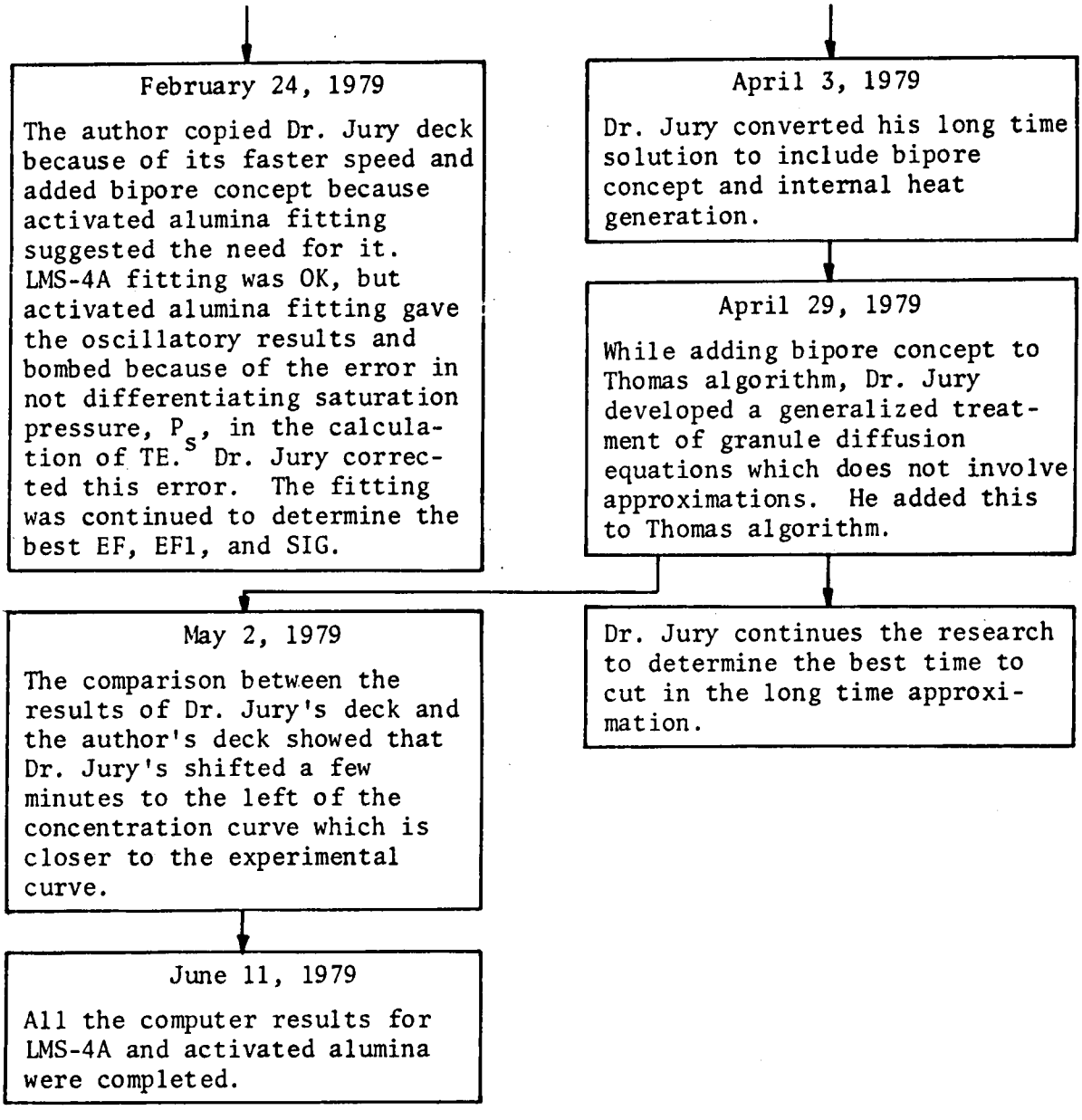


Figure 7 (continued)

In that which follows we will present a series of flow charts to illustrate the advances made during the course of program development in this present work. The starting program is shown in Figure 8. This was the end product of the original work by Jury, addition of the Drierite diffusion routine by Y. W. Kim, debug of Kim's routine by Van Brunt and the XFUN refinement of SUBROUTINE DOG by Pollock. Although the subroutines and DTSTDR and YJST estimating routines served a useful purpose in past development work they tended to decrease computational speed. Thus the objectives of the present work were to eliminate the temperature loop (T loop), the concentration loop (C loop), and subroutines if at all possible. By so doing the computational speed should be substantially increased.

Jury and Berbano (74) had already shown how to eliminate the T loop in the case of heat recuperation where YJST was absent and so we carried this the step further to include YJST and thereby eliminated the T loop.

From prior work and the concurrent work of Pollock it gradually became obvious that the subroutines and XFUN could be condensed into a routine which we added directly to the MAIN program. It remained now to do something about the elimination of the C loop.

A major step in the development was made on September 2, 1977, when we learned how to replace the concentration, C1, with the partial pressure, P, and temperature, τ. The remarkable advantage of the diffusion equation expressed in terms of partial pressure is that at the interface the chemical potentials, μ, of the two phases are equal and if

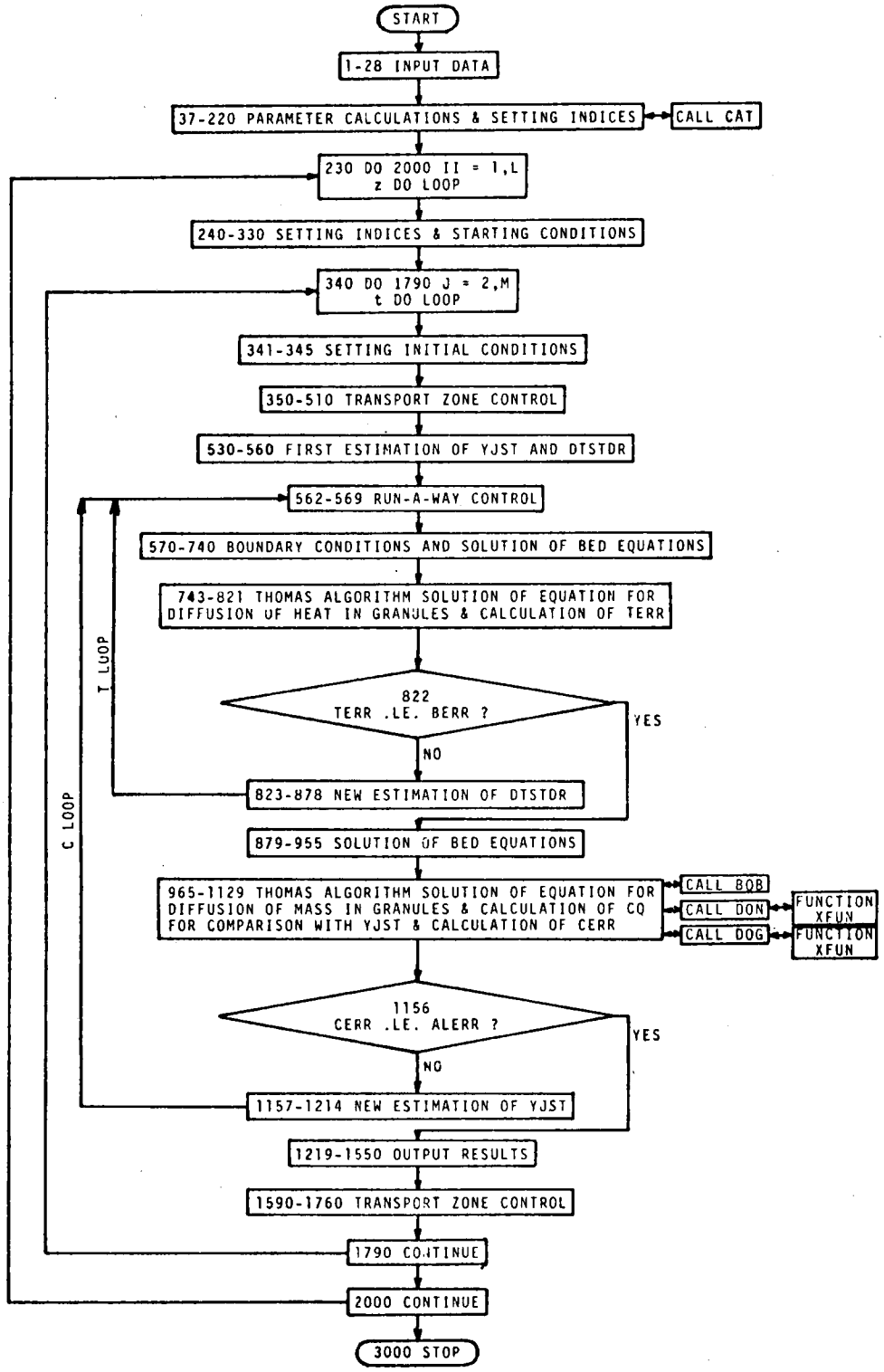


Figure 8. Flow Chart of the Earlier Computer Program.

the gas is ideal then

$$\mu = \mu^{\circ}+RT \ln P/P_o$$

and for the same temperature the vapor pressure and partial pressure are equal. This permits getting from the gas phase into the solid phase calculation to compute BE(1) and GE(1) in the Thomas relation

$$UP(t_2,1) = BE(1)*UP(t_2,2)+GE(1)$$

and then to start the Thomas algorithm for the UP solution. Because we know $UP(t_2,K)$ we can calculate P and then X directly without going through a function, XFUN. The concentration, C1, and $\partial C1/\partial X$ can also be calculated directly without using a subroutine BOBCAT (BOB + CAT). A new diffusion routine was designed in terms of diffusivity, D(K), and permeability, PE, and was inserted directly in the MAIN program as statements 1160 and 1200. Constant D(K) and PE which were varied between 1.D-7 to 1.D-2 were used sometimes to bypass this diffusion routine during testing of the program.

Emphasis was shifted to experimental work on January 11, 1978. On May 29, the program was applied to fit Dr. Jury's experimental results on Drierite (83) and the computer curve was too far left of the experimental curve. A lot of changes were made until the errors were found in August 8. Two types of errors were causing the trouble. The definition of UP that was used to derive the diffusion equations was wrong, and there were several dimensional inhomogeneities.

On August 15, the diffusion parameter calculations were moved to between the time incrementing DO loop and the run-a-way control. This

also speeded the program up because the size of inner DO loop was reduced. On August 24, the SUMJST, SUMCQ, and SUMGAS statements were added in order to check the material balance. On August 27, the run-a-way control was moved down to after bed parameter calculations. This also speeded the program up. The amplification factor, AMPF, was added on August 28 to reduce the number of iteration at the start for each ΔZ. The flow diagram is shown in Figure 9. Further minor adjustment had been made until September 12 when the experiment was run.

Between November 20 to December 12, new diffusion routines were written for Drierite, activated alumina, and Linde molecular sieve-4A based on Pollock's diffusivities and permeabilities expressions. Test runs had been made to compare with the experimental results and the computer results were found to be on the right side of experimental results.

On December 11, 1978, Dr. Jury's high speed deck with long time calculation was duplicated and the new diffusion parameter solutions were put in for each granule. The flow chart of this program is shown in Figure 10. It resembles the previous one except that the most inner loop is now eliminated. A new technique was used deriving the BE(1) and GE(1) as shown in Chapter III for the solution of granule mass transfer equations. The latter solution operation was then moved to precede the solution of granule heat transfer equation, thus eliminating the inner loop. The CPU time was reduced by a factor of 3 to 4 times when compared with the one with the inner loop.

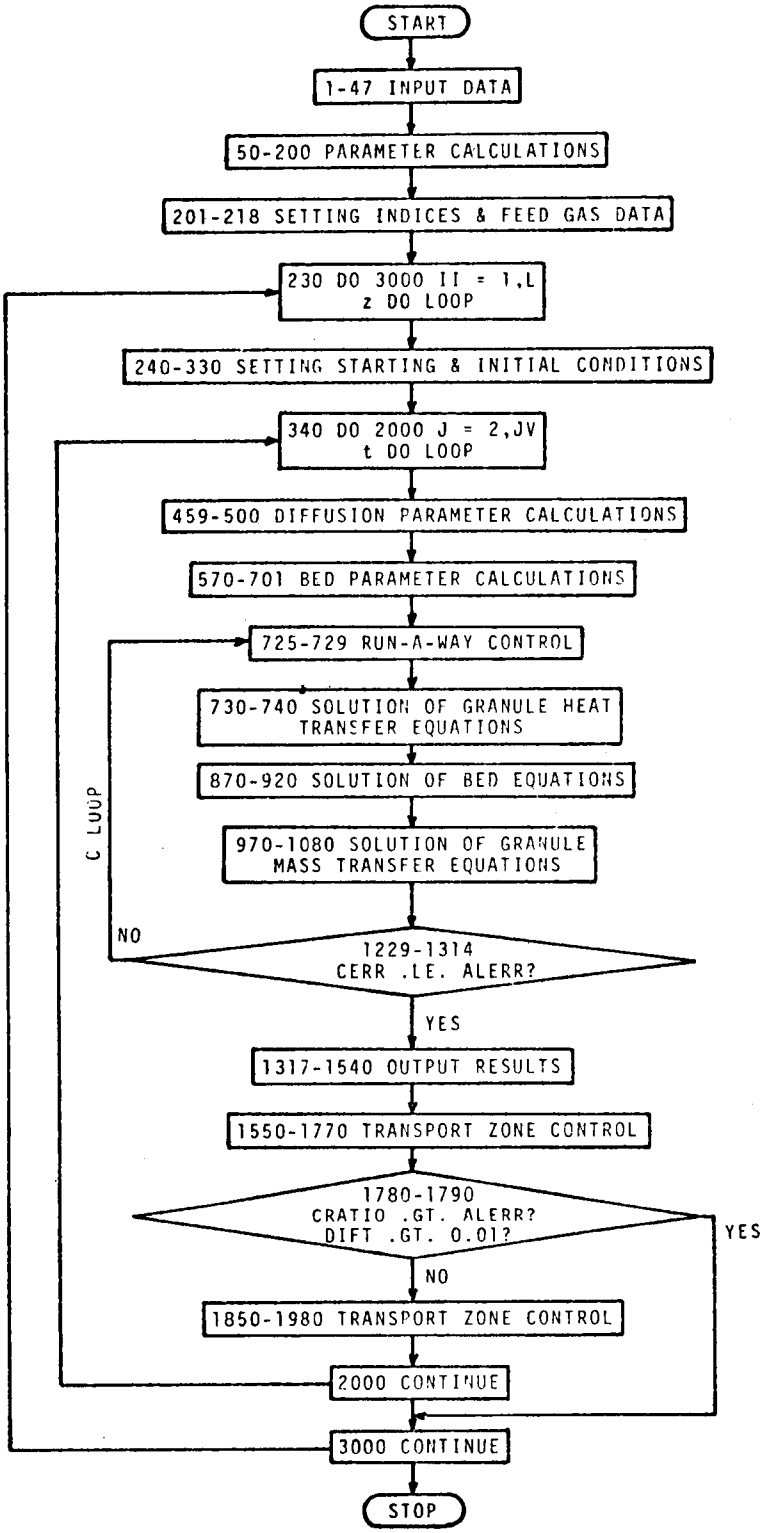


Figure 9. Flow Chart of the Intermediate Computer Program.

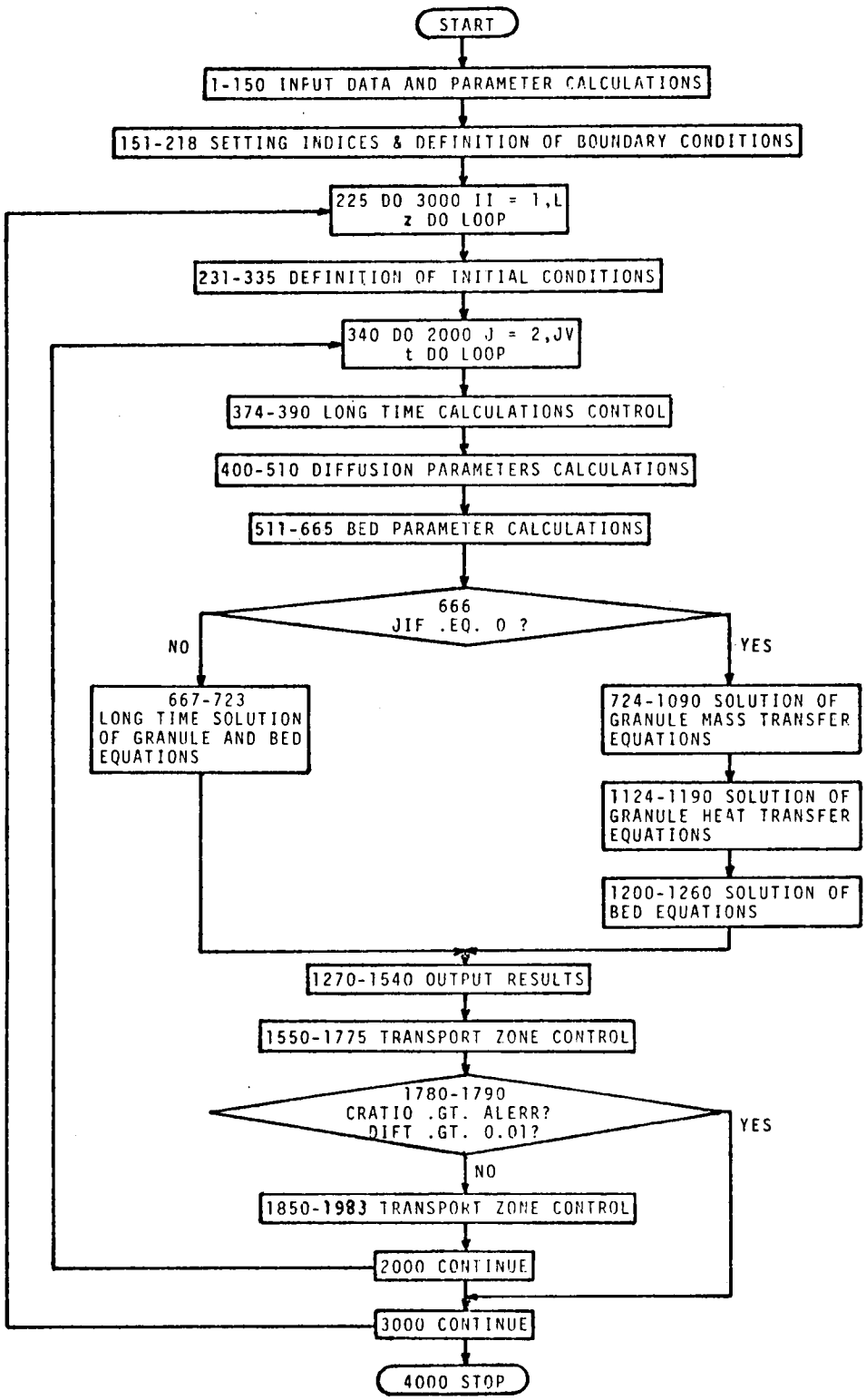


Figure 10. Flow Chart of the Present Computer Program.

To get rid of a negative partial pressure problem, the granule had to be divided into 224 divisions for LMS-4A and 448 for activated alumina which increased the CPU time. This problem was solved on January 19, 1979, by varying the granule division with the occurrence of negative partial pressure. This was satisfactory for LMS-4A but still gave too long a CPU time for activated alumina.

A new high speed deck by Dr. Jury was duplicated on February 2. The advantages of this new deck were the subdivision of some of the outer shells but not the inner ones and this reduced the total division of granule to 30 with the same accuracy as the previous 224 subdivisions. This deck made use of the Crank-Nicolson finite difference method, and the addition of internal heat generation. The bipore concept, which was discussed in Chapter III, was added because activated alumina fitting suggested the need for it. LMS-4A fitting was satisfactory without the bipore concept. Activated alumina fitting still had oscillation problems which were found to be due to the error in not differentiating the saturation pressure, P_s, in the calculation of $(\partial X/\partial \tau)_p$ for TE(K).

Another new Jury deck with the bipore concept and internal heat generation in both normal case and long time calculation was duplicated on May 1, 1979. This program also had a generalized treatment of granule diffusion equations which did not involve approximations in the Thomas algorithm. This new program was compared to the one before and the concentration curve of this new program shifted to the left which was closer to the experimental result. This new program without the

use of bipore concept and heat generation was used to fit the LMS-4A experimental results, and with the use of bipore concept and without the use of internal heat generation was used to fit the activated alumina experimental results. The multiplication factors had been determined to fit the first run of each granule, and then these factors were used for the other runs. All the runs were completed in June 11, 1979, and the result of each run will be shown in Chapter VII.

CHAPTER VI

EXPERIMENTAL EQUIPMENT AND PROCEDURE

Associated with this research is a good deal of sophisticated, though necessary, equipment. In fact, a high degree of precision has been designed into and is maintained in all individual pieces of equipment. This leads to high accuracy results using the integrated system. Many graduate students have made substantial contributions to the development of these systems (12,23,94,96,113,132).

During the course of this research new models have been developed. Likewise, the equipment has been continually refined and perfected. It is intended here to describe the equipment and operational procedures with emphasis upon the new developments which have occurred.

The air supplies are the backbone of the entire percolation research experimental program. Consequently, a good deal of work has gone into their design, and as a result, the supplies are very reliable and are essentially "standard" air supplies. The compressed air is supplied by a new large capacity Joy "oiless" compressor rated at 250 psig but operating at 180 psig. Our line is reduced to 150 psig. This air is passed through a Honeywell and two Pall air filters before passing through a dampening tank. The pressure is regulated to 125 psig with a Cash pressure regulator before supplying to all three humidity control systems.

The low air supply is produced by a Wilkerson air dryer operated at 106 psig. This dryer is an adiabatic "heatless" adsorption dryer

which uses a pair of molecular sieve adsorption columns. While one column is adsorbing, the other is being regenerated by a side stream from the 20 psig dried outlet air. It operates on a timed "pressure-swing" cycle, switching every 30 seconds. The result is dry air, the frost point of which is less than -105°F.

The intermediate air supply produces air which is saturated at 100 psig and 32°F in a mechanically refrigerated ice bath designed by Dr. Jury (71). The theoretical frost point of this air is approximately -9.6°F.

The high air supply is a humidification tower designed by Mattern (113) and improved by Pollock (132). It produces air saturated at 114°F and 40 psig and is reduced to 100°F and 40 psig in this research.

The laminar flowrators which were used to measure the SCFH were designed by Y. W. Kim (96). These instruments were calibrated as discussed in the Appendix C. One flowrator is used for each supply air stream, and any desired humidity air can be mixed by using two flowrators and the appropriate air supplies.

The percolator bed was designed by Berbano (12) and improved by the author and is shown in Figure 11. The adsorbent sample is placed in the inner tube called the bed holder, which is a 1-1/4 in. I.D. × 1-1/2 in. O.D. × 12-13/32 in. long polystyrene tube. This tube is enclosed by a 3 in. I.D. × 3-3/8 in. O.D. aluminum cylindrical casing. The space between the bed holder and the aluminum casing is adequately sealed by o-rings. During experimental runs the annular region is evacuated to less than 2×10^{-7} Torr pressure by means of a mechanical-oil diffusion pump combine to minimize gas space conduction losses.

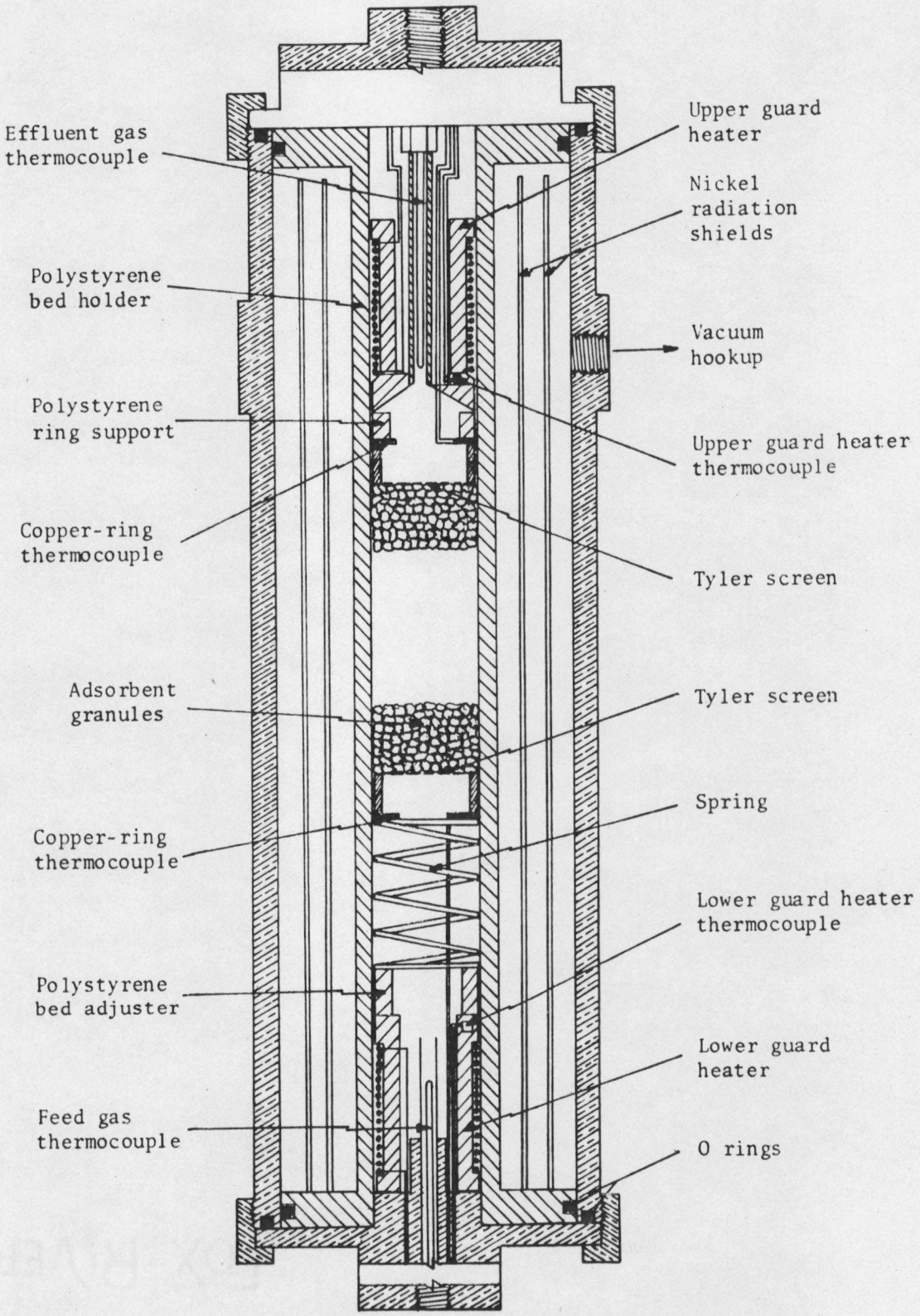


Figure 11. The Experimental Fixed Bed.

The radiation losses are reduced by polishing the inside wall of the aluminum casing and selecting a clear polystyrene, in addition to providing the two nickel radiation shields.

The bed head assembly consists of a Conax thermocouple and an eccentric bed adapter. The thermocouple is mounted on the bed cap for the measurement of effluent gas temperature.

The adsorbent sample is held in the polystyrene bed holder by two supported Tyler 32 mesh screens. The screens are soldered onto a one-half inch long piece of brass pipe that is machined to simply slip down inside the bed. Two copper-constantant thermocouple wires are soldered onto two 1/32 in. thick × 1/8 in. wide copper rings and placed onto the other side of the screens to measure the temperatures at those two points. The steel spring is placed between the copper ring and the bottom bed adjuster to make sure that the bed is a fixed bed at any flow rate. Both bed adjusters are made of polystyrene and the bottom one is interchangeable for 2 and 4 inches adsorbent samples. As a means of minimizing the heat loss by conduction, two guard heaters with thermocouples are placed at the upper and lower ends of the bed. These two guard heaters are adjusted by hand via the variacs to keep the temperatures of the copper ring and the guard heater thermocouples closed together. Both ballast resistors of the guard heaters are set to 500 ohms to make sure that the guard heaters can quickly respond to the temperature changes.

The miniature air heater and a thermocouple make up the bottom cap of the aluminum casing. The inlet air is preheated by the miniature

heater to the set point temperature, and the gas inlet temperature to the bed is monitored using the high-velocity thermocouple which is mounted on the cap.

The aluminum casing is designed so that bed holders of different diameters could be used. However, a bed diameter of 1-1/4 in. I.D. was used throughout the experimental work of this thesis.

The use of a mechanical pump alone for the vacuum insulation of the annular space between the inner and outer cylinders of the percolator bed is not adequate based on pegging the thermocouple vacuum gage, since this degree of vacuum required for vacuum insulation. For this purpose an oil diffusion pump backed up by a mechanical pump is used. Details of the mechanical-oil diffusion pump is presented in Appendix B.

The automatic vacuum controller is designed for the automation and safe operation of the oil diffusion pump. Details of this controller are also presented in Appendix B.

The apparent solid density, external and internal void fractions, average particle radius, the surface area per unit volume, the vapor pressure of moisture in the bed at initial condition, and the regeneration time were all measured in laboratory 316 for each adsorbent sample. Details of sample preparations are discussed in Appendix A.

All the percolation runs were done in laboratory 311. Each sample was packed into the bed holder for a desired bed length. After assembling the bed and connecting to the board, the vacuum system was started. The low humidity air was fed through the bed and the bed was leak tested. Then the temperature of the dry air was increased to 190°F

to regenerate the granules. During the regeneration, the miniature heater was controlled by the Thermotrol to maintain the temperature. After a period of time determined by the experiment which is discussed in Appendix A, the Thermotrol was cut off and the dry air was maintained at 78°F by the thermostated water passed through the miniature heater only.

When the bed temperature was equal to the room temperature, which was controlled at 78°F, the experiment was begun. The moist air was fed in at the desired concentration and flow rate. The effluent gas temperature was recorded by a Honeywell recorder before passing through the frost dew point hygrometer which was designed by Jury (76,81,82). The frost point temperature was recorded by an Esterline Angus recorder. The feed gas, upper and lower copper rings, and upper and lower guard heaters thermocouples were connected to a Bristol temperature indicator. Each temperature was checked and adjusted frequently in order to maintain the high precision of each run.

During each run the total pressure was recorded by reading the barometer in room 317 every 1/2 hour, so the best average total pressure could be made. The run was completed when the frost point of the effluent gas was equal to the frost point of the feed gas. This can be checked by connecting the high or intermediate air supply directly to the hygrometer, but for the mixed air supply we had to compare the effluent frost point with the calculated one and also had to wait long enough to make sure that the frost point was not going to change further.

After each run was completed, the regeneration was started again without removing the granules if the same size of granules and bed length were to be used in the next run.

All the equipment had to be calibrated according to Pollock's procedures (132), and the adjustment and minor repair work had to be done before almost all the runs. The most serious problem that terminated many of the runs was the lack of building distilled water supply during the middle of the run which caused the high air supply system to automatically shut down.

The previous plan was to study the percolation kinetics by flowing humid air through fixed beds under various conditions as follows: (1) two different gas flow rates, (2) two different feed gas concentrations, (3) two different particle sizes, (4) two different bed lengths, and (5) two different bed diameters. There was a time problem in finding polystyrene tubes to construct another bed holder, so the bed diameter was fixed. Three different particle sizes were used.

The experimental runs were designed to study various conditions. The plan of runs is shown in Table IV. All the experimental runs were based on the constant feed gas temperature equal to initial bed and room temperature which was 78°F. The experimental results are shown in Chapter VII in comparison with the calculated results.

Table IV. Design of Experimental Run.

Run No.	1	2	3	4	5	6
Gas flow rate (SCFH)	10	5	10	10	10	10
Feed gas concentration (Air supply)	HIGH	HIGH	MIXED	HIGH	HIGH	HIGH
Particle size (mesh)	12/14	12/14	12/14	8/10	16/20	12/14
Bed length (inch)	2	2	2	2	2	4

CHAPTER VII

COMPARISON OF EXPERIMENTAL AND CALCULATED RESULTS

During a run the temperature and frost point of the effluent air from a bed were constantly monitored and recorded on strip chart recorders. The recorded frost point temperatures from the Esterline Angus recorder were changed to partial pressures, P, by using data given in the International Critical Tables (156). Then the RATIOC were calculated from the following definition:

$$\text{RATIOC} = [P/P_T-(P/P_T)_{\text{initial}}]/[P/P_T)_{\text{feed}}-(P/P_T)_{\text{initial}}]$$

where P_T is the average total pressure throughout the run. This RATIOC and the effluent temperature from the Honeywell recorder were plotted versus time to produce the bed expiration curves determined experimentally. These are designated as LMSX or ACTX runs. The conditions of each experimental run are shown in Table V for LMS-4A and Table VI for activated alumina. The original data and the conversion to RATIOC are shown in Appendix D.

The next steps involved putting into the computer program the run conditions for the shortest bed and fastest run. The program was run and the results were compared with experiment until coincidence. These computer runs are designated as LMSC or ACTC runs.

Before embarking on the attempts at the best fit of data we must define what we mean by "the best fit of data." If all parameters in the computer program were precisely known then these would simply be

Table V. Conditions of Each LMS-4A Experimental Run.

Run No.	LMSX-1	LMSX-1N	LMSX-2	LMSX-3	LMSX-4	LMSX-5	LMSX-6
Feed gas flow rate, SCFH	10.31	10.31	5.22	9.89	10.41	10.27	10.44
Frost pt. of feed gas, °F	55.7	56.2	55.8	-9.1	55.5	56.8	55.7
Particle size, mesh	12/14	12/14	12/14	12/14	8/10	16/20	12/14
Bed length, inch	2.0	2.0	2.0	2.0	2.0	2.0	4.0
Initial partial pressure in bed, mm. Hg	.1326D-2	.1326D-2	.1326D-2	.1326D-2	.1875D-2	.9227D-3	.1326D-2
Feed gas partial pressure, mm. Hg	11.3568	11.5660	11.3938	0.5902	11.2754	11.8176	11.3568
Total pressure, mm. Hg	748.057	749.491	732.890	742.870	746.040	748.055	749.141

Remark: LMSX-1N ran without guard heater.

Table VI. Conditions of Each Activated Alumina Experimental Run.

Run No.	ACTX-1	ACTX-2	ACTX-3	ACTX-4	ACTX-5	ACTX-6
Feed gas flow rate, SCFH	9.35	4.89	9.26	9.40	9.48	9.64
Frost pt. of feed gas, °F	54.7	54.8	-10.0	55.0	55.2	55.7
Particle size, mesh	12/14	12/14	12/14	8/10	16/20	12/14
Bed length, inch	2.0	2.0	2.0	2.0	2.0	4.0
Initial partial pressure in bed, mm. Hg	.1110D-2	.1110D-2	.1110D-2	.1381D-2	.9448D-3	.1110D-2
Feed gas partial pressure, mm. Hg	10.9482	10.9914	0.5615	11.0706	11.1507	11.3568
Total pressure, mm. Hg	742.875	743.092	746.300	745.100	745.060	750.148

inserted into the program to produce "the fit." This, however, is not quite the case. Experimental measurements are themselves subject to errors even for the input conditions. Emissivities for the radiation shields around the bed container are actually best estimated and so the radiation coefficient HR may have to be adjusted to produce "the best fit." Likewise the latent heat of sorption, YLAMDA, taken from the literature is the best guess and so it too may have to be adjusted. Other parameters may also be involved and a complete discussion of these details is reserved for the following chapter.

In order that we as well as our reader may develop a feeling for the effects of parameter adjustments, we have made some of these for LMS-4A and the results are shown in Figures 12-15. Those for activated alumina are shown in Figures 16-17.

Armed with the foregoing information we can now proceed to adjust parameters until the best fits are obtained for LMS-4A run 1 and activated alumina run 1. These values of parameters are then fixed in computer runs 2-6 for LMS-4A and 2-6 for activated alumina. The best fit results for LMS-4A are shown in Figures 18-23 and those for activated alumina in Figures 24-29.

The input conditions for each LMS-4A computer run are given in Table VII. Those for each activated alumina computer run are given in Table VIII. The parameters that were adjusted and their final values to produce the best fits are given in Table IX. The tables of computer results for both LMS-4A and activated alumina are shown in Appendix E. These are the data that were used in plotting the computed portions of the figures.

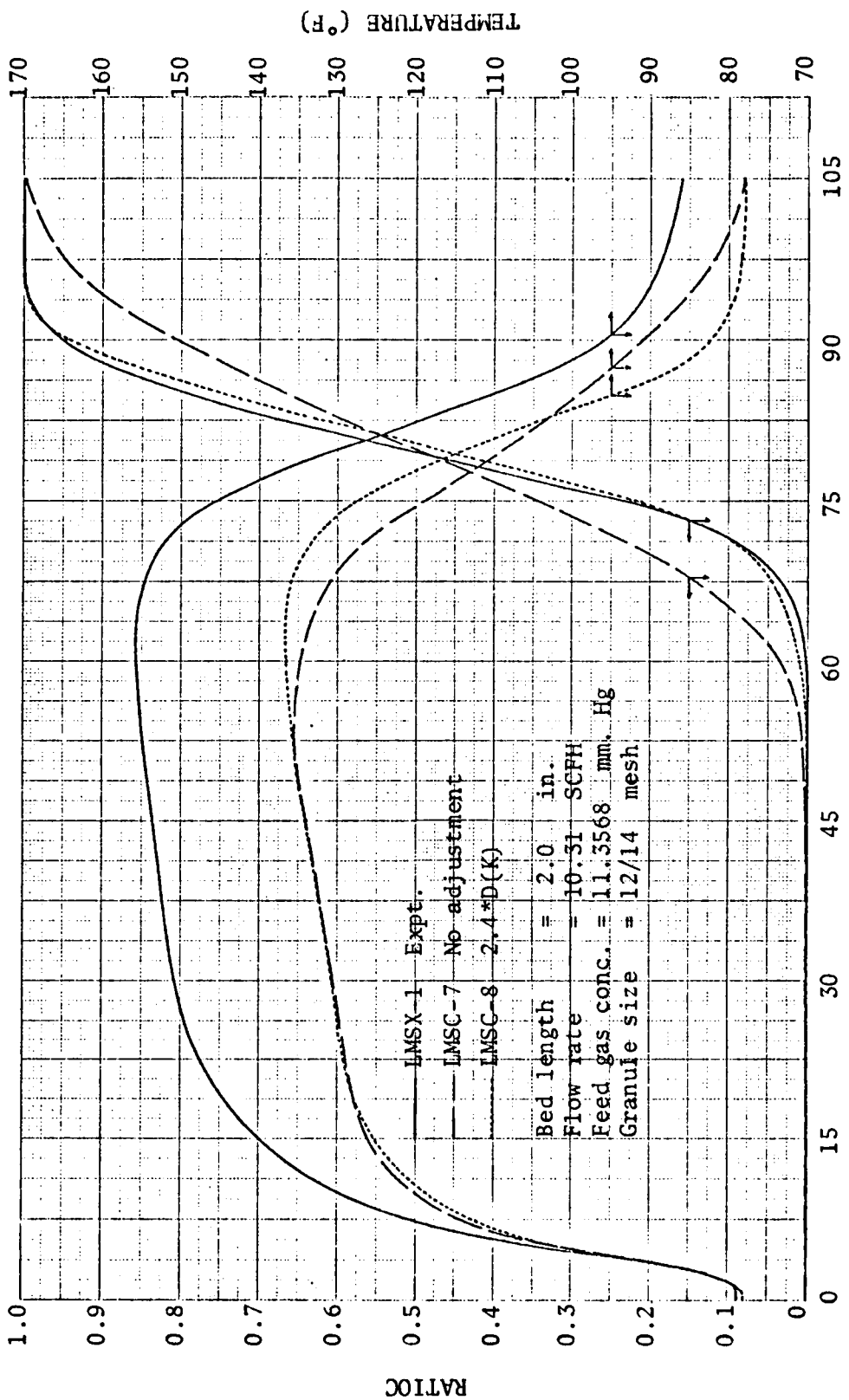


Figure 12. The Effect of a Change in D(K) on the Fit of LMS-4A Experimental Data Run No. 1. Here SIG = 1.0, EF1 = 1.0, and EF = 0.0.

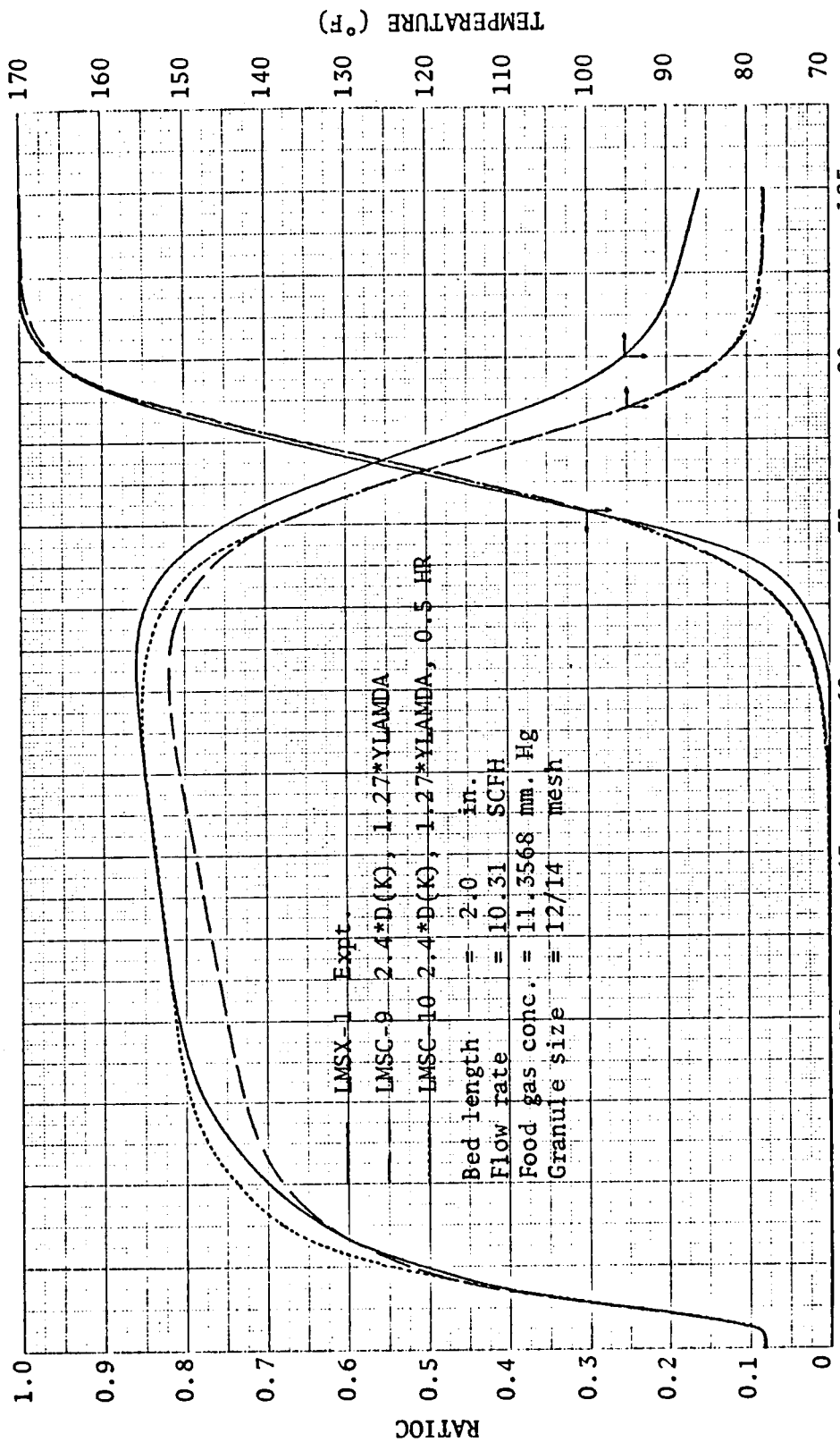


Figure 13. The Combined Effect of Changes in D(K) and YLAMDA, and D(K), YLAMDA, and HR on the Fit of LMS-4A Experimental Data Run No. 1. Here SIG = 1.0, EF1 = 1.0, and EF = 0.0.

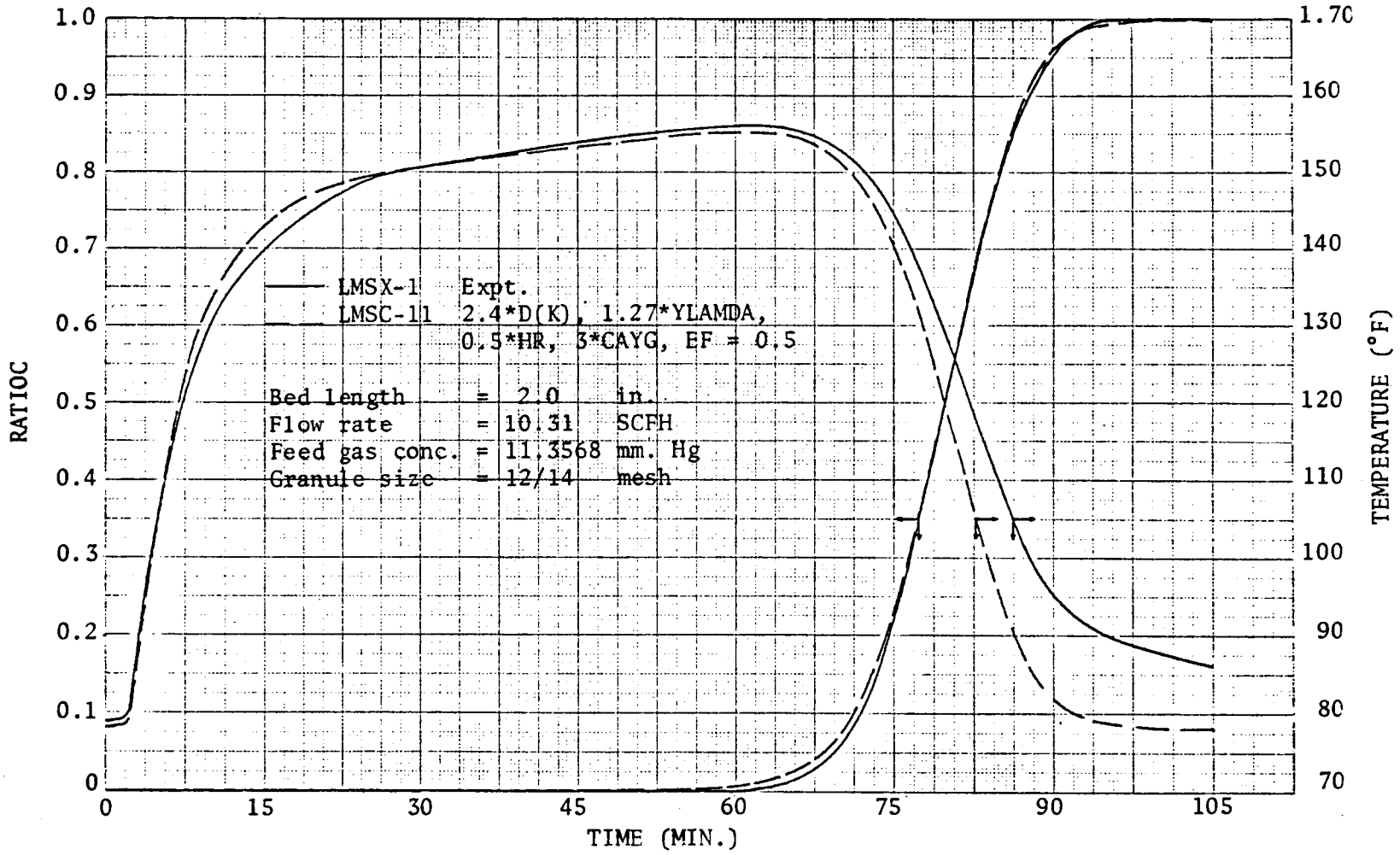


Figure 14. The Combined Effect of Changes in D(K), YLAMDA, HR, CAYG, and EF on the Fit of LMS-4A Experimental Data Run No. 1. Here SIG = 1.0, and EF1 = 1.0.

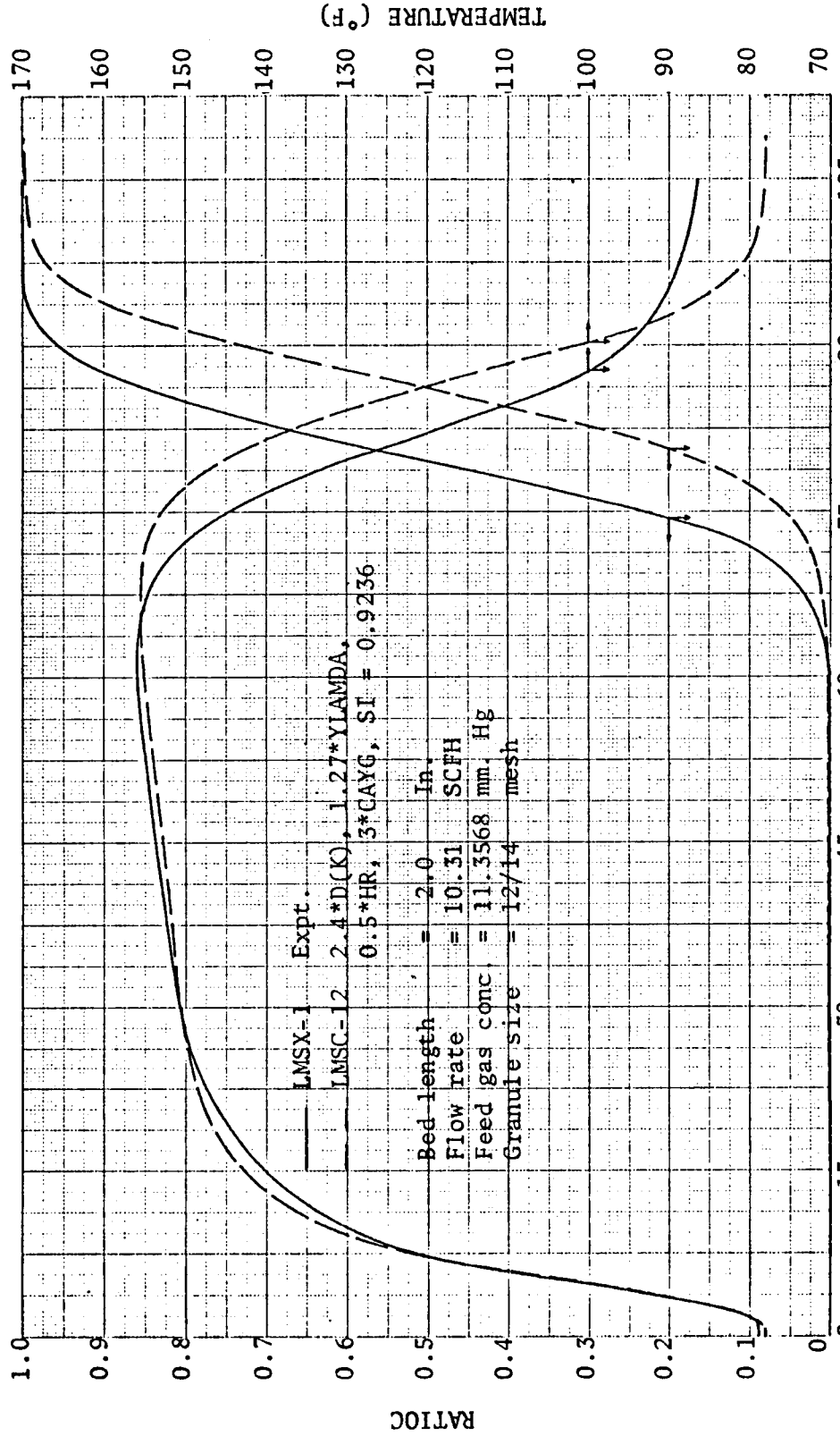


Figure 15. The Combined Effect of Changes in D(K), YLAMDA, HR, CAYG, and SI on the Fit of LMS-4A Experimental Data Run No. 1. Here SIG = 1.0, EF1 = 1.0, and EF = 0.0.

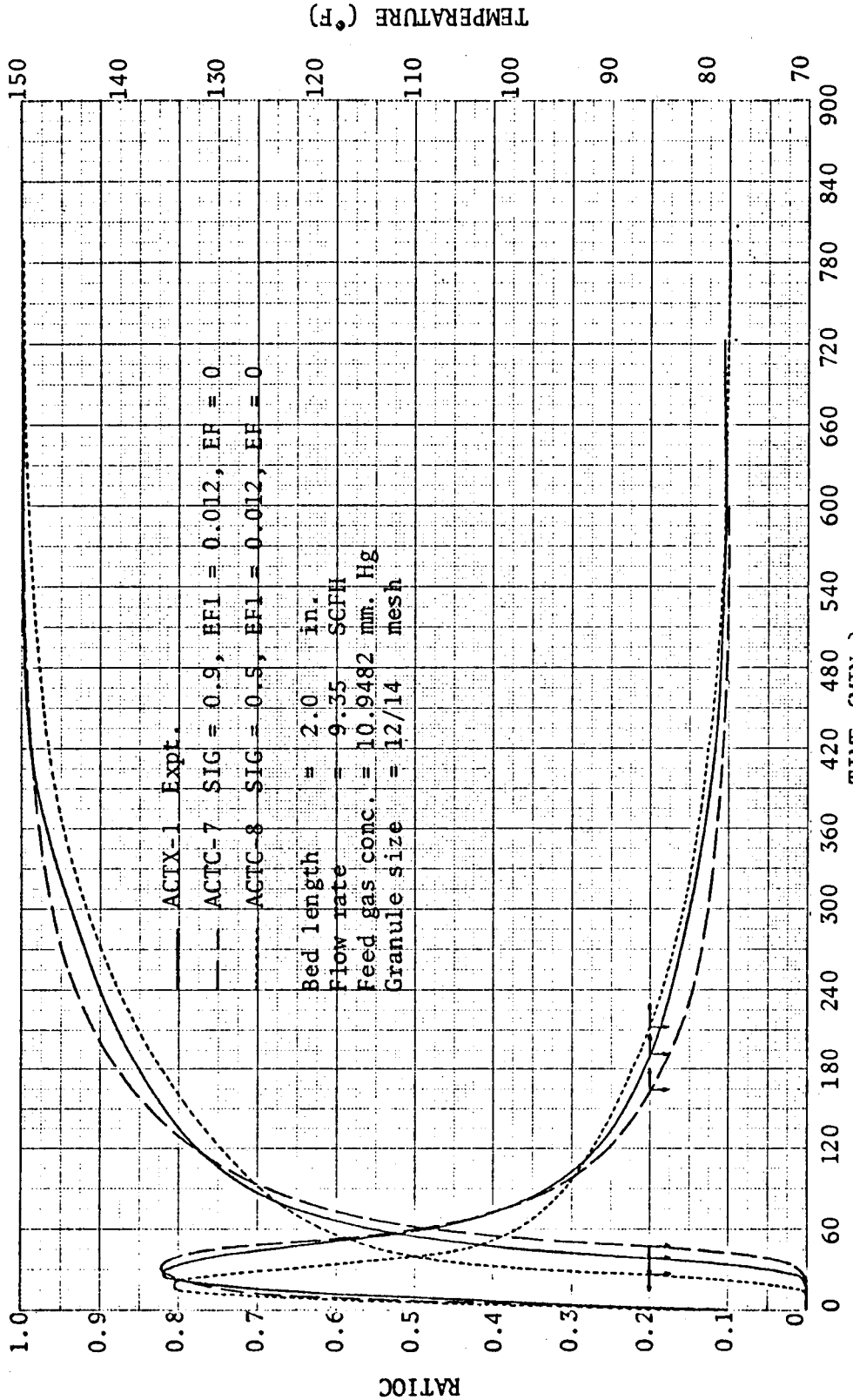


Figure 16. The Effect of Changes in SIG on the Fit of Activated Alumina Experimental Data Run No. 1. Here D(K)*3.0, YLAMDA*1.27, HR*0.5, CAYG*3.0, EF1 = 0.012, and EF = 0.0.

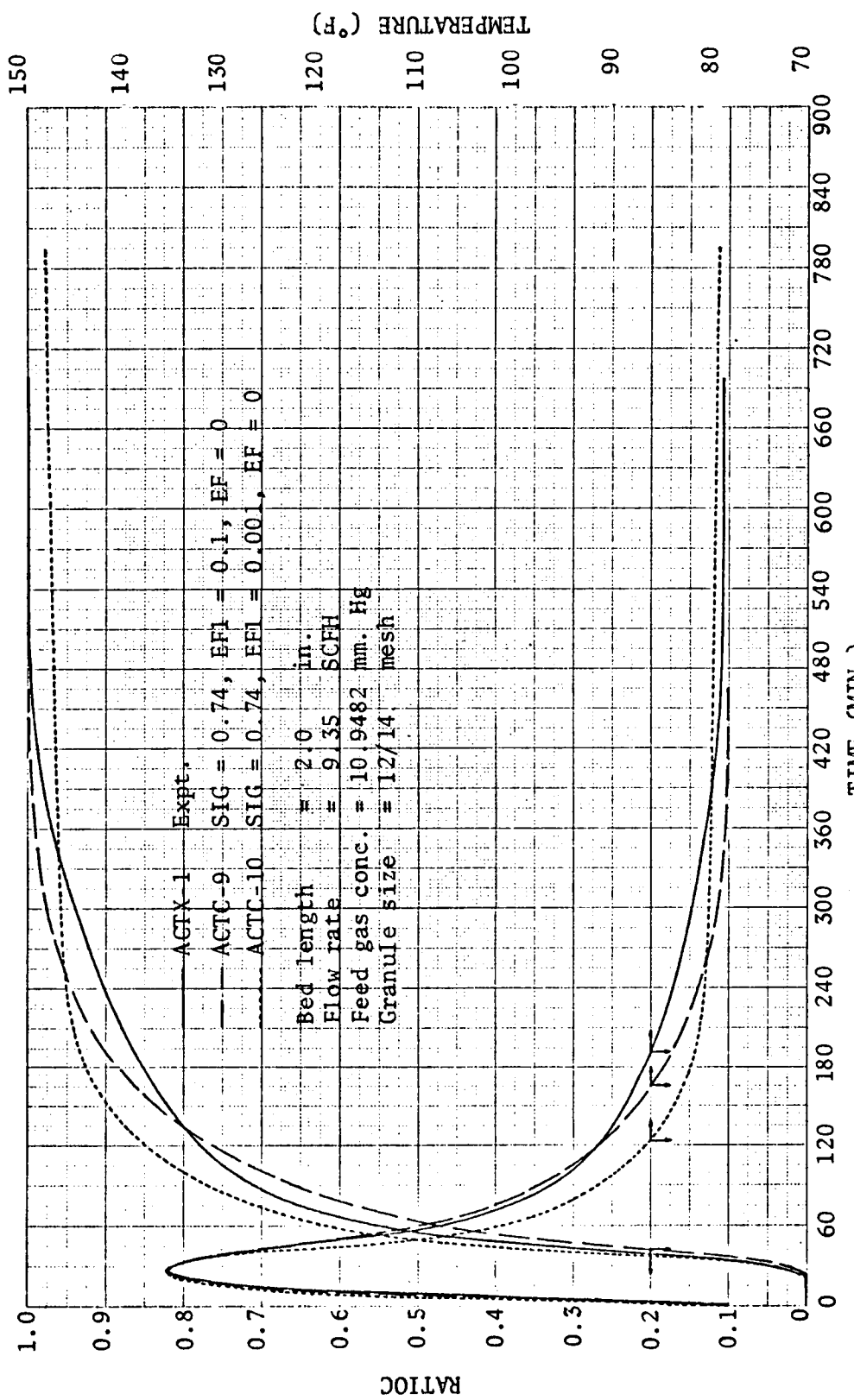


Figure 17. The Effect of Changes in EF1 on the Fit of Activated Alumina Experimental Data Run No. 1. Here D(K)*3.0, YLAMDA*1.27, HR*0.5, CAYG*3.0, SIG = 0.74, and EF = 0.0.

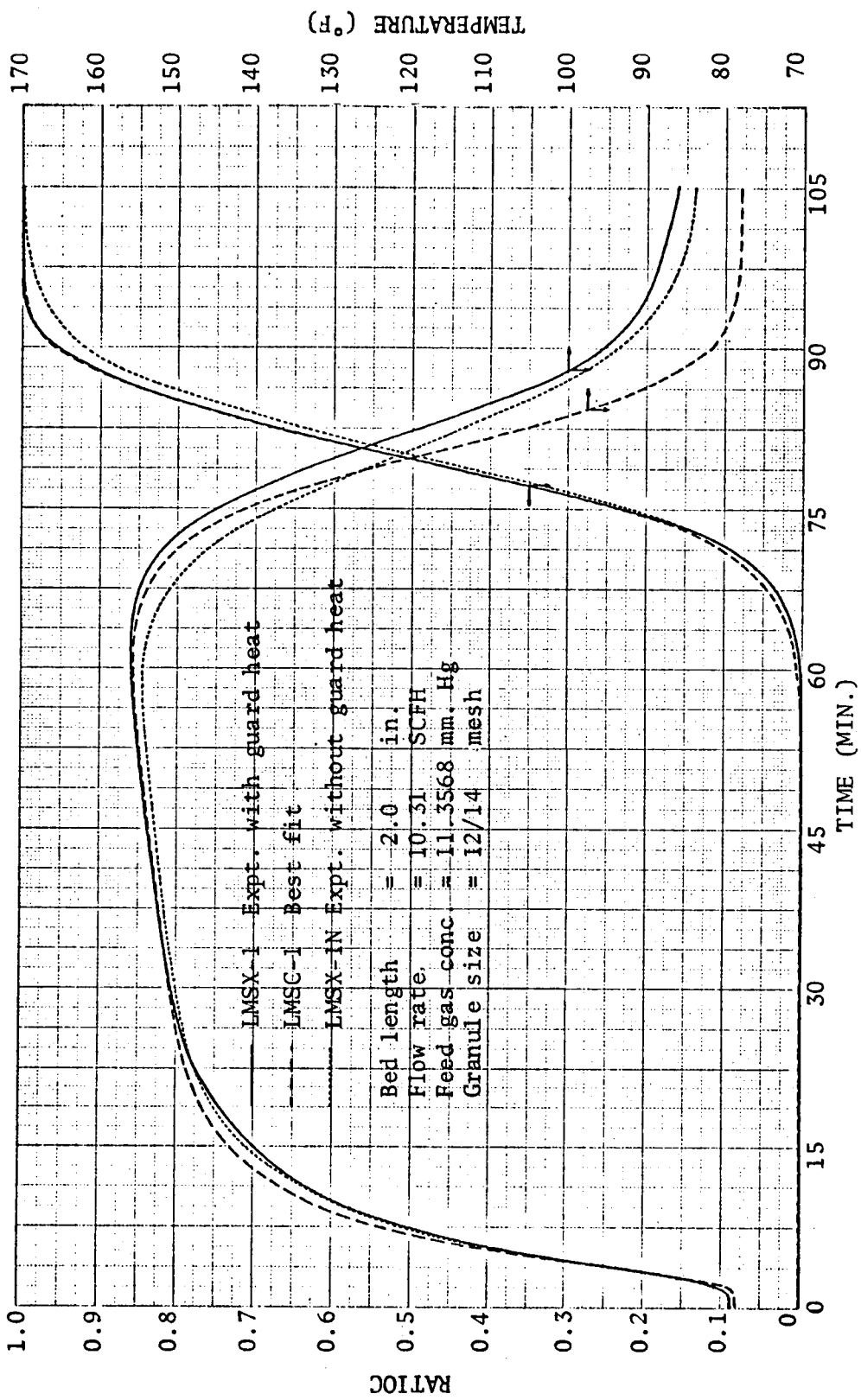


Figure 18. Comparison of Experimental Data and Best Fit of LMS-4A Run No. 1.

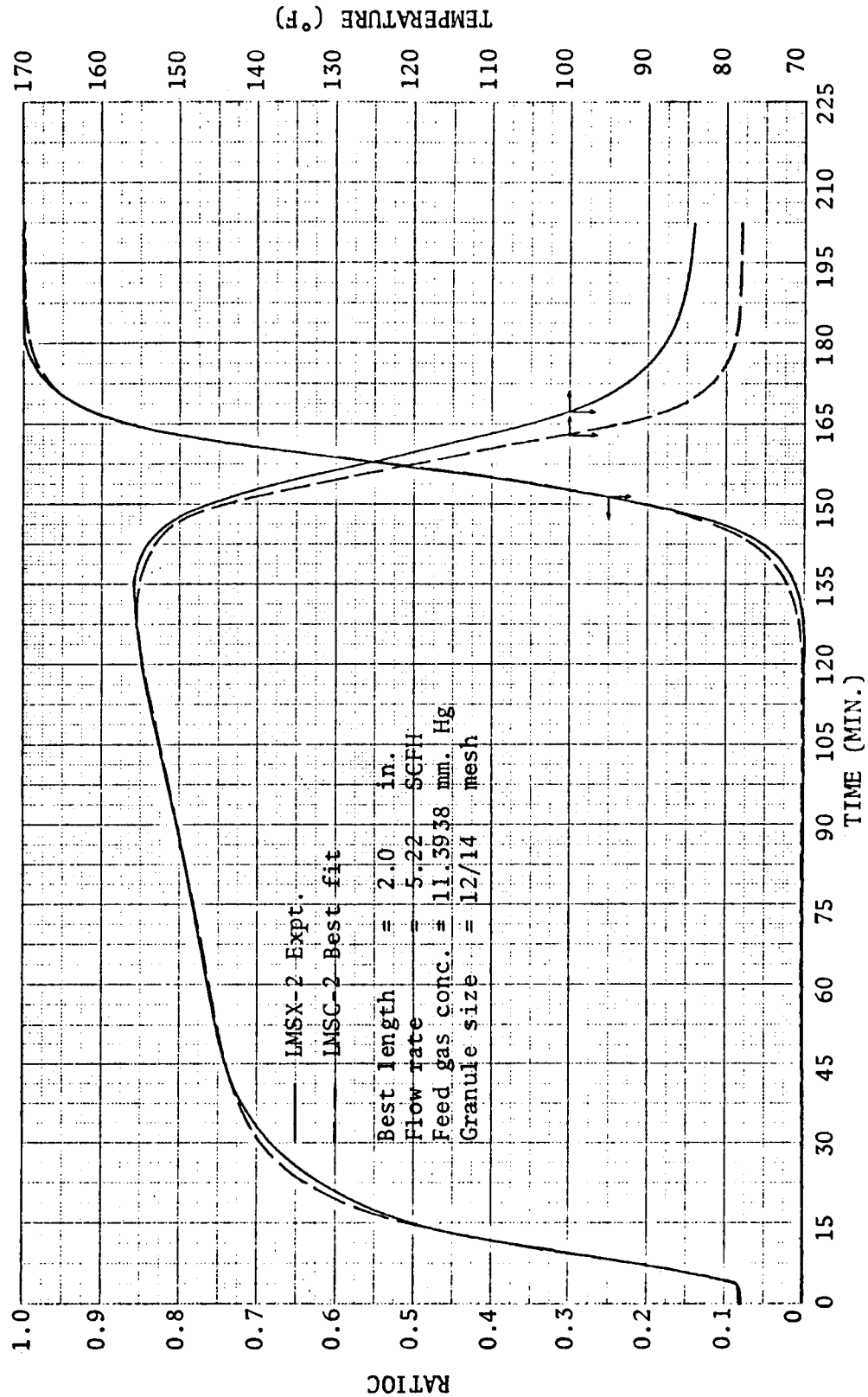


Figure 19. Comparison of Experimental Data and Best Fit of LMS-4A Run No. 2.

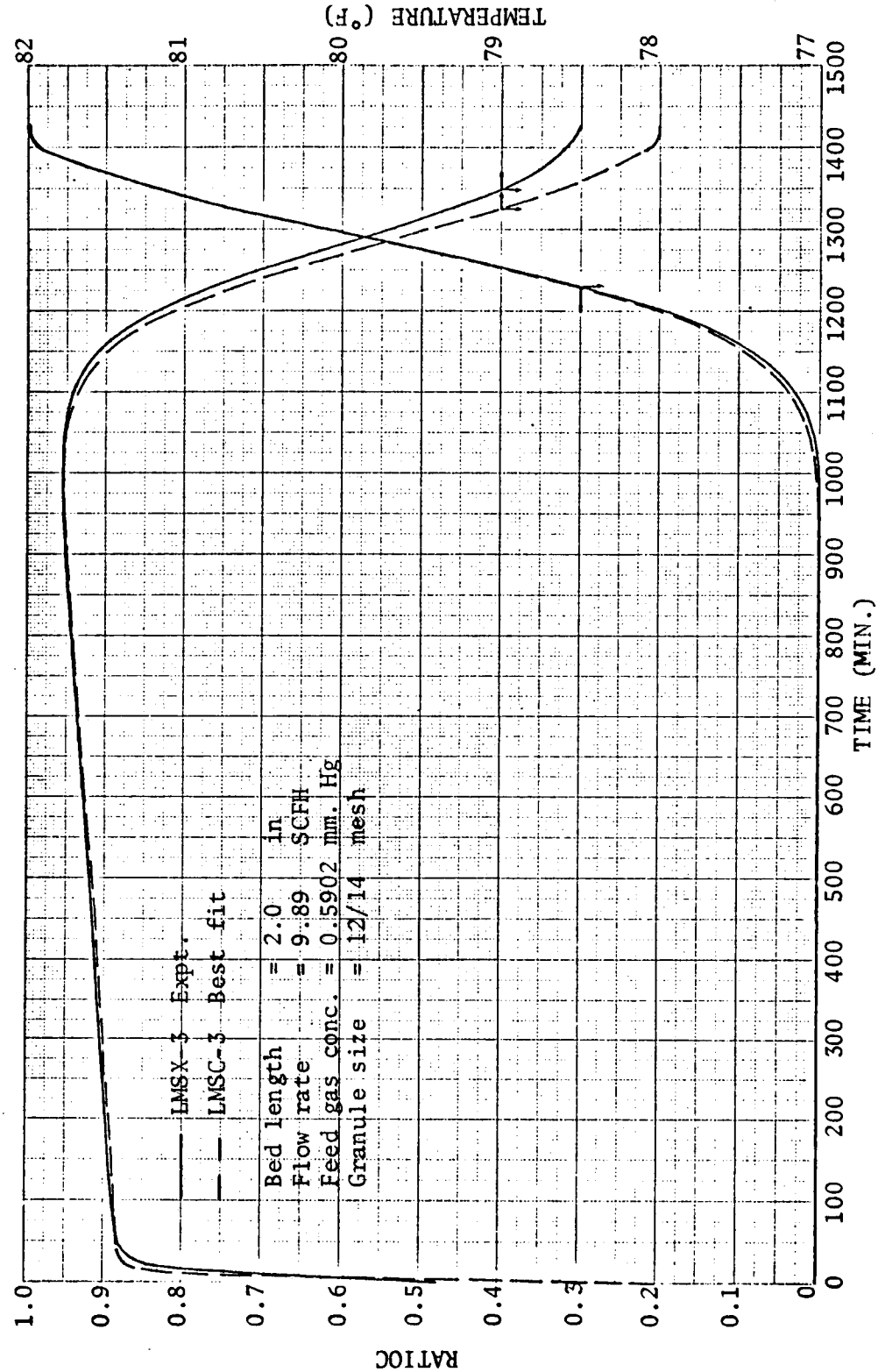


Figure 20. Comparison of Experimental Data and Best Fit of LMS-4A Run No. 3.

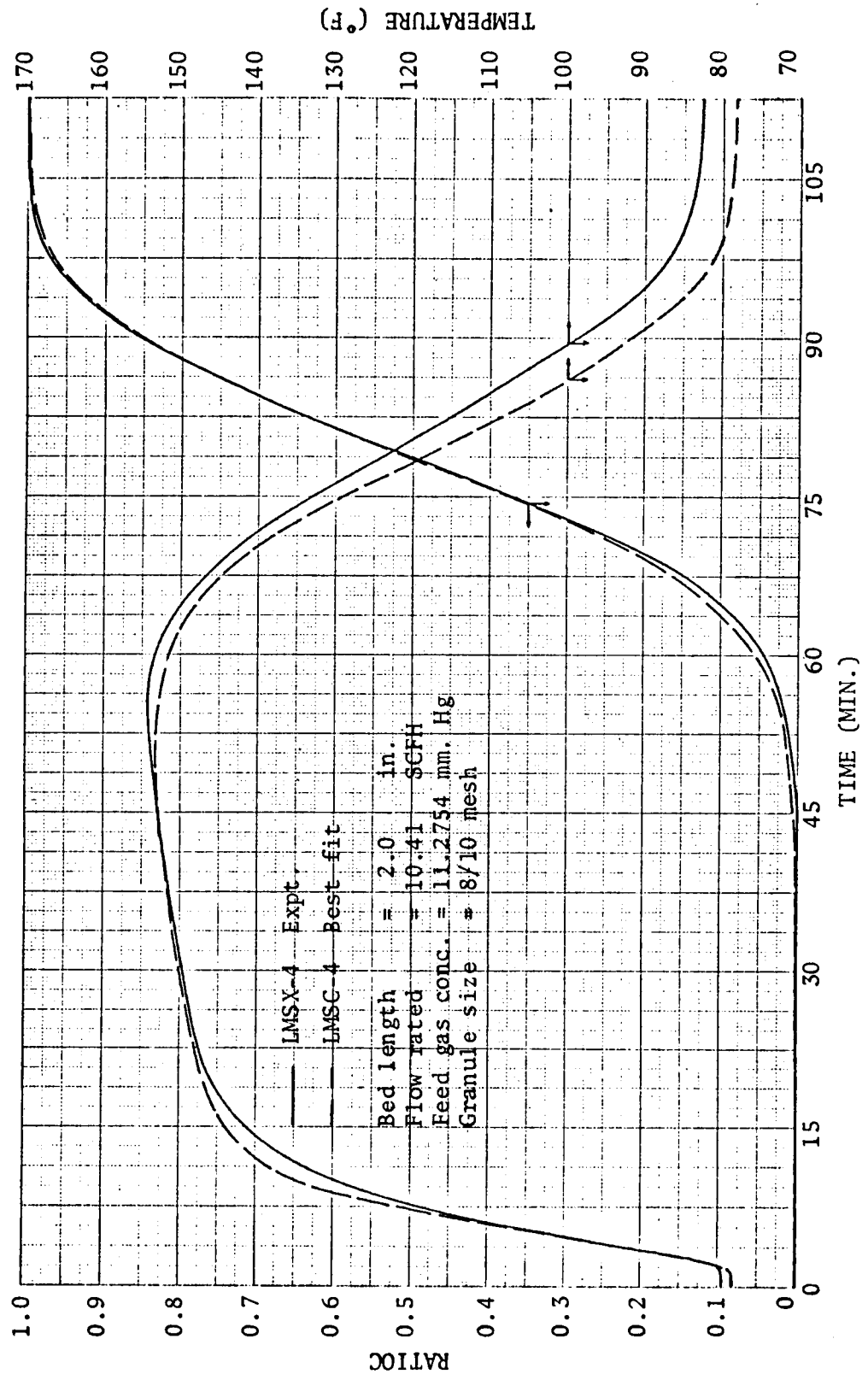


Figure 21. Comparison of Experimental Data and Best Fit of LMS-4A Run No. 4.

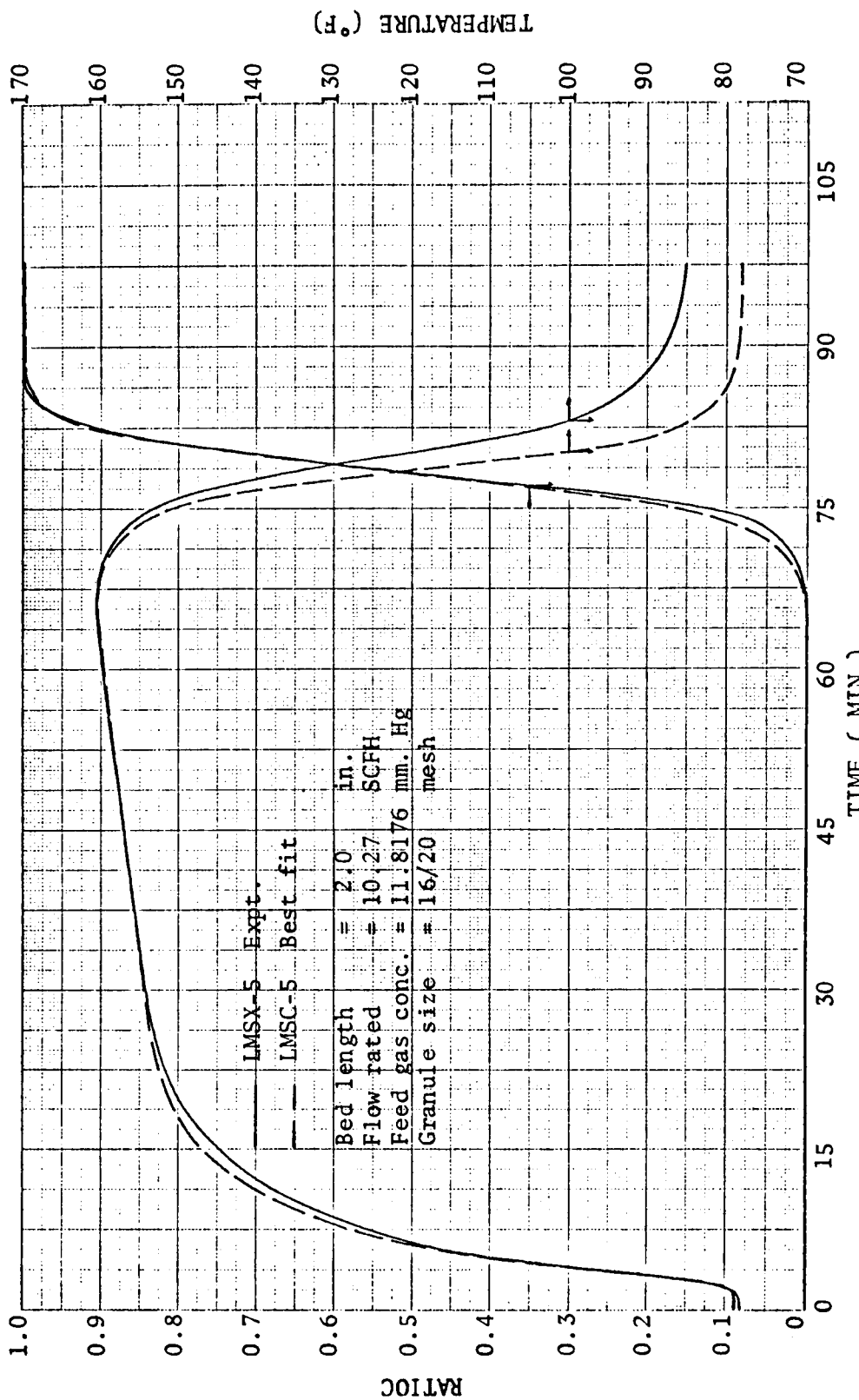


Figure 22. Comparison of Experimental Data and Best Fit of LMS-4A Run No. 5.

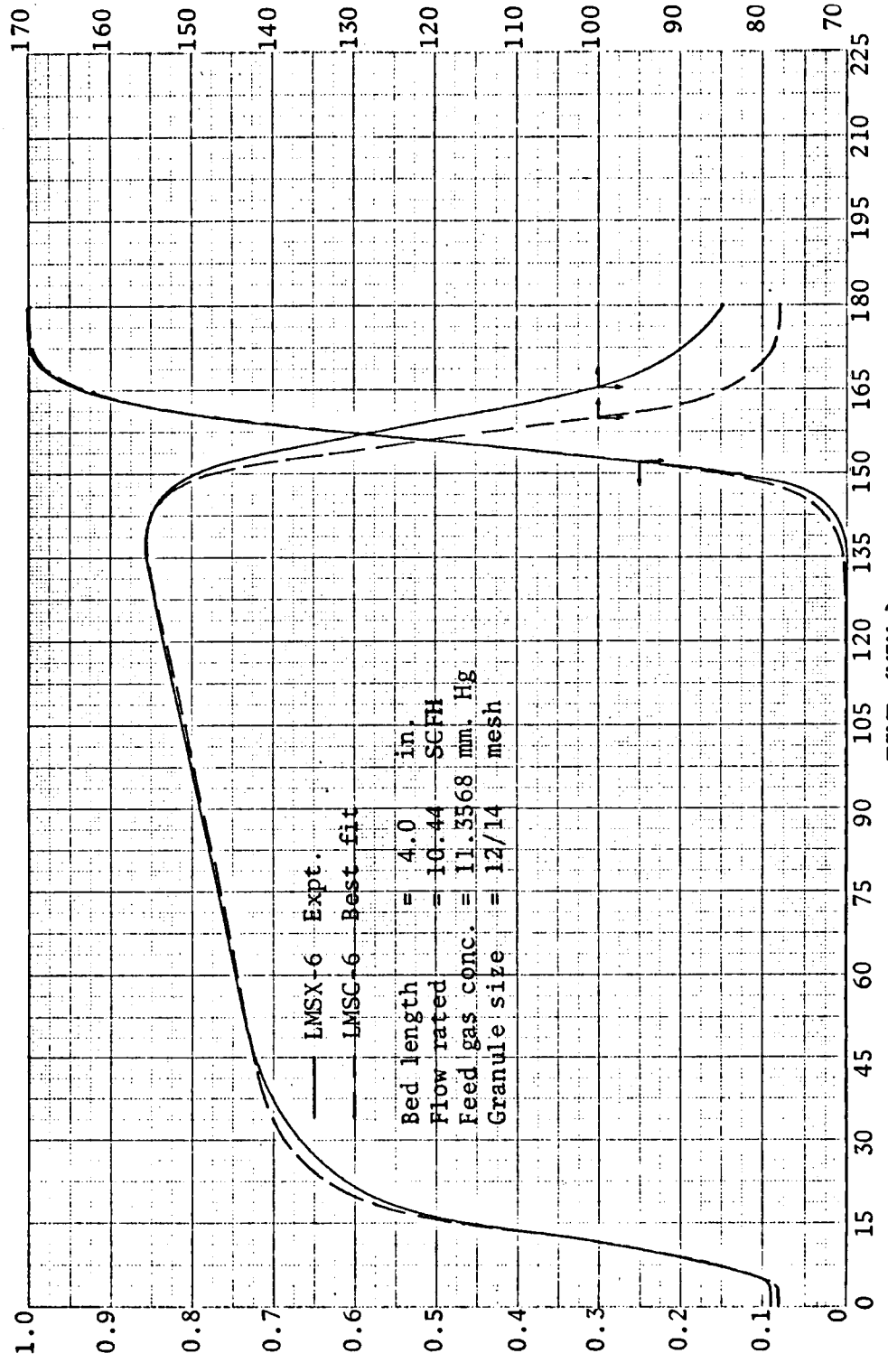


Figure 23. Comparison of Experimental Data and Best Fit of LMS-4A Run No. 6.

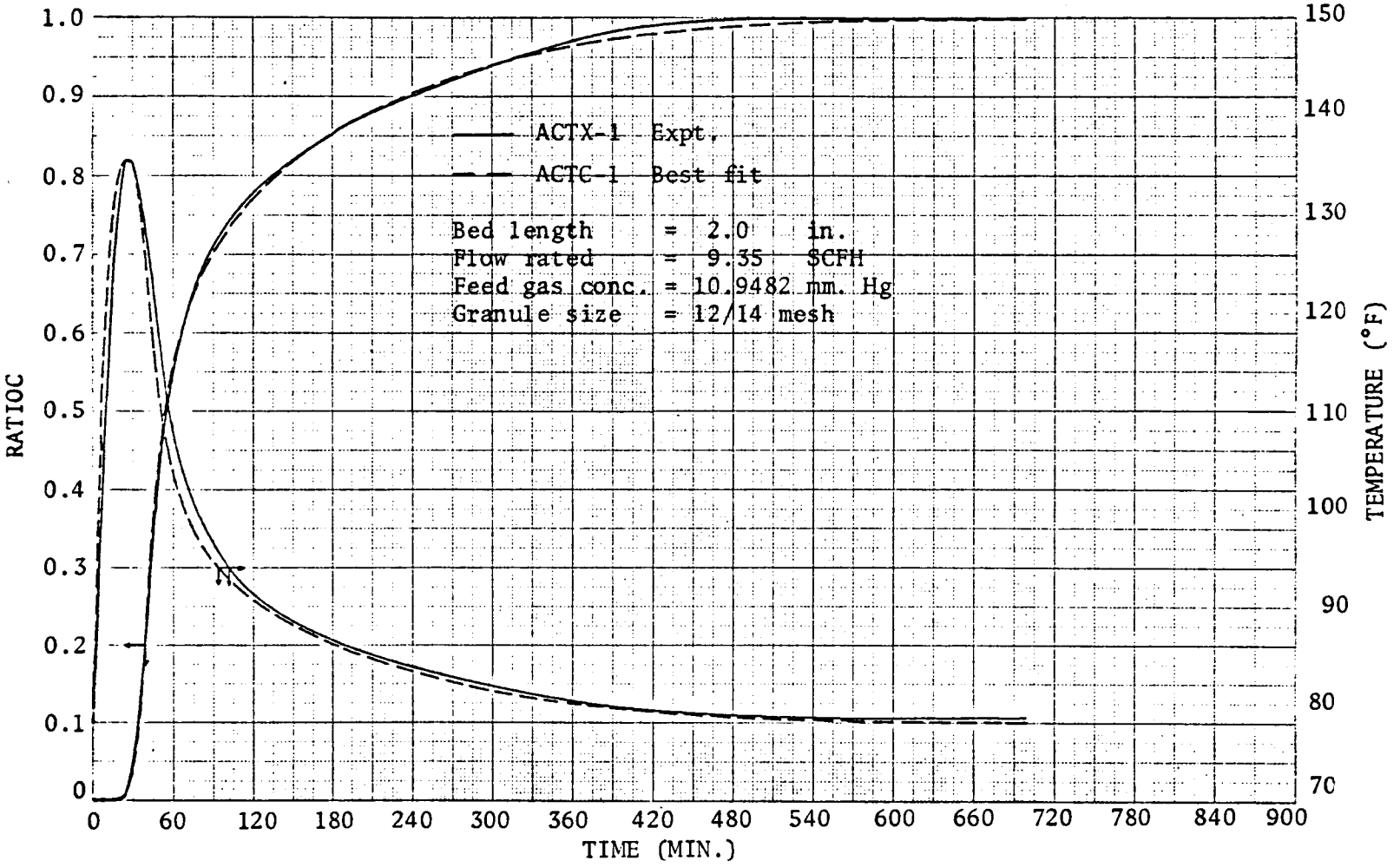


Figure 24. Comparison of Experimental Data and Best Fit of Activated Alumina Run No. 1.

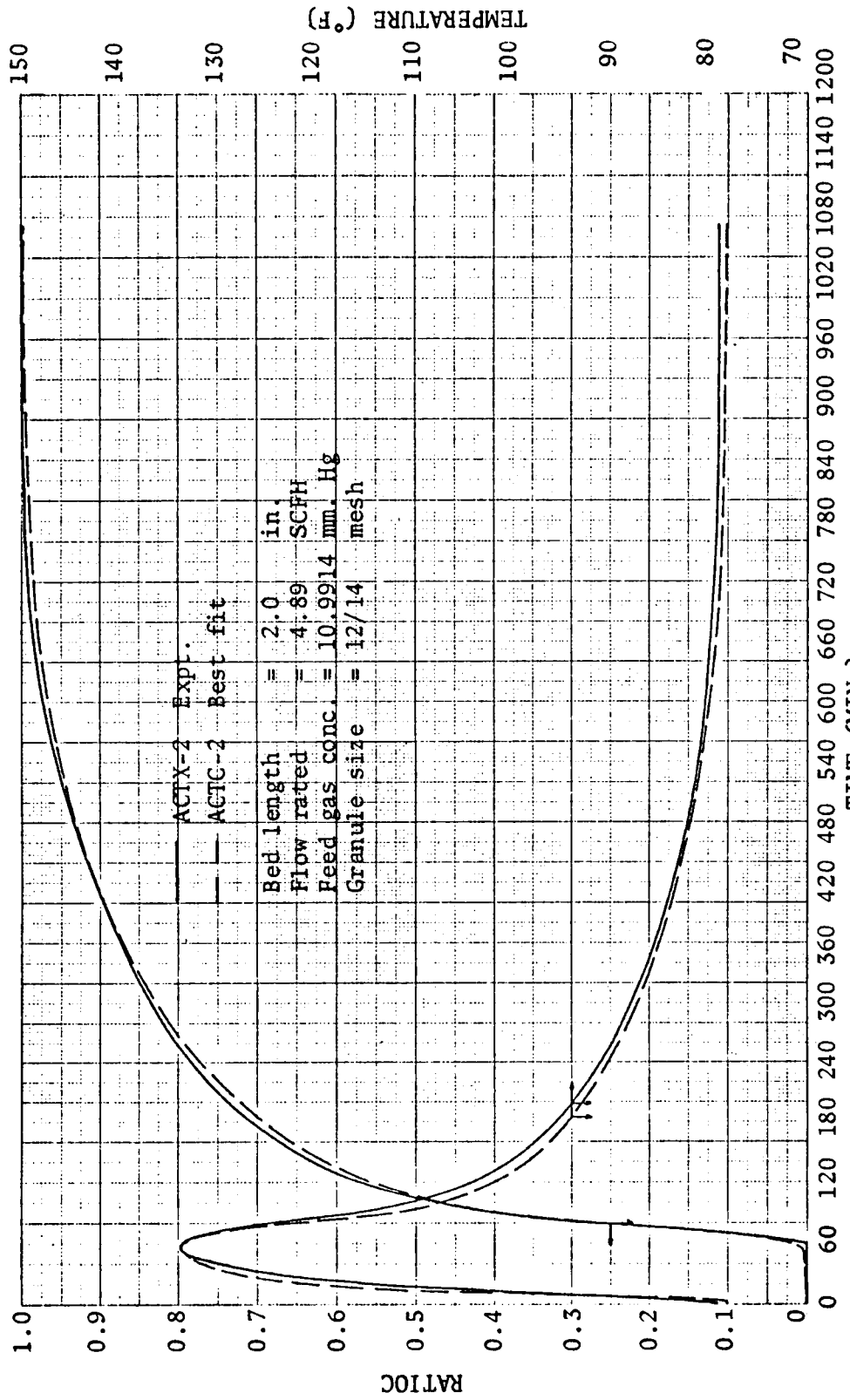


Figure 25. Comparison of Experimental Data and Best Fit of Activated Alumina Run No. 2.

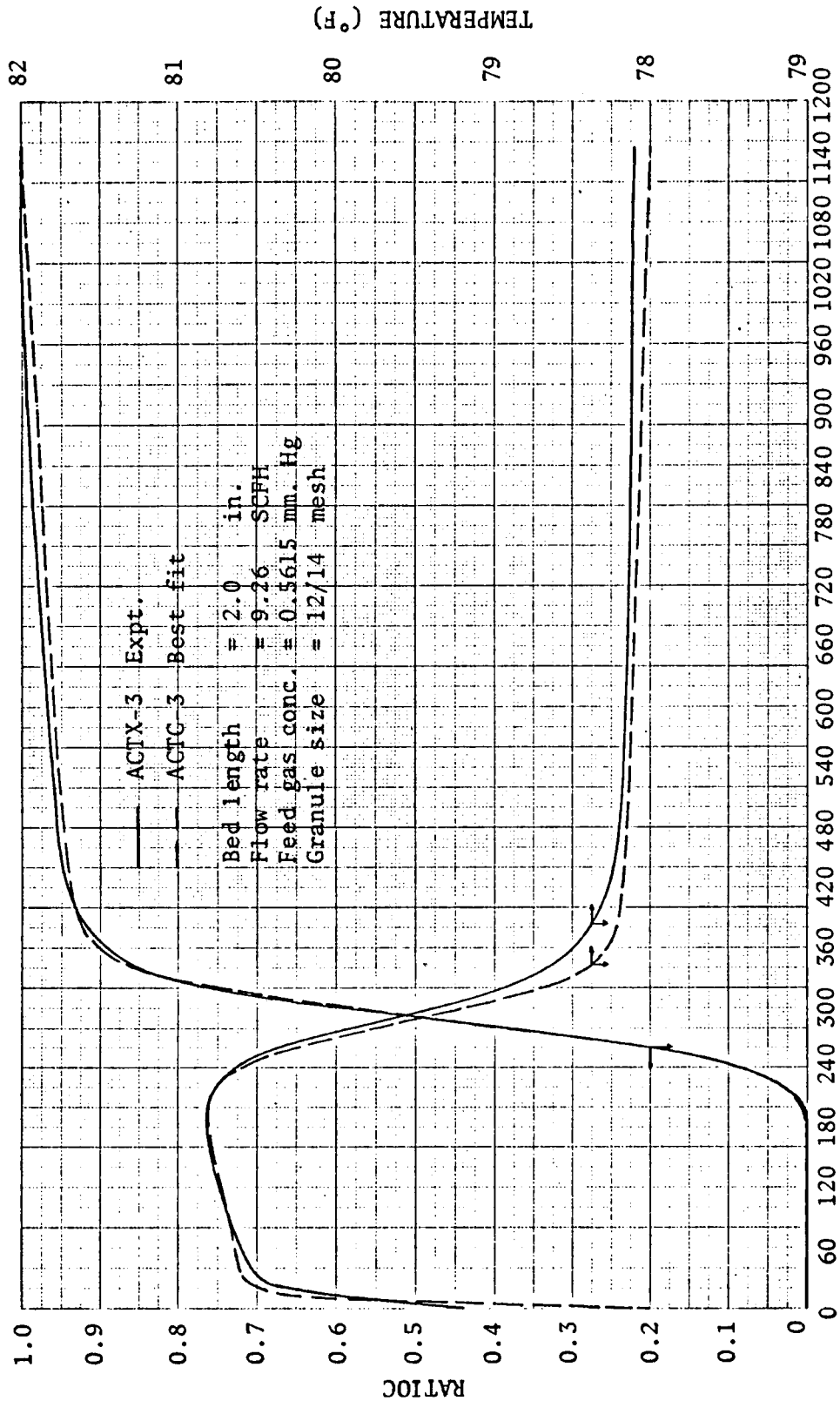


Figure 26. Comparison of Experimental Data and Best Fit of Activated Alumina Run No. 3.

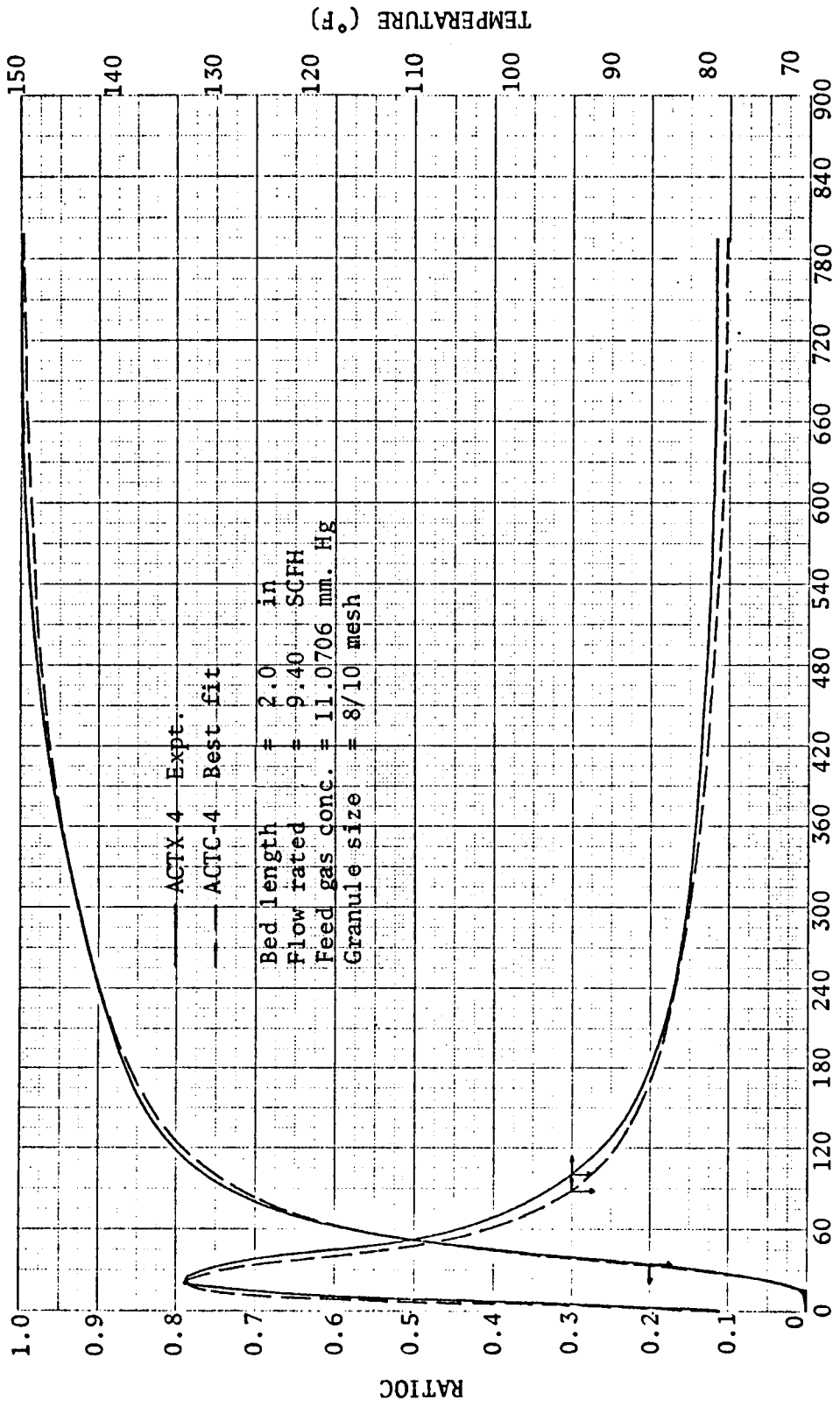


Figure 27. Comparison of Experimental Data and Best Fit of Activated Alumina Run No. 4.

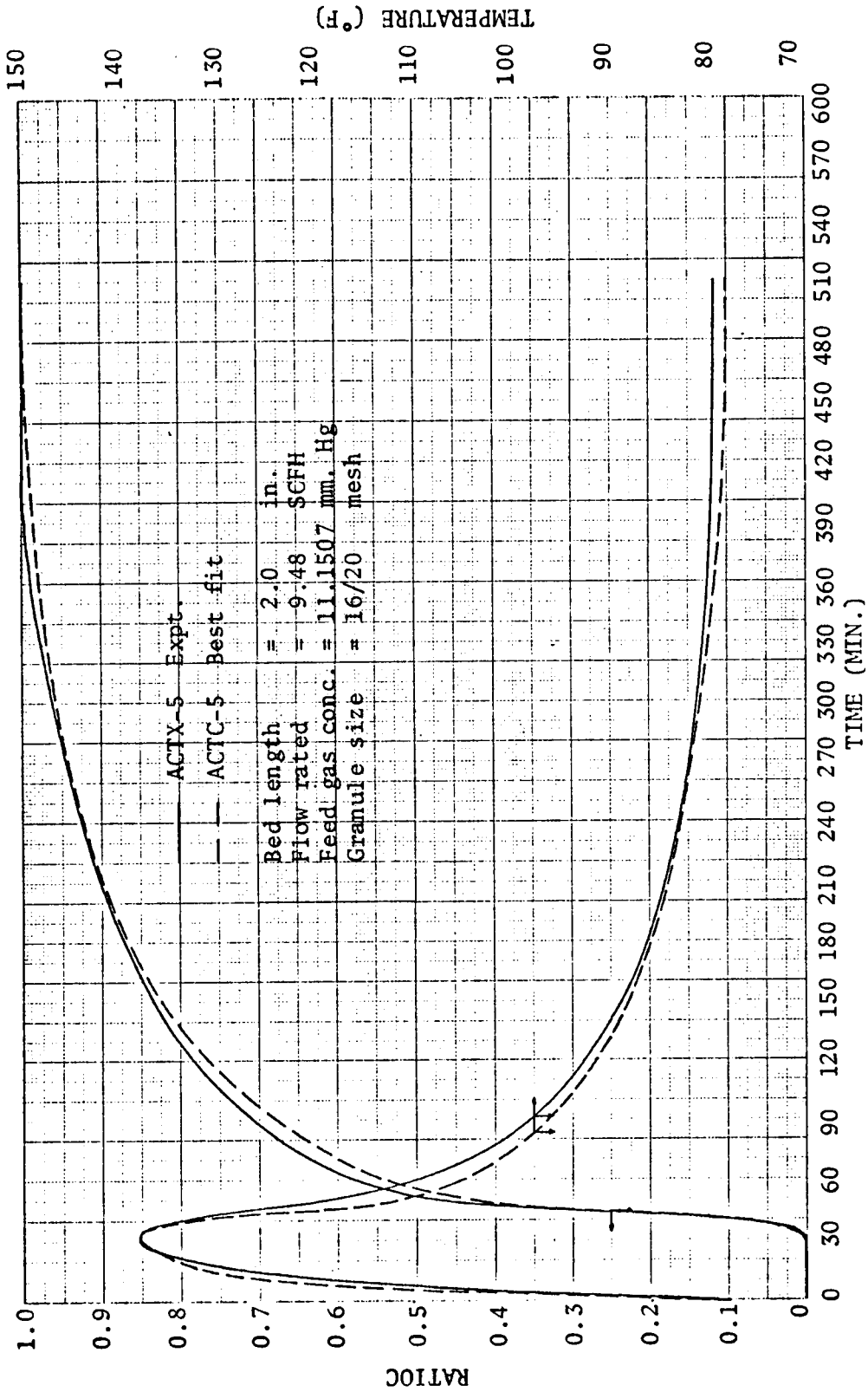


Figure 28. Comparison of Experimental Data and Best Fit of Activated Alumina Run No. 5.

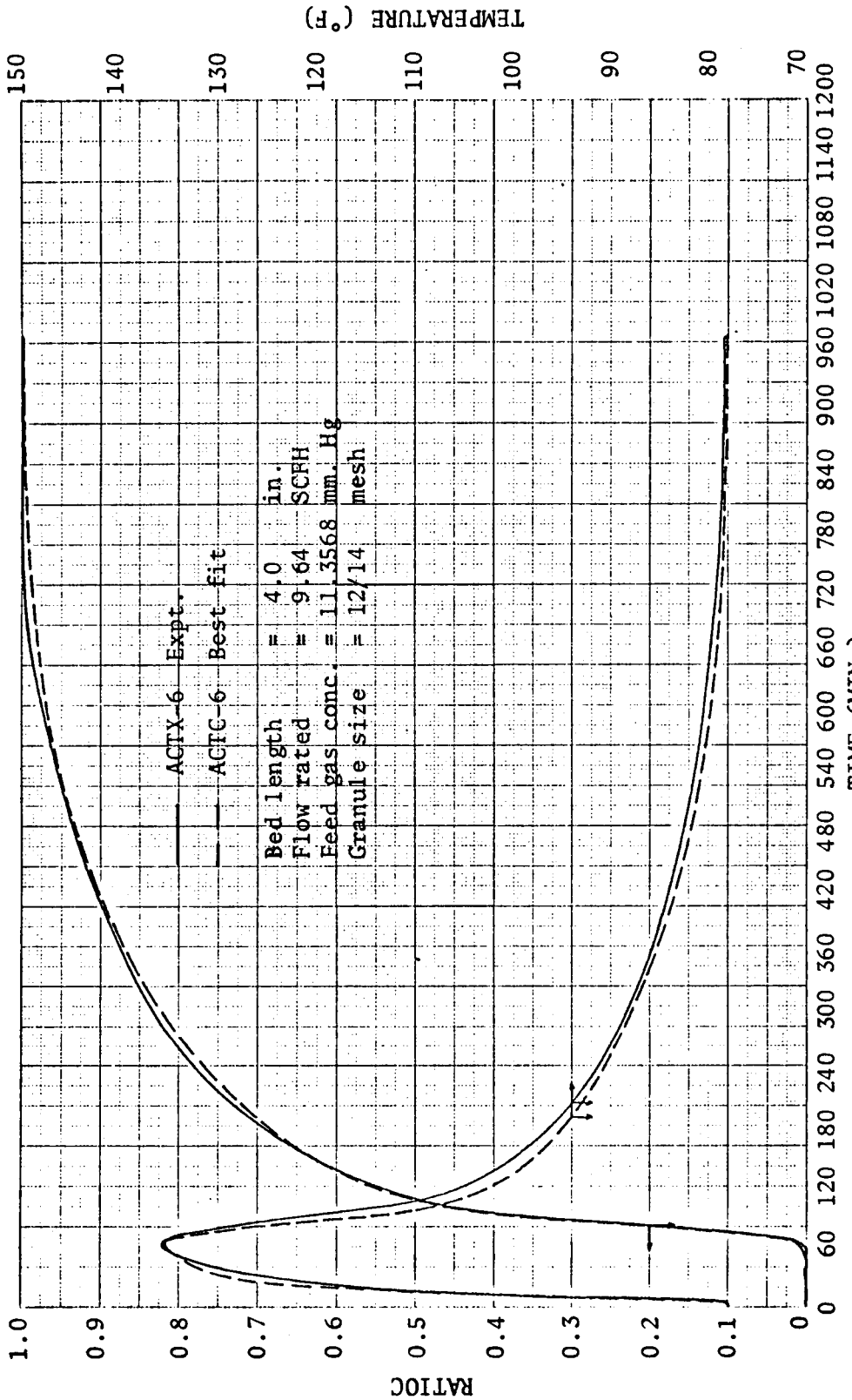


Figure 29. Comparison of Experimental Data and Best Fit of Activated Alumina Run No. 6.

Table VII. Input Data of Each LMS-4A Computer Run.

Run No.	LMSC-1	LMSC-2	LMSC-3	LMSC-4	LMSC-5	LMSC-6
Real SCFH	10.31	5.22	9.89	10.41	10.27	10.44
Adjusted SCFH	11.20	5.67	10.74	11.31	11.15	11.34
% SCFH increased	8.60	8.57	8.63	8.61	8.60	8.60
R, ft	.2412D-2	.2412D-2	.2412D-2	.3491D-2	.1595D-2	.2412D-2
EL, inch	2.0	2.0	2.0	2.0	2.0	4.0
BEDPI, mm. Hg	.1326D-2	.1326D-2	.1326D-2	.1875D-2	.9227D-3	.1326D-2
BEDPF, mm. Hg	11.3568	11.3938	0.5902	11.2754	11.8176	11.3568
P_T, mm. Hg	748.057	732.890	742.87	746.040	748.055	749.141
EPSLON, ε	.464	.464	.464	.460	.466	.464
DELTAT, sec	3.0	3.0	15.0	3.0	3.0	3.0

Table VIII. Input Data of Each Activated Alumina Computer Run.

Run No.	ACTC-1	ACTC-2	ACTC-3	ACTC-4	ACTC-5	ACTC-6
Real SCFH	9.35	4.89	9.26	9.40	9.48	9.64
Adjusted SCFH	10.00	5.23	9.90	10.05	10.14	10.31
% SCFH increase	6.93	7.02	6.95	6.95	6.89	6.92
R, ft	.2341D-2	.2341D-2	.2341D-2	.3242D-2	.1534D-2	.2341D-2
EL, inch	2.0	2.0	2.0	2.0	2.0	4.0
BEDPI, mm. Hg	.1110D-2	.1110D-2	.1110D-2	.1381D-2	.9448D-3	.1110D-2
BEDPF, mm. Hg	10.9482	10.9914	0.5615	11.0706	11.1507	11.3568
P_T, mm. Hg	742.875	743.092	746.300	745.100	745.060	750.148
EPSLON, ε	.4307	.4307	.4307	.4245	.4353	.4309
DELTAT, sec	12.0	12.0	12.0	12.0	12.0	12.0

Table IX. Parameters and Adjusted Parameter Values That Produced Best Fits of Experimental Data.

Parameter	Final Adjusted Value	
	LMS-4A	Activated Alumina
Fraction granule continuous phase, SIG	SIG = 1.0	SIG = 0.74
Time constant proportionality factor, EF1	EF = 1.0	EF1 = 0.012
Fraction of heat of sorption generated internally, EF	EF = 0.0	EF = 0.0
Latent heat of sorption, YLAMDA	1.27*YLAMDA	1.4*YLAMDA
Gas film mass transfer coeff., CAYG	3.0*CAYG	3.0*CAYG
Diffusivity of continuous phase, D(K)	2.4*D(K)	3.0*D(K)
Radiation coeff., HR	0.5*HR	0.5*HR
Shape factor, SI	SI = 1.0 (Correct Value = 0.9236)	SI = 1.0 (Correct Value = 0.9045)

CHAPTER VIII

DISCUSSION OF RESULTS AND CONCLUSIONS

In the previous chapter we have shown that our computer programs and consequently the mathematical descriptions of our kinetic mechanism models contained in them do an extremely good job of accounting for the expiration curves determined experimentally. It is reasonable to assume therefore that Linde molecular sieve 4A does not contain blind pores whereas activated alumina does. Also diffusion in LMS-4A takes place via Knudsen and interstitial means whereas in activated alumina diffusion takes place by free, Knudsen and surface means. Gas phase film resistance to heat and mass transfer does play a part. The sorption therms determined earlier in this project are completely compatible with our present findings.

If we were to analyze our work in detail we would invite attention to the temperature curves which show a very good fit at the start, but tend to drop down to the left faster than the experimental results. Many runs were made in which we adjusted each parameter to try to reduce the rapid drop but none of them tended to correct this problem. Run LMSX-1N was run without guard heaters in order to check that this problem didn't come from the guard heaters. From Figure 18 (page 106) it is obvious that this result drops between the guarded experiment and the calculated. The internal heat release factor EF was added to our program specifically to correct the rapid drop but it also distorted the rest of the temperature curve.

Figures 12 to 13 (pages 100 and 101) show the necessity of each of the multiplication factors. LMSC-8 with 2.4 D(K) moves the RATIOC curve to almost the same slope as the experimental curve and also extends the time before the temperature curve starts dropping down. LMSC-9 with 2.4 D(K) and 1.27 YLAMDA moves the RATIOC curve closer to the experimental curve and also moves the top of the bell-shaped temperature curve up closer to the experimental curve. LMSC-10 with 2.4 D(K), 1.27 YLAMDA, and 0.5 HR moves the temperature curve up to fit with the experimental curve. The only problem remaining is the starting point of RATIOC curve is not perfectly fitted with the experimental curve. This is corrected in LMSC-1 by adding 3 CAYG to LMSC-10 which makes not only the best fit of RATIOC for LMSX-1 but also the best fit for other LMS-4A runs, and it also moves the temperature curve to the best fit along the increasing part too.

Figure 14 (page 102) shows the effect of internal heat release in case of experimental run No. 1. The temperature curve is not high enough to perfectly fit with the experimental curve at the maximum temperature region, but the effect is not too much.

It was found after all runs were completed that the correct values of the shape factor, ψ or SI, used by Berbano (12) had been overlooked. Figure 15 (page 103) is intended to show the effect of SI by using our LMSC-1 program with the correct value SI = .9236 instead of 1.0. Both RATIOC and the decreasing part of the temperature curves move to the right of the experimental curves. This suggests that the flow rate of each run need not to be increased by the average of 8.6% as shown in

Table VII (page 118). If the shape factor has a linear effect on the results the effect can be estimated by $(1-\psi)/\psi$ = (1-.9236)/.9236 = 8.27% which is not much different from 8.6% increase of flowrate used in the fits. Some error can also come from the error in reading the flowrator pressure gauge because 8.6% error from 10 SCFH is only about 0.86 SCFH or less than 0.3 psig. The pressure gauge can be read to 1 psig and estimated to 0.2 psig.

All the calculated RATIOC curves for activated alumina reach 1.0 after the experimental curves but these differences are slight. For activated alumina the effects of SIG are shown in Figure 16 (page 104). The higher the SIG is, the sooner the RATIOC reaches 1.0, but the starting point starts slower. The effect of the lower SIG also makes the temperature curve drop a lot sooner than the experimental one. The effects of EF1 are shown in Figure 17 (page 105). The higher the EF1 is, the sooner the RATIOC reaches 1.0, and the slope of the RATIOC curve is less at the start, but more at the end when compared to the one with lower EF1.

For activated alumina the same problem with the shape factor was found here as discussed above. The flow rates in these cases were increased by the average of 6.94% as shown in Table VIII (page 119). If the shape factor produced a linear effect then we would estimate the effect to be (1-.9045)/.9045 = 10.56%. These two percentages are different because in the bipore model the effect of shape factor may not be a linear effect.

The multiplication factors require some explanation. The diffusivity equations for D(K) were taken from Pollock's dissertation

(132). These equations had to be multiplied by 2.4 for LMS-4A and 3.0 for activated alumina. In Pollock's diffusion cell only steady state experiments were run to determine the D(K) function. In these one cannot detect blind pores because their contents are in a state of equilibrium and do not play apart in the diffusion. If SIG were known at the time of these experiments the computed value of D(K) would have been

$$D(K) = [D(K)]_{Pollock}/SIG$$

It should also be noted that in the diffusion cell used by Pollock gases flowed over the two exposed faces of discs of the sorbent. Turbulence promoting screens were placed in the gas channels to minimize gas film resistance to the point where it could be neglected in calculating the results from the diffusion cell. Thus if gas film resistance is included in D(K) then of course D(K) would be higher without this effect. Apparently this is the case.

The heat of adsorption values, YLAMDA, were taken from Horng's thesis (61). These values had to be multiplied by 1.27 for LMS-4A and 1.4 for activated alumina. Horng's values were for the isosteric heats of adsorption determined from his sorption therms fit of experimental data. Actually there are five different sorption heats (39), i.e., the "integral," Q_{int}, the "differential," $Q_{diff} = dQ_{int}/dC$, the "isothermal," $Q_{isoth} = Q_{diff} + \bar{R}T$ and the "isosteric," $Q_{isosteric} = Q_{isoth}$. The "isosteric heat of adsorption" is determined from the equation of the sorption isostere as was done by Horng. The "Calorimetric heat of

adsorptions" will have a value between Q_{diff} and Q_{isoth} depending on conditions of the experiment. The Q_{diff} for macroporous adsorbents such as activated alumina is very high at low concentrations and drops rapidly toward the latent heat of condensation as the saturated sorbent condition is approached. The integral heat of adsorption is the integral average of this range of values. For zeolitic solids such as Drierite and LMS-4A the $Q_{diff} = Q_{int}$ because there is little change of Q_{diff} with concentration. Thus if Horng's value needs correction this should be the least for LMS-4A and of course it is. The actual difference of course remains a subject for further investigation.

The coefficient of heat transfer by radiation from the tube wall, HR, was taken from Berbano's dissertation (12). This coefficient had to be multiplied by 0.5 for both LMS-4A and activated alumina. This suggests that the repolishing of the inside wall of the aluminum casing and both sides of the two Nickel radiation shields reduced the radiation heat loss. There may also be some effect due to better control of guard heat.

The gas phase heat transfer film coefficient, CAYG, was calculated using the Lewis relation. This coefficient had to be multiplied by 3.0 for both LMS-4A and activated alumina. This value can vary widely due to the method of calculation as indicated in Treybal (151). It may not have to be multiplied by any multiplication factor if the correct relation was found and used. This too remains a subject for further investigation.

The computational speed was drastically improved through the high-speed explicit programming and the use of new functions to evaluate

equilibrium and diffusivities. All the computer programs were run by IBM 360/65. The execution time (not total CPU time) of the first program that was run with constant diffusivities D(K) = PE = 1.D-5 was 0.2275 sec. per each increment of J loop with the index parameter for radial increment, K, equal to 10 and the execution time of the last program that used the same constant diffusivities was 0.0347 sec. per each J increment with K = 16. The first program was run with WATFIV and the last one with FORTRAN G. The execution time of the program with variable K from 14 to 224 was 0.1154 sec. and 0.2133 sec. per J increment with FORTRAN G and the latest one was 0.0782 sec. and 0.1437 sec. per J increment with FORTRAN H and K = 30 for LMS-4A and activated alumina, respectively.

The long time approximation which was developed by Jury was used at the end of LMS-4A run No. 3 and also at the end of all activated alumina runs except run No. 4 and 8. If the factor that controlled the switching time to long time approximation, KL, was set lower the execution time would be faster. The optimum KL has not been determined yet and this again remains a subject for further investigation.

The accuracy of the results also depend upon the time increment, Δt, which was 3 sec. for LMS-4A and 12 sec. for activated alumina. If we reduce this time increment, the results will be more accurate but the execution time will be longer.

The results of these fittings could be slightly better if the turn around time of the computer was improved. The 6-8 weeks turn around

time for the 300 min. CPU job made it difficult to adjust parameters for better results. Frequent system crashes and constant changes did not improve matters any. The university computer center is not really set up to handle large scientific problems. It is ideal for beginning students with 10 sec. to 1 min. runs. We are, however, deeply grateful to the staff and management of the computing center for their continuous cooperation in improving this situation wherever humanly possible to do so.

LIST OF REFERENCES

LIST OF REFERENCES

1. Acrivos, A., "Method of Characteristic Technique: Application to Heat and Mass Transfer Problems," Ind. Eng. Chem., 48, 703-710 (1956).

2. Acrivos, A., "On the Combined Effect of Longitudinal Diffusion and External Mass Transfer Resistance in Fixed Bed Operation," Chem. Eng. Sci., 13, 1-6 (1960).

3. Ahlberg, J. E., "Rates of Water-Vapor Adsorption from Air by Silica Gel," Ind. Chem., 31, 988-992 (1939).

4. Aleksashenko, A. A., "Determination of the Coefficient of Internal Diffusion in Porous Sorbents from a Nonlinear Adsorption Isotherm," Teor. Osn. Khim. Tekhnol., 11, 6, 924-927 (1977).

5. Amero, R. C., J. W. Moore, and R. C. Capell, "Design and Use of Absorptive Drying Units," Chem. Eng. Prog., 43, 349-370 (1947).

6. Amundson, N. R., "Solid-Fluid Interactions in Fixed and Moving Beds with Small Particles," Ind. Eng. Chem., 48, 1, 26-35 (1956).

7. Amundson, N. R., R. Aris, and R. Swanson, "On Simple Exchange Waves in Fixed Beds, "Proc. Roy. Soc., 286A, 129-139 (1965).

8. Anzelius, A., "Uber Erwarmung Vermittels durch Stromender Medein," Zeit. Angew. Math. Mech., 6, 291 (1926).

9. Astakhov, V. A., P. G. Romankov, and V. D. Lukin, "Calculation of Equilibrium Adsorption in the Gas Vapor-Microporous Adsorbent System," Zh. Prikl. Khim. (Leningrad), 49, 8, 1754-1758 (1976).

10. Babcock, R. E., D. W. Green, and R. M. Perry, "Longitudinal Dispersion Mechanisms in Packed Beds," AIChE J., 12, 922 (1966).

11. Belyanina, I. V., and V. I. Ulin, "Internal Diffusion in a Granule of Adsorbent with Microporous Formations in the Form of Parallelepipeds," Zh. Fiz. Khim., 51, 71, 1816-1818 (1977).

12. Berbano, M. C., "The Kinetics of Heat Recuperation," Ph.D. Dissertation," The University of Tennessee, Knoxville (1974).

13. Binnie, A. M., and E. G. C. Poole, "The Theory of the Single-Pass Cross Flow Heat Exchanger," Proc. Cambridge Phil. Soc., 23, 403-411 (1937).

14. Bird, R. B., W. E. Stewart, and E. N. Lightfoot, Transport Phenomena, First Edition, John Wiley & Son, Inc., N.Y. (1960).

15. Blakely, R. L., and B. N. Taylor, "Computer Analysis Techniques for Spacecraft Adsorption Beds," Paper preprint 19 C. Presented at the symposium on Adsorption—Part III, 64th National Meeting AIChE, New Orleans, La., March, 16-20 (1969).

16. Blasinski, H., and M. Amanorwicz, "Methods of Determination of the Effective Diffusion Coefficient in Porous Solids," Inz. Chem., 7, 2, 293-301 (1977).

17. Bradshaw, A. V., and E. Myers, "Heat and Mass Transfer in Fixed and Fluidized Beds of Large Particle," AIChE J., 9, 5, 590-595 (1963).

18. Braener, P., "Adsorption on Heterogeneous Surfaces on the Basis of Langmuir Models," Math.-Natuwiss. Reihe, 25, 6, 813-823 (1976).

19. Brinkley, S. R., Jr., "Heat Transfer Between a Fluid and a Porous Solid Generating Heat," J. Applied Physics, 18, 582-585 (1947).

20. Brunovska, A., P. Brunovsky, and J. Ilavsky, "Estimation of the Diffusion Coefficient from Sorption Measurements," Chem. Eng. Sci., 32, 7, 717-722 (1977).

21. Bowen, J. H., "Sizing Adsorbers to Take a High Concentration Feed," Trans. Inst. Chem. Engrs., 42, T259-T265 (1964).

22. Bunke, G., K. H. Radeke, and D. Galbin, "Modeling of Temperature Breakthrough Curves," Chem. Tech. (Leipzig), 29, 2, 92-95 (1977).

23. Carlson, A. M., "The Determination of the Diffusivities of Porous Solids," M.S. Thesis, The University of Tennessee, Knoxville (1959).

24. Carmen, P. C., and R. A. W. Haul, "Measurement of Diffusion Coefficients," Proc. Roy. Soc. (London), 222A, 109-118 (1954).

25. Carter, J. W., "A Numerical Method for Prediction of Adiabatics Adsorption in Fixed Beds," Trans. Inst. Chem. Engrs., 44, T253-T259 (1966).

26. Carter, J. W., "Developments in Adsorption Processes," Brit. Chem. Eng., 13, 229 (1968).

27. Carter, J. W., "Isothermal and Adiabatic Adsorption in Fixed Beds," Trans. Inst. Chem. Engrs., 46, T213 (1968).

28. Carter, J. W., "Some Aspects of the Prediction of Performance of a Large Air-Dryer," Tran. Inst. Chem. Engrs., 46, T222 (1968).

29. Carter, J. W., "Adsorption of Carbon Dioxide in Fixed Beds of Molecular Sieves," Trans. Inst. Chem. Engrs., 50, 69 (1972).

30. Carter, J. W., and H. Husain, "The Prediction of the Performance of Fixed Bed Adsorptive Gas Purifiers," Chem. Eng. Tech., 49, 6, 517 (1977).

31. Chao, R., and H. E. Hoelscher, "Simultaneous Axial Dispersion of Adsorption in a Packed Bed," AIChE J., 12, 271-278 (1966).

32. Chen, J. W., J. A. Buege, F. L. Cunningham, and J. I. Northan, "Scale Up of a Column Adsorption Process by Computer Simulation," I.&.E.C. Proc. Design Develop., 7, I, 26-31 (1968).

33. Chi, C. W., and D. T. Wasan, "Fixed Bed Adsorption Drying," AIChE J., 16, 1, 23-31 (1970).

34. Chihara, K., M. Suzuki, and K. Kawazoe, "Review on Mechanism of Surface Diffusion and Intracrystalline Diffusion in Adsorbent Particles in Gaseous Phase. II. Surface Diffusion," Seison Kenkyu, 29, 6, 307-320 (1977).

35. Chihara, K., M. Suzuki, and K. Kawazoe, "Review on Mechanism of Surface Diffusion and Intracrystalline Diffusion in Adsorbent Particles in Gaseous Phase," Seison Kenkyu, 29, 4, 195-203 (1977).

36. Ciembroniewicz, A., and Schulz L., "Determination of Coefficients of Diffusion of Gases in Porous Solids," Zesz. Nauk. Akad. Gorn.-Hutn. (Krakow), Gorn., 85, 47-52 (1977).

37. Collins, R. E., Modern Chemical Engineering, Vol. I, Chapter 7, Reinhold Publishing Corporation, New York (1963).

38. Crittenden, J. C., "Mathematic Modeling of Fixed Bed Adsorber," Paper preprinted, U. of Michigan, Ann Arbor (1976).

39. De Boer, J. H., The Dynamical Character of Adsorption, Clarendon Press, Oxford, England, 48-49 (1953).

40. Deitz, V. R., "Gas Adsorption," Ind. Eng. Chem., 57, 5, 49-66 (1965).

41. Derr, R. B., "Drying Air and Commercial Gases with Activated Alumina," Ind. Eng. Chem., 30, 384-388 (1938).

42. Dubinin, M. M., "New Research on Equilibriums and the Kinetics of Gas and Vapor Adsorption by Microporous Adsorbents," Usp. Khim., 46, 1, 1929-1946 (1977).

43. Eagleton, L. C., and A. K. Bliss, "Drying of Air in Fixed Bed," Chem. Eng. Prog., 49, 543-548 (1953).

44. Edwards, H. R., "A Study of Sorption Equilibrium for the Drying of a Humid Air Stream by Fixed Beds of Silica Gel and Florite," M.S. Thesis, The University of Tennessee, Knoxville (1968).

45. Furnas, C. C., "Heat Transfer from a Gas Stream to a Bed of Broken Solids," Trans. Am. Inst. Chem. Engrs., 24, 142 (1930).

46. Furnas, C. C., "Heat Transfer from a Gas Stream to a Bed of Broken Solids—II," Ind. Eng. Chem., 22, 721 (1930).

47. Furnas, C. C., "Heat Transfer from a Gas Stream to a Bed of Broken Solids," U.S. Bur. Mines Bull., 361 (1932).

48. Gamson, B. W., G. Thodos, and O. A. Hougen, "Heat, Mass and Momentum Transfer in the Flowing of Gases Through Granular Solids," AIChE Trans., 39, 1-35 (1943).

49. Garg, D. R., and D. M. Ruthven, "On Fixed Sorption Behavior of Gases with Nonlinear Equilibria," AIChE J., 19, 4, 852-853 (1973).

50. Getty, R. J., and W. P. Armstrong, "Drying Air with Activated Alumina Under Adiabatic Conditions," I.&E.C. Proc. Design Develop., 3, 60-65 (1964).

51. Gould, R. F., "Solid Surfaces and the Gas-Solid Interface," Advances in Chemistry, Series 33, American Chemical Society (1961).

52. Granville, W. H., "Some Aspects of Gas Separation," Ind. Eng. Chem., 56, 5, 32-37 (1964).

53. Gregg, S. J., and K. S. W. Sing, "The Adsorption of Gases on Porous Solids," Surf. Colloid Sci., 9, 231-359 (1976).

54. Grossman, L. V., "The Calculation of Temperature Distribution in Catalytic Converters," Trans. A.I. Chem. Engrs., 42, 535-551 (1946).

55. Gupta, A. S., and G. Thodos, "Mass and Heat Transfer through Fixed and Fluidized Beds," Chem. Eng. Prog., 58, 7, 58-62 (1962).

56. Handley, D., and P. J. Heggs, "Momentum and Heat Transfer Mechanisms in Regular-Shaped Packings," Trans. Instn. Chem. Engr., 46, T251-T264 (1968).

57. Handley, D., and P. J. Heggs, "The Effect of Thermal Conductivity of the Packing Material on Transient Heat Transfer in a Fixed Bed." Int. J. Heat & Mass Transfer, 12, 549-570 (1969).

58. Henrion, P. N., "Introduction to the Analytical Use of Gas Adsorption on Solids," Cent. Etude Energ. Nucl. (1976).

59. Hougen, O. A., and F. S. Dodge, "The Drying of Gases," Ann Arbor, Michigan, Edwards Bros., Inc., 14, (1947).

60. Hougen, O. A., and W. R. Marshall, Jr., "Adsorption from A Fluid Stream Flowing Through a Stationary Granular Bed," Chem. Eng. Prog., 43, 197 (1947).

61. Horng, J. S., "A Study of Sorption Equilibrium for Activated Alumina and Linde Molecular Sieve Structure Type 4A," M.S. Thesis, The University of Tennessee, Knoxville (1970).

62. Hubard, S., "Equilibrium Data for Silica Gel and Water Vapor," Ind. Eng. Chem., 46, 356-358 (1954).

63. Innes, W. B., "Determination of Surface Area and Pore Structure of Catalysts," Experimental Methods in Catalytic Research, Edited by R. B. Anderson, Academic Press, New York, 44-49 (1968).

64. Jaroniec, M., "A Simple Procedure for Obtaining Adsorption Isotherms of Gas Mixtures on Heterogeneous Surfaces," Colloid Polym., Sci., 255, 2, 176-177 (1977).

65. Jaroniec, M., "Adsorption of Gas Mixture on Heterogeneous Solid Surfaces. II. Adsorption Isotherms for Gaseous Mixture Whose Pure Gas Isotherms Show the Freundlich Toth and Langmuir Behavior," Colloid Polym. Sci., 255, 1, 32-34 (1977).

66. Jaroniec, M., "Adsorption of Gas Mixtures on Heterogeneous Pressure," Colloid Interface Sci., 59, 2, 230-242 (1977).

67. Jaroniec, M., and M. Borowko, "Numerical Studies of Gas Adsorption on Heterogeneous Solid Surfaces by Using the Model of Associated Adsorbate," Colloid Interface Sci., 63, 2, 362-368 (1978).

68. Jefferson, C. P., "Prediction of Breakthrough Curves in Packed Beds: I. Applicability of Single Parameter Models," AIChE J., 18, 2, 409-420 (1970).

69. Jury, S. H., "A Rate Equation for Molecular Diffusion in a Dispersed Phase," AIChE J., 3, 8J (1957).

70. Jury, S. H., "An Improved Version of the Rate Equation for Molecular Diffusion in a Dispersed Phase," AIChE J., 13, 1124-1126 (1967).

71. Jury, S. R., "Mechanically Refrigerated Ice Bath," Instruments and Control System, 40, 118-119 (1967).

72. Jury, S. H., "Numerical Solution of Systems of Mixed Partial Differential Equations Associated with Transport Phenomena with Exchange," J. Franklin Institute, 292, 203-223 (1971).

73. Jury, S. H., "The Application of a New Hybrid Computer to Large Scientific Problems," I.S.A. Trans., 11, 201-208 (1972).

74. Jury, S. H., and M. C. Berbano, "Heat Transfer in Packed Bed Heat Recuperators—I. A Precision Numerical Analysis," J. Franklin Inst., 303, 285-299 (1977).

75. Jury, S. H., and M. C. Berbano, "Heat Transfer in Packed Bed Heat Recuperators—II. The Film Coefficient for Dry Sorbent Solids," J. Franklin Inst., 303, 329-343 (1977).

76. Jury, S. H., L. P. Bosanquet, and Y. W. Kim, "Fast Response Sensing Element for a Frost Point Hygrometer," The Rev. of Sci. Inst., 35, 1634-1637 (1967).

77. Jury, S. H., and H. R. Edwards, "The Silica Gel-Water Vapor Sorption Therm," Canadian J. Chem. Engineering, 49, 663-666 (1971).

78. Jury, S. H., and H. R. Edwards, "The Florite-Water Vapor Sorption Therm," AIChE J., 18, 639-642 (1972).

79. Jury, S. H., and J. S. Horng, "The Molecular Sieve 4-A-Water Vapor Sorption Therm," AIChE J., 19, 371-372 (1973).

80. Jury, S. H., and J. S. Horng, "The Activated Alumina-Water Vapor Sorption Therm," Canadian J. Chem. Engineering, 51, 131-133 (1973).

81. Jury, S. H., Y. W. Kim, and L. P. Bosanquet, "Fast Response Frost-Dew Point Hygrometer," Anal. Chem., 38, 912-917 (1967).

82. Jury, S. H., and W. Licht, "Automatic Frost Point Hygrometer," Anal. Chem., 22, 1936-1940 (1950).

83. Jury, S. H., and W. Licht, "Drying of Gases: Adsorption Wave in Desiccant Beds," Chem. Eng. Prog., 48, 102-109 (1952).

84. Jury, S. H., and W. Licht, "Static Adsorption Isotherm for Beta-soluble Anhydrite and Humid Air," Ind. Eng. Chem., 44, 591-594 (1952).

85. Jury, S. H., M. A. Pollock, and J. W. Mattern, "The Activated Calcium Sulfate-Water Vapor Sorption Therm," AIChE J., 18, 48-51 (1972).

86. Jury, S. H., M. A. Pollock, and E. K. Kim, "The Diffusion of Moisture in Sorbent Solids—I. Diffusion Cell and Pore Diffusion," J. Franklin Inst., 303, 345-355 (1977).

87. Jury, S. H., M. A. Pollock, and E. K. Kim, "The Diffusion of Moisture in Sorbent Solids—II. Activated Alumina," J. Franklin Inst., 303, 425-436 (1977).

88. Jury, S. H., M. A. Pollock, and E. K. Kim, "The Diffusion of Moisture in Florite," AIChE Symposium Series No. 179, 74, 27-33 (1978).

89. Kasten, P. R., L. Lapidus, and N. R. Amundson, "Mathematics of Adsorption in Beds. V. Effect of Intraparticle Diffusion in Flow Systems in Fixed Beds," J. Phys. Coll. Chem., 56, 683-688 (1952).

90. Kataeva, L. I., and V. I. Ulin, "Numerical Calculation and Analysis of Kinetic Curves for Biporous Adsorbents in the Case of Linear Adsorption Isotherm. 1. Procedure for Calculating Kinetics Curves," Izv. Akad. Nank SSSR, Ser. Khim., 5, 975-979 (1977).

91. Keda, K., C. Fujino, and K. Katoh, "Heat and Mass Transfer in the Nonisothermal Fixed Bed Adsorption Column with Nonlinear Equilibrium," Textes Conf. Cadre Congr. Int., "Contrib. Calc. Electron. Dev. Genic Chim. Chim. Ind.," Soc. Chim. Ind., Paris, France, B, 45-49 (1978).

92. Keenan, J. H., F. G. Keyes, P. G. Hill, and J. G. Moore, Steam Tables: Thermodynamic Properties of Water Including Vapor, Liquid and Solid Phases (International System of Units—S.I.), a Wiley Interscience Publication, John Wiley & Son, New York (1978).

93. Kendall, B. R., "Mercury Vapor Hazards in Vacuum Laboratories," Vacuum, 16, 125-127 (1966).

94. Kim, E. K., "Sorption Kinetics and Diffusion of Water in Commercial Desiccants," Ph.D. Dissertation, The University of Tennessee, Knoxville (1973).

95. Kim, S. G., "Simulation of the Concentration Distribution in a Fixed Bed Adsorption Column Under Constant Pattern Conditions," Yongnam Taehakkyo Kongop Kisul Yonguso Yongu Pogo, 5, 1, 51-55 (1977).

96. Kim, Y. W., "Sorption Kinetics in Beds of Granular Adsorbents," Ph.D. Dissertation, The University of Tennessee, Knoxville (1968).

97. Kondis, E. F., and J. S. Dranoff, "Nonisothermal Sorption of Etane by 4A Molecular Sieves," AIChE Symp. Ser., No. 117, 67, 25 (1971).

98. Kota, K., and H. Aoki, "Adiabatic Adsorption on Desiccant Kaken Gel," Rikugaku Kenkyusha Hokoku, 34, 344-354 (1958).

99. Kreith, F., Principles of Heat Transfer, Second Edition, International Textbooks Ltd., London (1966).

100. Lason, M., and A. Nodzenski, "Porous Structure of Adsorbents and Adsorption of a Two-Component Gas Mixture," Tr. Vses. Soveshch. Adsorbentam, 4th, 1976, Edited by T. G. Plachenov, Leningr. Otd., U.S.S.R. (1978).

101. Lawson, C. G., "The Diffusion of Water Vapor Through Granular Adsorbents," M.S. Thesis, The University of Tennessee, Knoxville (1951).

102. Leavitt, F. W., "Non-isothermal Adsorption in Large Fixed Beds," Chem. Eng. Progs., 58, 54-59 (1962).

103. Lee, H., and C. W. Chi, "Carbon Dioxide Removal from Air by Sodium-X Molecular Sieve Under Nonisothermal Conditions," AIChE Symp. Ser., No. 117, 67, 84 (1971).

104. Lee, R. G., and T. W. Weber, "Isothermal Adsorption in Fixed Beds," Canadian J. Chem. Engineering, 47, 54-59 (1969).

105. Leung, P. K., and D. Quon, "A Computer Model for the Regenerative Bed," Canadian J. Chem. Engineering, 44, 26-31 (1966).

106. Lowan, A. N., "On the Problem of the Recuperator," Trans. AIChE, 914-933 (1934).

107. Maachi, R., and J. M. Vergnaud, "Study of the Law of Diffusion Governing the Adsorption of Water Vapor by Type 4A and 3A Molecular Sieves," C. R. Hebd. Siances Acad. Sci., Ser. C, 286, 6, 173-176 (1978).

108. Major, C. J., B. J. Sollami, and K. Kammermeyer, "Carbondioxide Removal from Air by Adsorbents," I.&E.C. Proc. Design Develop., 4, 3, 327-333 (1965).

109. Marcussen, L., "The Kinetics of Water Adsorption of Porous Alumina," Chem. Eng. Sci., 25, 1487-1499 (1970).

110. Masamune, S., and J. M. Smith, "Transient Mass Transfer in a Fixed Bed," Ind. Eng. Chem. Fundam., 3, 179-181 (1963).

111. Masamune, S., and J. M. Smith, "Adsorption Rate Studies Significance of Pore Diffusion," AIChE J., 10, 246-252 (1964).

112. Masamune, S., and J. M. Smith, "Adsorption Rate Studies Interaction of Diffusion and Surface Processes," AIChE J., 11, 34-40 (1965).

113. Mattern, J. W., "A Study of Sorption and Recuperation using Drierite Desiccant," M.S. Thesis, The University of Tennessee, Knoxville (1967).

114. Mauzy, P. M., "A Preliminary Study of Diffusion In and Through Porous Solids," M.S. Thesis, The University of Tennessee, Knoxville (1951).

115. Meyer, O. A., and T. W. Weber, "Nonisothermal Adsorption in Fixed Beds," AIChE J., 13, 457-465 (1967).

116. McGreavy, C., and C. Nussey, "Heat and Mass Transfer Processes in Transient Operation of Fixed Beds," Textes Conf. Cadre Congr. Int., "Contrib. Calc. Electron. Dev. Genic Chim. Chim. Ind.," Soc. Chim. Ind., Paris, France, A, 118-123 (1978).

117. Miline, D. F., and J. O. Hougen, "Thermal Conductivity of Granular Solids through which Gases are Flowing," Chem. Eng. Prog., 48, 3, 147-149 (1952).

118. Miura, K., and K. Hashimoto, "Analytical Solutions for the Breakthrough Curves of Fixed Bed Adsorbers Under Constant Pattern and Linear Driving Force Approximations," J. Chem. Eng. Jpn., 10, 6, 490-493 (1977).

119. Mondt, J. R., "International Development in Heat Transfer," Boulder Meeting, 614 (1961).

120. Nagarev, V. V., Sh. G. Enikev, Yu. I. Shumyatskii, N. S. Torocheshnikov, and V. I. Ermakov, "Calculation of Thermal Effects During Study of Adsorption Processes," VINITI, 1850-1874 (1977).

121. Nam, Y. W., and H. K. Rhee, "Asympototic Solution and Effective Dispersion Coefficient for a Fixed Bed Adsorption System," Hwahak Konghak, 15, 1, 41-49 (1977).

122. Nazarok, V. I., and L. I. Kravetskii, "Kinetics of Adsorption of Readily Adsorbable Substances in Systems with a Langmuir Isotherm. I. Numerical Problem Solution," Adsorbtsiya Adsorbenty, 5, 94-98 (1977).

123. Nazarok, V. I., Yu. M. Ostrovskii, L. I. Kravetskii, and P. A. Khinkis, "Kinetics of Adsorption of Readily Adsorbable Substances in Systems with a Langmuir Isotherm. II. Approximate Analytical Problem Solution," Adsorbtsiya Adsorbenty, 5, 98-100 (1977).

124. Novak, L. T., "A Method for the Study of Interphase Mass Transfer at Very Low Reynolds Number in Packed Beds," AIChE J., 23, 3, 398-400 (1977).

125. Nusselt, W., "Die Theories des Winderhitzers," Zeit. Ver. Dent. Ing., 71, 85 (1927).

126. Nutter, J. I., and G. Burnett, Jr., "Drying of Air by Fixed Bed Adsorption with Molecular Sieves," AIChE J., 9, 2, 202-206 (1963).

127. Nutter, J. I., and G. Burnett, Jr., "Fixed-Bed Drying of Air Using Molecular Sieves," I.&E.C. Proc. Design Develop., 5, 1, 1-4 (1966).

128. Ostrovskii, V. E., "Development of Methods for Describing Adsorption Isotherms with the Framework of the Basic Postulates of the Langmuir Theory," Usp. Khim., 45, 5, 849-876 (1976).

129. Poepelt, P., J. Koehler, and K. Pilchowski, "The Determination of Diffusion Coefficients in Solids from Sorption Data IX. Numerical Calculation of Diffusion Coefficients Using the Paterson Series Development," Z. Phys. Chem. (Leipzig), 258, 6, 1081-1087 (1977).

130. Pollock, M. A., "Diffusion in Solid Sorbents," Research Report, The University of Tennessee, Knoxville (July 1969).

131. Pollock, M. A., and S. H. Jury, "A New Approach to Numerical Integration by Means of Steady-state Flux in a Slab," J. Franklin Inst., 299, 417-431 (1975).

132. Pollock, M. A., "Kinetic Mechanisms of Diffusion in Sorbent Solids," Ph.D. Dissertation, The University of Tennessee, Knoxville (1976).

133. Pollock, M. A., and S. H. Jury, "Maximum Temperature in Fixed-bed Sorption Column and Isosteric Heats of Adsorption," J. Franklin Inst., 302, 357-365 (1976).

134. Poundorf, W., and H. W. Knipping, "Sorption of Vapors from Circulating Gas by Solid Adsorbent and the Adaptation Activated Charcoal and Silica Gel to the Determination of Small Quantities of Vapors in Exhaled Breath," Beitr. Tuberk., 68, 751 (1928).

135. Reilly, P. M., "Unsteady State Heat Transfer in Stationary Packed Beds," AIChE J., 3, 4, 513-516 (1957).

136. Rhodin, T. N., and D. L. Adams, "Adsorption of Gases on Solids," Treatise Solid State Chem., 6A, 343-484 (1976).

137. Rimpel, A. E., Jr., D. T. Camp, J. A. Kostecki, and L. N. Canjar, "Kinetics of Physical Adsorption of Propane from Helium on Fixed Beds of Activated Alumina," AIChE J., 14, 19-24 (1968).

138. Rosen, J. B., "Kinetics of a Fixed Bed System for Solid Diffusion into Spherical Particles," J. Chem. Phys., 20, 387 (1952).

139. Rosen, J. B., "General Numerical Solution for Solid Diffusion in Fixed Beds," Ind. Eng. Chem., 46, 1590 (1954).

140. Ross, S., and J. P. Olivier, Physical Adsorption, Interscience Publishers, New York (1964).

141. Ruthven, D. M., "Sorption and Diffusion in Molecular Sieve Zeolites," Sep. Purif. Methods, 5, 2, 189-246 (1976).

142. Sanlaville, J., "Adsorption of Water Vapor by Activated Alumina and the Dynamic Drying of Gases," Genie Chim., 78, 102-122 (1957).

143. Saunders, O. A., and H. S. Ford, "Heat Transfer in the Flow of Gas Through a Bed of Solid Particles," J. Iron and Steel Inst., 141, 1, 291-316 (1940).

144. Saveleva, L. V., R. I. Zamashkin, L. N. Savelev, and G. V. Dvoretskii, "Possibility of Separating Vapor-Air Mixtures on Carbon Molecular Sieves," Poluch. Anal. Chist. Veshchestv, 2, 53-55 (1977).

145. Schumann, T. E. W., "Heat Transfer: A Liquid Flowing Through a Porous Prism," J. Franklin Inst., 208, 405 (1929).

146. Shestopalov, V. V., V. M. Kisarov, and R. Ya. Fisher, "Algorithm for the Calculation of Adsorption Desorption Processes in a Fixed Bed of a Sorbent," Khim. Prom. St., 6, 449-451 (1976).

147. Smith, D. M., "Mean Temperature Difference in Cross Flow," Engineering, 138, 479-481 (1934).

148. Smith, J. M., Chemical Engineering Kinetics, Second Edition, McGraw-Hill Book Co., Inc., N.Y. (1970).

149. Thomas, G., "Mechanism of Gas Fixation on a Zeolite, Adsorption Thermodynamics of One Gas," J. Chem. Phys., 73, 11, 967-974 (1976).

150. Tien, C., and G. Thodos, "Adsorption Kinetics in Fixed Beds with Nonlinear Equilibrium Relationships," AIChE J., 11, 845-847 (1965).

151. Treybal, R. E., Mass Transfer Operations, McGraw-Hill Book Company, Inc., New York (1955).

152. Vermeulen, T., "Separation by Adsorption Methods," Advan. Chem. Eng., 2, 147-208 (1958).

153. Voloshchuk, A. M., V. A. Gorlov, M. M. Dubinin, I. T. Erashko, P. P. Zolotarev, and V. I. Ulin, "Kinetics of Adsorption in Biporous Adsorbents in the Case of Sharply Convex Isotherms of Adsorption," Adsorbenty, Ikh. Poluch., Svoistva Primen., Tr. Vses. Soveshch. Adsorbentam, 4th 1976, Edited by T. G. Plachenov, "Nauka," Leningr. Otd., Leningrad, USSR, 98-102 (Pub. 1978).

154. Von Rosenberg, D. U., R. P. Chambers, and G. A. Swan, "Numerical Solution of Surface Controlled Fixed Bed Adsorption," Ind. Eng. Chem., Fundam., 16, 1, 154-157 (1977).

155. Weber, T. W., and R. K. Chakravorti, "Pore and Solid Diffusion Models for Fixed Bed Absorbers," AIChE J., 20, 228-238 (1974).

156. Washburn, E. W., "The Vapor Pressures of Ice and Water Up to 100°C," International Critical Tables, 3, 210-212 (1928).

157. Watson, J. E., "An Investigation of Diffusion In and Through Porous Solids," M.S. Thesis, The University of Tennessee, Knoxville (1951).

158. Wicke, E., "Empirische und Theoretische Untersuchungen der Sorptions-ges hwindigkeit von Gases an Porösen Stoffen," Kolloid Z., 86, 167, 296 (1939).

159. Wicke, E., "Untersuchung über Ad und Desorptionvorgänge in Kornigen, Durchströmen Adsorber Schicten," Kolloid Z., 93, 129 (1940).

160. Zolotarev, P. P., L. I. Kataeva, and V. I. Ulin, "Numerical Calculation and Analysis of the Kinetic Curves for Biporous Adsorbents in the Case of Linear Adsorption Isotherms. Part 2. Analysis of the Results," Izv. Akad. Nauk SSSR., Ser. Khim., 12, 2657-2661 (1977).

161. Zolotarev, P. P., V. M. Starov, and V. I. Ulin, "Internal Diffusion in a Biporous Adsorbent in the Case of a Rectangular Adsorption Isotherm. 3. Exact Integral Equation for the Adsorption Wave Front Boundary," Izv. Akad. Nauk. SSSR, Ser. Khim., 5, 980-985 (1977).

162. Zolotarev, P. P., and V. I. Ulin, "Internal Diffusion in a Biporous Adsorbent in the Case of Rectangular Adsorption Isotherm. 1. Formulation of the Problem and Principal Equations," Izv. Akad. Nauk. SSSR, Ser. Khim., 3, 500-505 (1977).

163. Zolotarev, P. P., and V. I. Ulin, "Internal Diffusion in a Biporous Adsorbent in the Case of Rectangular Adsorption Isotherms. 2. Solution of the Problem for Approximate Kinetic Functions of Microporous Formations," Izv. Akad. Nauk SSSR, Ser. Khim., 3, 505-510 (1977).

APPENDICES

APPENDIX A

PREPARATION OF SAMPLES

Both activated alumina (Alcoa F-1) and Linde molecular sieve-4A were prepared from new materials, and from the same containers that were used before in the previous research. LMS-4A samples were ground because they were pellets. Each of the desiccants was classified using Tyler sieve screens to select the desired sizes 8/10, 12/14 and 16/20 mesh. The roto-tap at the Geology department was used to shake the screens. The classification time was 3 hours.

After each desiccant was prepared, the apparent solid density, external void fraction, internal void fraction, particle count, average particle radius, the surface area per unit bed volume, and the initial vapor pressure of moisture in the regenerated bed were all measured in laboratory 316. Prior to the determination of these physical properties, all the samples were dried in the oven for 15 hours at 300^{o}F.

Three methods were applied to determine the volume of the granules: the mercury displacement method which was used by Berbano (12), the wet cloth method which was used by E. K. Kim (94), and the Di-n-butyl Phthalate displacement method which was suggested by Dr. Jury. The details of each method follow.

The mercury displacement method (148) was used in the measurement of the apparent solid density and the void fraction of the bed. The procedure is as follows: 30cc. of granules was carefully measured in the 100 cc. measuring cylinder which has almost the same diameter as the

polystyrene bed holder. This amount of granules was weighed with the Sarterius balance, and then was put into the oven and weighed periodically until the weight did not change. The sample was introduced and pressed into a 50 cc. special designed syringe containing 25 cc. of mercury. The volume of mercury displaced was measured. The weight of the sample of particles divided by the volume of mercury displaced was the apparent solid density, ρ_s, that is

ρ_s = weight of sample, W_S/volume of displacement mercury, V_H

The void fraction, ϵ, was calculated from the relation

ϵ = 1 - volume of displaced mercury, V_H/volume of bed, V_B

where here the volume of displaced mercury, V_H, is the same as the volume of the weighed sample. This procedure for the estimation of ρ_s and ϵ was repeated three times for each size of sample and the average values calculated are shown in Table X. To make sure that no air pockets were trapped between the sample particles before reading the mercury displacement, the syringe shaft was pushed and pulled to move the sample particles up and down in the mercury column at least eight times. In addition one must be careful in working with the mercury as pointed out by Kendall (93) on account of its relatively high vapor pressure of 1 micron at room temperature. Good air flow is required.

The wet cloth method is described in Innes (63). Distilled water was used. The basic principles of this method to determine the internal

Table X. Physical Properties of the Adsorbent Sample.

Properties	LMS-4A			Activated Alumina		
	8/10 mesh	12/14 mesh	16/20 mesh	8/10 mesh	12/14 mesh	16/20 mesh
Average solid density, ρ_s, lb/ft^3						
- by mercury displacement	*	*	*	99.7308	101.0756	100.6854
- by wet cloth method	77.9088	77.0989	78.9076	103.4197	105.4494	105.0591
- by Di-n-butyl Phthalate	76.286	70.667	69.793	102.5738	104.3592	104.2031
External void fraction, ε, ft^3 void/ft^3 bed						
- by mercury displacement	*	*	*	0.4245	0.4307	0.4353
- by wet cloth method	0.460	0.464	0.466	0.4225	0.4308	0.4445
- by Di-n-butyl Phthalate	0.433	0.454	0.470	0.4255	0.4306	0.4376

Table X (continued)

Properties	LMS-4A			Activated Alumina		
	8/10 mesh	12/14 mesh	16/20 mesh	8/10 mesh	12/14 mesh	16/20 mesh
Internal porosity, θ_i, ft^3 pore/ft^3 solid						
- by wet cloth method	0.481	0.477	0.495	0.5015	0.4360	0.4510
- by Di-n-butyl Phthalate	0.531	0.578	0.581	0.5421	0.5551	0.5592
Number of particles per cc. of bed	107	322	1110	140	374	1329
Average particle radius, R, ft.	.3491D-2	.2412D-2	.1595D-2	.3242D-2	.2341D-2	.1534D-2
Water content of dry bed, W, gm H_2O/gm solid	.8362D-2	.6005D-2	.4228D-2	.3604D-2	.3312D-2	.3111D-2
Partial pressure-temperature coordinate, X, consistent units	.8763D 7	.6196D 7	.4311D 7	.1946D-1	.1782D-1	.1670D-1
Initial partial pressure, BEDPI, mm.Hg	.1875D-2	.1326D-2	.9227D-3	.1381D-2	.1110D-2	.9448D-3

Table X (continued)

Properties	LMS-4A			Activated Alumina		
	8/10 mesh	12/14 mesh	16/20 mesh	8/10 mesh	12/14 mesh	16/20 mesh
Average surface area, a_v, ft^2 (with $\psi = 1$)	464.0	666.6	1004.5	532.5	729.5	1104.4
Shape factor, ψ		0.9236			0.9045	
Specific heat of granules, C ρ_s, Btu/lb ^oF		0.230			0.183	
Solid thermal conductivity, $\bar{k}_s$ Btu/hr ft ^oF		0.084			0.0745	
Berbano's average solid density, ρ_s, lb/ft^3		83.681			100.451	
E. K. Kim's average solid density, ρ_s, lb/ft^3		83.95			98.62	

Note: * = Unknown

porosity, θ_i, the apparent solid density, ρ_s, and the external void fraction, ε, of the samples are summarized as follows:

θ_i = internal void volume, V_{vi}/volume of displaced water, V_H

ρ_s = dry weight of sample, W_s/volume of displaced water, V_H

ε = 1-volume of displaced water, V_H/volume of bed, V_B

After measureing the volume of bed, V_B, and the dry weight, W_s, as discussed before the internal void volume, V_i, and the volume of displaced water were determined by the following procedure:

1. The granules were saturated with distilled water by boiling in distilled water for 4 hours and were allowed to cool down to room temperature over night. This duration of time is necessary for the complete saturation of the granules.

2. The excess water was drained by decantation and the granules were transfered into a paper towel and the excess water remaining at the granule interfaces was removed.

3. The wetted weight of the granules, W_w, was measured. Thus the internal void volume, V_{vi}, could be computed from the relation

$$V_{vi} = (W_w - W_s)/\rho_{H_2O}$$

where ρ_{H_2O} is the density of water at room temperature.

4. The volume of the sample or the volume of displaced water, V_H, was measured by placing the granules in a graduated cylinder containing a known volume of distilled water. The difference between the volume of water before and after placing was the desired volume, V_H. To

make sure that no air pockets were trapped between the sample particles before reading the water displacement, a stirrer was used to stir the granules.

After all these values were determined, the internal porosity, θ_i, the apparent solid density, ρ_s, and the external void fraction, ε, of the samples were calculated from the relations shown above. This procedure was repeated three times for each size of sample and the average values calculated are shown in Table X.

The Di-n-butyl Phthalate method is exactly the same as the wet cloth method described above except distilled water is replaced by Di-n-butyl Phthalate. The results calculated are shown in Table X.

G. M. Lawson, a part-time employee, assisted us in measuring the physical properties of LMS-4A. He used the wet cloth and the Di-n-butyl Phthalate displacement methods. We used the results of the wet cloth method in our calculations because they showed the best agreement among repeated measurements. The data of the mercury displacement method were used in the calculations of activated alumina because of the same reason. The average density of LMS-4A or activated alumina should be the same no matter what the granule size, the average density of the size 12/14 mesh which was used 4 out of 6 runs was assumed to represent the average density in all the calculations of each granule. It is noticeable that the average solid density, ρ_s, and the external void fraction, ε, determined by the wet cloth is the highest one because the paper towel removed too much water from the granules, not only the excess water remaining at the granule interfaces. For the Di-n-butyl Phthalate displacement method, it is slower and harder to remove the excess

Di-n-butyl Phthalate so the calculated values are lower and not well agreed among repeated measurements. The mercury displacement method is suggested to be the best method.

The average particle radius for each size of the sample was determined by counting the sample particles of known volume. The average radius was calculated from the following relations:

$$V_G = n\ 4\pi R^3/3 = 1 - \varepsilon$$

$$R = [3(1 - \varepsilon)/(4\ n\pi)]^{1/3}$$

where V_G = volume of particles/volume of bed

n = number of particles/volume of bed

R = average radius of particle

ε = external void fraction of bed

The results are shown in Table X.

With both the external void fraction and the average particle radius already measured, one could then calculate the interstitial surface area per unit bed volume, a_v, for each size of sample particles from the relation

$$a_v = 3(1 - \varepsilon)/(R\psi)$$

where the shape factor ψ was assumed equal to 1 for all the calculated results as discussed in Chapter VIII. Later it was realized that the values are available in Berbano's dissertation (12).

The values for specific heat were taken from the literature, and the thermal conductivity of granules, $\bar{k}_s$, for LMS-4A and activated alumina were obtained from the thermal conductivity approximation method of Moline and Hougen (117) which was calculated by Berbano. These values are shown in Table X.

The initial vapor pressure of moisture in the regenerated bed was measured using the isothermal bed designed by Edward (44). The desiccant sample is placed in a sample holder which is an aluminum capsule that has a fixed Tyler 32 mesh screen on the bottom end and a removable one on the top end. This sample holder was designed to slide into and out of the bed support tube with a clearance of 0.015 in. The bed support tube is surrounded by the bed wall heater which acts as a constant temperature shield between the sample and the room, thus maintaining the sample at the desired temperature. The bed wall temperature is monitored by a thermocouple that is connected to a Speedomax W recorder, and this temperature can be adjusted by hand via a variac. Outside of the bed wall heater is the insulation which is used to prevent the heat loss. The inlet and outlet air temperatures were monitored by two thermocouple assemblies. The outlet air thermocouple assembly is attached to the bed cap, and both cap and thermocouple assembly were removed as a unit when the sample holder was taken out of the bed for weighing. The miniature air heater is used to control the inlet air temperature. This temperature is monitored by a thermocouple that is connected to an Esterline Angus recorder, and this temperature can be adjusted by hand via a variac.

To calculate the initial vapor pressure, the water content of the granules at initial condition has to be determined first. This was done by passing 20 SCFH of low air at 190°F through the granules in the sample holder and periodically weighing until the weight was constant, this weight, after subtracting the weight of the sample holder, was assumed to be the dry weight of granules. Then the temperature was reduced to 78°F, and the granules in the sample holder were periodically weighed again until the weight was constant. The difference between these two weights divided by the dry weight of granules was the water content of the granules, W. Then it was changed to partial pressure-temperature coordinate, X, and then partial pressure, P or BEDPI, by the sorption therms shown in Table II, p. 66. The calculated values of W, X, and BEDPI are shown in Table X.

The average regeneration time was the combination of time that used to dry the granules with dry air at 190°F and 78°F, which are about 36 hours for LMS 4-A and 72 hours for activated alumina. But in practice, these drying times were longer and the frost point temperature was checked to make sure that it was below -105°F before each experimental run was started.

APPENDIX B

MECHANICAL-OIL DIFFUSION PUMP AND VACUUM CONTROLLER

The oil diffusion pump is used to evacuate space around the bed container-enclosure for the purpose of attaining an adiabatic condition in the percolator bed. The pump is a Consolidated Vacuum Company Type VMF-10 pump which has an ultimate pressure of $1x10^{-6}$ Torr and a limiting forepressure of 0.1 Torr. The rating of the diffusion pump heater is 135 W., 115 V. The mechanical pump, which serves as back-up pump, is a Duo-seal No. 1400B type with a motor rating of 1/3 HP and 1725 RPM. For the oil diffusion pump fluid 55 milliliters of Octoil (Di-octyl Phthalate) was used.

The automatic vacuum controller is designed for the automation and safe operation of the oil diffusion pump. The purposes of this vacuum controller were:

1. Normal open-START button.
2. Normal shut down-STOP button.
3. Automatic shut down if the pot of the diffusion pump is too hot.
4. Automatic shut down if the cooling water flowrate is too small and the effluent water temperature rises above a specified value which will cause the low temperature thermostat to open.

This vacuum controller was designed by Dr. Jury and first constructed by E. K. Kim, but it did not operate properly until it was debugged and rebuilt by the author. Some bad components and wrong wiring caused the

trouble. It is intended here to describe the details of this controller which is shown in Figure 30. The principal features of the vacuum control systems are:

1. A Hastings-Raydist thermocouple vacuum guage, Model DV-23.

2. A Hastings-Raydist Controller, Model CVH-3, which has a control pressure range 0-5 Torr.

3. Four relays mounted on an aluminum chassis.

4. A Veeco vacuum valve, No. SV-62, which will open when the mechanical pump is started.

5. Two Fenwal bimetallic thermal switches; one is at the effluent end of the cooling water and the other one is at the bottom of the oil diffusion pump heater.

6. A solenoid valve, Automatic Switch Company, No. 8262 C22.

7. A solenoid relief valve, Automatic Switch Company, No. Air JS-346B, which is used to prevent any backflow of the oil from the oil diffusion pump when the whole system is shut off.

The vacuum controller panel is mounted in a standard 19-inch relay rack. Operation of the vacuum system is initiated by pressing the "start" button on the panel and this will automatically start the mechanical pump. When the set point pressure of 0.35 Torr is reached, the oil diffusion pump heater automatically turns on, and minimum system pressure (pegging) is attained after about 20 minutes from start-up. With the installation of a Hoke bellows valve near the vacuum hook-up for the percolator bed, one can isolate the bed and do work on it, e.g. change the bed granules, without necessarily shutting off the

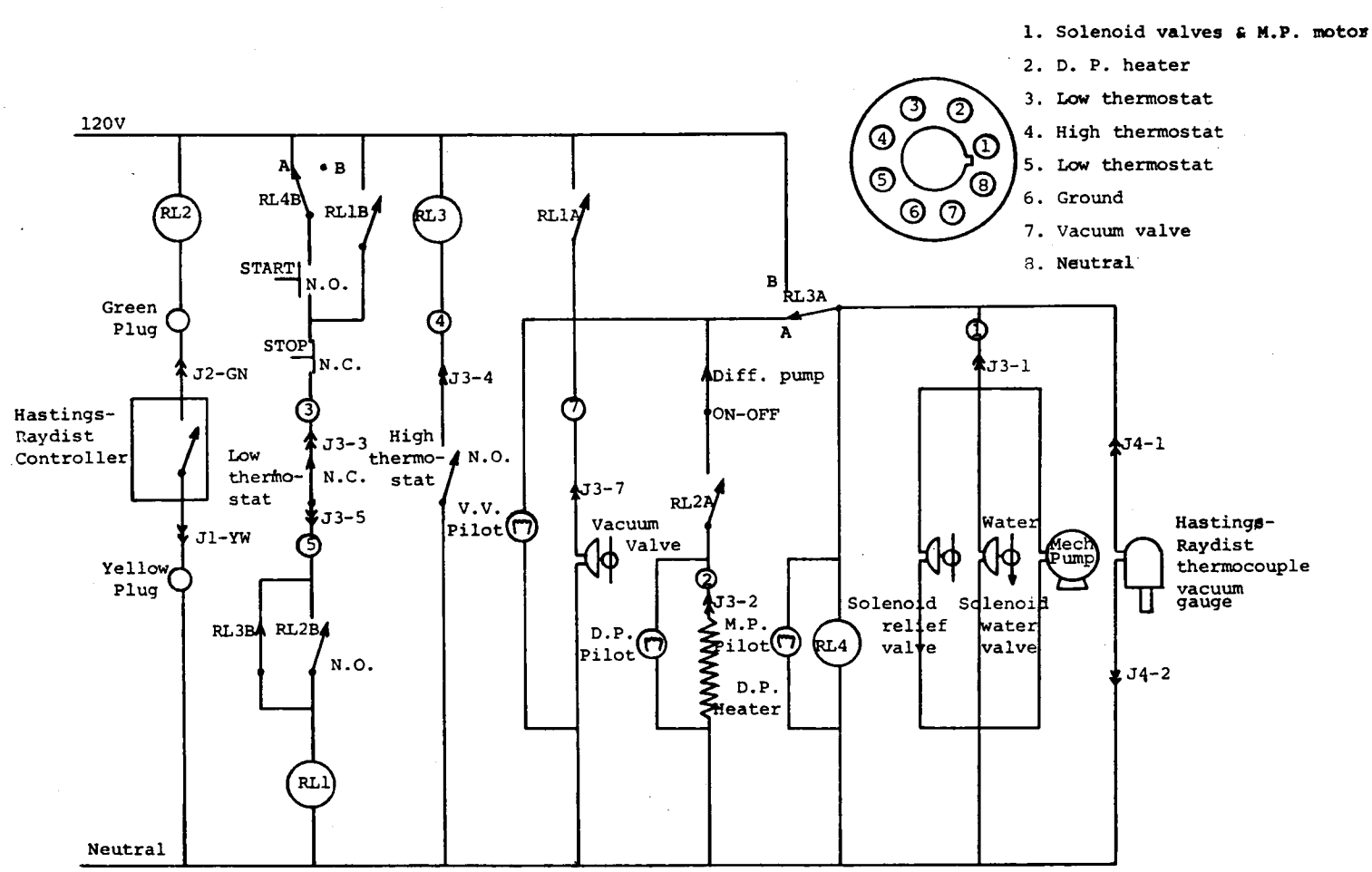


Figure 30. Schematic Diagram of the Vacuum Control System.

vacuum system. After the "stop" button is pushed to shut off the system, the oil diffusion pump and the vacuum valve are shut off first. The mechanical pump continues working until the diffusion pump heater temperature drops down to about 85^{o}F before the system automatically shuts off, which causes the solenoid relief valve to open and the solenoid cooling water valve to close.

The controller has four relays in it as follows:

Relay No. 1 responds to the START button and turns on power. It also responds to reset loop in general.

Relay No. 2 responds to the Hastings-Raydist vacuum guage when vacuum is below the set point.

Relay No. 3 responds to the high temperature thermostat when the oil diffusion pot temperature is above the set point which is a little above the ambient temperature. This insures that the mechanical pump, cooling water and relief valve cannot deactivate until the pot is cooled back down. The high temperature thermostat must be normally open.

Relay No. 4 responds to relay No. 1 to insure that START button remains inactive during operation.

The reset loop consists of the following:

1. START button.
2. STOP button.
3. Low temperature thermostat.
4. Coil RL1 and switches RL4B, RL1B, RL3B, and RL2B.

Anytime this loop is opened RL1 is deactivated and the shutdown sequence is initiated. This sequence is immediate if the pot is cold. Otherwise the shut down (deactivation of mechanical pump, solenoid cooling water valve, and solenoid relief valve) is delayed until the pot has cooled down and RL3 is deactivated.

RL2B and RL3B are in parallel because in normal operation RL2B is closed and RL3B is opened. Thus if the vacuum is lost (system is opened) the RL2B opens and initiates the shut down cycle.

The low temperature thermostat will also initiate shut down if it opens because effluent cooling water becomes too hot. This will happen if the cooling water is not turned full on or if calcium in the cooling system restricts the flow of water too much.

It should be noted that if system leaks at the start then RL2 will not be activated and system will run but Hastings-Raydist guage will indicate the trouble and the oil diffusion pump heater light will not come on.

Basically the purpose of the controller is to prevent damage to the oil in the diffusion pump. It also prevents inter-mixing of oils in the diffusion pump and mechanical pump.

When all the system was completed, tests showed that the vacuum system was so good that the Hastings-Raydist guage went 1 centimeter below 0 millitorr. The electronic shop checked this guage twice and the answer was at 0 millitorr of the guage was not 0 millitor but 1×10^{-6} Torr, so for an operating pressure of 2×10^{-7} Torr the guage went down below zero.

One should not use acetone as a leak detector fluid because it will be drawn into the oil diffusion pot and contaminate the oil. If this happens all the pump system must be taken apart and cleaned.

APPENDIX C

CALIBRATION CHARTS OF WET TEST METER AND LAMINAR FLOWRATORS

The precision laminar flowrators were calibrated with the use of a wet test meter. The wet test meter, 24ft^3/hr, Precision Scientific Company, No. 63115, was first calibrated according to the weighed water method whereby the volume of air drawn through the meter for a given number of revolutions is calculated from the corresponding weight of displaced water. This procedure is discussed in Pollock's dissertation (132) as well as the method to calibrate the laminar flowrators. The calibration curve for wet test is shown in Figure 31. Three laminar flowrators were thus calibrated as shown in Figure 32 to 34 for low, intermediate, and high air supplies at room temperature, 78^{o}F, respectively. These calibration curves are presented in terms of air flow rate in SCFH as a function of the guage pressure, psig, at the exit of the air channel in the flowrators.

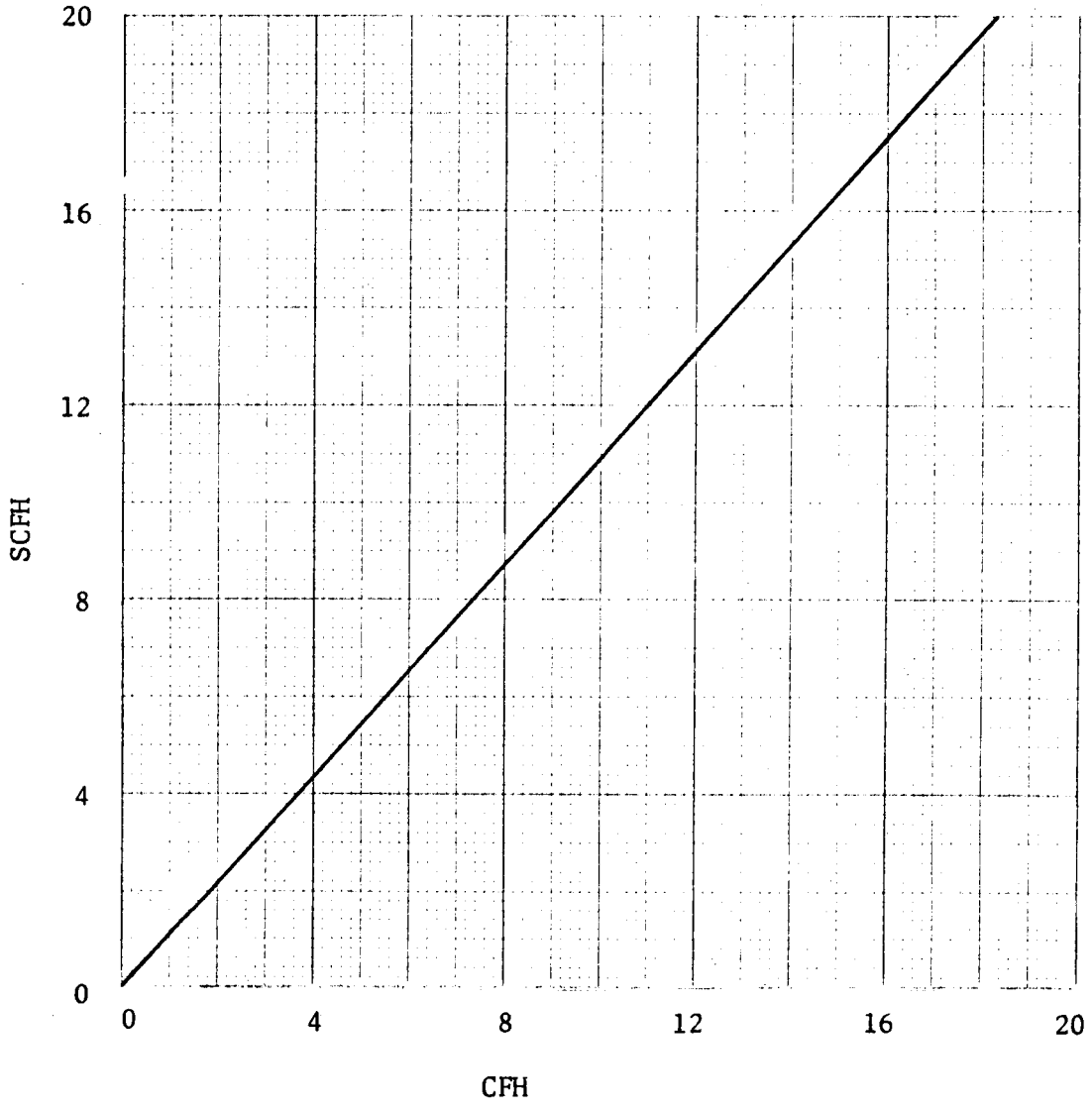


Figure 31. Calibration Curve of Wet Test Meter No. 63115 at 78°F.

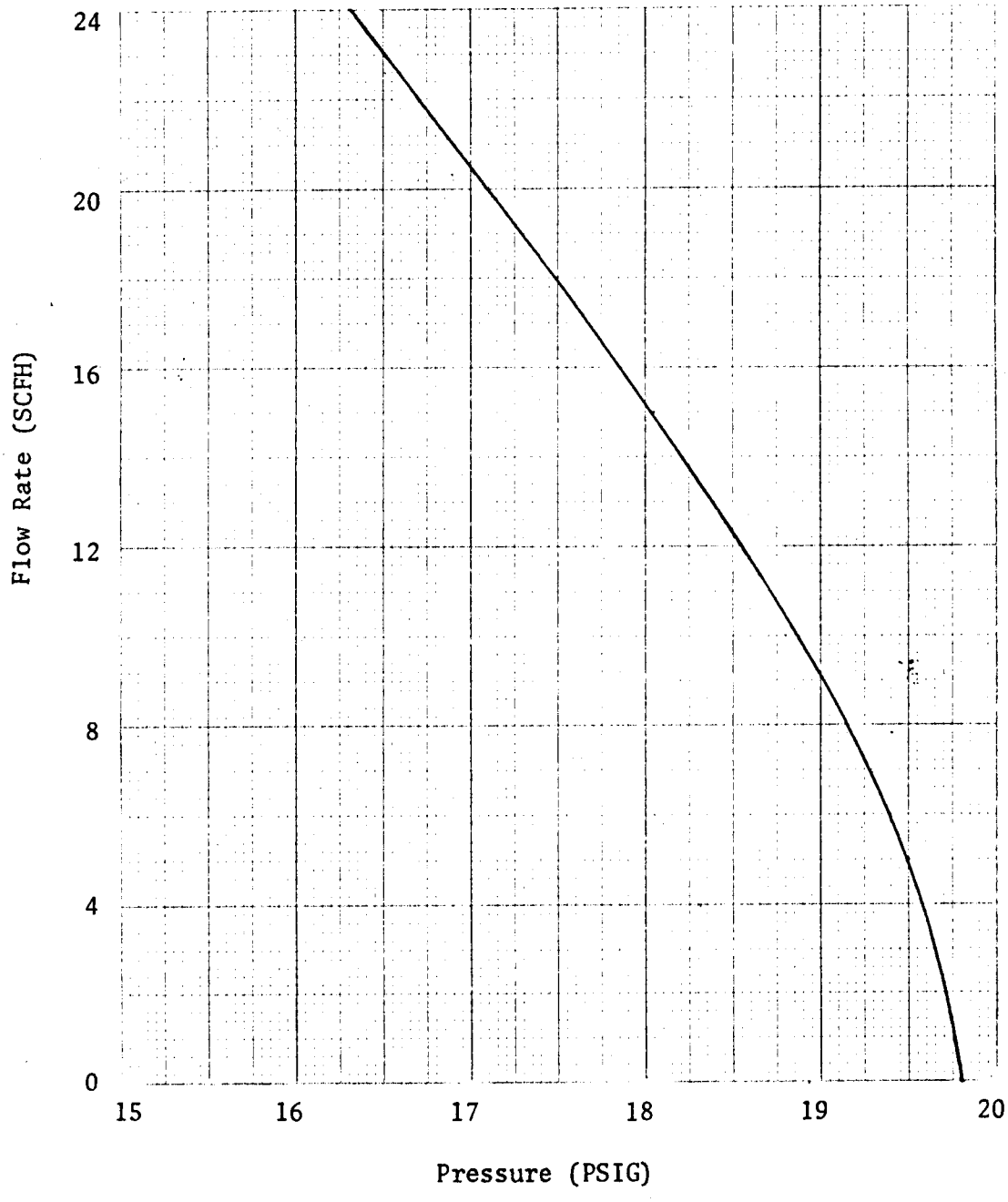


Figure 32. Calibration Curve of Laminar Flowrator No. A For Low Air Supply at 78°F.

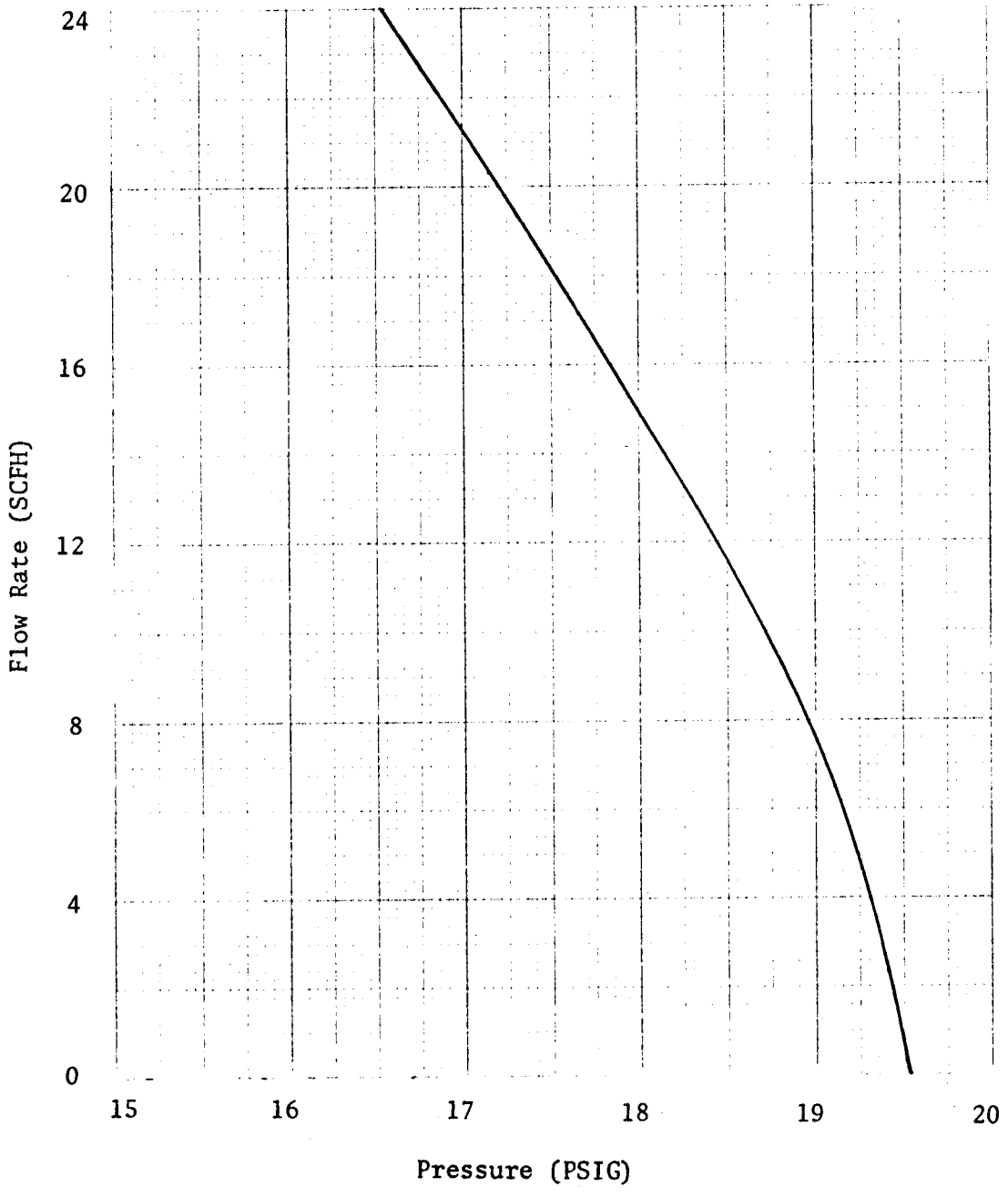


Figure 33. Calibration Curve of Laminar Flowrator No. C for Intermediate Air Supply at 78°F.

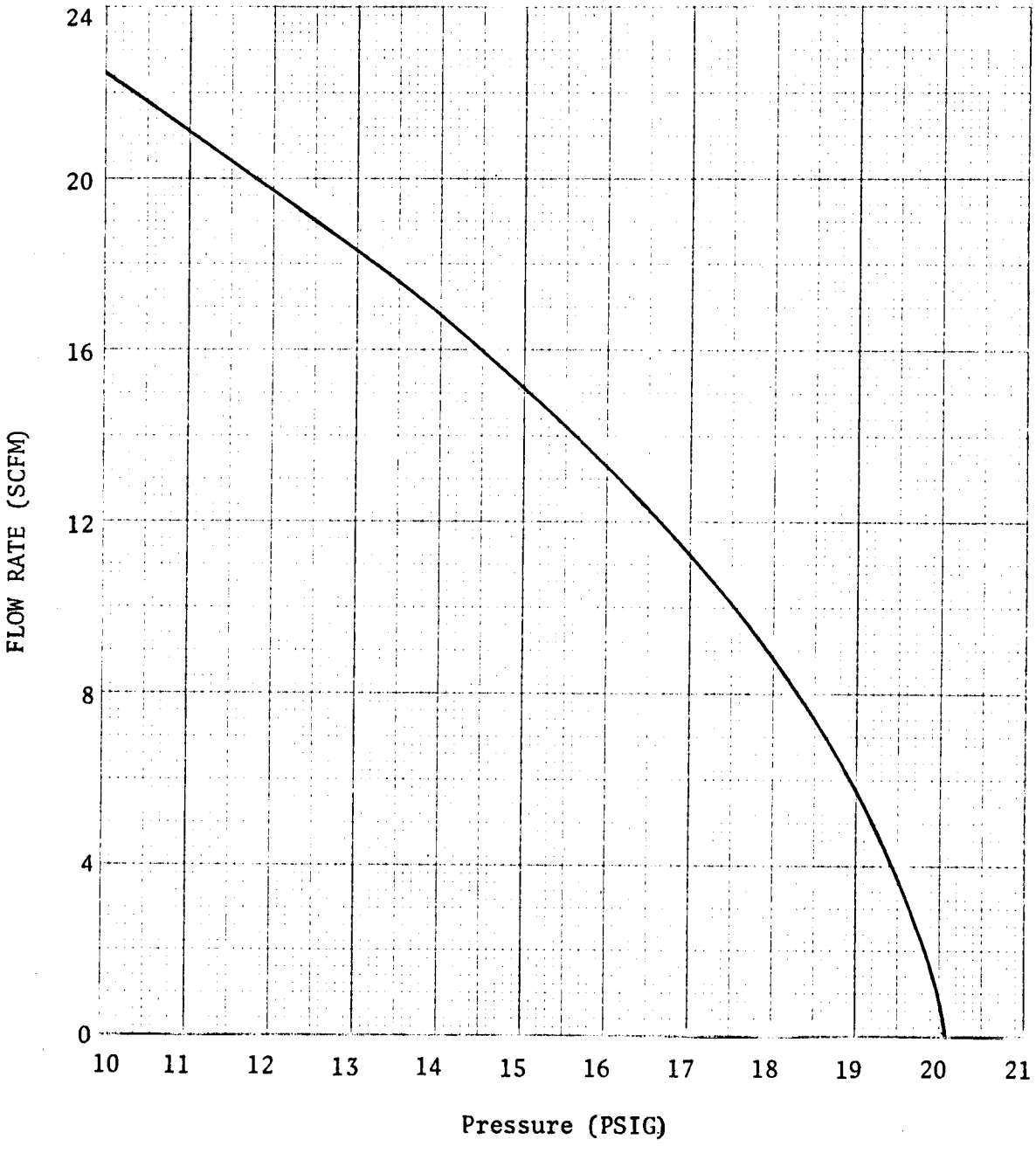


Figure 34. Calibration Curve of Laminar Flowrator No. D for High Air Supply At 78°F.

APPENDIX D

TABLES OF ORIGINAL EXPERIMENTAL DATA AND CONVERSION TO RATIOC

The primary purpose of this appendix is to present the original experimental data in terms of frost point temperature and the temperature of the effluent at each time interval of 7.5 min. The second purpose is to show the partial pressure and RATIOC which are calculated from the frost point temperature as discussed in Chapter VII. The sample of conversion for the first set of data, time=0 min., of LMS-4A run No. 1 is as follows:

The frost point temperature reading from Esterline Angus recorder	= -106.3		^{o}F
	or = -76.83		^{o}C
The vapor pressure reading from the International Critical Table (156)	= 0.0006787		mm.Hg
The average total pressure reading from the barometer	= 748.057		mm.Hg
The initial partial pressure of moisture in bed calculated in Appendix A	= 0.0013259793		mm.Hg

$$\text{RATIOC} = \frac{(0.0006787/748.057)-(0.0013259793/748.057)}{(11.3568/748.057)-(0.0013259793/748.057)}$$

$$= -0.0000570015$$

Tables XI - XVII and XVIII - XXIII show the experimental results of LMS-4A and activated alumina from run 1 - 6 for each desiccant respectively.

The operating temperature range of the hygrometer is primarily from $-100^{o}F$ to $78^{o}F$ so any temperature out of this range is unacceptable. All our starting frost point temperatures are less than $-100^{o}F$ which we converted to partial pressure and then RATIOC, the slightly negative RATIOC would appear until the frost point temperature is in the acceptable range.

Table XI. Experimental Results of LMS-4A Run No. 1 (LMSX-1).

Time Min.	Frost Pt. °F	Partial Pressure mm. Hg	RATIOC	Gas Temp. °F
.0000D 0	-.1063D 3	.6787D-3	-.5700D-4	.7880D 2
.7500D 1	-.1063D 3	.6787D-3	-.5700D-4	.1206D 3
.1500D 2	-.1063D 3	.6787D-3	-.5700D-4	.1401D 3
.2250D 2	-.1063D 3	.6787D-3	-.5700D-4	.1475D 3
.3000D 2	-.1063D 3	.6787D-3	-.5700D-4	.1507D 3
.3750D 2	-.1063D 3	.6787D-3	-.5700D-4	.1524D 3
.4500D 2	-.1063D 3	.6787D-3	-.5700D-4	.1538D 3
.5250D 2	-.1063D 3	.6787D-3	-.5700D-4	.1551D 3
.6000D 2	-.6060D 2	.2474D-1	.2062D-2	.1560D 3
.6750D 2	-.1770D 2	.3656D 0	.3208D-1	.1550D 3
.7500D 2	.1920D 2	.2513D 1	.2212D 0	.1447D 3
.8250D 2	.4470D 2	.7544D 1	.6643D 0	.1192D 3
.9000D 2	.5450D 2	.1087D 2	.9571D 0	.9550D 2
.9750D 2	.5570D 2	.1136D 2	.1000D 1	.8860D 2
.1050D 3	.5570D 2	.1136D 2	.1000D 1	.8600D 2

Table XII. Experimental Results of LMS-4A Run No. 1N (LMSX-1N).

Time Min.	Frost Pt. °F	Partial Pressure mm. Hg	RATIOC	Gas Temp. °F
.0000D 0	-.1043D 3	.8064D-3	-.4493D-4	.7880D 2
.7500D 1	-.1043D 3	.8064D-3	-.4493D-4	.1212D 3
.1500D 2	-.1043D 3	.8064D-3	-.4493D-4	.1410D 3
.2250D 2	-.1043D 3	.8064D-3	-.4493D-4	.1476D 3
.3000D 2	-.1043D 3	.8064D-3	-.4493D-4	.1501D 3
.3750D 2	-.1043D 3	.8064D-3	-.4493D-4	.1516D 3
.4500D 2	-.1043D 3	.8064D-3	-.4493D-4	.1528D 3
.5250D 2	-.1043D 3	.8064D-3	-.4493D-4	.1539D 3
.6000D 2	-.5900D 2	.2762D-1	.2273D-2	.1545D 3
.6750D 2	-.1550D 2	.4144D 0	.3572D-1	.1508D 3
.7500D 2	.1900D 2	.2489D 1	.2151D 0	.1373D 3
.8250D 2	.4410D 2	.7370D 1	.6372D 0	.1135D 3
.9000D 2	.5390D 2	.1064D 2	.9197D 0	.9360D 2
.9750D 2	.5590D 2	.1144D 2	.9889D 0	.8590D 2
.1050D 3	.5620D 2	.1157D 2	.1000D 1	.8380D 2

Table XIII. Experimental Results of LMS-4A Run No. 2 (LMSX-2).

Time Min.	Frost Pt. °F	Partial Pressure mm. Hg	RATIOC	Gas Temp. °F
.0000D 0	-.1090D 3	.5303D-3	-.6984D-4	.7780D 2
.7500D 1	-.1090D 3	.5303D-3	-.6984D-4	.9100D 2
.1500D 2	-.1090D 3	.5303D-3	-.6984D-4	.1200D 3
.2250D 2	-.1090D 3	.5303D-3	-.6984D-4	.1316D 3
.3000D 2	-.1090D 3	.5303D-3	-.6984D-4	.1380D 3
.3750D 2	-.1090D 3	.5303D-3	-.6984D-4	.1420D 3
.4500D 2	-.1090D 3	.5303D-3	-.6984D-4	.1440D 3
.5250D 2	-.1090D 3	.5303D-3	-.6984D-4	.1455D 3
.6000D 2	-.1090D 3	.5303D-3	-.6984D-4	.1465D 3
.6750D 2	-.1090D 3	.5303D-3	-.6984D-4	.1475D 3
.7500D 2	-.1090D 3	.5303D-3	-.6984D-4	.1483D 3
.8250D 2	-.1090D 3	.5303D-3	-.6984D-4	.1492D 3
.9000D 2	-.1090D 3	.5303D-3	-.6984D-4	.1504D 3
.9750D 2	-.1090D 3	.5303D-3	-.6984D-4	.1515D 3
.1050D 3	-.1090D 3	.5303D-3	-.6984D-4	.1525D 3
.1125D 3	-.1090D 3	.5303D-3	-.6984D-4	.1539D 3
.1200D 3	-.1090D 3	.5303D-3	-.6984D-4	.1549D 3
.1275D 3	-.7000D 2	.1266D-1	.9950D-3	.1555D 3
.1350D 3	-.3720D 2	.1153D 0	.1000D-2	.1560D 3
.1425D 3	-.9700D 1	.5705D 0	.4996D-1	.1540D 3
.1500D 3	.1720D 2	.2281D 1	.2001D 0	.1460D 3
.1575D 3	.3800D 2	.5819D 1	.5107D 0	.1260D 3
.1650D 3	.5170D 2	.9805D 1	.8605D 0	.1050D 3
.1725D 3	.5500D 2	.1007D 2	.9716D 0	.9250D 2
.1800D 3	.5570D 2	.1136D 2	.9968D 0	.8780D 2
.1875D 3	.5580D 2	.1139D 2	.1000D 1	.8550D 2
.1950D 3	.5580D 2	.1139D 2	.1000D 1	.8450D 2
.2025D 3	.5580D 2	.1139D 2	.1000D 1	.8400D 2

Table XIV. Experimental Results of LMS-4A Run No. 3 (LMSX-3).

Time Min.	Frost Pt. °F	Partial Pressure mm. Hg	RATIOC	Gas Temp. °F
.0000D 0	-.1045D 3	.7921D-3	-.9066D-3	.7940D 2
.7500D 1	-.1045D 3	.7921D-3	-.9066D-3	.8030D 2
.1500D 2	-.1045D 3	.7921D-3	-.9066D-3	.8090D 2
.2250D 2	-.1045D 3	.7921D-3	-.9066D-3	.8120D 2
.3000D 2	-.1045D 3	.7921D-3	-.9066D-3	.8130D 2
.3750D 2	-.1045D 3	.7921D-3	-.9066D-3	.8140D 2
.4500D 2	-.1045D 3	.7921D-3	-.9066D-3	.8140D 2
.5250D 2	-.1045D 3	.7921D-3	-.9066D-3	.8140D 2
.6000D 2	-.1045D 3	.7921D-3	-.9066D-3	.8140D 2
.6750D 2	-.1045D 3	.7921D-3	-.9066D-3	.8140D 2
.7500D 2	-.1045D 3	.7921D-3	-.9066D-3	.8140D 2
.8250D 2	-.1045D 3	.7921D-3	-.9066D-3	.8140D 2
.9000D 2	-.1045D 3	.7921D-3	-.9066D-3	.8140D 2
.9750D 2	-.1045D 3	.7921D-3	-.9066D-3	.8140D 2
.1050D 3	-.1045D 3	.7921D-3	-.9066D-3	.8140D 2
.1125D 3	-.1045D 3	.7921D-3	-.9066D-3	.8140D 2
.1200D 3	-.1045D 3	.7921D-3	-.9066D-3	.8140D 2
.1275D 3	-.1045D 3	.7921D-3	-.9066D-3	.8150D 2
.1350D 3	-.1045D 3	.7921D-3	-.9066D-3	.8150D 2
.1425D 3	-.1045D 3	.7921D-3	-.9066D-3	.8150D 2
.1500D 3	-.1045D 3	.7921D-3	-.9066D-3	.8150D 2
.1575D 3	-.1045D 3	.7921D-3	-.9066D-3	.8150D 2
.1650D 3	-.1045D 3	.7921D-3	-.9066D-3	.8150D 2
.1725D 3	-.1045D 3	.7921D-3	-.9066D-3	.8150D 2
.1800D 3	-.1045D 3	.7921D-3	-.9066D-3	.8150D 2
.1875D 3	-.1045D 3	.7921D-3	-.9066D-3	.8150D 2
.1950D 3	-.1045D 3	.7921D-3	-.9066D-3	.8150D 2
.2025D 3	-.1045D 3	.7921D-3	-.9066D-3	.8150D 2

Table XIV (continued)

Time Min.	Frost Pt. °F	Partial Pressure mm. Hg	RATIOC	Gas Temp. °F
.2100D 3	-.1045D 3	.7921D-3	-.9066D-3	.8150D 2
.2175D 3	-.1045D 3	.7921D-3	-.9066D-3	.8150D 2
.2250D 3	-.1045D 3	.7921D-3	-.9066D-3	.8150D 2
.2325D 3	-.1045D 3	.7921D-3	-.9066D-3	.8150D 2
.2400D 3	-.1045D 3	.7921D-3	-.9066D-3	.8150D 2
.2475D 3	-.1045D 3	.7921D-3	-.9066D-3	.8150D 2
.2550D 3	-.1045D 3	.7921D-3	-.9066D-3	.8150D 2
.2625D 3	-.1045D 3	.7921D-3	-.9066D-3	.8150D 2
.2700D 3	-.1045D 3	.7921D-3	-.9066D-3	.8150D 2
.2775D 3	-.1045D 3	.7921D-3	-.9066D-3	.8150D 2
.2850D 3	-.1045D 3	.7921D-3	-.9066D-3	.8150D 2
.2925D 3	-.1045D 3	.7921D-3	-.9066D-3	.8150D 2
.3000D 3	-.1045D 3	.7921D-3	-.9066D-3	.8150D 2
.3075D 3	-.1045D 3	.7921D-3	-.9066D-3	.8150D 2
.3150D 3	-.1045D 3	.7921D-3	-.9066D-3	.8150D 2
.3225D 3	-.1045D 3	.7921D-3	-.9066D-3	.8150D 2
.3300D 3	-.1045D 3	.7921D-3	-.9066D-3	.8150D 2
.3375D 3	-.1045D 3	.7921D-3	-.9066D-3	.8150D 2
.3450D 3	-.1045D 3	.7921D-3	-.9066D-3	.8150D 2
.3525D 3	-.1045D 3	.7921D-3	-.9066D-3	.8150D 2
.3600D 3	-.1045D 3	.7921D-3	-.9066D-3	.8150D 2
.3675D 3	-.1045D 3	.7921D-3	-.9066D-3	.8150D 2
.3750D 3	-.1045D 3	.7921D-3	-.9066D-3	.8160D 2
.3825D 3	-.1045D 3	.7921D-3	-.9066D-3	.8160D 2
.3900D 3	-.1045D 3	.7921D-3	-.9066D-3	.8160D 2
.3975D 3	-.1045D 3	.7921D-3	-.9066D-3	.8160D 2
.4050D 3	-.1045D 3	.7921D-3	-.9066D-3	.8160D 2
.4125D 3	-.1045D 3	.7921D-3	-.9066D-3	.8160D 2
.4200D 3	-.1045D 3	.7921D-3	-.9066D-3	.8160D 2

Table XIV (continued)

Time Min.	Frost Pt. °F	Partial Pressure mm. Hg	RATIOC	Gas Temp. °F
.4275D 3	-.1045D 3	.7921D-3	-.9066D-3	.8160D 2
.4350D 3	-.1045D 3	.7921D-3	-.9066D-3	.8160D 2
.4425D 3	-.1045D 3	.7921D-3	-.9066D-3	.8160D 2
.4500D 3	-.1045D 3	.7921D-3	-.9066D-3	.8160D 2
.4575D 3	-.1045D 3	.7921D-3	-.9066D-3	.8160D 2
.4650D 3	-.1045D 3	.7921D-3	-.9066D-3	.8160D 2
.4725D 3	-.1045D 3	.7921D-3	-.9066D-3	.8160D 2
.4800D 3	-.1045D 3	.7921D-3	-.9066D-3	.8160D 2
.4875D 3	-.1045D 3	.7921D-3	-.9066D-3	.8160D 2
.4950D 3	-.1045D 3	.7921D-3	-.9066D-3	.8160D 2
.5025D 3	-.1045D 3	.7921D-3	-.9066D-3	.8160D 2
.5100D 3	-.1045D 3	.7921D-3	-.9066D-3	.8160D 2
.5175D 3	-.1045D 3	.7921D-3	-.9066D-3	.8160D 2
.5250D 3	-.1045D 3	.7921D-3	-.9066D-3	.8160D 2
.5325D 3	-.1045D 3	.7921D-3	-.9066D-3	.8160D 2
.5400D 3	-.1045D 3	.7921D-3	-.9066D-3	.8160D 2
.5475D 3	-.1045D 3	.7921D-3	-.9066D-3	.8160D 2
.5550D 3	-.1045D 3	.7921D-3	-.9066D-3	.8160D 2
.5625D 3	-.1045D 3	.7921D-3	-.9066D-3	.8160D 2
.5700D 3	-.1045D 3	.7921D-3	-.9066D-3	.8160D 2
.5775D 3	-.1045D 3	.7921D-3	-.9066D-3	.8160D 2
.5850D 3	-.1045D 3	.7921D-3	-.9066D-3	.8160D 2
.5925D 3	-.1045D 3	.7921D-3	-.9066D-3	.8160D 2
.6000D 3	-.1045D 3	.7921D-3	-.9066D-3	.8160D 2
.6075D 3	-.1045D 3	.7921D-3	-.9066D-3	.8160D 2
.6150D 3	-.1045D 3	.7921D-3	-.9066D-3	.8160D 2
.6225D 3	-.1045D 3	.7921D-3	-.9066D-3	.8160D 2
.6300D 3	-.1045D 3	.7921D-3	-.9066D-3	.8160D 2

Table XIV (continued)

Time Min.	Frost Pt. °F	Partial Pressure mm. Hg	RATIOC	Gas Temp. °F
.6375D 3	-.1045D 3	.7921D-3	-.9066D-3	.8160D 2
.6450D 3	-.1045D 3	.7921D-3	-.9066D-3	.8160D 2
.6525D 3	-.1045D 3	.7921D-3	-.9066D-3	.8160D 2
.6600D 3	-.1045D 3	.7921D-3	-.9066D-3	.8170D 2
.6675D 3	-.1045D 3	.7921D-3	-.9066D-3	.8170D 2
.6750D 3	-.1045D 3	.7921D-3	-.9066D-3	.8170D 2
.6825D 3	-.1045D 3	.7921D-3	-.9066D-3	.8170D 2
.6900D 3	-.1045D 3	.7921D-3	-.9066D-3	.8170D 2
.6975D 3	-.1045D 3	.7921D-3	-.9066D-3	.8170D 2
.7050D 3	-.1045D 3	.7921D-3	-.9066D-3	.8170D 2
.7125D 3	-.1045D 3	.7921D-3	-.9066D-3	.8170D 2
.7200D 3	-.1045D 3	.7921D-3	-.9066D-3	.8170D 2
.7275D 3	-.1045D 3	.7921D-3	-.9066D-3	.8170D 2
.7350D 3	-.1045D 3	.7921D-3	-.9066D-3	.8170D 2
.7425D 3	-.1045D 3	.7921D-3	-.9066D-3	.8170D 2
.7500D 3	-.1045D 3	.7921D-3	-.9066D-3	.8170D 2
.7575D 3	-.1045D 3	.7921D-3	-.9066D-3	.8170D 2
.7650D 3	-.1045D 3	.7921D-3	-.9066D-3	.8170D 2
.7725D 3	-.1045D 3	.7921D-3	-.9066D-3	.8170D 2
.7800D 3	-.1045D 3	.7921D-3	-.9066D-3	.8170D 2
.7875D 3	-.1045D 3	.7921D-3	-.9066D-3	.8170D 2
.7950D 3	-.1045D 3	.7921D-3	-.9066D-3	.8170D 2
.8025D 3	-.1045D 3	.7921D-3	-.9066D-3	.8170D 2
.8100D 3	-.1045D 3	.7921D-3	-.9066D-3	.8170D 2
.8175D 3	-.1045D 3	.7921D-3	-.9066D-3	.8170D 2
.8250D 3	-.1045D 3	.7921D-3	-.9066D-3	.8170D 2
.8325D 3	-.1045D 3	.7921D-3	-.9066D-3	.8170D 2
.8400D 3	-.1045D 3	.7921D-3	-.9066D-3	.8170D 2

Table XIV (continued)

Time Min.	Frost Pt. °F	Partial Pressure mm. Hg	RATIOC	Gas Temp. °F
.8475D 3	-.1045D 3	.7921D-3	-.9066D-3	.8170D 2
.8550D 3	-.1045D 3	.7921D-3	-.9066D-3	.8170D 2
.8625D 3	-.1045D 3	.7921D-3	-.9066D-3	.8170D 2
.8700D 3	-.1045D 3	.7921D-3	-.9066D-3	.8170D 2
.8775D 3	-.1045D 3	.7921D-3	-.9066D-3	.8170D 2
.8850D 3	-.1045D 3	.7921D-3	-.9066D-3	.8170D 2
.8925D 3	-.1045D 3	.7921D-3	-.9066D-3	.8170D 2
.9000D 3	-.1045D 3	.7921D-3	-.9066D-3	.8170D 2
.9075D 3	-.1045D 3	.7921D-3	-.9066D-3	.8170D 2
.9150D 3	-.1045D 3	.7921D-3	-.9066D-3	.8170D 2
.9225D 3	-.1045D 3	.7921D-3	-.9066D-3	.8170D 2
.9300D 3	-.1045D 3	.7921D-3	-.9066D-3	.8180D 2
.9375D 3	-.1045D 3	.7921D-3	-.9066D-3	.8180D 2
.9450D 3	-.1045D 3	.7921D-3	-.9066D-3	.8180D 2
.9525D 3	-.1045D 3	.7921D-3	-.9066D-3	.8180D 2
.9600D 3	-.1045D 3	.7921D-3	-.9066D-3	.8180D 2
.9675D 3	-.1045D 3	.7921D-3	-.9066D-3	.8180D 2
.9750D 3	-.1045D 3	.7921D-3	-.9066D-3	.8180D 2
.9825D 3	-.1045D 3	.7921D-3	-.9066D-3	.8180D 2
.9900D 3	-.1045D 3	.7921D-3	-.9066D-3	.8180D 2
.9975D 3	-.1045D 3	.7921D-3	-.9066D-3	.8180D 2
.1005D 4	-.9620D 2	.1617D-2	.4946D-3	.8180D 2
.1013D 4	-.9420D 2	.1910D-2	.9923D-3	.8180D 2
.1020D 4	-.8830D 2	.3100D-2	.3012D-2	.8180D 2
.1027D 4	-.8620D 2	.3668D-2	.3978D-2	.8180D 2
.1035D 4	-.8430D 2	.4268D-2	.4996D-2	.8180D 2
.1043D 4	-.8260D 2	.4871D-2	.6020D-2	.8180D 2
.1050D 4	-.8110D 2	.5476D-2	.7047D-2	.8180D 2

Table XIV (continued)

Time Min.	Frost Pt. °F	Partial Pressure mm. Hg	RATIOC	Gas Temp. °F
.1057D 4	-.7750D 2	.7209D-2	.9989D-2	.8180D 2
.1065D 4	-.7460D 2	.8993D-2	.1302D-1	.8170D 2
.1073D 4	-.7300D 2	.1015D-1	.14990-1	.8170D 2
.1080D 4	-.7020D 2	.1247D-1	.1893D-1	.8170D 2
.1087D 4	-.6840D 2	.1422D-1	.2189D-1	.8170D 2
.1095D 4	-.6570D 2	.1721D-1	.2698D-1	.8170D 2
.1102D 4	-.6350D 2	.2015D-1	.3197D-1	.8170D 2
.1110D 4	-.6120D 2	.2368D-1	.3796D-1	.8170D 2
.1118D 4	-.5920D 2	.2724D-1	.4400D-1	.8170D 2
.1125D 4	-.5740D 2	.3082D-1	.5009D-1	.8160D 2
.1132D 4	-.5580D 2	.3437D-1	.5611D-1	.8160D 2
.1140D 4	-.5260D 2	.4260D-1	.7009D-1	.8160D 2
.1148D 4	-.5070D 2	.4846D-1	.8004D-1	.8150D 2
.1155D 4	-.4890D 2	.5451D-1	.9031D-1	.8150D 2
.1162D 4	-.4710D 2	.6135D-1	.1019D 0	.8140D 2
.1170D 4	-.4460D 2	.7210D-1	.1202D 0	.8130D 2
.1178D 4	-.4280D 2	.8094D-1	.1352D 0	.8130D 2
.1185D 4	-.4120D 2	.8963D-1	.1500D 0	.8120D 2
.1192D 4	-.3880D 2	.1043D 0	.1749D 0	.8120D 2
.1200D 4	-.3710D 2	.1159D 0	.1946D 0	.8120D 2
.1207D 4	-.3480D 2	.1335D 0	.2245D 0	.8110D 2
.1215D 4	-.3310D 2	.1480D 0	.2492D 0	.8100D 2
.1222D 4	-.3150D 2	.1632D 0	.2749D 0	.8090D 2
.1230D 4	-.3010D 2	.1777D 0	.2995D 0	.8080D 2
.1237D 4	-.2850D 2	.1955D 0	.3298D 0	.8070D 2
.1245D 4	-.2700D 2	.2135D 0	.3604D 0	.8060D 2
.1253D 4	-.2550D 2	.2333D 0	.3940D 0	.8050D 2
.1260D 4	-.2420D 2	.2518D 0	.4254D 0	.8040D 2

Table XIV (continued)

Time Min.	Frost Pt. °F	Partial Pressure mm. Hg	RATIOC	Gas Temp. °F
.1268D 4	-.2230D 2	.2811D 0	.4751D 0	.8030D 2
.1275D 4	-.2160D 2	.2926D 0	.4946D 0	.8010D 2
.1283D 4	-.2040D 2	.3137D 0	.5305D 0	.8000D 2
.1290D 4	-.1930D 2	.3340D 0	.5649D 0	.7990D 2
.1298D 4	-.1810D 2	.3578D 0	.6053D 0	.7980D 2
.1305D 4	-.1700D 2	.3802D 0	.6434D 0	.7970D 2
.1313D 4	-.1590D 2	.4046D 0	.6848D 0	.7960D 2
.1320D 4	-.1500D 2	.4256D 0	.7205D 0	.7950D 2
.1328D 4	-.1430D 2	.4430D 0	.7500D 0	.7930D 2
.1335D 4	-.1370D 2	.4575D 0	.7747D 0	.7920D 2
.1342D 4	-.1300D 2	.4760D 0	.8061D 0	.7910D 2
.1350D 4	-.1250D 2	.4892D 0	.8285D 0	.7900D 2
.1358D 4	-.1190D 2	.5055D 0	.8562D 0	.7890D 2
.1365D 4	-.1140D 2	.5195D 0	.8799D 0	.7880D 2
.1372D 4	-.1090D 2	.5345D 0	.9054D 0	.7880D 2
.1380D 4	-.1040D 2	.5490D 0	.9300D 0	.7870D 2
.1388D 4	-.9700D 1	.5705D 0	.9665D 0	.7870D 2
.1395D 4	-.9500D 1	.5764D 0	.9766D 0	.7860D 2
.1402D 4	-.9300D 1	.5836D 0	.9888D 0	.7860D 2
.1410D 4	-.9200D 1	.5866D 0	.9939D 0	.7850D 2
.1418D 4	-.9100D 1	.5902D 0	.1000D 1	.7850D 2
.1425D 4	-.9100D 1	.5902D 0	.1000D 1	.7850D 2

Table XV. Experimental Results of LMS-4A Run No. 4 (LMSX-4).

Time Min.	Frost Pt. °F	Partial Pressure mm. Hg	RATIOC	Gas Temp. °F
.0000D 0	-.1035D 3	.8636D-3	-.8975D-4	.7950D 2
.7500D 1	-.1035D 3	.8636D-3	-.8975D-4	.1185D 3
.1500D 2	-.1035D 3	.8636D-3	-.8975D-4	.1410D 3
.2250D 2	-.1035D 3	.8636D-3	-.8975D-4	.1475D 3
.3000D 2	-.1035D 3	.8636D-3	-.8975D-4	.1495D 3
.3750D 2	-.1035D 3	.8636D-3	-.8975D-4	.1515D 3
.4500D 2	-.1035D 3	.8636D-3	-.8975D-4	.1530D 3
.5250D 2	-.3440D 2	.1368D 0	.1190D-1	.1540D 3
.6000D 2	-.1590D 2	.7323D 0	.6479D-1	.1532D 3
.6750D 2	.1050D 2	.1640D 1	.1453D 0	.1467D 3
.7500D 2	.3000D 2	.4179D 1	.3705D 0	.1330D 3
.8250D 2	.4350D 2	.7204D 1	.6389D 0	.1150D 3
.9000D 2	.5110D 2	.9591D 1	.8506D 0	.9850D 2
.9750D 2	.5470D 2	.1095D 2	.9710D 0	.8700D 2
.1050D 3	.5520D 2	.1115D 2	.9889D 0	.8320D 2
.1125D 3	.5550D 2	.1128D 2	.1000D 1	.8250D 2

Table XVI. Experimental Results of LMS-4A Run No. 5 (LMSX-5).

Time Min.	Frost Pt. °F	Partial Pressure mm. Hg	RATIOC	Gas Temp. °F
.0000D 0	-.1040D 3	.8272D-3	-.8082D-5	.7900D 2
.7500D 1	-.1040D 3	.8272D-3	-.8082D-5	.1250D 3
.1500D 2	-.1040D 3	.8272D-3	-.8082D 5	.1445D 3
.2250D 2	-.1040D 3	.8272D-3	-.8082D 5	.1535D 3
.3000D 2	-.1040D 3	.8272D-3	-.8082D 5	.1542D 3
.3750D 2	-.1040D 3	.8272D-3	-.8082D-5	.1557D 3
.4500D 2	-.1040D 3	.8272D-3	-.8082D-5	.1570D 3
.5250D 2	-.1040D 3	.8272D-3	-.8082D-5	.1585D 3
.6000D 2	-.1040D 3	.8272D-3	-.8082D-5	.1593D 3
.6750D 2	-.5500D 2	.3635D-1	.2998D-2	.1605D 3
.7500D 2	.7700D 1	.1424D 1	.1204D 0	.1530D 3
.8250D 2	.5390D 2	.1064D 2	.9000D 0	.1030D 3
.9000D 2	.5680D 2	.1182D 2	.1000D 1	.9200D 2
.9750D 2	.5680D 2	.1182D 2	.1000D 1	.8500D 2

Table XVII. Experimental Results of LMS-4A Run No. 6 (LMSX-6).

Time Min.	Frost Pt. °F	Partial Pressure mm. hg	RATIOC	Gas Temp. °F
.0000D 0	-.1034D 3	.8714D-3	-.4003D-4	.7920D 2
.7500D 1	-.1034D 3	.8714D-3	-.4003D-4	.8500D 2
.1500D 2	-.1034D 3	.8714D-3	-.4003D-4	.1150D 3
.2250D 2	-.1034D 3	.8714D-3	-.4003D-4	.1310D 3
.3000D 2	-.1034D 3	.8714D-3	-.4003D-4	.1365D 3
.3750D 2	-.1034D 3	.8714D-3	-.4003D-4	.1400D 3
.4500D 2	-.1034D 3	.8714D-3	-.4003D-4	.1422D 3
.5250D 2	-.1034D 3	.8714D-3	-.4003D-4	.1435D 3
.6000D 2	-.1034D 3	.8714D-3	-.4003D-4	.1446D 3
.6750D 2	-.1034D 3	.8714D-3	-.4003D-4	.1459D 3
.7500D 2	-.1034D 3	.8714D-3	-.4003D-4	.1468D 3
.8250D 2	-.1034D 3	.8714D-3	-.4003D-4	.1480D 3
.9000D 2	-.1034D 3	.8714D-3	-.4003D-4	.1490D 3
.9750D 2	-.1034D 3	.8714D-3	-.4003D-4	.1501D 3
.1050D 3	-.1034D 3	.8714D-3	-.4003D-4	.1512D 3
.1125D 3	-.1034D 3	.8714D-3	-.4003D-4	.1525D 3
.1200D 3	-.1034D 3	.8714D 3	-.4003D-4	.1532D 3
.1275D 3	-.1034D 3	.8714D-3	-.4003D-4	.1545D 3
.1350D 3	-.1034D 3	.8714D-3	-.4003D-4	.1552D 3
.1425D 3	-.3060D 2	.1723D 0	.1506D-1	.1550D 3
.1500D 3	.8400D 1	.1476D 1	.1298D 0	.1495D 3
.1575D 3	.4180D 2	.6747D 1	.5940D 0	.1270D 3
.1650D 3	.5370D 2	.1056D 2	.9298D 0	.1010D 3
.1725D 3	.5560D 2	.1131D 2	.9961D 0	.8950D 2
.1800D 3	.5570D 2	.1136D 2	.1000D 1	.8500D 2

Table XVIII. Experimental Results of Activated Alumina Run No. 1 (ACTX-1).

Time Min.	Frost Pt. °F	Partial Pressure mm. hg	RATIOC	Gas Temp. °F
.0000D 0	-.1055D 3	.7271D-3	-.3497D-4	.8000D 2
.7500D 1	-.1055D 3	.7271D-3	-.3497D-4	.9800D 2
.1500D 2	-.1055D 3	.7271D-3	-.3497D-4	.1220D 3
.2250D 2	-.5090D 2	.4777D-1	.4262D-6	.1335D 3
.3000D 2	-.7600D 1	.6400D 0	.5836D-1	.1350D 3
.3750D 2	.1410D 2	.1961D 1	.1790D 0	.1295D 3
.4500D 2	.2640D 2	.3536D 1	.3229D 0	.1205D 3
.5250D 2	.3430D 2	.5027D 1	.4591D 0	.1130D 3
.6000D 2	.3860D 2	.5960D 1	.5444D 0	.1075D 3
.6750D 2	.4120D 2	.6594D 1	.6022D 0	.1035D 3
.7500D 2	.4320D 2	.7121D 1	.6504D 0	.1005D 3
.8250D 2	.4460D 2	.7513D 1	.6862D 0	.9820D 2
.9000D 2	.4560D 2	.7807D 1	.7130D 0	.9650D 2
.9750D 2	.4630D 2	.8012D 1	.7318D 0	.9500D 2
.1050D 3	.4700D 2	.8228D 1	.7515D 0	.9350D 2
.1125D 3	.4740D 2	.8357D 1	.7633D 0	.9230D 2
.1200D 3	.4800D 2	.8545D 1	.7805D 0	.9130D 2
.1275D 3	.4830D 2	.8644D 1	.7895D 0	.9040D 2
.1350D 3	.4870D 2	.8774D 1	.8014D 0	.8970D 2
.1425D 3	.4900D 2	.8869D 1	.8101D 0	.8900D 2
.1500D 3	.4930D 2	.8971D 1	.8194D 0	.8850D 2
.1575D 3	.4960D 2	.9074D 1	.8288D 0	.8800D 2
.1650D 3	.4980D 2	.9141D 1	.8349D 0	.8750D 2
.1725D 3	.5010D 2	.9246D 1	.8445D 0	.8700D 2
.1800D 3	.5030D 2	.9314D 1	.8508D 0	.8660D 2
.1875D 3	.5060D 2	.9414D 1	.8598D 0	.8610D 2
.1950D 3	.5080D 2	.9483D 1	.8662D 0	.8580D 2
.2025D 3	.5100D 2	.9559D 1	.8731D 0	.8550D 2

Table XVIII (continued)

Time Min.	Frost Pt. °F	Partial Pressure mm. Hg	RATIOC	Gas Temp. °F
.2100D 3	.5120D 2	.9630D 1	.8796D 0	.8510D 2
.2175D 3	.5130D 2	.9662D 1	.8825D 0	.8470D 2
.2250D 3	.5150D 2	.9734D 1	.8890D 0	.8430D 2
.2325D 3	.5170D 2	.9805D 1	.8966D 0	.8400D 2
.2400D 3	.5190D 2	.9884D 1	.9028D 0	.8380D 2
.2475D 3	.5200D 2	.9917D 1	.9058D 0	.8350D 2
.2550D 3	.5220D 2	.9989D 1	.9124D 0	.8330D 2
.2625D 3	.5230D 2	.1003D 2	.9160D 0	.8300D 2
.2700D 3	.5250D 2	.1010D 2	.9227D 0	.8280D 2
.2775D 3	.5260D 2	.1014D 2	.9258D 0	.8250D 2
.2850D 3	.5270D 2	.1018D 2	.9295D 0	.8230D 2
.2925D 3	.5290D 2	.1025D 2	.9363D 0	.8200D 2
.3000D 3	.5300D 2	.1029D 2	.9400D 0	.8180D 2
.3070D 3	.5320D 2	.1037D 2	.9469D 0	.8160D 2
.3150D 3	.5330D 2	.1040D 2	.9500D 0	.8140D 2
.3225D 3	.5340D 2	.1044D 2	.9538D 0	.8120D 2
.3300D 3	.5350D 2	.1048D 2	.9569D 0	.8100D 2
.3375D 3	.5360D 2	.1052D 2	.9607D 0	.8080D 2
.3450D 3	.5370D 2	.1053D 2	.9613D 0	.8060D 2
.3525D 3	.5380D 2	.1060D 2	.9677D 0	.8040D 2
.3600D 3	.5390D 2	.1064D 2	.9716D 0	.8020D 2
.3675D 3	.5400D 2	.1067D 2	.9748D 0	.8000D 2
.3750D 3	.5410D 2	.1071D 2	.9786D 0	.7990D 2
.3825D 3	.5420D 2	.1075D 2	.9818D 0	.7980D 2
.3900D 3	.5420D 2	.1075D 2	.9818D 0	.7970D 2
.3975D 3	.5430D 2	.1079D 2	.9857D 0	.7960D 2
.4050D 3	.5430D 2	.1079D 2	.9857D 0	.7950D 2
.4125D 3	.5440D 2	.1083D 2	.9890D 0	.7940D 2

Table XVIII (continued)

Time Min.	Frost Pt. °F	Partial Pressure mm. Hg	RATIOC	Gas Temp. °F
.4200D 3	.5440D 2	.1083D 2	.9890D 0	.7930D 2
.4275D 3	.5450D 2	.1087D 2	.9929D 0	.7920D 2
.4350D 3	.5450D 2	.1087D 2	.9929D 0	.7910D 2
.4425D 3	.5450D 2	.1087D 2	.9929D 0	.7890D 2
.4500D 3	.5460D 2	.1091D 2	.9967D 0	.7880D 2
.4575D 3	.5460D 2	.1091D 2	.9967D 0	.7880D 2
.4650D 3	.5460D 2	.1091D 2	.9967D 0	.7870D 2
.4725D 3	.5460D 2	.1091D 2	.9967D 0	.7870D 2
.4800D 3	.5470D 2	.1095D 2	.1000D 1	.7870D 2
.4875D 3	.5470D 2	.1095D 2	.1000D 1	.7870D 2
.4950D 3	.5470D 2	.1095D 2	.1000D 1	.7870D 2
.5025D 3	.5470D 2	.1095D 2	.1000D 1	.7870D 2
.5100D 3	.5470D 2	.1095D 2	.1000D 1	.7860D 2
.5175D 3	.5470D 2	.1095D 2	.1000D 1	.7860D 2
.5250D 3	.5470D 2	.1095D 2	.1000D 1	.7860D 2
.5325D 3	.5470D 2	.1095D 2	.1000D 1	.7850D 2
.5400D 3	.5470D 2	.1095D 2	.1000D 1	.7850D 2
.5475D 3	.5470D 2	.1095D 2	.1000D 1	.7850D 2
.5550D 3	.5470D 2	.1095D 2	.1000D 1	.7850D 2
.5625D 3	.5470D 2	.1095D 2	.1000D 1	.7850D 2
.5700D 3	.5470D 2	.1095D 2	.1000D 1	.7850D 2
.5775D 3	.5470D 2	.1095D 2	.1000D 1	.7850D 2
.5850D 3	.5470D 2	.1095D 2	.1000D 1	.7850D 2
.5925D 3	.5470D 2	.1095D 2	.1000D 1	.7850D 2
.6000D 3	.5470D 2	.1095D 2	.1000D 1	.7850D 2
.6075D 3	.5470D 2	.1095D 2	.1000D 1	.7850D 2
.6150D 3	.5470D 2	.1095D 2	.1000D 1	.7850D 2
.6225D 3	.5470D 2	.1095D 2	.1000D 1	.7850D 2

Table XVIII (continued)

Time Min.	Frost Pt. °F	Partial Pressure mm. Hg	RATIOC	Gas Temp. °F
.6300D 3	.5470D 2	.1095D 2	.1000D 1	.7850D 2
.6375D 3	.5470D 2	.1095D 2	.1000D 1	.7850D 2
.6450D 3	.5470D 2	.1095D 2	.1000D 1	.7850D 2
.6525D 3	.5470D 2	.1095D 2	.1000D 1	.7850D 2
.6600D 3	.5470D 2	.1095D 2	.1000D 1	.7850D 2
.6675D 3	.5470D 2	.1095D 2	.1000D 1	.7850D 2
.6750D 3	.5470D 2	.1095D 2	.1000D 1	.7850D 2
.6825D 3	.5470D 2	.1095D 2	.1000D 1	.7850D 2
.6900D 3	.5470D 2	.1095D 2	.1000D 1	.7850D 2
.6975D 3	.5470D 2	.1095D 2	.1000D 1	.7850D 2

Table XIX. Experimental Results of Activated Alumina Run No. 2 (ACTX-2).

Time Min.	Frost Pt. °F	Partial Pressure mm. Hg	RATIOC	Gas Temp. °F
.0000D 0	-.1069D 3	.6430D-3	-.4248D-4	.7900D 2
.7500D 1	-.1069D 3	.6430D-3	-.4248D-4	.8800D 2
.1500D 2	-.1069D 3	.6430D-3	-.4248D-4	.1044D 3
.2250D 2	-.1069D 3	.6430D-3	-.4248D-4	.1168D 3
.3000D 2	-.1069D 3	.6430D-3	-.4248D-4	.1240D 3
.3750D 2	-.1069D 3	.6430D-3	-.4248D-4	.1288D 3
.4500D 2	-.1069D 3	.6430D-3	-.4248D 4	.1312D 3
.5250D 2	-.1069D 3	.6430D-3	-.4248D-4	.1334D 3
.6000D 2	-.1069D 3	.6430D-3	-.4248D-4	.1334D 3
.6750D 2	-.5500D 1	.7169D 0	.6513D-1	.1320D 3
.7500D 2	.1190D 2	.1758D 1	.1598D 0	.1280D 3
.8250D 2	.2310D 2	.3029D 1	.2755D 0	.1230D 3
.9000D 2	.3080D 2	.4334D 1	.3942D 0	.1160D 3
.9750D 2	.3420D 2	.5005D 1	.3443D 0	.1136D 3
.1050D 3	.3600D 2	.5378D 1	.4892D 0	.1090D 3
.1125D 3	.3820D 2	.5864D 1	.5335D 0	.1063D 3
.1200D 3	.3970D 2	.6221D 1	.5660D 0	.1040D 3
.1275D 3	.4100D 2	.6543D 1	.5952D 0	.1028D 3
.1350D 3	.4210D 2	.6827D 1	.6211D 0	.1012D 3
.1425D 3	.4270D 2	.6984D 1	.6354D 0	.1000D 3
.1500D 3	.4330D 2	.7150D 1	.6505D 0	.9900D 2
.1575D 3	.4400D 2	.7345D 1	.6682D 0	.9790D 2
.1650D 3	.4450D 2	.7482D 1	.6807D 0	.9720D 2
.1725D 3	.4500D 2	.7627D 1	.6939D 0	.9640D 2
.1800D 3	.4540D 2	.7743D 1	.7044D 0	.9560D 2
.1875D 3	.4590D 2	.7893D 1	.7181D 0	.9500D 2
.1950D 3	.4630D 2	.8012D 1	.7289D 0	.9420D 2

Table XIX (continued)

Time Min.	Frost Pt. °F	Partial Pressure mm. Hg	RATIOC	Gas Temp. °F
.2025D 3	.4670D 2	.8139D 1	.7404D 0	.9360D 2
.2100D 3	.4700D 2	.8228D 1	.7485D 0	.9300D 2
.2175D 3	.4740D 2	.8357D 1	.7603D 0	.9240D 2
.2250D 3	.4760D 2	.8420D 1	.7660D 0	.9190D 2
.2325D 3	.4790D 2	.8511D 1	.7743D 0	.9140D 2
.2400D 3	.4820D 2	.8609D 1	.7832D 0	.9100D 2
.2475D 3	.4840D 2	.8674D 1	.7891D 0	.9060D 2
.2550D 3	.4870D 2	.8774D 1	.7983D 0	.9010D 2
.2625D 3	.4890D 2	.8839D 1	.8042D 0	.8960D 2
.2700D 3	.4910D 2	.8905D 1	.8102D 0	.8920D 2
.2775D 3	.4930D 2	.8971D 1	.8162D 0	.8880D 2
.2850D 3	.4940D 2	.9007D 1	.8194D 0	.8850D 2
.2925D 3	.4970D 2	.9104D 1	.8283D 0	.8820D 2
.3000D 3	.4990D 2	.9172D 1	.8344D 0	.8790D 2
.3075D 3	.5010D 2	.9213D 1	.8382D 0	.8760D 2
.3150D 3	.5020D 2	.9277D 1	.8440D 0	.8720D 2
.3225D 3	.5040D 2	.9345D 1	.8502D 0	.8680D 2
.3300D 3	.5050D 2	.9383D 1	.8536D 0	.8660D 2
.3375D 3	.5070D 2	.9452D 1	.8599D 0	.8620D 2
.3450D 3	.5090D 2	.9521D 1	.8662D 0	.8600D 2
.3525D 3	.5100D 2	.9559D 1	.8697D 0	.8560D 2
.3600D 3	.5110D 2	.9591D 1	.8726D 0	.8540D 2
.3675D 3	.5130D 2	.9662D 1	.8790D 0	.8520D 2
.3750D 3	.5140D 2	.9701D 1	.8826D 0	.8480D 2
.3825D 3	.5150D 2	.9734D 1	.8855D 0	.8460D 2
.3900D 3	.5160D 2	.9773D 1	.8891D 0	.8440D 2
.3975D 3	.5180D 2	.9844D 1	.8956D 0	.8420D 2
.4050D 3	.5190D 2	.9884D 1	.8992D 0	.8400D 2

Table XIX (continued)

Time Min.	Frost Pt. °F	Partial Pressure mm. Hg	RATIOC	Gas Temp. °F
.4125D 3	.5200D 2	.9917D 1	.9022D 0	.8380D 2
.4200D 3	.5210D 2	.9956D 1	.9058D 0	.8360D 2
.4275D 3	.5220D 2	.9989D 1	.9088D 0	.8340D 2
.4350D 3	.5230D 2	.1003D 2	.9124D 0	.8320D 2
.4425D 3	.5240D 2	.1006D 2	.9154D 0	.8300D 2
.4500D 3	.5250D 2	.1010D 2	.9191D 0	.8280D 2
.4575D 3	.5260D 2	.1014D 2	.9221D 0	.8260D 2
.4650D 3	.5280D 2	.1022D 2	.9295D 0	.8240D 2
.4725D 3	.5290D 2	.1025D 2	.9326D 0	.8220D 2
.4800D 3	.5300D 2	.1029D 2	.9363D 0	.8200D 2
.4875D 3	.5300D 2	.1029D 2	.9363D 0	.8180D 2
.4950D 3	.5310D 2	.1033D 2	.9394D 0	.8170D 2
.5025D 3	.5320D 2	.1037D 2	.9431D0	.8160D 2
.5100D 3	.5330D 2	.1040D 2	.9463D 0	.8150D 2
.5175D 3	.5330D 2	.1040D 2	.9463D 0	.8140D 2
.5250D 3	.5340D 2	.1044D 2	.9500D 0	.8130D 2
.5325D 3	.5350D 2	.1048D 2	.9532D 0	.8120D 2
.5400D 3	.5350D 2	.1048D 2	.9532D 0	.8110D 2
.5475D 3	.5360D 2	.1052D 2	.9569D 0	.8100D 2
.5550D 3	.5370D 2	.1056D 2	.9607D 0	.8090D 2
.5625D 3	.5380D 2	.1060D 2	.9639D 0	.8080D 2
.5700D 3	.5380D 2	.1060D 2	.9639D 0	.8070D 2
.5775D 3	.5390D 2	.1063D 2	.9671D 0	.8060D 2
.5850D 3	.5400D 2	.1067D 2	.9709D 0	.8050D 2
.5925D 3	.5400D 2	.1067D 2	.9709D.0	.8040D 2
.6000D 3	.5410D 2	.1071D 2	.9748D 0	.8030D 2
.6075D 3	.5410D 2	.1071D 2	.9748D 0	.8020D 2
.6150D 3	.5410D 2	.1071D 2	.9748D 0	.8010D 2

Table XIX (continued)

Time Min.	Frost Pt. °F	Partial Pressure mm. Hg	RATIOC	Gas Temp. °F
.6225D 3	.5420D 2	.1075D 2	.9780D 0	.8000D 2
.6300D 3	.5420D 2	.1075D 2	.9780D 0	.8000D 2
.6375D 3	.5430D 2	.1079D 2	.9818D 0	.7990D 2
.6450D 3	.5430D 2	.1079D 2	.9818D 0	.7990D 2
.6525D 3	.5440D 2	.1083D 2	.9851D 0	.7980D 2
.6600D 3	.5440D 2	.1083D 2	.9851D 0	.7980D 2
.6675D 3	.5440D 2	.1083D 2	.9851D 0	.7970D 2
.6750D 3	.5440D 2	.1083D 2	.9851D 0	.7970D 2
.6825D 3	.5450D 2	.1087D 2	.9890D 0	.7960D 2
.6900D 3	.5450D 2	.1087D 2	.9890D 0	.7960D 2
.6975D 3	.5450D 2	.1087D 2	.9890D 0	.7950D 2
.7050D 3	.5460D 2	.1091D 2	.9928D 0	.7950D 2
.7125D 3	.5460D 2	.1091D 2	.9928D 0	.7940D 2
.7200D 3	.5460D 2	.1091D 2	.9928D 0	.7940D 2
.7275D 3	.5460D 2	.1091D 2	.9928D 0	.7930D 2
.7350D 3	.5460D 2	.1091D 2	.9928D 0	.7930D 2
.7425D 3	.5460D 2	.1091D 2	.9928D 0	.7920D 2
.7500D 3	.5470D 2	.1095D 2	.9961D 0	.7920D 2
.7575D 3	.5470D 2	.1095D 2	.9961D 0	.7920D 2
.7650D 3	.5470D 2	.1095D 2	.9961D 0	.7920D 2
.7725D 3	.5470D 2	.1095D 2	.9961D 0	.7910D 0
.7800D 3	.5470D 2	.1095D 2	.9961D 0	.7910D 0
.7875D 3	.5470D 2	.1095D 2	.9961D 0	.7910D 2
.7950D 3	.5470D 2	.1095D 2	.9961D 0	.7910D 2
.8025D 3	.5470D 2	.1095D 2	.9961D 0	.7910D 2
.8100D 3	.5470D 2	.1095D 2	.9961D 0	.7900D 2
.8175D 3	.5470D 2	.1095D 2	.9961D 0	.7900D 2
.8250D 3	.5470D 2	.1095D 2	.9961D 0	.7900D 2

Table XIX (continued)

Time Min.	Frost Pt. °F	Partial Pressure mm. Hg	RATIOC	Gas Temp. °F
.8325D 3	.5480D 2	.1099D 2	.1000D 1	.7900D 2
.8400D 3	.5480D 2	.1099D 2	.1000D 1	.7900D 2
.8475D 3	.5480D 2	.1099D 2	.1000D 1	.7900D 2
.8550D 3	.5480D 2	.1099D 2	.1000D 1	.7900D 2
.8625D 3	.5480D 2	.1099D 2	.1000D 1	.7890D 2
.8700D 3	.5480D 2	.1099D 2	.1000D 1	.7890D 2
.8775D 3	.5480D 2	.1099D 2	.1000D 1	.7890D 2
.8850D 3	.5480D 2	.1900D 2	.1000D 1	.7890D 2
.8925D 3	.5480D 2	.1099D 2	.1000D 1	.7890D 2
.9000D 3	.5480D 2	.1099D 2	.1000D 1	.7890D 2
.9075D 3	.5480D 2	.1099D 2	.1000D 1	.7890D 2
.9150D 3	.5480D 2	.1099D 2	.1000D 1	.7890D 2
.9225D 3	.5480D 2	.1099D 2	.1000D 1	.7890D 2
.9300D 3	.5480D 2	.1099D 2	.1000D 1	.7890D 2
.9375D 3	.5480D 2	.1099D 2	.1000D 1	.7890D 2
.9450D 3	.5480D 2	.1099D 2	.1000D 1	.7890D 2
.9525D 3	.5480D 2	.1099D 2	.1000D 1	.7890D 2
.9600D 3	.5480D 2	.1099D 2	.1000D 1	.7890D 2
.9675D 3	.5480D 2	.1099D 2	.1000D 1	.7890D 2
.9750D 3	.5480D 2	.1099D 2	.1000D 1	.7890D 2
.9825D 3	.5480D 2	.1099D 2	.1000D 1	.7890D 2
.9900D 3	.5480D 2	.1099D 2	.1000D 1	.7890D 2
.9975D 3	.5480D 2	.1099D 2	.1000D 1	.7890D 2
.1005D 4	.5480D 2	.1099D 2	.1000D 1	.7890D 2
.1013D 4	.5480D 2	.1099D 2	.1000D 1	.7890D 2
.1020D 4	.5480D 2	.1099D 2	.1000D 1	.7890D 2
.1027D 4	.5480D 2	.1099D 2	.1000D 1	.7890D 2

Table XIX (continued)

Time Min.	Frost Pt. °F	Partial Pressure mm. Hg	RATIOC	Gas Temp. °F
.1035D 4	.5480D 2	.1099D 2	.1000D 1	.7890D 2
.1043D 4	.5480D 2	.1099D 2	.1000D 1	.7890D 2
.1050D 4	.5480D 2	.1099D 2	.1000D 1	.7890D 2
.1057D 4	.5480D 2	.1099D 2	.1000D 1	.7890D 2
.1065D 4	.5480D 2	.1099D 2	.1000D 1	.7890D 2
.1073D 4	.5480D 2	.1099D 2	.1000D 1	.7890D 2

Table XX. Experimental Results of Activated Alumina Run No. 3 (ACTX-3).

Time Min.	Frost Pt. °F	Partial Pressure mm. Hg	RATIOC	Gas Temp. °F
.0000D 0	-.1042D 3	.8129D-3	-.5300D-3	.7920D 2
.7500D 1	-.1042D 3	.8129D-3	-.5300D-3	.7980D 2
.1500D 2	-.1042D 3	.8129D-3	-.5300D-3	.8010D 2
.2250D 2	-.1042D 3	.8129D-3	-.5300D 3	.8030D 2
.3000D 2	-.1042D 3	.8129D-3	-.5300D-3	.8040D 2
.3750D 2	-.1042D 3	.8129D-3	-.5300D-3	.8050D 2
.4500D 2	-.1042D 3	.8129D-3	-.5300D-3	.8050D 2
.5250D 2	-.1042D 3	.8129D-3	-.5300D-3	.8060D 2
.6000D 2	-.1042D 3	.8129D-3	-.5300D-3	.8060D 2
.6750D 2	-.1042D 3	.8129D-3	-.5300D-3	.8060D 2
.7500D 2	-.1042D 3	.8129D-3	-.5300D-3	.8060D 2
.8250D 2	-.1042D 3	.8129D-3	-.5300D-3	.8070D 2
.9000D 2	-.1042D 3	.8129D-3	-.5300D-3	.8070D 2
.9750D 2	-.1042D 3	.8129D-3	-.5300D-3	.8070D 2
.1050D 3	-.1042D 3	.8129D-3	-.5300D-3	.8070D 2
.1125D 3	-.1042D 3	.8129D-3	-.5300D-3	.8070D 2
.1200D 3	-.1042D 3	.8129D-3	-.5300D-3	.8070D 2
.1275D 3	-.1042D 3	.8129D-3	-.5300D-3	.8080D 2
.1350D 3	-.1042D 3	.8129D-3	-.5300D-3	.8080D 2
.1425D 3	-.1042D 3	.8129D-3	-.5300D-3	.8080D 2
.1500D 3	-.1042D 3	.8129D-3	-.5300D-3	.8080D 2
.1575D 3	-.1042D 3	.8129D-3	-.5300D-3	.8080D 2
.1650D 3	-.1042D 3	.8129D-3	-.5300D-3	.8080D 2
.1725D 3	-.1042D 3	.8129D-3	-.5300D-3	.8080D 2
.1800D 3	-.1042D 3	.8129D-3	-.5300D-3	.8080D 2
.1875D 3	-.9580D 2	.1670D-2	.9995D-3	.8080D 2
.1950D 3	-.9220D 2	.2250D-2	.2034D-2	.8080D 2
.2025D 3	-.8540D 2	.3911D-2	.4999D-2	.8080D 2

Table XX (continued)

Time Min.	Frost Pt. °F	Partial Pressure mm. Hg	RATIOC	Gas Temp. °F
.2100D 3	-.7380D 2	.9547D-2	.1506D-1	.8080D 2
.2175D 3	-.6700D 2	.1570D-1	.2604D-1	.8080D 2
.2250D 3	-.6120D 2	.2368D-1	.4028D-1	.8070D 2
.2325D 3	-.5450D 2	.3754D-1	.6500D-1	.8070D 2
.2400D 3	-.5060D 2	.4876D-1	.8503D-1	.8060D 2
.2475D 3	-.4540D 2	.6840D-1	.1201D 0	.8050D 2
.2550D 3	-.4000D 2	.9660D-1	.1704D 0	.8040D 2
.2625D 3	-.3560D 2	.1271D 0	.2249D 0	.8030D 2
.2700D 3	-.3200D 2	.1584D 0	.2806D 0	.8010D 2
.2775D 3	-.2910D 2	.1886D 0	.3345D 0	.7990D 2
.2850D 3	-.2480D 2	.2431D 0	.4318D 0	.7970D 2
.2925D 3	-.2180D 2	.2893D 0	.5143D 0	.7960D 2
.3000D 3	-.1920D 2	.3358D 0	.5972D 0	.7940D 2
.3075D 3	-.1760D 2	.3680D 0	.6547D 0	.7920D 2
.3150D 3	-.1600D 2	.4018D 0	.7150D 0	.7900D 2
.3225D 3	-.1480D 2	.4300D 0	.7653D 0	.7890D 2
.3300D 3	-.1370D 2	.4575D 0	.8144D 0	.7880D 2
.3375D 3	-.1300D 2	.4760D 0	.8474D 0	.7870D 2
.3450D 3	-.1270D 2	.4845D 0	.8626D 0	.7860D 2
.3525D 3	-.1240D 2	.4915D 0	.8751D 0	.7860D 2
.3600D 3	-.1210D 2	.5000D 0	.8903D 0	.7850D 2
.3675D 3	-.1190D 2	.5055D 0	.9001D 0	.7850D 2
.3750D 3	-.1170D 2	.5110D 0	.9099D 0	.7840D 2
.3825D 3	-.1160D 2	.5140D 0	.9152D 0	.7840D 2
.3900D 3	-.1140D 2	.5200D 0	.9251D 0	.7840D 2
.3975D 3	-.1130D 2	.5224D 0	.9302D 0	.7830D 2
.4050D 3	-.1120D 2	.5260D 0	.9367D 0	.7830D 2
.4125D 3	-.1120D 2	.5260D 0	.9367D 0	.7830D 2

Table XX (continued)

Time Min.	Frost Pt. °F	Partial Pressure mm. Hg	RATIOC	Gas Temp. °F
.4200D 3	-.1110D 2	.5290D 0	.9420D 0	.7830D 2
.4275D 3	-.1100D 2	.5315D 0	.9465D 0	.7820D 2
.4350D 3	-.1100D 2	.5315D 0	.9465D 0	.7820D 2
.4425D 3	-.1090D 2	.5345D 0	.9518D 0	.7820D 2
.4500D 3	-.1090D 2	.5345D 0	.9518D 0	.7820D 2
.4575D 3	-.1090D 2	.5345D 0	.9518D 0	.7820D 2
.4650D 3	-.1080D 2	.5370D 0	.9563D 0	.7820D 2
.4725D 3	-.1080D 2	.5370D 0	.9563D 0	.7820D 2
.4800D 3	-.1080D 2	.5370D 0	.9563D 0	.7820D 2
.4875D 3	-.1080D 2	.5370D 0	.9563D 0	.7820D 2
.4950D 3	-.1080D 2	.5370D 0	.9563D 0	.7820D 2
.5025D 3	-.1080D 2	.5370D 0	.9563D 0	.7820D 2
.5100D 3	-.1080D 2	.5370D 0	.9563D 0	.7820D 2
.5175D 3	-.1070D 2	.5400D 0	.9616D 0	.7820D 2
.5250D 3	-.1070D 2	.5400D 0	.9616D 0	.7820D 2
.5325D 3	-.1070D 2	.5400D 0	.9616D 0	.7820D 2
.5400D 3	-.1070D 2	.5400D 0	.9616D 0	.7820D 2
.5475D 3	-.1070D 2	.5400D 0	.9616D 0	.7820D 2
.5550D 3	-.1060D 2	.5428D 0	.9666D 0	.7820D 2
.5625D 3	-.1060D 2	.5428D 0	.9666D 0	.7820D 2
.5700D 3	-.1060D 2	.5428D 0	.9666D 0	.7820D 2
.5775D 3	-.1060D 2	.5428D 0	.9666D 0	.7820D 2
.5850D 3	-.1060D 2	.5428D 0	.9666D 0	.7820D 2
.5925D 3	-.1060D 2	.5428D 0	.9666D 0	.7820D 2
.6000D 3	-.1060D 2	.5428D 0	.9666D 0	.7820D 2
.6075D 3	-.1060D 2	.5428D 0	.9666D 0	.7820D 2
.6150D 3	-.1050D 2	.5464D 0	.9731D 0	.7820D 2
.6225D 3	-.1050D 2	.5460D 0	.9731D 0	.7820D 2

Table XX (continued)

Time Min.	Frost Pt. °F	Partial Pressure mm. Hg	RATIOC	Gas Temp. °F
.6300D 3	-.1050D 2	.5464D 0	.9731D 0	.7820D 2
.6375D 3	-.1050D 2	.5464D 0	.9731D 0	.7820D 2
.6450D 3	-.1050D 2	.5464D 0	.9731D 0	.7820D 2
.6525D 3	-.1050D 2	.5464D 0	.9731D 0	.7820D 2
.6600D 3	-.1050D 2	.5464D 0	.9731D 0	.7820D 2
.6675D 3	-.1050D 2	.5464D 0	.9731D 0	.7810D 2
.6750D 3	-.1040D 2	.5490D 0	.9777D 0	.7810D 2
.6825D 3	-.1040D 2	.5490D 0	.9777D 0	.7810D 2
.6900D 3	-.1040D 2	.5490D 0	.9777D 0	.7810D 2
.6975D 3	-.1040D 2	.5490D 0	.9777D 0	.7810D 2
.7050D 3	-.1040D 2	.5490D 0	.9777D 0	.7810D 2
.7125D 3	-.1040D 2	.5490D 0	.9777D 0	.7810D 2
.7200D 3	-.1040D 2	.5490D 0	.9777D 0	.7810D 2
.7275D 3	-.1040D 2	.5490D 0	.9777D 0	.7810D 2
.7350D 3	-.1030D 2	.5520D 0	.9830D 0	.7810D 2
.7425D 3	-.1030D 2	.5520D 0	.9830D 0	.7810D 2
.7500D 3	-.1030D 2	.5520D 0	.9830D 0	.7810D 2
.7575D 3	-.1030D 2	.5520D 0	.9830D 0	.7810D 2
.7650D 3	-.1030D 2	.5520D 0	.9830D 0	.7810D 2
.7725D 3	-.1030D 2	.5520D 0	.9830D 0	.7810D 2
.7800D 3	-.1030D 2	.5520D 0	.9830D 0	.7810D 2
.7875D 3	-.1030D 2	.5520D 0	.9830D 0	.7810D 2
.7950D 3	-.1030D 2	.5520D 0	.9830D 0	.7810D 2
.8025D 3	-.1020D 2	.5556D 0	.9895D 0	.7810D 2
.8100D 3	-.1020D 2	.5556D 0	.9895D 0	.7810D 2
.8175D 3	-.1020D 2	.5556D 0	.9895D 0	.7810D 2
.8250D 3	-.1020D 2	.5556D 0	.9895D 0	.7810D 2
.8325D 3	-.1020D 2	.5556D 0	.9895D 0	.7810D 2

Table XX (continued)

Time Min.	Frost Pt. °F	Partial Pressure mm.Hg	RATIOC	Gas Temp. °F
.8400D 3	-.1020D 2	.5556D 0	.9895D 0	.7810D 2
.8475D 3	-.1020D 2	.5556D 0	.9895D 0	.7810D 2
.8550D 3	-.1020D 2	.5556D 0	.9895D 0	.7810D 2
.8625D 3	-.1020D 2	.5556D 0	.9895D 0	.7810D 2
.8700D 3	-.1020D 2	.5556D 0	.9895D 0	.7810D 2
.8775D 3	-.1020D 2	.5556D 0	.9895D 0	.7810D 2
.8850D 3	-.1020D 2	.5556D 0	.9895D 0	.7810D 2
.8925D 3	-.1020D 2	.5556D 0	.9895D 0	.7810D 2
.9000D 3	-.1010D 2	.5585D 0	.9946D 0	.7810D 2
.9075D 3	-.1010D 2	.5585D 0	.9946D 0	.7810D 2
.9150D 3	-.1010D 2	.5585D 0	.9946D 0	.7810D 2
.9225D 3	-.1010D 2	.5585D 0	.9946D 0	.7810D 2
.9300D 3	-.1010D 2	.5585D 0	.9946D 0	.7810D 2
.9375D 3	-.1010D 2	.5585D 0	.9946D 0	.7810D 2
.9450D 3	-.1010D 2	.5585D 0	.9946D 0	.7810D 2
.9525D 3	-.1010D 2	.5585D 0	.9946D 0	.7810D 2
.9600D 3	-.1010D 2	.5585D 0	.9946D 0	.7810D 2
.9675D 3	-.1010D 2	.5585D 0	.9946D 0	.7810D 2
.9750D 3	-.1010D 2	.5585D 0	.9946D 0	.7810D 2
.9825D 3	-.1010D 2	.5585D 0	.9946D 0	.7810D 2
.9900D 3	-.1010D 2	.5585D 0	.9946D 0	.7810D 2
.9975D 3	-.1000D 2	.5615D 0	.1000D 1	.7810D 2
.1005D 4	-.1000D 2	.5615D 0	.1000D 1	.7810D 2
.1013D 4	-.1000D 2	.5615D 0	.1000D 1	.7810D 2
.1020D 4	-.1000D 2	.5615D 0	.1000D 1	.7810D 2
.1027D 4	-.1000D 2	.5615D 0	.1000D 1	.7810D 2
.1035D 4	-.1000D 2	.5615D 0	.1000D 1	.7810D 2

Table XX (continued)

Time Min.	Frost Pt. °F	Partial Pressure mm. Hg	RATIOC	Gas Temp. °F
.1043D 4	-.1000D 2	.5615D 0	.1000D 1	.7810D 2
.1050D 4	-.1000D 2	.5615D 0	.1000D 1	.7810D 2
.1057D 4	-.1000D 2	.5615D 0	.1000D 1	.7810D 2
.1065D 4	-.1000D 2	.5615D 0	.1000D 1	.7810D 2
.1073D 4	-.1000D 2	.5615D 0	.1000D 1	.7810D 2
.1080D 4	-.1000D 2	.5615D 0	.1000D 1	.7810D 2
.1087D 4	-.1000D 2	.5615D 0	.1000D 1	.7810D 2
.1095D 4	-.1000D 2	.5615D 0	.1000D 1	.7810D 2
.1102D 4	-.1000D 2	.5615D 0	.1000D 1	.7810D 2
.1110D 4	-.1000D 2	.5615D 0	.1000D 1	.7810D 2
.1118D 4	-.1000D 2	.5615D 0	.1000D 1	.7810D 2
.1125D 4	-.1000D 2	.5615D 0	.1000D 1	.7810D 2
.1132D 4	-.1000D 2	.5615D 0	.1000D 1	.7810D 2
.1140D 4	-.1000D 2	.5615D 0	.1000D 1	.7810D 2
.1148D 4	-.1000D 2	.5615D 0	.1000D 1	.7810D 2
.1155D 4	-.1000D 2	.5615D 0	.1000D 1	.7810D 2

Table XXI. Experimental Results of Activated Alumina Run No. 4 (ACTX-4).

Time Min.	Frost Pt. °F	Partial Pressure mm. Hg	RATIOC	Gas Temp. °F
.0000D 0	-.1054D 3	.7337D-3	-.5847D-4	.7920D 2
.7500D 1	-.1054D 3	.7337D-3	-.5847D-4	.1020D 3
.1500D 2	-.1054D 3	.7337D-3	-.5847D-4	.1252D 3
.2250D 2	-.1020D 3	.5556D 0	.5007D-1	.1330D 3
.3000D 2	.7100D 1	.1382D 1	.1247D 0	.1308D 3
.3750D 2	.2120D 2	.2765D 1	.2497D 0	.1266D 3
.4500D 2	.3070D 2	.4316D 1	.3898D 0	.1170D 3
.5250D 2	.3670D 2	.5529D 1	.4994D 0	.1100D 3
.6000D 2	.4030D 2	.6368D 1	.5751D 0	.1052D 3
.6750D 2	.4300D 2	.7067D 1	.6383D 0	.1024D 3
.7500D 2	.4470D 2	.7544D 1	.6814D 0	.1000D 3
.8250D 2	.4580D 2	.7866D 1	.7105D 0	.9800D 2
.9000D 2	.4670D 2	.8139D 1	.7351D 0	.9600D 2
.9750D 2	.4740D 2	.8357D 1	.7549D 0	.9460D 2
.1050D 3	.4810D 2	.8574D 1	.7745D 0	.9320D 2
.1125D 3	.4860D 2	.8739D 1	.7893D 0	.9200D 2
.1200D 3	.4900D 2	.8869D 1	.8011D 0	.9100D 2
.1275D 3	.4950D 2	.9037D 1	.8163D 0	.9000D 2
.1350D 3	.4980D 2	.9141D 1	.8257D 0	.8920D 2
.1425D 3	.5010D 2	.9246D 1	.8352D 0	.8840D 2
.1500D 3	.5030D 2	.9314D 1	.8413D 0	.8780D 2
.1575D 3	.5040D 2	.9345D 1	.8441D 0	.8740D 2
.1650D 3	.5070D 2	.9452D 1	.8537D 0	.8680D 2
.1725D 3	.5090D 2	.9521D 1	.8600D 0	.8640D 2
.1800D 3	.5110D 2	.9591D 1	.8664D 0	.8600D 2
.1875D 3	.5120D 2	.9630D 1	.8698D 0	.8570D 2
.1950D 3	.5140D 2	.9701D 1	.8763D 0	.8540D 2

Table XXI (continued)

Time Min.	Frost Pt. °F	Partial Pressure mm. Hg	RATIOC	Gas Temp. °F
.2025D 3	.5150D 2	.9734D 1	.8792D 0	.8500D 2
.2100D 3	.5170D 2	.9805D 1	.8857D 0	.8480D 2
.2175D 3	.5180D 2	.9844D 1	.8892D 0	.8440D 2
.2250D 3	.5190D 2	.9884D 1	.8928D 0	.8410D 2
.2325D 3	.5200D 2	.9917D 1	.8957D 0	.8380D 2
.2400D 3	.5210D 2	.9956D 1	.8993D 0	.8360D 2
.2475D 3	.5220D 2	.9989D 1	.9023D 0	.8330D 2
.2550D 3	.5230D 2	.1003D 2	.9059D 0	.8320D 2
.2625D 3	.5240D 2	.1006D 2	.9089D 0	.8300D 2
.2700D 3	.5250D 2	.1010D 2	.9125D 0	.8280D 2
.2775D 3	.5260D 2	.1014D 2	.9155D 0	.8270D 2
.2850D 3	.5270D 2	.1018D 2	.9192D 0	.8260D 2
.2925D 3	.5280D 2	.1022D 2	.9229D 0	.8240D 2
.3000D 3	.5290D 2	.1025D 2	.9259D 0	.8230D 2
.3075D 3	.5300D 2	.1029D 2	.9296D 0	.8220D 2
.3150D 3	.5310D 2	.1033D 2	.9327D 0	.8210D 2
.3225D 3	.5320D 2	.1037D 2	.9364D 0	.8200D 2
.3300D 3	.5320D 2	.1037D 2	.9364D 0	.8190D 2
.3375D 3	.5330D 2	.1040D 2	.9395D 0	.8180D 2
.3450D 3	.5340D 2	.1044D 2	.9432D 0	.8170D 2
.3525D 3	.5350D 2	.1048D 2	.9463D 0	.8160D 2
.3600D 3	.5360D 2	.1052D 2	.9501D 0	.8150D 2
.3675D 3	.5360D 2	.1052D 2	.9501D 0	.8140D 2
.3750D 3	.5370D 2	.1056D 2	.9539D 0	.8130D 2
.3850D 3	.5380D 2	.1060D 2	.9570D 0	.8120D 2
.3900D 3	.5380D 2	.1060D 2	.9570D 0	.8110D 2
.3975D 3	.5390D 2	.1064D 2	.9608D 0	.8100D 2
.4050D 3	.5390D 2	.1064D 2	.9608D 0	.8090D 2

Table XXI (continued)

Time Min.	Frost Pt. °F	Partial Pressure mm. Hg	RATIOC	Gas Temp. °F
.4125D 3	.5400D 2	.1067D 2	.9640D 0	.8080D 2
.4200D 3	.5410D 2	.1071D 2	.9678D 0	.8080D 2
.4275D 3	.5410D 2	.1071D 2	.9678D 0	.8080D 2
.4350D 3	.5420D 2	.1075D 2	.9710D 0	.8070D 2
.4425D 3	.5420D 2	.1075D 2	.9710D 0	.8070D 2
.4500D 3	.5430D 2	.1079D 2	.9748D 0	.8070D 2
.4575D 3	.5430D 2	.1079D 2	.9748D 0	.8060D 2
.4650D 3	.5430D 2	.1079D 2	.9748D 0	.8050D 2
.4725D 3	.5440D 2	.1083D 2	.9780D 0	.8040D 2
.4800D 3	.5440D 2	.1083D 2	.9780D 0	.8040D 2
.4875D 3	.5450D 2	.1087D 2	.9819D 0	.8030D 2
.4950D 3	.5450D 2	.1087D 2	.9819D 0	.8020D 2
.5025D 3	.5450D 2	.1087D 2	.9819D 0	.8010D 2
.5100D 3	.5460D 2	.1091D 2	.9857D 0	.8010D 2
.5175D 3	.5460D 2	.1091D 2	.9857D 0	.8000D 2
.5250D 3	.5460D 2	.1091D 2	.9857D 0	.8000D 2
.5324D 3	.5460D 2	.1091D 2	.9857D 0	.7990D 2
.5400D 3	.5470D 2	.1095D 2	.9889D 0	.7990D 2
.5475D 3	.5470D 2	.1095D 2	.9889D 0	.7980D 2
.5550D 3	.5470D 2	.1095D 2	.9889D 0	.7980D 2
.5625D 3	.5470D 2	.1095D 2	.9889D 0	.7970D 2
.5700D 3	.5480D 2	.1099D 2	.9928D 0	.7970D 2
.5775D 3	.5480D 2	.1099D 2	.9928D 0	.7970D 2
.5850D 3	.5480D 2	.1099D 2	.9928D 0	.7960D 2
.5925D 3	.5480D 2	.1099D 2	.9928D 0	.7960D 2
.6000D 3	.5490D 2	.1103D 2	.9961D 0	.7960D 2
.6075D 3	.5490D 2	.1103D 2	.9961D 0	.7960D 2
.6150D 3	.5490D 2	.1103D 2	.9961D 0	.7960D 2

Table XXI (continued)

Time Min.	Frost Pt. °F	Partial Pressure mm. Hg	RATIOC	Gas Temp. °F
.6225D 3	.5490D 2	.1103D 2	.9961D 0	.7950D 2
.6300D 3	.5490D 2	.1103D 2	.9961D 0	.7950D 2
.6375D 3	.5490D 2	.1103D 2	.9961D 0	.7950D 2
.6450D 3	.5490D 2	.1103D 2	.9961D 0	.7950D 2
.6525D 3	.5490D 2	.1103D 2	.9961D 0	.7940D 2
.6600D 3	.5500D 2	.1107D 2	.1000D 1	.7940D 2
.6675D 3	.5500D 2	.1107D 2	.1000D 1	.7940D 2
.6750D 3	.5500D 2	.1107D 2	.1000D 1	.7940D 2
.6825D 3	.5500D 2	.1107D 2	.1000D 1	.7930D 2
.6900D 3	.5500D 2	.1107D 2	.1000D 1	.7930D 2
.6975D 3	.5500D 2	.1107D 2	.1000D 1	.7930D 2
.7050D 3	.5500D 2	.1107D 2	.1000D 1	.7930D 2
.7125D 3	.5500D 2	.1107D 2	.1000D 1	.7930D 2
.7200D 3	.5500D 2	.1107D 2	.1000D 1	.7930D 2
.7275D 3	.5500D 2	.1107D 2	.1000D 1	.7930D 2
.7350D 3	.5500D 2	.1107D 2	.1000D 1	.7930D 2
.7425D 3	.5500D 2	.1107D 2	.1000D 1	.7930D 2
.7500D 3	.5500D 2	.1107D 2	.1000D 1	.7930D 2
.7575D 3	.5500D 2	.1107D 2	.1000D 1	.7930D 2
.7650D 3	.5500D 2	.1107D 2	.1000D 1	.7930D 2
.7725D 3	.5500D 2	.1107D 2	.1000D 1	.7920D 2
.7800D 3	.5500D 2	.1107D 2	.1000D 1	.7920D 2
.7875D 3	.5500D 2	.1107D 2	.1000D 1	.7920D 2
.7950D 3	.5500D 2	.1107D 2	.1000D 1	.7920D 2

Table XXII. Experimental Results of Activated Alumina Run No. 5 (ACTX-5).

Time Min.	Frost Pt. °F	Partial Pressure mm. Hg	RATIOC	Gas Temp. °F
.0000D 0	-.1060D 3	.6963D-3	-.2228D-4	.7950D 2
.7500D 1	-.1060D 3	.6963D-3	-.2228D-4	.1096D 3
.1500D 2	-.1060D 3	.6963D-3	-.2228D-4	.1272D 3
.2250D 2	-.1060D 3	.6963D-3	-.2228D-4	.1344D 3
.3000D 2	-.1060D 3	.6963D-3	-.2228D-4	.1380D 3
.3750D 2	-.1330D 2	.4682D 0	.4191D-1	.1352D 3
.4500D 2	.2520D 2	.3342D 1	.2996D 0	.1276D 3
.5250D 2	.3610D 2	.5400D 1	.4843D 0	.1160D 3
.6000D 2	.4050D 2	.6417D 1	.5754D 0	.1100D 3
.6750D 2	.4240D 2	.6907D 1	.6194D 0	.1058D 3
.7500D 2	.4390D 2	.7314D 1	.6559D 0	.1028D 3
.8250D 2	.4480D 2	.7570D 1	.6789D 0	.1004D 3
.9000D 2	.4600D 2	.7925D 1	.7107D 0	.9840D 2
.9750D 2	.4670D 2	.8139D 1	.7298D 0	.9640D 2
.1050D 3	.4730D 2	.8323D 1	.7464D 0	.9520D 2
.1125D 3	.4800D 2	.8545D 1	.7663D 0	.9390D 2
.1200D 3	.4860D 2	.8739D 1	.7837D 0	.9280D 2
.1275D 3	.4900D 2	.8867D 1	.7954D 0	.9160D 2
.1350D 3	.4950D 2	.9037D 1	.8104D 0	.9060D 2
.1425D 3	.4990D 2	.9172D 1	.8225D 0	.8960D 2
.1550D 3	.5030D 2	.9314D 1	.8353D 0	.8880D 2
.1575D 3	.5060D 2	.9414D 1	.8442D 0	.8800D 2
.1650D 3	.5090D 2	.9521D 1	.8531D 0	.8730D 2
.1725D 3	.5120D 2	.9630D 1	.8636D 0	.8680D 2
.1880D 3	.5140D 2	.9701D 1	.8700D 0	.8620D 2
.1875D 3	.5170D 2	.9805D 1	.8793D 0	.8560D 2
.1950D 3	.5190D 2	.9884D 1	.8864D 0	.8520D 2
.2025D 3	.5220D 2	.9989D 1	.8958D 0	.8480D 2

Table XXII (continued)

Time Min.	Frost Pt. °F	Partial Pressure mm. Hg	RATIOC	Gas Temp. °F
.2100D 3	.5240D 2	.1006D 2	.9024D 0	.8440D 2
.2175D 3	.5260D 2	.1014D 2	.9090D 0	.8400D 2
.2250D 3	.5280D 2	.1022D 2	.9162D 0	.8360D 2
.2325D 3	.5290D 2	.1025D 2	.9193D 0	.8320D 2
.2400D 3	.5310D 2	.1033D 2	.9260D 0	.8300D 2
.2475D 3	.5320D 2	.1037D 2	.9297D 0	.8270D 2
.2550D 3	.5340D 2	.1044D 2	.9364D 0	.8240D 2
.2625D 3	.5350D 2	.1048D 2	.9395D 0	.8210D 2
.2700D 3	.5370D 2	.1056D 2	.9470D 0	.8190D 2
.2775D 3	.5380D 2	.1060D 2	.9502D 0	.8170D 2
.2850D 3	.5390D 2	.1064D 2	.9539D 0	.8150D 2
.2925D 3	.5400D 2	.1067D 2	.9571D 0	.8130D 2
.3000D 3	.5410D 2	.1071D 2	.9608D 0	.8110D 2
.3075D 3	.5420D 2	.1075D 2	.9640D 0	.8090D 2
.3150D 3	.5430D 2	.1079D 2	.9678D 0	.8070D 2
.3225D 3	.5440D 2	.1083D 2	.9710D 0	.8060D 2
.3300D 3	.5450D 2	.1087D 2	.9748D 0	.8050D 2
.3375D 3	.5460D 2	.1091D 2	.9786D 0	.8040D 2
.3450D 3	.5470D 2	.1095D 2	.9818D 0	.8030D 2
.3525D 3	.5480D 2	.1099D 2	.9857D 0	.8020D 2
.3600D 3	.5490D 2	.1103D 2	.9889D 0	.8010D 2
.3675D 3	.5500D 2	.1107D 2	.9928D 0	.8000D 2
.3750D 3	.5500D 2	.1107D 2	.9928D 0	.7990D 2
.3825D 3	.5510D 2	.1111D 2	.9961D 0	.7980D 2
.3900D 3	.5510D 2	.1111D 2	.9961D 0	.7970D 2
.3975D 3	.5520D 2	.1115D 2	.1000D 1	.7960D 2
.4050D 3	.5520D 2	.1115D 2	.1000D 1	.7960D 2
.4125D 3	.5520D 2	.1115D 2	.1000D 1	.7960D 2

Table XXII (continued)

Time Min.	Frost Pt. °F	Partial Pressure mm. Hg	RATIOC	Gas Temp. °F
.4200D 3	.5520D 2	.1115D 2	.1000D 1	.7950D 2
.4275D 3	.5520D 2	.1115D 2	.1000D 1	.7950D 2
.4350D 3	.5520D 2	.1115D 2	.1000D 1	.7950D 2
.4425D 3	.5520D 2	.1115D 2	.1000D 1	.7940D 2
.4500D 3	.5520D 2	.1115D 2	.1000D 1	.7940D 2
.4575D 3	.5520D 2	.1115D 2	.1000D 1	.7940D 2
.4650D 3	.5520D 2	.1115D 2	.1000D 1	.7940D 2
.4725D 3	.5520D 2	.1115D 2	.1000D 1	.7930D 2
.4800D 3	.5520D 2	.1115D 2	.1000D 1	.7930D 2
.4875D 3	.5520D 2	.1115D 2	.1000D 1	.7930D 2
.4950D 3	.5520D 2	.1115D 2	.1000D 1	.7920D 2
.5025D 3	.5520D 2	.1115D 2	.1000D 1	.7920D 2
.5100D 3	.5520D 2	.1115D 2	.1000D 1	.7920D 2

Table XXIII. Experimental Results of Activated Alumina Run No. 6 (ACTX-6).

Time Min.	Frost Pt. °F	Partial Pressure mm. Hg	RATIOC	Gas Temp. °F
.0000D 0	-.1063D 3	.6787D-3	-.5700D-4	.7880D 2
.7500D 1	-.1063D 3	.6787D-3	-.5700D-4	.8000D 2
.1500D 2	-.1063D 3	.6787D-3	-.5700D-4	.1068D 3
.2250D 2	-.1063D 3	.6787D-3	-.5700D-4	.1184D 3
.3000D 2	-.1063D 3	.6787D-3	-.5700D-4	.1248D 3
.3750D 2	-.1063D 3	.6787D-3	-.5700D-4	.1296D 3
.4500D 2	-.1063D 3	.6787D-3	-.5700D-4	.1320D 3
.5250D 2	-.1063D 3	.6787D-3	-.5700D-4	.1342D 3
.6000D 2	-.1063D 3	.6787D-3	-.5700D-4	.1357D 3
.6750D 2	-.3070D 2	.1714D 0	.1499D-1	.1352D 3
.7500D 2	.2300D 1	.1080D 1	.9499D-1	.1324D 3
.8250D 2	.1910D 1	.2500D 1	.2200D 0	.1272D 3
.9000D 2	.2890D 2	.3972D 1	.3496D 0	.1212D 3
.9750D 2	.3470D 2	.5107D 1	.4495D 0	.1150D 3
.1050D 3	.3640D 2	.5463D 1	.4809D 0	.1100D 3
.1125D 3	.3840D 2	.5914D 1	.5206D 0	.1068D 3
.1200D 3	.3960D 2	.6196D 1	.5454D 0	.1052D 3
.1275D 3	.4070D 2	.6467D 1	.5692D 0	.1032D 3
.1350D 3	.4180D 2	.6746D 1	.5939D 0	.1016D 3
.1425D 3	.4270D 2	.7042D 1	.6199D 0	.1004D 3
.1500D 3	.4360D 2	.7229D 1	.6364D 0	.9960D 2
.1575D 3	.4430D 2	.7426D 1	.6537D 0	.9880D 2
.1650D 3	.4530D 2	.7717D 1	.6793D 0	.9760D 2
.1725D 3	.4560D 2	.7807D 1	.6872D 0	.9670D 2
.1800D 3	.4590D 2	.7893D 1	.6948D 0	.9600D 2
.1875D 3	.4650D 2	.8078D 1	.7111D 0	.9520D 2
.1950D 3	.4680D 2	.8166D 1	.7189D 0	.9450D 2
.2025D 3	.4720D 2	.8289D 1	.7297D 0	.9400D 2

Table XXIII (continued)

Time Min.	Frost Pt. °F	Partial Pressure mm. Hg	RATIOC	Gas Temp. °F
.2100D 3	.4700D 2	.8448D 1	.7437D 0	.9320D 2
.2175D 3	.4790D 2	.8511D 1	.7493D 0	.9270D 2
.2250D 3	.4830D 2	.8644D 1	.7610D 0	.9220D 2
.2325D 3	.4860D 2	.8739D 1	.7693D 0	.9170D 2
.2400D 3	.4890D 2	.8839D 1	.7781D 0	.9120D 2
.2475D 3	.4930D 2	.8971D 1	.7897D 0	.9080D 2
.2550D 3	.4950D 2	.9037D 1	.7956D 0	.9040D 2
.2625D 3	.4980D 2	.9141D 1	.8047D 0	.9000D 2
.2700D 3	.5000D 2	.9209D 1	.8107D 0	.8960D 2
.2750D 3	.5020D 2	.9277D 1	.8167D 0	.8920D 2
.2850D 3	.5050D 2	.9338D 1	.8221D 0	.8880D 2
.2925D 3	.5070D 2	.9452D 1	.8321D 0	.8840D 2
.3000D 3	.5090D 2	.9521D 1	.8382D 0	.8800D 2
.3075D 3	.5110D 2	.9591D 1	.8444D 0	.8770D 2
.3150D 3	.5120D 2	.9630D 1	.8478D 0	.8740D 2
.3225D 2	.5140D 2	.9701D 1	.8540D 0	.8710D 2
.3300D 3	.5150D 2	.9734D 1	.8569D 0	.8680D 2
.3375D 3	.5170D 2	.9805D 1	.8632D 0	.8650D 2
.3450D 3	.5180D 2	.9844D 1	.8666D 0	.8620D 2
.3525D 3	.5190D 2	.9884D 1	.8701D 0	.8590D 2
.3600D 3	.5200D 2	.9917D 1	.8730D 0	.8560D 2
.3675D 3	.5210D 2	.9956D 1	.8765D 0	.8530D 2
.3750D 3	.5220D 2	.9989D 1	.8794D 0	.8510D 2
.3825D 3	.5250D 2	.1010D 2	.8894D 0	.8490D 2
.3900D 3	.5260D 2	.1014D 2	.8923D 0	.8470D 2
.3975D 3	.5270D 2	.1018D 2	.8958D 0	.8450D 2
.4050D 3	.5280D 2	.1022D 2	.8994D 0	.8440D 2
.4125D 3	.5300D 2	.1029D 2	.9060D 0	.8400D 2

Table XXIII (continued)

Time Min.	Frost Pt. °F	Partial Pressure mm. Hg	RATIOC	Gas Temp. °F
.4200D 3	.5310D 2	.1033D 2	.9090D 0	.8380D 2
.4275D 3	.5320D 2	.1037D 2	.9126D 0	.8360D 2
.4350D 3	.5340D 2	.1044D 2	.9193D 0	.8340D 2
.4425D 3	.5350D 2	.1048D 2	.9223D 0	.8320D 2
.4500D 3	.5350D 2	.1048D 2	.9223D 0	.8300D 2
.4575D 3	.5360D 2	.1052D 2	.9260D 0	.8290D 2
.4650D 3	.5370D 2	.1056D 2	.9297D 0	.8270D 2
.4725D 3	.5380D 2	.1060D 2	.9327D 0	.8250D 2
.4800D 3	.5390D 2	.1064D 2	.9364D 0	.8240D 2
.4875D 3	.5390D 2	.1064D 2	.9364D 0	.8220D 2
.4950D 3	.5400D 2	.1067D 2	.9395D 0	.8210D 2
.5025D 3	.5410D 2	.1071D 2	.9432D 0	.8190D 2
.5100D 3	.5420D 2	.1075D 2	.9463D 0	.8180D 2
.5175D 3	.5420D 2	.1075D 2	.9463D 0	.8150D 2
.5250D 3	.5430D 2	.1079D 2	.9500D 0	.8140D 2
.5325D 3	.5440D 2	.1083D 2	.9532D 0	.8130D 2
.5400D 3	.5440D 2	.1083D 2	.9532D 0	.8120D 2
.5475D 3	.5450D 2	.1087D 2	.9569D 0	.8110D 2
.5550D 3	.5460D 2	.1091D 2	.9607D 0	.8100D 2
.5625D 3	.5470D 2	.1095D 2	.9638D 0	.8090D 2
.5700D 3	.5470D 2	.1095D 2	.9638D 0	.8080D 2
.5775D 3	.5480D 2	.1099D 2	.9676D 0	.8070D 2
.5850D 3	.5490D 2	.1103D 2	.9708D 0	.8060D 2
.5925D 3	.5500D 2	.1107D 2	.9746D 0	.8050D 2
.6000D 3	.5500D 2	.1107D 2	.9746D 0	.8040D 2
.6075D 3	.5510D 2	.1111D 2	.9778D 0	.8040D 2
.6150D 3	.5510D 2	.1111D 2	.9778D 0	.8030D 2
.6225D 3	.5520D 2	.1115D 2	.9817D 0	.8020D 2
.6300D 3	.5520D 2	.1115D 2	.9817D 0	.8010D 2

Table XXIII (continued)

Time Min.	Frost Pt. °F	Partial Pressure mm. Hg	RATIOC	Gas Temp. °F
.6375D 3	.5530D 2	.1119D 2	.9849D 0	.8000D 2
.6450D 3	.5530D 2	.1119D 2	.9849D 0	.7990D 2
.6525D 3	.5540D 2	.1123D 2	.9887D 0	.7980D 2
.6600D 3	.5540D 2	.1123D 2	.9887D 0	.7970D 2
.6675D 3	.5550D 2	.1123D 2	.9887D 0	.7970D 2
.6750D 3	.5550D 2	.1128D 2	.9926D 0	.7960D 2
.6825D 3	.5550D 2	.1128D 2	.9926D 0	.7960D 2
.6900D 3	.5550D 2	.1128D 2	.9926D 0	.7950D 2
.6975D 3	.5550D 2	.1128D 2	.9926D 0	.7950D 2
.7050D 3	.5550D 2	.1128D 2	.9926D 0	.7940D 2
.7125D 3	.5560D 2	.1131D 2	.9959D 0	.7930D 2
.7200D 3	.5560D 2	.1131D 2	.9959D 0	.7920D 2
.7275D 3	.5560D 2	.1131D 2	.9959D 0	.7920D 2
.7350D 3	.5560D 2	.1131D 2	.9959D 0	.7910D 2
.7425D 3	.5560D 2	.1131D 2	.9959D 0	.7900D 2
.7500D 3	.5560D 2	.1131D 2	.9959D 0	.7900D 2
.7575D 3	.5560D 2	.1131D 2	.9959D 0	.7890D 2
.7650D 3	.5560D 2	.1131D 2	.9959D 0	.7890D 2
.7725D 3	.5560D 2	.1131D 2	.9959D 0	.7880D 2
.7800D 3	.5570D 2	.1136D 2	.1000D 1	.7880D 2
.7875D 3	.5570D 2	.1136D 2	.1000D 1	.7870D 2
.7950D 3	.5570D 2	.1136D 2	.1000D 1	.7870D 2
.8025D 3	.5570D 2	.1136D 2	.1000D 1	.7870D 2
.8100D 3	.5570D 2	.1136D 2	.1000D 1	.7860D 2
.8175D 3	.5570D 2	.1136D 2	.1000D 1	.7860D 2
.8250D 3	.5570D 2	.1136D 2	.1000D 1	.7860D 2
.8325D 3	.5570D 2	.1136D 2	.1000D 1	.7860D 2
.8400D 3	.5570D 2	.1136D 2	.1000D 1	.7860D 2

Table XXIII (continued)

Time Min.	Frost Pt. °F	Partial Pressure mm. Hg	RATIOC	Gas Temp. °F
.8475D 3	.5570D 2	.1136D 2	.1000D 1	.7860D 2
.8550D 3	.5570D 2	.1136D 2	.1000D 1	.7850D 2
.8625D 3	.5570D 2	.1136D 2	.1000D 1	.7850D 2
.8700D 3	.5570D 2	.1136D 2	.1000D 1	.7850D 2
.8775D 3	.5570D 2	.1136D 2	.1000D 1	.7850D 2
.8850D 3	.5570D 2	.1136D 2	.1000D 1	.7850D 2
.8925D 3	.5570D 2	.1136D 2	.1000D 1	.7840D 2
.9000D 3	.5570D 2	.1136D 2	.1000D 1	.7840D 2
.9075D 3	.5570D 2	.1136D 2	.1000D 1	.7840D 2
.9150D 3	.5570D 2	.1136D 2	.1000D 1	.7840D 2
.9225D 3	.5570D 2	.1136D 2	.1000D 1	.7840D 2
.9300D 3	.5570D 2	.1136D 2	.1000D 1	.7840D 2
.9375D 3	.5570D 2	.1137D 2	.1000D 1	.7840D 2
.9450D 3	.5570D 2	.1136D 2	.1000D 1	.7840D 2
.9525D 3	.5570D 2	.1136D 2	.1000D 1	.7840D 2
.9600D 3	.5570D 2	.1136D 2	.1000D 1	.7840D 2
.9675D 3	.5570D 2	.1136D 2	.1000D 1	.7840D 2

APPENDIX E

TABLES OF COMPUTER RESULTS

The tables of the computer results of LMS-4A and activated alumina are shown in Table XXIV - XXXV for LMSC-1 - LMSC-13 and XXXVI - XLV for ACTC-1 - ACTC-10 respectively. The details of each run are already discussed in Chapter VIII.

All RATIOC are positive in the computer results because they are calculated from the initial and feed gas conditions not depending upon the hygrometer.

Table XXIV. Computer Results of LMS-4A Run No. 1 (LMSC-1).

Time Min.	RATIOC	Gas Temp. ^{o}F	Time Min.	RATIOC	Gas Temp. ^{o}F
.7500D 1	.7448D-3	.1238D 3	.1500D 2	.1792D-2	.1437D 3
.2250D 2	.2235D-2	.1491D 3	.3000D 2	.2430D-2	.1512D 3
.3750D 2	.2572D-2	.1525D 3	.4500D 2	.2771D-2	.1537D 3
.5250D 2	.3488D-2	.1549D 3	.6000D 2	.8258D-2	.1558D 3
.6750D 2	.4280D-1	.1544D 3	.7500D 2	.2309D 0	.1412D 3
.8250D 2	.6778D 0	.1065D 3	.9000D 2	.9645D 0	.8190D 2
.9750D 2	.9975D 0	.7833D 2	.1050D 3	.9998D 0	.7802D 2

Table XXV. Computer Results of LMS-4A Run No. 2 (LMSC-2).

Time Min.	RATIOC	Gas Temp. °F	Time Min.	RATIOC	Gas Temp. °F
.7500D 1	.1026D-3	.9209D 2	.1500D 2	.6506D-3	.1208D 3
.2250D 2	.1181D-2	.1336D 3	.3000D 2	.1523D-2	.1396D 3
.3750D 2	.1713D-2	.1423D 3	.4500D 2	.1833D-2	.1440D 3
.5250D 2	.1929D-2	.1452D 3	.6000D 2	.2020D-2	.1462D 3
.6750D 2	.2113D-2	.1473D 3	.7500D 2	.2210D-2	.1483D 3
.8250D 2	.2307D-2	.1494D 3	.9000D 2	.2412D-2	.1504D 3
.9750D 2	.2542D-2	.1514D 3	.1050D 3	.2737D-2	.1525D 3
.1125D 3	.3154D-2	.1536D 3	.1200D 3	.4371D-2	.1548D 3
.1275D 3	.8453D-2	.1557D 3	.1350D 3	.2248D-1	.1556D 3
.1425D 3	.6942D-1	.1531D 3	.1500D 3	.2062D 0	.1436D 3
.1575D 3	.5033D 0	.1211D 3	.1650D 3	.8596D 0	.9229D 2
.1725D 3	.9689D 0	.8156D 2	.1800D 3	.9927D 0	.7890D 2
.1875D 3	.9982D 0	.7823D 2	.1950D 3	.9996D 0	.7806D 2
.2025D 3	.9999D 0	.7801D 2			

Table XXVI. Computer Results of LMS-4A Run No. 3 (LMSC-3).

Time Min.	RATIOC	Gas ^{o}F Temp.	Time Min.	RATIOC	Gas ^{o}F Temp.
.7500D 1	.2311D-3	.8012D 2	.1500D 2	.3622D-3	.8115D 2
.2250D 2	.3913D-3	.8137D 2	.3000D 2	.3964D-3	.8141D 2
.3750D 2	.3973D-3	.8142D 2	.4500D 2	.3976D-3	.8142D 2
.5250D 2	.3979D-3	.8142D 2	.6000D 2	.3981D-3	.8142D 2
.6750D 2	.3983D-3	.8143D 2	.7500D 2	.3986D-3	.8143D 2
.8250D 2	.3988D-3	.8143D 2	.9000D 2	.3991D-3	.8143D 2
.9750D 2	.3994D-3	.8143D 2	.1050D 3	.3997D-3	.8144D 2
.1125D 3	.4000D-3	.8144D 2	.1200D 3	.4003D-3	.8144D 2
.1275D 3	.4006D-3	.8144D 2	.1350D 3	.4009D-3	.8144D 2
.1425D 3	.4013D-3	.8145D 2	.1500D 3	.4016D-3	.8145D 2
.1575D 3	.4020D-3	.8145D 2	.1650D 3	.4024D-3	.8146D 2
.1725D 3	.4029D-3	.8146D 2	.1800D 3	.4330D-3	.8146D 2
.1875D 3	.4039D-3	.8147D 2	.1950D 3	.4046D-3	.8147D 2
.2025D 3	.4051D-3	.8148D 2	.2100D 3	.4054D-3	.8148D 2
.2175D 3	.4056D-3	.8148D 2	.2250D 3	.4058D-3	.8148D 2
.2325D 3	.4061D-3	.8148D 2	.2400D 3	.4064D-3	.8149D 2
.2475D 3	.4068D-3	.8149D 2	.2550D 3	.4073D-3	.8149D 2
.2625D 3	.4079D-3	.8150D 2	.2700D 3	.4086D-3	.8150D 2
.2775D 3	.4090D-3	.8150D 2	.2850D 3	.4092D-3	.8151D 2
.2925D 3	.4094D-3	.8151D 2	.3000D 3	.4097D-3	.8151D 2
.3075D 3	.4100D-3	.8151D 2	.3150D 3	.4103D-3	.8151D 2
.3225D 3	.4108D-3	.8152D 2	.3300D 3	.4112D-3	.8152D 2
.3375D 3	.4118D-3	.8152D 2	.3450D 3	.4125D-3	.8153D 2
.3525D 3	.4129D-3	.8153D 2	.3600D 3	.4131D-3	.8153D 2
.3675D 3	.4133D-3	.8154D 2	.3750D 3	.4136D-3	.8154D 2
.3825D 3	.4139D-3	.8154D 2	.3900D 3	.4143D-3	.8154D 2
.3975D 3	.4147D-3	.8155D 2	.4050D 3	.4152D-3	.8155D 2
.4125D 3	.4158D-3	.8155D 2	.4200D 3	.4165D-3	.8156D 2
.4275D 3	.4169D-3	.8156D 2	.4350D 3	.4171D-3	.8156D 2

Table XXVI (continued)

Time Min.	RATIOC	Gas ^{o}F Temp.	Time Min.	RATIOC	Gas ^{o}F Temp.
.4425D 3	.4173D-3	.8156D 2	.4500D 3	.4176D-3	.8157D 2
.4575D 3	.4179D-3	.8157D 2	.4650D 3	.4183D-3	.8157D 2
.4725D 3	.4188D-3	.8157D 2	.4800D 3	.4193D-3	.8158D 2
.4875D 3	.4200D-3	.8158D 2	.4950D 3	.4207D-3	.8159D 2
.5025D 3	.4211D-3	.8159D 2	.5100D 3	.4213D-3	.8159D 2
.5175D 3	.4216D-3	.8159D 2	.5250D 3	.4219D-3	.8160D 2
.5325D 3	.4223D-3	.8160D 2	.5400D 3	.4228D-3	.8160D 2
.5475D 3	.4234D-3	.8160D 2	.5550D 3	.4240D-3	.8161D 2
.5625D 3	.4249D-3	.8161D 2	.5700D 3	.4256D-3	.8162D 2
.5775D 3	.4261D-3	.8162D 2	.5850D 3	.4265D-3	.8162D 2
.5925D 3	.4270D-3	.8162D 2	.6000D 3	.4276D-3	.8163D 2
.6075D 3	.4283D-3	.8163D 2	.6150D 3	.4291D-3	.8163D 2
.6225D 3	.4300D-3	.8163D 2	.6300D 3	.4311D-3	.8164D 2
.6375D 3	.4324D-3	.8164D 2	.6450D 3	.4337D-3	.8165D 2
.6525D 3	.4348D-3	.8165D 2	.6600D 3	.4360D-3	.8165D 2
.6675D 3	.4373D-3	.8165D 2	.6750D 3	.4389D-3	.8165D 2
.6825D 3	.4408D-3	.8166D 2	.6900D 3	.4429D-3	.8166D 2
.6975D 3	.4454D-3	.8166D 2	.7050D 3	.4484D-3	.8167D 2
.7125D 3	.4518D-3	.8167D 2	.7200D 3	.4555D-3	.8168D 2
.7275D 3	.4594D-3	.8168D 2	.7350D 3	.4638D-3	.8168D 2
.7425D 3	.4690D-3	.8168D 2	.7500D 3	.4750D 3	.8168D 2
.7575D 3	.4819D-3	.8169D 2	.7650D 3	.4900D-3	.8169D 2
.7725D 3	.4994D-3	.8169D 2	.7800D 3	.5102D-3	.8170D 2
.7875D 3	.5229D-3	.8170D 2	.7950D 3	.5371D-3	.8171D 2
.8025D 3	.5533D-3	.8171D 2	.8100D 3	.5721D-3	.8171D 2
.8175D 3	.5938D-3	.8171D 2	.8250D 3	.6191D-3	.8171D 2
.8325D 3	.6483D-3	.8172D 2	.8400D 3	.6822D-3	.8172D 2
.8475D 3	.7214D-3	.8172D 2	.8550D 3	.7668D-3	.8173D 2
.8625D 3	.8195D-3	.8173D 2	.8700D 3	.8801D-3	.8174D 2

Table XXVI (continued)

Time Min.	RATIOC	Gas Temp. °F	Time Min.	RATIOC	Gas Temp. °F
.8775D 3	.9502D-3	.8174D 2	.8850D 3	.1032D-2	.8174D 2
.8925D 3	.1126D-2	.8174D 2	.9000D 3	.1235D-2	.8174D 2
.9075D 3	.1361D-2	.8174D 2	.9150D 3	.1507D-2	.8175D 2
.9225D 3	.1676D-2	.8175D 2	.9300D 3	.1872D-2	.8176D 2
.9375D 3	.2098D-2	.8176D 2	.9450D 3	.2361D-2	.8176D 2
.9525D 3	.2666D-2	.8176D 2	.9600D 3	.3020D-2	.8176D 2
.9675D 3	.3429D-2	.8176D 2	.9750D 3	.3902D-2	.8176D 2
.9825D 3	.4447D-2	.8176D 2	.9900D 3	.5076D-2	.8176D 2
.9975D 3	.5801D-2	.8177D 2	.1005D 4	.6641D-2	.8177D 2
.1013D 4	.7616D-2	.8177D 2	.1020D 4	.8749D-2	.8177D 2
.1027D 4	.1006D-1	.8176D 2	.1035D 4	.1158D-1	.8176D 2
.1043D 4	.1332D-1	.8175D 2	.1050D 4	.1532D-1	.8175D 2
.1057D 4	.1761D-1	.8174D 2	.1065D 4	.2023D-1	.8174D 2
.1073D 4	.2325D-1	.8173D 2	.1080D 4	.2672D-1	.8172D 2
.1087D 4	.3074D-1	.8171D 2	.1095D 4	.3538D-1	.8169D 2
.1102D 4	.4070D-1	.8167D 2	.1110D 4	.4674D-1	.8165D 2
.1118D 4	.5356D-1	.8163D 2	.1125D 4	.6123D-1	.8160D 2
.1132D 4	.6983D-1	.8157D 2	.1140D 4	.7950D-1	.8154D 2
.1148D 4	.9036D-1	.8150D 2	.1155D 4	.1027D 0	.8146D 2
.1162D 4	.1166D 0	.8141D 2	.1170D 4	.1323D 0	.8135D 2
.1178D 4	.1494D 0	.8128D 2	.1185D 4	.1680D 0	.8121D 2
.1192D 4	.1878D 0	.8113D 2	.1200D 4	.2091D 0	.8105D 2
.1207D 4	.2317D 0	.8097D 2	.1215D 4	.2561D 0	.8088D 2
.1222D 4	.2824D 0	.8078D 2	.1230D 4	.3111D 0	.8067D 2
.1237D 4	.3425D 0	.8055D 2	.1245D 4	.3753D 0	.8042D 2
.1253D 4	.4084D 0	.8030D 2	.1260D 4	.4414D 0	.8017D 2
.1268D 4	.4742D 0	.8004D 2	.1275D 4	.5072D 0	.7991D 2
.1283D 4	.5404D 0	.7979D 2	.1290D 4	.5745D 0	.7965D 2
.1298D 4	.6096D 0	.7952D 2	.1305D 4	.6475D 0	.7938D 2

Table XXVI (continued)

Time Min.	RATIOC	Gas ^{o}F Temp.	Time Min.	RATIOC	Gas ^{o}F Temp.
.1313D 4	.6868D 0	.7922D 2	.1320D 4	.7230D 0	.7908D 2
.1328D 4	.7550D 0	.7896D 2	.1335D 4	.7835D 0	.7884D 2
.1342D 4	.8095D 0	.7874D 2	.1350D 4	.8340D 0	.7865D 2
.1358D 4	.8581D 0	.7855D 2	.1365D 4	.8820D 0	.7846D 2
.1372D 4	.9069D 0	.7837D 2	.1380D 4	.9359D 0	.7826D 2
.1388D 4	.9623D 0	.7815D 2	.1395D 4	.9791D 0	.7808D 2
.1402D 4	.9888D 0	.7805D 2	.1410D 4	.9940D 0	.7802D 2
.1418D 4	.9969D 0	.7801D 2	.1425D 4	.9984D 0	.7801D 2

Table XXVII. Computer Results of LMS-4A Run No. 4 (LMSC-4).

Time Min.	RATIOC	Gas ^{o}F Temp.	Time Min.	RATIOC	Gas ^{o}F Temp.
.7500D 1	.9992D-3	.1224D 3	.1500D 2	.2632D-3	.1440D 3
.2250D 2	.3128D-2	.1478D 3	.3000D 2	.3613D-2	.1502D 3
.3750D 2	.4672D-2	.1519D 3	.4500D 2	.8016D-2	.1530D 3
.5250D 2	.1972D-1	.1534D 3	.6000D 2	.5861D-1	.1517D 3
.6750D 2	.1652D 0	.1447D 3	.7500D 2	.3741D 0	.1295D 3
.8250D 2	.6370D 0	.1089D 3	.9000D 2	.8450D 0	.9181D 2
.9750D 2	.9680D 0	.8122D 3	.1050D 3	.9952D 0	.7851D 2
.1125D 3	.9993D 0	.7807D 2			

Table XXVIII. Computer Results of LMS-4A Run No. 5 (LMSC-5).

Time Min.	RATIOC	Gas ^{o}F Temp.	Time Min.	RATIOC	Gas ^{o}F Temp.
.7500D 1	.6061D-3	.1284D 3	.1500D 2	.1350D-2	.1471D 3
.2250D 2	.1675D-2	.1525D 3	.3000D 2	.1821D-2	.1546D 3
.3750D 2	.1922D-2	.1559D 3	.4500D 2	.2029D-2	.1572D 3
.5250D 2	.2138D-2	.1585D 3	.6000D 2	.2421D-2	.1597D 3
.6750D 2	.8518D-2	.1606D 3	.7500D 2	.1672D 0	.1492D 3
.8250D 2	.9242D 0	.8689D 2	.9000D 2	.9977D 0	.7855D 2
.9750D 2	.9998D 0	.7806D 2			

Table XXIX. Computer Results of LMS-4A Run No. 6 (LMSC-6).

Time Min.	RATIOC	Gas ^{o}F Temp.	Time Min.	RATIOC	Gas ^{o}F Temp.
.7500D 1	.5113D-4	.8604D 2	.1500D 2	.5794D-3	.1183D 3
.2250D 2	.1196D-2	.1338D 3	.3000D 2	.1506D-2	.1392D 3
.3750D 2	.1642D-2	.1412D 3	.4500D 2	.1729D-2	.1424D 3
.5250D 2	.1808D-2	.1435D 3	.6000D 2	.1890D-2	.1445D 3
.6750D 2	.1976D-2	.1455D 3	.7500D 2	.2068D-2	.1466D 3
.8250D 2	.2165D-2	.1477D 3	.9000D 2	.2267D-2	.1488D 3
.9750D 2	.2378D-2	.1499D 3	.1050D 3	.2498D-2	.1510D 3
.1125D 3	.2626D-2	.1522D 3	.1200D 3	.2789D-2	.1533D 3
.1275D 3	.3225D-2	.1545D 3	.1350D 3	.5924D-2	.1556D 3
.1425D 3	.2682D-1	.1553D 3	.1500D 3	.1594D 0	.1463D 3
.1575D 3	.5713D 0	.1149D 3	.1650D 3	.9350D 0	.8471D 2
.1725D 3	.9961D 0	.7851D 2	.1800D 3	.9997D 0	.7804D 2

Table XXX. Computer Results of LMS-4A Run No. 7 (LMSC-7).

Time Min.	RATIOC	Gas Temp. °F	Time Min.	RATIOC	Gas Temp. °F
.7500D 1	.4743D-3	.1140D 3	.1500D 2	.8683D-3	.1262D 3
.2250D 2	.9818D-3	.1288D 3	.3000D 2	.1115D-2	.1306D 3
.3750D 2	.1449D-2	.1324D 3	.4500D 2	.2806D-2	.1340D 3
.5250D 2	.9316D-2	.1351D 3	.6000D 2	.3927D-1	.1349D 3
.6750D 2	.1432D 0	.1301D 3	.7500D 2	.3495D 0	.1186D 3
.8250D 2	.5950D 0	.1039D 3	.9000D 2	.8036D 0	.9103D 2
.9750D 2	.9466D 0	.8178D 2	.1050D 3	.9971D 0	.7827D 2
.1125D 3	.9999D 0	.7801D 2			

Table XXXI. Computer Results of LMS-4A Run No. 8 (LMSC-8).

Time Min.	RATIOC	Gas ^{o}F Temp.	Time Min.	RATIOC	Gas ^{o}F Temp.
.7500D 1	.4422D-3	.1129D 3	.1500D 2	.8291D-3	.1255D 3
.2250D 2	.9807D-3	.1291D 3	.3000D 2	.1068D-2	.1309D 3
.3750D 2	.1162D-2	.1324D 3	.4500D 2	.1376D-2	.1339D 3
.5250D 2	.2340D-2	.1354D 3	.6000D 2	.8099D-2	.1365D 3
.6750D 2	.4311D-1	.1362D 3	.7500D 2	.2110D 0	.1276D 3
.8250D 2	.6113D 0	.1037D 3	.9000D 2	.9467D 0	.8229D 2
.9750D 2	.9982D 0	.7820D 2	.1050D 3	.9999D 0	.7801D 2

Table XXXII. Computer Results of LMS-4A Run No. 9 (LMSC-9).

Time Min.	RATIOC	Gas Temp. °F	Time Min.	RATIOC	Gas Temp. °F
.7500D 1	.7168D-3	.1225D 3	.1500D 2	.1449D-2	.1383D 3
.2250D 2	.1748D-2	.1426D 3	.3000D 2	.1940D-2	.1449D 3
.3750D 2	.2162D-2	.1468D 3	.4500D 2	.2669D-2	.1488D 3
.5250D 2	.4658D-2	.1507D 3	.6000D 2	.1429D-1	.1519D 3
.6750D 2	.6103D-1	.1505D 3	.7500D 2	.2467D 0	.1383D 3
.8250D 2	.6550D 0	.1073D 3	.9000D 2	.9560D 0	.8245D 2
.9750D 2	.9973D 0	.7833D 2	.1050D 3	.9998D 0	.7802D 2

Table XXXIII. Computer Results of LMS-4A Run No. 10 (LMSC-10).

Time Min.	RATIOC	Gas ^{o}F Temp.	Time Min.	RATIOC	Gas ^{o}F Temp.
.7500D 1	.7698D-3	.1241D 3	.1500D 2	.1799D-2	.1436D 3
.2250D 2	.2244D-2	.1491D 3	.3000D 2	.2456D-2	.1512D 3
.3750D 2	.2664D-2	.1525D 3	.4500D 2	.3186D-2	.1537D 3
.5250D 2	.5334D-2	.1548D 3	.6000D 2	.1551D-1	.1553D 3
.6750D 2	.6324D-1	.1528D 3	.7500D 2	.2492D 0	.1397D 3
.8250D 2	.6583D 0	.1079D 3	.9000D 2	.9562D 0	.8268D 3
.9750D 2	.9969D 0	.7840D 2	.1050D 3	.9998D 0	.7803D 3

Table XXXIV. Computer Results of LMS-4A Run No. 11 (LMSC-11).

Time Min.	RATIOC	Gas ^{o}F Temp.	Time Min.	RATIOC	Gas ^{o}F Temp.
.7500D 1	.7305D-3	.1234D 3	.1500D 2	.1746D-2	.1431D 3
.2250D 2	.2187D-2	.1486D 3	.3000D 2	.2382D-2	.1507D 3
.3750D 2	.2518D-2	.1520D 3	.4500D 2	.2710D-2	.1532D 3
.5250D 2	.3408D-2	.1545D 3	.6000D 2	.8058D-2	.1553D 3
.6750D 2	.4209D-1	.1539D 3	.7500D 2	.2297D 0	.1408D 3
.8250D 2	.6780D 0	.1062D 3	.9000D 2	.9646D 0	.8187D 2
.9750D 2	.9976D 0	.7833D 2	.1050D 3	.9998D 0	.7802D 2

Table XXXV. Computer Results of LMS-4A Run No. 12 (LMSC-12).

Time Min.	RATIOC	Gas ^{o}F Temp.	Time Min.	RATIOC	Gas ^{o}F Temp.
.7500D 1	.6800D-3	.1219D 3	.1500D 2	.1738D-2	.1429D 3
.2250D 2	.2186D-2	.1486D 3	.3000D 2	.2367D-2	.1506D 3
.3750D 2	.2495D-2	.1518D 3	.4500D 2	.2633D-2	.1530D 3
.5250D 2	.2883D-2	.1540D 3	.6000D 2	.4024D-2	.1552D 3
.6750D 2	.1142D-1	.1556D 3	.7500D 2	.6033D-1	.1532D 3
.8250D 2	.2855D 0	.1368D 3	.9000D 2	.7344D 0	.1017D 3
.9750D 2	.9735D 0	.8094D 2	.1050D 3	.9979D 0	.7827D 2
.1125D 3	.9999D 0	.7802D 2			

Table XXXVI. Computer Results of Activated Alumina Run No. 1 (ACTC-1).

Time Min.	RATIOC	Gas ^{o}F Temp.	Time Min.	RATIOC	Gas ^{o}F Temp.
.6000D 1	.2685D-3	.1063D 3	.1500D 2	.1133D-2	.1299D 3
.2100D 2	.3783D-2	.1347D 3	.3000D 2	.4884D-2	.1351D 3
.3600D 2	.1486D 0	.1298D 3	.4500D 2	.3634D 0	.1165D 3
.5100D 2	.4670D 0	.1096D 3	.6000D 2	.5600D 0	.1034D 3
.6600D 2	.6015D 0	.1008D 3	.7500D 2	.6479D 0	.9788D 2
.8100D 2	.6723D 0	.9641D 2	.9000D 2	.7024D 0	.9463D 2
.9600D 2	.7194D 0	.9364D 2	.1050D 3	.7415D 0	.9237D 2
.1110D 3	.7544D 0	.9164D 2	.1200D 3	.7718D 0	.9066D 2
.1260D 3	.7824D 0	.9007D 2	.1350D 3	.7968D 0	.8927D 2
.1410D 3	.8057D 0	.8878D 2	.1500D 3	.8181D 0	.8809D 2
.1560D 3	.8258D 0	.8767D 2	.1650D 3	.8367D 0	.8707D 2
.1710D 3	.8436D 0	.8669D 2	.1800D 3	.8533D 0	.8615D 2
.1860D 3	.8595D 0	.8582D 2	.1950D 3	.8683D 0	.8533D 2
.2010D 3	.8739D 0	.8503D 2	.2100D 3	.8819D 0	.8459D 2
.2160D 3	.8870D 0	.8431D 2	.2250D 3	.8943D 0	.8390D 2
.2310D 3	.8989D 0	.8365D 2	.2400D 3	.9055D 0	.8328D 2
.2460D 3	.9098D 0	.8305D 2	.2550D 3	.9158D 0	.8271D 2
.2610D 3	.9197D 0	.8250D 2	.2700D 3	.9252D 0	.8220D 2
.2760D 3	.9287D 0	.8200D 2	.2850D 3	.9337D 0	.8172D 2
.2910D 3	.9368D 0	.8155D 2	.3000D 3	.9414D 0	.8130D 2
.3060D 3	.9442D 0	.8114D 2	.3150D 3	.9483D 0	.8091D 2
.3210D 3	.9509D 0	.8076D 2	.3300D 3	.9546D 0	.8056D 2
.3360D 3	.9569D 0	.8043D 2	.3450D 3	.9602D 0	.8025D 2
.3510D 3	.9625D 0	.8013D 2	.3600D 3	.9652D 0	.7996D 2
.3660D 3	.9671D 0	.7986D 2	.3750D 3	.9697D 0	.7971D 2
.3810D 3	.9713D 0	.7962D 2	.3900D 3	.9736D 0	.7949D 2
.3960D 3	.9751D 0	.7941D 2	.4050D 3	.9772D 0	.7929D 2
.4110D 3	.9785D 0	.7922D 2	.4200D 3	.9803D 0	.7912D 2
.4260D 3	.9814D 0	.7906D 2	.4350D 3	.9830D 0	.7897D 2

Table XXXVI (continued)

Time Min.	RATIOC	Gas Temp. °F	Time Min.	RATIOC	Gas Temp. °F
.4410D 3	.9840D 0	.7891D 2	.4500D 3	.9854D 0	.7883D 2
.4560D 3	.9862D 0	.7878D 2	.4650D 3	.9874D 0	.7871D 2
.4710D 3	.9882D 0	.7867D 2	.4800D 3	.9893D 0	.7861D 2
.4860D 3	.9899D 0	.7857D 2	.4950D 3	.9909D 0	.7852D 2
.5010D 3	.9914D 0	.7849D 2	.5100D 3	.9922D 0	.7844D 2
.5160D 3	.9927D 0	.7841D 2	.5250D 3	.9934D 0	.7838D 2
.5310D 3	.9939D 0	.7835D 2	.5400D 3	.9945D 0	.7832D 2
.5460D 3	.9949D 0	.7829D 2	.5550D 3	.9954D 0	.7826D 2
.5610D 3	.9957D 0	.7825D 2	.5700D 3	.9962D 0	.7822D 2
.5760D 3	.9965D 0	.7820D 2	.5850D 3	.9969D 0	.7818D 2
.5910D 3	.9971D 0	.7817D 2	.6000D 3	.9974D 0	.7815D 2
.6060D 3	.9977D 0	.7814D 2	.6150D 3	.9980D 0	.7812D 2
.6210D 3	.9982D 0	.7811D 2	.6300D 3	.9984D 0	.7809D 2
.6360D 3	.9986D 0	.7808D 2	.6450D 3	.9988D 0	.7807D 2
.6510D 3	.9989D 0	.7806D 2	.6600D 3	.9991D 0	.7805D 2
.6660D 3	.9993D 0	.7804D 2	.6750D 3	.9995D 0	.7803D 2
.6810D 3	.9995D 0	.7803D 2	.6900D 3	.9997D 0	.7802D 2
.6960D 3	.9998D 0	.7801D 2			

Table XXXVII. Computer Results of Activated Alumina Run No 2 (ACTC-2).

Time Min.	RATIOC	Gas Temp. °F	Time Min.	RATIOC	Gas Temp. °F
.6000D 1	.1294D-4	.8090D 2	.1500D 2	.4603D-3	.1139D 3
.2100D 2	.7140D-3	.1219D 3	.3000D 2	.9875D-3	.1282D 3
.3600D 2	.1156D-2	.1304D 3	.4500D 2	.2026D-2	.1324D 3
.5100D 2	.4854D-2	.1332D 3	.6000D 2	.2485D-1	.1332D 3
.6600D 2	.6473D-1	.1314D 3	.7500D 2	.1829D 0	.1249D 3
.8100D 2	.2822D 0	.1189D 3	.9000D 2	.3956D 0	.1118D 3
.9600D 2	.4453D 0	.1086D 3	.1050D 3	.4990D 0	.1053D 3
.1110D 3	.5266D 0	.1036D 3	.1200D 3	.5604D 0	.1016D 3
.1260D 3	.5795D 0	.1005D 3	.1350D 3	.6044D 0	.9910D 2
.1410D 3	.6193D 0	.9828D 2	.1500D 3	.6394D 0	.9718D 2
.1560D 3	.6516D 0	.9652D 2	.1650D 3	.6686D 0	.9561D 2
.1710D 3	.6792D 0	.9505D 2	.1800D 3	.6940D 0	.9426D 2
.1860D 3	.7033D 0	.9377D 2	.1950D 3	.7165D 0	.9308D 2
.2010D 3	.7249D 0	.9264D 2	.2100D 3	.7368D 0	.9201D 2
.2160D 3	.7445D 0	.9162D 2	.2250D 3	.7554D 0	.9105D 2
.2310D 3	.7623D 0	.9068D 2	.2400D 3	.7724D 0	.9016D 2
.2460D 3	.7788D 0	.8982D 2	.2550D 3	.7881D 0	.8934D 2
.2610D 3	.7941D 0	.8903D 2	.2700D 3	.8027D 0	.8858D 2
.2760D 3	.8083D 0	.8829D 2	.2850D 3	.8164D 0	.8787D 2
.2910D 3	.8216D 0	.8759D 2	.3000D 3	.8291D 0	.8720D 2
.3060D 3	.8339D 0	.8695D 2	.3150D 3	.8410D 0	.8658D 2
.3210D 3	.8455D 0	.8634D 2	.3300D 3	.8522D 0	.8599D 2
.3360D 3	.8564D 0	.8576D 2	.3450D 3	.8626D 0	.8544D 2
.3510D 3	.8666D 0	.8523D 2	.3600D 3	.8724D 0	.8492D 2
.3660D 3	.8762D 0	.8472D 2	.3750D 3	.8817D 0	.8443D 2
.3810D 3	.8852D 0	.8424D 2	.3900D 3	.8903D 0	.8397D 2
.3960D 3	.8937D 0	.8379D 2	.4050D 3	.8985D 0	.8354D 2
.4110D 3	.9016D 0	.8337D 2	.4200D 3	.9061D 0	.8313D 2

Table XXXVII (continued)

Time Min.	RATIOC	Gas Temp. °F	Time Min.	RATIOC	Gas Temp. °F
.4260D 3	.9090D 0	.8297D 2	.4350D 3	.9133D 0	.8275D 2
.4410D 3	.9160D 0	.8260D 2	.4500D 3	.9200D 0	.8239D 2
.4560D 3	.9226D 0	.8225D 2	.4650D 3	.9263D 0	.8205D 2
.4710D 3	.9287D 0	.8192D 2	.4800D 3	.9322D 0	.8173D 2
.4860D 3	.9344D 0	.8161D 2	.4950D 3	.9377D 0	.8143D 2
.5010D 3	.9398D 0	.8132D 2	.5100D 3	.9429D 0	.8115D 2
.5160D 3	.9448D 0	.8105D 2	.5250D 3	.9477D 0	.8089D 2
.5310D 3	.9495D 0	.8079D 2	.5400D 3	.9521D 0	.8065D 2
.5460D 3	.9538D 0	.8055D 2	.5550D 3	.9563D 0	.8042D 2
.5610D 3	.9579D 0	.8033D 2	.5700D 3	.9602D 0	.8021D 2
.5760D 3	.9616D 0	.8013D 2	.5850D 3	.9638D 0	.8001D 2
.5910D 3	.9651D 0	.7994D 2	.6000D 3	.9671D 0	.7983D 2
.6060D 3	.9683D 0	.7976D 2	.6150D 3	.9701D 0	.7966D 2
.6210D 3	.9713D 0	.7960D 2	.6300D 3	.9730D 0	.7951D 2
.6360D 3	.9740D 0	.7945D 2	.6450D 3	.9756D 0	.7936D 2
.6510D 3	.9765D 0	.7931D 2	.6600D 3	.9779D 0	.7923D 2
.6660D 3	.9789D 0	.7918D 2	.6750D 3	.9801D 0	.7911D 2
.6810D 3	.9810D 0	.7907D 2	.6900D 3	.9821D 0	.7900D 2
.6960D 3	.9829D 0	.7896D 2	.7050D 3	.9840D 0	.7890D 2
.7110D 3	.9847D 0	.7886D 2	.7200D 3	.9857D 0	.7881D 2
.7260D 3	.9863D 0	.7877D 2	.7350D 3	.9872D 0	.7872D 2
.7410D 3	.9877D 0	.7869D 2	.7500D 3	.9886D 0	.7864D 2
.7560D 3	.9891D 0	.7862D 2	.7650D 3	.9898D 0	.7857D 2
.7710D 3	.9903D 0	.7855D 2	.7800D 3	.9909D 0	.7851D 2
.7860D 3	.9914D 0	.7849D 2	.7950D 3	.9920D 0	.7845D 2
.8010D 3	.9924D 0	.7843D 2	.8100D 3	.9929D 0	.7840D 2
.8160D 3	.9932D 0	.7838D 2	.8250D 3	.9937D 0	.7835D 2
.8310D 3	.9940D 0	.7834D 2	.8400D 3	.9945D 0	.7831D 2

Table XXXVII (continued)

Time Min.	RATIOC	Gas Temp. °F	Time Min.	RATIOC	Gas Temp. °F
.8460D 3	.9948D 0	.7830D 2	.8550D 3	.9952D 0	.7827D 2
.8610D 3	.9954D 0	.7826D 2	.8700D 3	.9958D 0	.7824D 2
.8760D 3	.9960D 0	.7823D 2	.8850D 3	.9963D 0	.7821D 2
.8910D 3	.9965D 0	.7820D 2	.9000D 3	.9968D 0	.7818D 2
.9060D 3	.9970D 0	.7817D 2	.9150D 3	.9973D 0	.7816D 2
.9210D 3	.9974D 0	.7815D 2	.9300D 3	.9976D 0	.7814D 2
.9360D 3	.9978D 0	.7813D 2	.9450D 3	.9980D 0	.7811D 2
.9510D 3	.9981D 0	.7811D 2	.9600D 3	.9983D 0	.7810D 2
.9660D 3	.9984D 0	.7809D 2	.9750D 3	.9986D 0	.7808D 2
.9810D 3	.9987D 0	.7808D 2	.9900D 3	.9989D 0	.7807D 2
.9960D 3	.9989D 0	.7806D 2	.1005D 4	.9991D 0	.7805D 2
.1011D 4	.9992D 0	.7805D 2	.1020D 4	.9993D 0	.7804D 2
.1026D 4	.9994D 0	.7804D 2	.1035D 4	.9995D 0	.7803D 2
.1041D 4	.9995D 0	.7803D 2	.1050D 4	.9997D 0	.7803D 2
.1056D 4	.9997D 0	.7802D 2	.1065D 4	.9998D 0	.7801D 2
.1071D 4	.9998D 0	.7801D 2			

Table XXXVIII. Computer Results of Activated Alumina Run No. 3 (ACTC-3).

Time Min.	RATIOC	Gas ^{o}F Temp.	Time Min.	RATIOC	Gas ^{o}F Temp.
.6000D 1	.1303D-3	.7929D 2	.1500D 2	.2532D-3	.8032D 2
.2100D 2	.2739D-3	.8050D 2	.3000D 2	.2841D-3	.8058D 2
.3600D 2	.2864D-3	.8060D 2	.4500D 2	.2882D-3	.8062D 2
.5100D 2	.2893D-3	.8063D 2	.6000D 2	.2910D-3	.8064D 2
.6600D 2	.2921D-3	.8065D 2	.7500D 2	.2940D-3	.8066D 2
.8100D 2	.2953D-3	.8067D 2	.9000D 2	.2978D-3	.8068D 2
.9600D 2	.3000D-3	.8069D 2	.1050D 3	.3048D-3	.8070D 2
.1110D 3	.3098D-3	.8071D 2	.1200D 3	.3223D-3	.8072D 2
.1260D 3	.3365D-3	.8073D 2	.1350D 3	.3739D-3	.8074D 2
.1410D 3	.4170D-3	.8075D 2	.1500D 3	.5317D-3	.8076D 2
.1560D 3	.6645D-3	.8077D 2	.1650D 3	.1017D-2	.8078D 2
.1710D 3	.1421D-2	.8079D 2	.1800D 3	.2481D-2	.8080D 2
.1860D 3	.3678D-2	.8080D 2	.1950D 3	.6721D-2	.8080D 2
.2010D 3	.1002D-1	.8080D 2	.2100D 3	.1793D-1	.8079D 2
.2160D 3	.2595D-1	.8077D 2	.2250D 3	.4370D-1	.8073D 2
.2310D 3	.6037D-1	.8069D 2	.2400D 3	.9430D-1	.8060D 2
.2460D 3	.1236D 0	.8052D 2	.2550D 3	.1783D 0	.8036D 2
.2610D 3	.2216D 0	.8025D 2	.2700D 3	.2959D 0	.8004D 2
.2760D 3	.3503D 0	.7989D 2	.2850D 3	.4368D 0	.7964D 2
.2910D 3	.4958D 0	.7947D 2	.3000D 3	.5831D 0	.7921D 2
.3060D 3	.6387D 0	.7905D 2	.3150D 3	.7152D 0	.7883D 2
.3210D 3	.7600D 0	.7870D 2	.3300D 3	.8149D 0	.7853D 2
.3360D 3	.8430D 0	.7845D 2	.3450D 3	.8742D 0	.7836D 2
.3510D 3	.8891D 0	.7831D 2	.3600D 3	.9052D 0	.7827D 2
.3660D 3	.9128D 0	.7824D 2	.3750D 3	.9209D 0	.7822D 2
.3810D 3	.9249D 0	.7821D 2	.3900D 3	.9293D 0	.7820D 2
.3960D 3	.9315D 0	.7819D 2	.4050D 3	.9341D 0	.7818D 2
.4110D 3	.9356D 0	.7818D 2	.4200D 3	.9374D 0	.7817D 2
.4260D 3	.9385D 0	.7817D 2	.4350D 3	.9400D 0	.7816D 2

Table XXXVIII (continued)

Time Min.	RATIOC	Gas Temp. °F	Time Min.	RATIOC	Gas Temp. °F
.4410D 3	.9409D 0	.7816D 2	.4500D 3	.9422D 0	.7816D 2
.4560D 3	.9430D 0	.7816D 2	.4650D 3	.9442D 0	.7815D 2
.4710D 3	.9449D 0	.7815D 2	.4800D 3	.9460D 0	.7815D 2
.4860D 3	.9468D 0	.7815D 2	.4950D 3	.9478D 0	.7814D 2
.5010D 3	.9485D 0	.7814D 2	.5100D 3	.9495D 0	.7814D 2
.5160D 3	.9502D 0	.7814D 2	.5250D 3	.9512D 0	.7813D 2
.5310D 3	.9519D 0	.7813D 2	.5400D 3	.9528D 0	.7813D 2
.5460D 3	.9534D 0	.7813D 2	.5550D 3	.9544D 0	.7813D 2
.5610D 3	.9550D 0	.7812D 2	.5700D 3	.9559D 0	.7812D 2
.5760D 3	.9565D 0	.7812D 2	.5850D 3	.9573D 0	.7812D 2
.5910D 3	.9579D 0	.7812D 2	.6000D 3	.9587D 0	.7811D 2
.6060D 3	.9593D 0	.7811D 2	.6150D 3	.9601D 0	.7811D 2
.6210D 3	.9606D 0	.7811D 2	.6300D 3	.9614D 0	.7811D 2
.6360D 3	.9619D 0	.7810D 2	.6450D 3	.9627D 0	.7810D 2
.6510D 3	.9632D 0	.7810D 2	.6600D 3	.9639D 0	.7810D 2
.6660D 3	.9644D 0	.7810D 2	.6750D 3	.9651D 0	.7810D 2
.6810D 3	.9656D 0	.7809D 2	.6900D 3	.9663D 0	.7809D 2
.6960D 3	.9667D 0	.7809D 2	.7050D 3	.9674D 0	.7809D 2
.7110D 3	.9678D 0	.7809D 2	.7200D 3	.9685D 0	.7809D 2
.7260D 3	.9689D 0	.7809D 2	.7350D 3	.9695D 0	.7808D 2
.7410D 3	.9699D 0	.7808D 2	.7500D 3	.9705D 0	.7808D 2
.7560D 3	.9709D 0	.7808D 2	.7650D 3	.9715D 0	.7808D 2
.7710D 3	.9719D 0	.7808D 2	.7800D 3	.9725D 0	.7808D 2
.7860D 3	.9729D 0	.7807D 2	.7950D 3	.9734D 0	.7807D 2
.8010D 3	.9738D 0	.7807D 2	.8100D 3	.9744D 0	.7807D 2
.8160D 3	.9748D 0	.7807D 2	.8250D 3	.9754D 0	.7807D 2
.8310D 3	.9758D 0	.7807D 2	.8400D 3	.9764D 0	.7807D 2
.8460D 3	.9768D 0	.7806D 2	.8550D 3	.9775D 0	.7806D 2
.8610D 3	.9779D 0	.7806D 2	.8700D 3	.9786D 0	.7806D 2
.8760D 3	.9790D 0	.7806D 2	.8850D 3	.9797D 0	.7806D 2

Table XXXVIII (continued)

Time Min.	RATIOC	Gas Temp. °F	Time Min.	RATIOC	Gas Temp. °F
.8910D 3	.9801D 0	.7806D 2	.9000D 3	.9808D 0	.7805D 2
.9060D 3	.9813D 0	.7805D 2	.9150D 3	.9819D 0	.7805D 2
.9210D 3	.9824D 0	.7805D 2	.9300D 3	.9831D 0	.7805D 2
.9360D 3	.9835D 0	.7805D 2	.9450D 3	.9842D 0	.7804D 2
.9510D 3	.9847D 0	.7804D 2	.9600D 3	.9854D 0	.7804D 2
.9660D 3	.9858D 0	.7804D 2	.9750D 3	.9865D 0	.7804D 2
.9810D 3	.9870D 0	.7804D 2	.9900D 3	.9876D 0	.7804D 2
.9960D 3	.9881D 0	.7803D 2	.1005D 4	.9888D 0	.7803D 2
.1011D 4	.9892D 0	.7803D 2	.1020D 4	.9899D 0	.7803D 2
.1026D 4	.9903D 0	.7803D 2	.1035D 4	.9909D 0	.7803D 2
.1041D 4	.9914D 0	.7802D 2	.1050D 4	.9920D 0	.7802D 2
.1056D 4	.9924D 0	.7802D 2	.1065D 4	.9931D 0	.7802D 2
.1071D 4	.9935D 0	.7802D 2	.1080D 4	.9941D 0	.7802D 2
.1086D 4	.9946D 0	.7802D 2	.1095D 4	.9951D 0	.7801D 2
.1101D 4	.9956D 0	.7801D 2	.1110D 4	.9962D 0	.7801D 2
.1116D 4	.9965D 0	.7801D 2	.1125D 4	.9972D 0	.7801D 2
.1131D 4	.9976D 0	.7801D 2	.1140D 4	.9979D 0	.7801D 2
.1146D 4	.9989D 0	.7800D 2	.1155D 4	.9989D 0	.7800D 2

Table XXXIX. Computer Results of Activated Alumina Run No. 4 (ACTC-4).

Time Min	RATIOC	Gas Temp. °F	Time Min.	RATIOC	Gas Temp. °F
.6000D 1	.3137D-3	.1047D 3	.1500D 2	.8355D-2	.1312D 3
.2100D 2	.4123D-1	.1339D 3	.3000D 2	.1535D 0	.1294D 3
.3600D 2	.2554D 0	.1235D 3	.4500D 2	.4097D 0	.1138D 3
.5100D 2	.4923D 0	.1083D 3	.6000D 2	.5789D 0	.1027D 3
.6600D 2	.6206D 0	.1000D 3	.7500D 2	.6685D 0	.9700D 2
.8100D 2	.6938D 0	.9545D 2	.9000D 2	.7249D 0	.9356D 2
.9600D 2	.7422D 0	.9253D 2	.1050D 3	.7642D 0	.9122D 2
.1110D 3	.7769D 0	.9048D 2	.1200D 3	.7935D 0	.8952D 2
.1260D 3	.8032D 0	.8895D 2	.1350D 3	.8162D 0	.8821D 2
.1410D 3	.8239D 0	.8776D 2	.1500D 3	.8344D 0	.8717D 2
.1560D 3	.8408D 0	.8681D 2	.1650D 3	.8495D 0	.8632D 2
.1710D 3	.8549D 0	.8602D 2	.1800D 3	.8624D 0	.8560D 2
.1860D 3	.8670D 0	.8534D 2	.1950D 3	.8735D 0	.8498D 2
.2010D 3	.8776D 0	.8476D 2	.2100D 3	.8834D 0	.8444D 2
.2160D 3	.8871D 0	.8424D 2	.2250D 3	.8923D 0	.8395D 2
.2310D 3	.8957D 0	.8377D 2	.2400D 3	.9005D 0	.8350D 2
.2460D 3	.9036D 0	.8333D 2	.2550D 3	.9080D 0	.8309D 2
.2610D 3	.9108D 0	.8294D 2	.2700D 3	.9149D 0	.8271D 2
.2760D 3	.9176D 0	.8257D 2	.2850D 3	.9214D 0	.8236D 2
.2910D 3	.9239D 0	.8222D 2	.3000D 3	.9274D 0	.8203D 2
.3060D 3	.9297D 0	.8190D 2	.3150D 3	.9331D 0	.8172D 2
.3210D 3	.9352D 0	.8160D 2	.3300D 3	.9383D 0	.8143D 2
.3360D 3	.9403D 0	.8132D 2	.3450D 3	.9432D 0	.8116D 2
.3510D 3	.9451D 0	.8105D 2	.3600D 3	.9478D 0	.8091D 2
.3660D 3	.9495D 0	.8081D 2	.3750D 3	.9520D 0	.8067D 2
.3810D 3	.9537D 0	.8058D 2	.3900D 3	.9560D 0	.8045D 2
.3960D 3	.9575D 0	.8037D 2	.4050D 3	.9597D 0	.8025D 2
.4110D 3	.9611D 0	.8017D 2	.4200D 3	.9631D 0	.8006D 2
.4260D 3	.9644D 0	.7999D 2	.4350D 3	.9662D 0	.7989D 2

Table XXXIX (continued)

Time Min.	RATIOC	Gas Temp. °F	Time Min.	RATIOC	Gas Temp. °F
.4410D 3	.9674D 0	.7982D 2	.4500D 3	.9692D 0	.7972D 2
.4560D 3	.9703D 0	.7966D 2	.4650D 3	.9719D 0	.7957D 2
.4710D 3	.9729D 0	.7952D 2	.4800D 3	.9743D 0	.7944D 2
.4860D 3	.9753D 0	.7938D 2	.4950D 3	.9766D 0	.7931D 2
.5010D 3	.9775D 0	.7926D 2	.5100D 3	.9787D 0	.7919D 2
.5160D 3	.9795D 0	.7915D 2	.5250D 3	.9806D 0	.7908D 2
.5310D 3	.9814D 0	.7904D 2	.5400D 3	.9823D 0	.7899D 2
.5460D 3	.9831D 0	.7895D 2	.5550D 3	.9840D 0	.7890D 2
.5610D 3	.9846D 0	.7886D 2	.5700D 3	.9855D 0	.7881D 2
.5760D 3	.9861D 0	.7878D 2	.5850D 3	.9869D 0	.7874D 2
.5910D 3	.9874D 0	.7871D 2	.6000D 3	.9881D 0	.7867D 2
.6060D 3	.9886D 0	.7864D 2	.6150D 3	.9892D 0	.7861D 2
.6210D 3	.9896D 0	.7858D 2	.6300D 3	.9902D 0	.7855D 2
.6360D 3	.9906D 0	.7853D 2	.6450D 3	.9912D 0	.7850D 2
.6510D 3	.9915D 0	.7848D 2	.6600D 3	.9920D 0	.7845D 2
.6660D 3	.9924D 0	.7843D 2	.6750D 3	.9928D 0	.7841D 2
.6810D 3	.9931D 0	.7839D 2	.6900D 3	.9935D 0	.7837D 2
.6960D 3	.9938D 0	.7835D 2	.7050D 3	.9942D 0	.7833D 2
.7110D 3	.9944D 0	.7832D 2	.7200D 3	.9948D 0	.7830D 2
.7260D 3	.9950D 0	.7828D 2	.7350D 3	.9953D 0	.7827D 2
.7410D 3	.9955D 0	.7825D 2	.7500D 3	.9958D 0	.7824D 2
.7560D 3	.9960D 0	.7823D 2	.7650D 3	.9963D 0	.7821D 2
.7710D 3	.9965D 0	.7820D 2	.7800D 3	.9967D 0	.7819D 2
.7860D 3	.9968D 0	.7818D 2	.7950D 3	.9971D 0	.7817D 2

Table XL. Computer Results of Activated Alumina Run No. 5 (ACTC-5).

Time Min.	RATIOC	Gas Temp. °F	Time Min.	RATIOC	Gas Temp. °F
.6000D 1	.3068D-3	.1122D 3	.1500D 2	.8713D-3	.1309D 3
.2100D 2	.1067D-2	.1351D 3	.3000D 2	.3017D-2	.1379D 3
.3600D 2	.3679D-1	.1370D 3	.4500D 2	.3225D 0	.1194D 3
.5100D 2	.4493D 0	.1109D 3	.6000D 2	.5366D 0	.1051D 3
.6600D 2	.5750D 0	.1026D 3	.7500D 2	.6206D 0	.9985D 2
.8100D 2	.6460D 0	.9835D 2	.9000D 2	.6790D 0	.9642D 2
.9600D 2	.6986D 0	.9530D 2	.1050D 3	.7250D 0	.9378D 2
.1110D 3	.7410D 0	.9287D 2	.1200D 3	.7630D 0	.9161D 2
.1260D 3	.7765D 0	.9084D 2	.1350D 3	.7953D 0	.8977D 2
.1410D 3	.8070D 0	.8911D 2	.1500D 3	.8233D 0	.8818D 2
.1560D 3	.8335D 0	.8760D 2	.1650D 3	.8477D 0	.8679D 2
.1710D 3	.8567D 0	.8628D 2	.1800D 3	.8651D 0	.8578D 2
.1860D 3	.8726D 0	.8539D 2	.1950D 3	.8839D 0	.8479D 2
.2010D 3	.8889D 0	.8442D 2	.2100D 3	.8979D 0	.8403D 2
.2160D 3	.9038D 0	.8371D 2	.2250D 3	.9119D 0	.8334D 2
.2310D 3	.9163D 0	.8302D 2	.2400D 3	.9223D 0	.8279D 2
.2460D 3	.9264D 0	.8248D 2	.2550D 3	.9331D 0	.8221D 2
.2610D 3	.9370D 0	.8199D 2	.2700D 3	.9419D 0	.8171D 2
.2760D 3	.9456D 0	.8143D 2	.2850D 3	.9506D 0	.8119D 2
.2910D 3	.9539D 0	.8102D 2	.3000D 3	.9572D 0	.8080D 2
.3060D 3	.9600D 0	.8051D 2	.3150D 3	.9638D 0	.8035D 2
.3210D 3	.9663D 0	.8020D 2	.3300D 3	.9697D 0	.7997D 2
.3360D 3	.9712D 0	.7977D 2	.3450D 3	.9747D 0	.7959D 2
.3510D 3	.9758D 0	.7936D 2	.3600D 3	.9784D 0	.7919D 2
.3660D 3	.9806D 0	.7910D 2	.3750D 3	.9823D 0	.7900D 2
.3810D 3	.9837D 0	.7887D 2	.3900D 3	.9851D 0	.7871D 2
.3960D 3	.9868D 0	.7864D 2	.4050D 3	.9883D 0	.7852D 2
.4110D 3	.9901D 0	.7839D 2	.4200D 3	.9923D 0	.7833D 2
.4260D 3	.9938D 0	.7831D 2	.4350D 3	.9953D 0	.7828D 2

Table XL (continued)

Time Min.	RATIOC	Gas ^{o}F Temp.	Time Min.	RATIOC	Gas ^{o}F Temp.
.4410D 3	.9960D 0	.7824D 2	.4500D 3	.9968D 0	.7819D 2
.4560D 3	.9974D 0	.7816D 2	.4650D 3	.9980D 0	.7812D 2
.4710D 3	.9984D 0	.7810D 2	.4800D 3	.9988D 0	.7807D 2
.4860D 3	.9991D 0	.7805D 2	.4950D 3	.9994D 0	.7803D 2
.5010D 3	.9996D 0	.7802D 2	.5100D 3	.9998D 0	.7801D 2

Table XLI. Computer Results of Activated Alumina Run No. 6 (ACTC-6).

Time Min.	RATIOC	Gas ^{o}F Temp.	Time Min.	RATIOC	Gas ^{o}F Temp.
.6000D 1	.2549D-5	.7868D 2	.1500D 2	.3466D-3	.1095D 3
.2100D 2	.6592D-3	.1209D 3	.3000D 2	.9867D-3	.1288D 3
.3600D 2	.1108D-2	.1312D 3	.4500D 2	.1533D-2	.1342D 3
.5100D 2	.1533D-2	.1342D 3	.6000D 2	.6010D-2	.1352D 3
.6600D 2	.2433D-1	.1350D 3	.7500D 2	.1224D 0	.1298D 3
.8100D 2	.2341D 0	.1229D 3	.9000D 2	.3803D 0	.1133D 3
.9600D 2	.4379D 0	.1095D 3	.1050D 3	.4949D 0	.1058D 3
.1110D 3	.5228D 0	.1041D 3	.1200D 3	.5566D 0	.1021D 3
.1260D 3	.5755D 0	.1010D 3	.1350D 3	.6003D 0	.9962D 2
.1410D 3	.6150D 0	.9880D 2	.1500D 3	.6350D 0	.9770D 2
.1560D 3	.6473D 0	.9704D 2	.1650D 3	.6643D 0	.9612D 2
.1710D 3	.6749D 0	.9555D 2	.1800D 3	.6898D 0	.9475D 2
.1860D 3	.6992D 0	.9425D 2	.1950D 3	.7126D 0	.9355D 2
.2010D 3	.7210D 0	.9310D 2	.2100D 3	.7331D 0	.9246D 2
.2160D 3	.7408D 0	.9205D 2	.2250D 3	.7519D 0	.9147D 2
.2310D 3	.7590D 0	.9110D 2	.2400D 3	.7692D 0	.9056D 2
.2460D 3	.7757D 0	.9021D 2	.2550D 3	.7852D 0	.8972D 2
.2610D 3	.7913D 0	.8939D 2	.2700D 3	.8001D 0	.8893D 2
.2760D 3	.8058D 0	.8863D 2	.2850D 3	.8140D 0	.8819D 2
.2910D 3	.8194D 0	.8791D 2	.3000D 3	.8271D 0	.8750D 2
.3060D 3	.8321D 0	.8724D 2	.3150D 3	.8393D 0	.8685D 2
.3210D 3	.8440D 0	.8660D 2	.3300D 3	.8508D 0	.8624D 2
.3360D 3	.8551D 0	.8600D 2	.3450D 3	.8619D 0	.8568D 2
.3510D 3	.8655D 0	.8544D 2	.3600D 3	.8717D 0	.8512D 2
.3660D 3	.8756D 0	.8491D 2	.3750D 3	.8806D 0	.8461D 2
.3810D 3	.8851D 0	.8440D 2	.3900D 3	.8902D 0	.8421D 2
.3960D 3	.8936D 0	.8393D 2	.4050D 3	.8990D 0	.8365D 2
.4110D 3	.9019D 0	.8349D 2	.4200D 3	.9065D 0	.8323D 2
.4260D 3	.9093D 0	.8208D 2	.4350D 3	.9141D 0	.8283D 2

Table XLI (continued)

Time Min.	RATIOC	Gas ^{o}F Temp.	Time Min.	RATIOC	Gas ^{o}F Temp.
.4410D 3	.9169D 0	.8267D 2	.4500D 3	.9115D 0	.8243D 2
.4560D 3	.9238D 0	.8230D 2	.4650D 3	.9275D 0	.8208D 2
.4710D 3	.9294D 0	.8193D 2	.4800D 3	.9337D 0	.8174D 2
.4860D 3	.9360D 0	.8161D 2	.4950D 3	.9399D 0	.8143D 2
.5010D 3	.9416D 0	.8130D 2	.5100D 3	.9444D 0	.8112D 2
.5160D 3	.9470D 0	.8101D 2	.5250D 3	.9497D 0	.8085D 2
.5310D 3	.9519D 0	.8076D 2	.5400D 3	.9544D 0	.8059D 2
.5460D 3	.9560D 0	.8050D 2	.5550D 3	.9585D 0	.8035D 2
.5610D 3	.9603D 0	.8026D 2	.5700D 3	.9629D 0	.8013D 2
.5760D 3	.9642D 0	.8005D 2	.5850D 3	.9662D 0	.7993D 2
.5910D 3	.9677D 0	.7984D 2	.6000D 3	.9697D 0	.7973D 2
.6060D 3	.9711D 0	.7967D 2	.6150D 3	.9738D 0	.7956D 2
.6210D 3	.9739D 0	.7950D 2	.6300D 3	.9757D 0	.7940D 2
.6360D 3	.9767D 0	.7934D 2	.6450D 3	.9783D 0	.7925D 2
.6510D 3	.9792D 0	.7919D 2	.6600D 3	.9806D 0	.7912D 2
.6660D 3	.9815D 0	.7906D 2	.6750D 3	.9828D 0	.7899D 2
.6810D 3	.9836D 0	.7895D 2	.6900D 3	.9848D 0	.7888D 2
.6960D 3	.9855D 0	.7884D 2	.7050D 3	.9866D 0	.7878D 2
.7110D 3	.9872D 0	.7874D 2	.7200D 3	.9881D 0	.7869D 2
.7260D 3	.9888D 0	.7865D 2	.7350D 3	.9896D 0	.7860D 2
.7410D 3	.9901D 0	.7857D 2	.7500D 3	.9909D 0	.7853D 2
.7560D 3	.9914D 0	.7850D 2	.7650D 3	.9921D 0	.7846D 2
.7710D 3	.9925D 0	.7844D 2	.7800D 3	.9931D 0	.7840D 2
.7870D 3	.9935D 0	.7838D 2	.7950D 3	.9941D 0	.7835D 2
.8010D 3	.9944D 0	.7833D 2	.8100D 3	.9949D 0	.7830D 2
.8160D 3	.9952D 0	.7828D 2	.8250D 3	.9957D 0	.7825D 2
.8310D 3	.9960D 0	.7824D 2	.8400D 3	.9964D 0	.7822D 2
.8460D 3	.9966D 0	.7820D 2	.8550D 3	.9970D 0	.7818D 2
.8610D 3	.9972D 0	.7817D 2	.8700D 3	.9975D 0	.7815D 2

Table XLI (continued)

Time Min.	RATIOC	Gas Temp. °F	Time Min.	RATIOC	Gas Temp. °F
.8760D 3	.9977D 0	.7814D 2	.8850D 3	.9980D 0	.7812D 2
.8910D 3	.9981D 0	.7811D 2	.9000D 3	.9984D 0	.7810D 2
.9060D 3	.9986D 0	.7809D 2	.9150D 3	.9988D 0	.7807D 2
.9210D 3	.9989D 0	.7806D 2	.9300D 3	.9991D 0	.7805D 2
.9360D 3	.9993D 0	.7804D 2	.9450D 3	.9995D 0	.7803D 2
.9510D 3	.9996D 0	.7803D 2	.9600D 3	.9997D 0	.7802D 2
.9660D 3	.9998D 0	.7801D 2			

Table XLII. Computer Results of Activated Alumina Run No. 7 (ACTC-7).

Time Min.	RATIOC	Gas Temp. °F	Time Min.	RATIOC	Gas Temp. °F
.6000D 1	.2532D-3	.1056D 3	.1500D 2	.9551D-3	.1283D 3
.2100D 2	.1368D-2	.1330D 3	.3000D 2	.7407D-2	.1357D 3
.3600D 2	.3375D-1	.1352D 3	.4500D 2	.1676D 0	.1281D 3
.5100D 2	.3080D 0	.1196D 3	.6000D 2	.4747D 0	.1090D 3
.6600D 2	.5423D 0	.1047D 3	.7500D 2	.6124D 0	.1003D 3
.8100D 2	.6474D 0	.9821D 2	.9000D 2	.6895D 0	.9570D 2
.9600D 2	.7128D 0	.9433D 2	.1050D 3	.7425D 0	.9260D 2
.1110D 3	.7597D 0	.9160D 2	.1200D 3	.7825D 0	.9029D 2
.1260D 3	.7961D 0	.8952D 2	.1350D 3	.8144D 0	.8848D 2
.1410D 3	.8254D 0	.8785D 2	.1500D 3	.8405D 0	.8699D 2
.1560D 3	.8498D 0	.8647D 2	.1650D 3	.8625D 0	.8575D 2
.1710D 3	.8704D 0	.8531D 2	.1800D 3	.8813D 0	.8470D 2
.1860D 3	.8880D 0	.8432D 2	.1950D 3	.8974D 0	.8379D 2
.2010D 3	.9033D 0	.8346D 2	.2100D 3	.9114D 0	.8300D 2
.2160D 3	.9165D 0	.8272D 2	.2250D 3	.9236D 0	.8232D 2
.2310D 3	.9280D 0	.8207D 2	.2400D 3	.9342D 0	.8172D 2
.2460D 3	.9380D 0	.8150D 2	.2550D 3	.9434D 0	.8120D 2
.2610D 3	.9468D 0	.8101D 2	.2700D 3	.9515D 0	.8075D 2
.2760D 3	.9545D 0	.8058D 2	.2850D 3	.9586D 0	.8035D 2
.2910D 3	.9611D 0	.8021D 2	.3000D 3	.9647D 0	.8001D 2
.3060D 3	.9669D 0	.7988D 2	.3150D 3	.9700D 0	.7970D 2
.3210D 3	.9719D 0	.7960D 2	.3300D 3	.9746D 0	.7944D 2
.3370D 3	.9763D 0	.7935D 2	.3450D 3	.9786D 0	.7922D 2
.3510D 3	.9800D 0	.7914D 2	.3600D 3	.9820D 0	.7903D 2
.3660D 3	.9832D 0	.7896D 2	.3750D 3	.9849D 0	.7886D 2
.3810D 3	.9859D 0	.7880D 2	.3900D 3	.9874D 0	.7872D 2
.3960D 3	.9883D 0	.7867D 2	.4050D 3	.9895D 0	.7860D 2
.4110D 3	.9903D 0	.7856D 2	.4200D 3	.9913D 0	.7850D 2
.4260D 3	.9920D 0	.7846D 2	.4350D 3	.9928D 0	.7841D 2

Table XLII (continued)

Time Min.	RATIOC	Gas ^{o}F Temp.	Time Min.	RATIOC	Gas ^{o}F Temp.
.4410D 3	.9934D 0	.7838D 2	.4500D 3	.9941D 0	.7834D 2
.4560D 3	.9946D 0	.7831D 2	.4650D 3	.9952D 0	.7828D 2
.4710D 3	.9956D 0	.7825D 2	.4800D 3	.9961D 0	.7822D 2
.4860D 3	.9965D 0	.7820D 2	.4950D 3	.9969D 0	.7818D 2
.5010D 3	.9972D 0	.7816D 2	.5100D 3	.9976D 0	.7814D 2
.5160D 3	.9978D 0	.7813D 2	.5250D 3	.9982D 0	.7811D 2
.5310D 3	.9984D 0	.7810D 2	.5400D 3	.9986D 0	.7808D 2
.5460D 3	.9988D 0	.7807D 2	.5550D 3	.9991D 0	.7806D 2
.5610D 3	.9992D 0	.7805D 2	.5700D 3	.9994D 0	.7803D 2
.5760D 3	.9995D 0	.7803D 2	.5850D 3	.9997D 0	.7802D 2
.5910D 3	.9998D 0	.7801D 2			

Table XLIII. Computer Results of Activated Alumina Run No. 8 (ACTC-8).

Time Min.	RATIOC	Gas ^{o}F Temp.	Time Min.	RATIOC	Gas ^{o}F Temp.
.6000D 1	.3203D-3	.1086D 3	.1500D 2	.1279D-1	.1336D 3
.2100D 2	.8874D-1	.1341D 3	.3000D 2	.3151D 0	.1208D 3
.3600D 2	.4418D 0	.1118D 3	.4500D 2	.5402D 0	.1045D 3
.5100D 2	.5787D 0	.1018D 3	.6000D 2	.6190D 0	.9915D 2
.6600D 2	.6393D 0	.9789D 2	.7500D 2	.6638D 0	.9644D 2
.8100D 2	.6777D 0	.9564D 2	.9000D 2	.6962D 0	.9461D 2
.9600D 2	.7074D 0	.9400D 2	.1050D 3	.7230D 0	.9315D 2
.1110D 3	.7328D 0	.9262D 2	.1200D 3	.7467D 0	.9187D 2
.1260D 3	.7556D 0	.9139D 2	.1350D 3	.7682D 0	.9071D 2
.1410D 3	.7763D 0	.9038D 2	.1500D 3	.7880D 0	.8965D 2
.1560D 3	.7954D 0	.8925D 2	.1650D 3	.8061D 0	.8867D 2
.1710D 3	.8130D 0	.8830D 2	.1800D 3	.8229D 0	.8776D 2
.1860D 3	.8292D 0	.8742D 2	.1950D 3	.8384D 0	.8692D 2
.2010D 3	.8442D 0	.8660D 2	.2100D 3	.8527D 0	.8615D 2
.2160D 3	.8581D 0	.8585D 2	.2250D 3	.8659D 0	.8543D 2
.2310D 3	.8709D 0	.8515D 2	.2400D 3	.8781D 0	.8476D 2
.2460D 3	.8827D 0	.8451D 2	.2550D 3	.8893D 0	.8414D 2
.2610D 3	.8936D 0	.8391D 2	.2700D 3	.8997D 0	.8353D 2
.2760D 3	.9037D 0	.8336D 2	.2850D 3	.9093D 0	.8305D 2
.2910D 3	.9129D 0	.8285D 2	.3000D 3	.9181D 0	.8257D 2
.3060D 3	.9214D 0	.8238D 2	.3150D 3	.9262D 0	.8212D 2
.3210D 3	.9292D 0	.8195D 2	.3300D 3	.9336D 0	.8171D 2
.3360D 3	.9364D 0	.8156D 2	.3450D 3	.9404D 0	.8133D 2
.3510D 3	.9429D 0	.8119D 2	.3600D 3	.9466D 0	.8099D 2
.3660D 3	.9439D 0	.8086D 2	.3750D 3	.9522D 0	.8068D 2
.3810D 3	.9554D 0	.8056D 2	.3900D 3	.9574D 0	.8039D 2
.3960D 3	.9593D 0	.8028D 2	.4050D 3	.9620D 0	.8013D 2
.4110D 3	.9638D 0	.8004D 2	.4200D 3	.9663D 0	.7990D 2
.4260D 3	.9678D 0	.7981D 2	.4350D 3	.9701D 0	.7968D 2

Table XLIII (continued)

Time Min.	RATIOC	Gas ^{o}F Temp.	Time Min.	RATIOC	Gas ^{o}F Temp.
.4410D 3	.9715D 0	.7961D 2	.4500D 3	.9735D 0	.7949D 2
.4560D 3	.9748D 0	.7942D 2	.4650D 3	.9766D 0	.7932D 2
.4710D 3	.9777D 0	.7926D 2	.4800D 3	.9793D 0	.7917D 2
.4860D 3	.9804D 0	.7911D 2	.4950D 3	.9818D 0	.7903D 2
.5010D 3	.9827D 0	.7898D 2	.5100D 3	.9840D 0	.7890D 2
.5160D 3	.9849D 0	.7886D 2	.5250D 3	.9860D 0	.7879D 2
.5310D 3	.9867D 0	.7875D 2	.5400D 3	.9878D 0	.7869D 2
.5460D 3	.9884D 0	.7866D 2	.5550D 3	.9893D 0	.7860D 2
.5610D 3	.9899D 0	.7857D 2	.5700D 3	.9907D 0	.7853D 2
.5760D 3	.9912D 0	.7850D 2	.5850D 3	.9919D 0	.7846D 2
.5910D 3	.9924D 0	.7843D 2	.6000D 3	.9930D 0	.7840D 2
.6060D 3	.9934D 0	.7837D 2	.6150D 3	.9940D 0	.7834D 2
.6210D 3	.9943D 0	.7832D 2	.6300D 3	.9948D 0	.7829D 2
.6360D 3	.9952D 0	.7828D 2	.6450D 3	.9956D 0	.7825D 2
.6510D 3	.9959D 0	.7824D 2	.6600D 3	.9963D 0	.7821D 2
.6660D 3	.9965D 0	.7820D 2	.6750D 3	.9968D 0	.7818D 2
.6810D 3	.9971D 0	.7817D 2	.6900D 3	.9974D 0	.7815D 2
.6960D 3	.9976D 0	.7814D 2	.7050D 3	.9978D 0	.7813D 2
.7110D 3	.9980D 0	.7812D 2	.7200D 3	.9982D 0	.7810D 2
.7260D 3	.9984D 0	.7809D 2	.7350D 3	.9986D 0	.7808D 2
.7410D 3	.9987D 0	.7807D 2	.7500D 3	.9989D 0	.7806D 2
.7560D 3	.9990D 0	.7806D 2	.7650D 3	.9992D 0	.7805D 2
.7710D 3	.9993D 0	.7804D 2	.7800D 3	.9995D 0	.7803D 2
.7860D 3	.9995D 0	.7803D 2	.7950D 3	.9997D 0	.7802D 2

Table XLIV. Computer Results of Activated Alumina Run No. 9 (ACTC-9).

Time Min.	RATIOC	Gas ^{o}F Temp.	Time Min.	RATIOC	Gas ^{o}F Temp.
.6000D 1	.2680D-3	.1063D 3	.1500D 2	.1084D-2	.1292D 3
.2100D 2	.3004D-2	.1336D 3	.3000D 2	.3216D-1	.1345D 3
.3600D 2	.9862D-1	.1313D 3	.4500D 2	.2616D 0	.1217D 3
.5110D 2	.3641D 0	.1154D 3	.6000D 2	.4693D 0	.1088D 3
.6600D 2	.5216D 0	.1056D 3	.7500D 2	.5848D 0	.1019D 3
.8100D 2	.6196D 0	.9981D 2	.9000D 2	.6639D 0	.9722D 2
.9600D 2	.6893D 0	.9575D 2	.1050D 3	.7226D 0	.9383D 2
.1110D 3	.7422D 0	.9271D 2	.1200D 3	.7685D 0	.9121D 2
.1260D 3	.7842D 0	.9031D 2	.1350D 3	.8057D 0	.8909D 2
.1410D 3	.8186D 0	.8835D 2	.1500D 3	.8365D 0	.8734D 2
.1560D 3	.8475D 0	.8672D 2	.1650D 3	.8626D 0	.8586D 2
.1710D 3	.8719D 0	.8533D 2	.1800D 3	.8849D 0	.8459D 2
.1860D 3	.8929D 0	.8414D 2	.1950D 3	.9040D 0	.8351D 2
.2010D 3	.9109D 0	.8311D 2	.2100D 3	.9205D 0	.8257D 2
.2160D 3	.9264D 0	.8223D 2	.2250D 3	.9347D 0	.8176D 2
.2310D 3	.9397D 0	.8147D 2	.2400D 3	.9468D 0	.8107D 2
.2460D 3	.9511D 0	.8082D 2	.2550D 3	.9571D 0	.8048D 2
.2610D 3	.9608D 0	.8026D 2	.2700D 3	.9658D 0	.7998D 2
.2760D 3	.9689D 0	.7980D 2	.2850D 3	.9731D 0	.7956D 2
.2910D 3	.9756D 0	.7941D 2	.3000D 3	.9791D 0	.7921D 2
.3060D 3	.9812D 0	.7909D 2	.3150D 3	.9840D 0	.7893D 2
.3210D 3	.9857D 0	.7883D 2	.3300D 3	.9879D 0	.7870D 2
.3360D 3	.9892D 0	.7863D 2	.3450D 3	.9910D 0	.7852D 2
.3510D 3	.9921D 0	.7846D 2	.3600D 3	.9934D 0	.7838D 2
.3660D 3	.9942D 0	.7834D 2	.3750D 3	.9953D 0	.7827D 2
.3860D 3	.9959D 0	.7824D 2	.3900D 3	.9967D 0	.7819D 2
.3960D 3	.9972D 0	.7817D 2	.4050D 3	.9978D 0	.7813D 2
.4110D 3	.9981D 0	.7811D 2	.4200D 3	.9986D 0	.7808D 2
.4260D 3	.9988D 0	.7807D 2	.4350D 3	.9991D 0	.7805D 2
.4410D 3	.9993D 0	.7804D 2	.4500D 3	.9996D 0	.7803D 2
.4560D 3	.9997D 0	.7802D 2	.4650D 3	.9998D 0	.7801D 2

Table XLV. Computer Results of Activated Alumina Run No. 10 (ACTC-10).

Time Min.	RATIOC	Gas Temp. °F	Time Min.	RATIOC	Gas Temp. °F
.6000D 1	.2686D-3	.1063D 3	.1500D 2	.1143D-2	.1300D 3
.2100D 2	.3978D-2	.1350D 3	.3000D 2	.5372D-1	.1355D 3
.3600D 2	.1638D 0	.1297D 3	.4500D 2	.3948D 0	.1153D 3
.5100D 2	.5049D 0	.1081D 3	.6000D 2	.6063D 0	.1014D 3
.6600D 2	.6531D 0	.9845D 2	.7500D 2	.7067D 0	.9513D 2
.8100D 2	.7352D 0	.9340D 2	.9000D 2	.7707D 0	.9126D 2
.9600D 2	.7907D 0	.9007D 2	.1050D 3	.8166D 0	.8854D 2
.1110D 3	.8316D 0	.8766D 2	.1200D 3	.8513D 0	.8650D 2
.1260D 3	.8628D 0	.8583D 2	.1350D 3	.8782D 0	.8493D 2
.1410D 3	.8872D 0	.8440D 2	.1500D 3	.8992D 0	.8370D 2
.1560D 3	.9062D 0	.8328D 2	.1650D 3	.9156D 0	.8274D 2
.1710D 3	.9210D 0	.8242D 2	.1800D 3	.9282D 0	.8200D 2
.1860D 3	.9323D 0	.8176D 2	.1950D 3	.9377D 0	.8144D 2
.2010D 3	.9408D 0	.8126D 2	.2100D 3	.9448D 0	.8103D 2
.2160D 3	.9470D 0	.8090D 2	.2250D 3	.9499D 0	.8073D 2
.2310D 3	.9515D 0	.8064D 2	.2400D 3	.9536D 0	.8052D 2
.2460D 3	.9548D 0	.8045D 2	.2550D 3	.9562D 0	.8036D 2
.2610D 3	.9571D 0	.8032D 2	.2700D 3	.9582D 0	.8025D 2
.2760D 3	.9588D 0	.8022D 2	.2850D 3	.9596D 0	.8017D 2
.2910D 3	.9610D 0	.8015D 2	.3000D 3	.9607D 0	.8011D 2
.3060D 3	.9611D 0	.8009D 2	.3150D 3	.9617D 0	.8006D 2
.3210D 2	.9620D 0	.8004D 2	.3300D 3	.9625D 0	.8001D 2
.3360D 3	.9628D 0	.8000D 2	.3450D 3	.9633D 0	.7997D 2
.3510D 3	.9635D 0	.7996D 2	.3600D 3	.9640D 0	.7993D 2
.3660D 3	.9642D 0	.7992D 2	.3750D 3	.9647D 0	.7990D 2
.3860D 3	.9649D 0	.7988D 2	.3900D 3	.9653D 0	.7986D 2
.3960D 3	.9656D 0	.7985D 2	.4050D 3	.9660D 0	.7983D 2
.4110D 3	.9662D 0	.7981D 2	.4200D 3	.9666D 0	.7979D 2
.4260D 3	.9669D 0	.7978D 2	.4350D 3	.9672D 0	.7976D 2

Table XLV (continued)

Time Min.	RATIOC	Gas Temp. °F	Time Min.	RATIOC	Gas Temp. °F
.4410D 3	.9675D 0	.7974D 2	.4500D 3	.9679D 0	.7973D 2
.4560D 3	.9681D 0	.7971D 2	.4650D 3	.9685D 0	.7969D 2
.4710D 3	.9687D 0	.7968D 2	.4800D 3	.9691D 0	.7966D 2
.4860D 3	.9693D 0	.7965D 2	.4950D 3	.9697D 0	.7963D 2
.5010D 3	.9699D 0	.7962D 2	.5100D 3	.9702D 0	.7960D 2
.5160D 3	.9705D 0	.7959D 2	.5250D 3	.9708D 0	.7957D 2
.5310D 3	.9710D 0	.7956D 2	.5400D 3	.9714D 0	.7954D 2
.5460D 3	.9716D 0	.7953D 2	.5550D 3	.9719D 0	.7951D 2
.5610D 3	.9721D 0	.7950D 2	.5700D 3	.9724D 0	.7948D 2
.5760D 3	.9726D 0	.7947D 2	.5850D 3	.9730D 0	.7945D 2
.5910D 3	.9732D 0	.7944D 2	.6000D 3	.9735D 0	.7942D 2
.6060D 3	.9737D 0	.7941D 2	.6150D 3	.9740D 0	.7940D 2
.6210D 3	.9742D 0	.7939D 2	.6300D 3	.9745D 0	.7937D 2
.6360D 3	.9747D 0	.7936D 2	.6450D 3	.9750D 0	.7934D 2
.6510D 3	.9753D 0	.7933D 2	.6600D 3	.9755D 0	.7932D 2
.6660D 3	.9757D 0	.7931D 2	.6750D 3	.9759D 0	.7929D 2
.6810D 3	.9761D 0	.7928D 2	.6900D 3	.9764D 0	.7927D 2
.6960D 3	.9766D 0	.7926D 2	.7050D 3	.9769D 0	.7924D 2
.7110D 3	.9770D 0	.7923D 2	.7200D 3	.9773D 0	.7922D 2
.7260D 3	.9775D 0	.7921D 2	.7350D 3	.9777D 0	.7920D 2
.7410D 3	.9779D 0	.7919D 2	.7500D 3	.9782D 0	.7917D 2
.7560D 3	.9784D 0	.7916D 2	.7650D 3	.9786D 0	.7915D 2
.7710D 3	.9788D 0	.7914D 2	.7800D 3	.9790D 0	.7913D 2
.7860D 3	.9792D 0	.7912D 2	.7950D 3	.9794D 0	.7911D 2

APPENDIX F

COMPUTER PROGRAM FOR LMS-4A AND ACTIVATED ALUMINA

The complete Fortran IV program of activated alumina is presented in Table XLVI. Most of the LMS-4A program is the same as activated alumina except the input data and the diffusion parameter calculations. so here we present only these two parts in Table XLVII.

Table XLVI. The Complete Fortran IV Program of Activated Alumina.

```
//ACT1   JOB (038441,054178,BINS,T-150,L-999,R-512),C,MSGLEVEL=(1,1)
//*RESOURCE INSTR360
// EXEC FORTHCLG,GOREG=512K,OPT=2,FORTREG=512K
//FORT.SYSIN DD *
      IMPLICIT REAL*8(A-H,O-Z)
      REAL*8 DEXP,DABS,DERF,DSQRT,DLOG,DMAX1,DLOG10
      INTEGER*4 IDINT
      DIMENSION TG(2,4000),RHOG(2,4000),G(2,4000),Y(2,4000)
      DIMENSION UT(2,31),UP(2,31),UPD(2,31),PE(2,31),DELUTI(2,31)
      DIMENSION RE(30),GE(30),D(30),TE(30),DI(30)
      DIMENSION RATIOC(3),TIME(3),YTEMP(3),ICHEK(3)
      DIMENSION TW(2),AAP(2),BBP(2),CCP(2)
C
C*****************************S. H. JURY CARD DECK*********************************
C
C*********************************INPUT DATA START*********************************
C
C***********************GRANULE PARAMETERS*****************************************
C
C EF IS THE FRACTION OF ADSORPTION HEAT LIBERATED IN THE GRANULE. THE FRACTION
C (1.D0-EF) IS THE HEAT LIBERATED AT THE GRANULE SURFACE.
C SIG IS THE FRACTION OF CONTINUOUS PHASE IN GRANULE.
C EF1 IS A FRACTION IN THE RELATION  EF1=(DD(K)/RD**2)/(D(K)/R**2)  WHERE DD(K)
C AND RD ARE THE MICROSPHERE DIFFUSIVITY AND RADIUS.
C
    1 SIG=.74D0
    2 EF1=0.012D0
    3 EF=0.0D0
    4 R=0.002341236 9D0                                                    A12/14
    5 CAY=0.0745D0
    6 YLAMDA=19093.97905D0
      YLAMDA=YLAMDA*1.4D0
    7 EPSLON=0.430 7D0                                                     A12/14
    8 RDS=101.0756D0
    9 SI=0.9045D0
C
C************************PERCOLATOR PARAMETERS*************************************
C
   10 DI=1.25D0/12.D0
   11 DO=1.5D0/12.D0
   12 ROT=1.0525D0*62.427D0
   13 CPT=0.32D0
C
C************************FEED GAS PARAMETERS***************************************
C
   15 SCFH=10.00D0                                                         ACT1
   16 TFEED=537.69D0
   17 BEDTI=537.69D0
   18 UNITP=14.696D0*144.0D0/760.0D0
   19 BEDPI=0.001109917 9D0*UNITP                                          A12/14
   20 BEDPF=10.9482D0*UNITP                                                ACT1
   21 P=742.875D0*UNITP                                                    ACT1
C
C*************************R RUN DESIGN*********************************************
C
   28 NR=11
   29 NA=1
   30 NS=20
   31 YNR=NR
   32 YNA=NA
   33 YNS=NS
```

Table XLVI (continued)

```
    34 N=NS-NA+NA*NR
    35 YN=N
    36 NN=N-1
    37 YT=YNS*YNR
    38 RN=YT-1.D0
    39 DELTAS=R/YNS
    40 DELTAR=DELTAS/YNR
    41 DRDS=DELTAR/DELTAS
C
C*************************************************************************
C JPRINT IS THE TIME INTERVAL BETWEEN THE PRINTS FOR EACH IPRINT INCREMENTS OF
C BED. PRIOR TO A COMPUTER RUN THE USER SHOULD USE A CALCULATOR TO EXECUTE
C STATEMENTS LISTED UNDER Z- AND T- RUN DESIGN TO INSURE PROPER COMPUTER RUN
C DESIGN.
C*************************************************************************
C
C*************************Z RUN DESIGN************************************
C
    45 EL=2.D0/12.D0
    46 DELTAZ=4.D0*R
    47 IPRINT=1
    48 YIP=IPRINT
    49 LW=IDINT(EL/(DELTAZ*YIP)+.5D0)
    51 L=LW*IPRINT
    52 YL=L
    53 DELTAZ=EL/YL
C
C*************************T RUN DESIGN************************************
C
    64 DELTAT=12.D0/3600.D0
    65 TTIME=4000.D0*DELTAT
    66 JPRINT=1
    68 YJP=JPRINT
    69 MW=IDINT(TTIME/(DELTAT*YJP)+.5D0)
    70 M=MW*JPRINT
    71 YM=M
    72 DELTAT=TTIME/YM
C
C*********************MISCELLANEOUS CONSTANTS*******************************
C
    73 ALERR=1.D-3
    74 V21=0.64152D0
    76 V22=0.67160D0
    77 V23=0.34685D0
    78 CW=1.5651D0
    80 CR=0.8130SD0
    82 RBAR=1545.33D0
C
C*****************************INPUT DATA END*******************************
C
C****************PARAMETER CALCULATIONS FROM INPUT DATA START***************
C
    83 DP=BEDPF-BEDPI
    84 KL=0
    85 ROCPS=ROS*0.183D0
    86 ALFA=CAY/ROCPS
    89 VFEED=SCFH*P*TFEED*4.D0/(519.69D0*14.696D0*144.D0*EPSLON*3.1415926
      *5400*DI**2)
    90 RT=RBAR*TFEED
    91 RB=RBAR*BEDTI
    92 CFEED=BEDPF/RT
```

Table XLVI (continued)

```
   93 BEDCGI=BEDPI/RB
   95 BEDROG=P/RB
  100 B=DELTAZ/DELTAT
  110 AA=(DELTAR**2)/DELTAT
  115 AY=3.D0*(1.D0-EPSLON)/(R*SI)
      AY=AY*SI
  120 AT=SIG*AY*DELTAZ*(3.14159265D0/4.0D0)*DI**2*DELTAT
  140 A3=(SIG*AY*DELTAZ)/EPSLON
  141 A4=15.D0*DELTAT/R**2
  142 A9=A4*ALFA
  144 A7=5.D0*CAY/R
  145 A8=(1.0D0-EF)*YLAMDA
  146 W02=(1.D0-SIG)/SIG
  147 W03=3.D0*DELTAT/R
  148 W04=1.D0+A9
  150 ROGIN=P/RT
C
C*****************PARAMETER CALCULATIONS FROM INPUT DATA END*********************
C
  151 SUMJST=0.D0
  152 SUMCO=0.D0
  153 SGFILM=0.D0
  154 SUMGAS=0.D0
  201 CF=1.D0
  203 I=0
  204 JTF=0
  205 JTF2=0
  206 JU=0
  207 UJ=JU
  208 TTMEJU=0.0D0
  209 ITSUM=0
  210 DO 218 J=2,M
  215 TG(1,J)=(TFEED-BEDTI)/BEDTI
  216 RHOG(1,J)=ROGIN
  217 G(1,J)=VFEED*ROGIN
  218 Y(1,J)=CFEED/ROGIN
C
C*****************************THE Z LOOP FOLLOWS*************************************
C
  225 DO 3000 II=1,L
  231 I=I+1
  232 IF(I .LE. IPRINT) GO TO 250
  233 I=1
C
C*************************INITIALS CONDITIONS START*********************************
C
  250 TW(1)=.0D0
  290 TG(2,1)=0.0D0
  291 RHOG(2,1)=BEDROG
  292 G(2,1)=VFEED*BEDROG
  293 Y(2,1)=BEDCGI/BEDROG
  300 DO 310 K=1,N
  301 DELUTI(2,K)=0.D0
  305 UT(1,K)=0.0D0
  308 UP(1,K)=0.0D0
  310 UPD(1,K)=0.0D0
  315 TG1=BEDTI
  319 PG1=BEDPI
  320 PC1=BEDPI
  321 THUM=0.D0
  322 JMAX=0
```

Table XLVI (continued)

```
C
C*************************INITIAL CONDITIONS END*********************************
C
  323 JWRITE=0
  324 JAY=2
  325 J0=0
  330 JV=M-JU
C
C*******************LONG TIME CALCULATION CONTROL-START*************************
C
  332 IF(JIF2.EQ.0)GO TO 340
  334 IF(JIF.EQ.1.OR.JU.LT.KL)GO TO 340
  335 JTF=1
C
C*******************LONG TIME CALCULATION CONTROL-END***************************
C
C*************************THE TIME LOOP FOLLOWS*********************************
C
  340 DO 2000 J=2,JV
C
C*******************LONG TIME CALCULATION CONTROL-START*************************
C
  374 IF(JIF.EQ.0)GO TO 400
  376 YK=1.D0
  378 K=1
  380 T=TC1
  385 PP=PC1
  390 GO TO 430
C
C*******************LONG TIME CALCULATION CONTROL-END***************************
C
C*****************************************************************************
C THE FOLLOWING ALGORITHM FOR COMPUTING THE DIFFUSION PARAMETERS,D(K),TE(K) AND
C PE(K) MUST BE SUPPLIED BY THE USER FOR HIS PARTICULAR ADSORBENT.
C*****************************************************************************
C
C*********************DIFFUSION PARAMETER CALCULATION START*******************
C
C ACTIVATED ALUMINA
C
  400 K=0
  410 K=K+1
  412 YK=K
  415 IF(K.GE.NR*NA+1)GO TO 420
  418 DUM=YNS/(YNS-YNA+(YNR*YNA-YK+1.D0)/YNR)
  419 GO TO 421
  420 DUM=YNS/(YN-YK+1.D0)
  421 T=(DUM*UT(1,K)+1.D0)*BEDTI
  427 PP=DUM*UP(1,K)*DP+BEDPI
  430 TC=T/1.8D0-273.16111111111D0
  450 TK=TC+273.15D0
  451 TD=0.65D0-0.01*TC
  452 TD2=TD**2
  453 TD3=TD*TD2
  454 TD4=TD*TD3
  455 TD5=TD*TD4
  456 TD6=TD*TD5
  457 TD7=TD*TD6
  459 SUM=-741.9242D0-29.721D0*TD-11.5528600*TD2-0.8685635D0*TD3+
     @0.1094098D0*TD4+0.4399930D0*TD5+0.2520658*TD6+0.0521868400*TD7
  460 EPA=1.D-2/TK*(374.1360D0-TC)*SUM
```

Table XLVI (continued)

```
  461 PSAT=220.88D0*DEXP(EPA)/1.01325D0*14.696D0*144.D0
  462 XPP=(PP/PSAT)**(T/1335.56922D0-1.D0)/PSAT
  463 X=XPP*PP
  464 X1=X**10.023BD0
  465 IF(DABS(X*X1).GT.1.D-30)GO TO 469
  466 X2=0.D0
  467 X3=0.D0
  468 GO TO 472
  469 X2=X*X1
  470 X3=X*X2
  472 ZA=1.D0-12.023BD0*X2+11.023BD0*X3
  473 ZB=1.D0+3.3676D0*X-4.3676D0*X3
  475 V1=R0S*.0107399603D0
  476 VP=V1*XPP/(1.D0-X)
  477 V2=VP*PP
  478 V3=V1/((1.D0-X)**2)
  480 C1PP=VP*ZA/ZB
  481 C1=C1PP*PP
  483 S1=132.5479664D0*X1*(X-1.0D0)
  487 S3=3.3676D0-52.51514888D0*X2
  490 DC1=V2*(S1/ZB-ZA*S3/ZB**2)+ZA/ZB*V3
  491 E1=-10764.36D0/T
  492 E2=1335.56922D0/T-1.D0
  495 Y1=332.1801042D0*DSQRT(T)*DEXP(E1)*C1PP*C1**2.D0
  496 Y2=1.952347015D-9*DSQRT(T)*(1.D0-0.678501720BD0*C1)
  497 Y3=2.176666667D-2*T+1.D0-0.2114D0*PP/P
  498 Y4=PSAT*1335.56922D0*X**E2/(T*DC1)
  499 D(K)=(Y1+Y2/Y3)*Y4
      D(K)=D(K)*3.0D0
  502 PE(2,K)=D(K)/Y4
  503 DSUM=-(1.D0/180.D0)*(-29.721D0-23.10572D0*TD-2.6056905D0*TD2+.4376
     @392D0*TD3+2.199965D0*TD4+1.5123948D0*TD5+.3653076D0*TD6)
  504 DLPSAT=(1.D-2/(1.8D0*TK**2))*(-647.286D0*SUM+1.8D0*TK*(374.136D0-T
     @C)*DSUM)
  505 TE(K)=-ALFA*DC1*X*(DLOG(PSAT/PP)+T*DLPSAT)/1335.56922D0
  506 IF(JIF.EQ.1.OR.J.NE.2)GO TO 510
  507 PE(1,K)=PE(2,K)
  508 D1(K)=D(K)
  510 IF(K.LT.N.AND.JIF.NE.1)GO TO 410
C
C*********************DIFFUSION PARAMETER CALCULATION END*************************
C
C*********************BED PARAMETER CALCULATIONS-START*****************************
C
  511 A5=5.D0*PE(2,1)/R
C
C*******************LONG TIME CALCULATION CONTROL-START*****************************
C
  520 IF(JIF2.EQ.1)GO TO 570
  522 KL=IDINT(.101D0*R**2*DMAX1(1.D0/ALFA,1.D0/D(1))/DELTAT)
  523 JIF2=1
  525 GO TO 334
C
C*******************LONG TIME CALCULATION CONTROL-END*******************************
C
  570 TG1=TG(2,J-1)*BEDTI+BEDTI
  571 TG15=TG1**1.5D0
  572 CPG=(0.02609D-2+(0.0354D-5-(0.08052D-9*TG1))*TG1)*TG1+6.713D0
  575 VIS=9.0648104D-5*TG15/(TG1+198.72D0)
  580 GGAY=9.2246260-4*TG15/(TG1+225.D0)
  590 RE=2.D0*G(2,J-1)*R/VIS
```

Table XLVI (continued)

```
  595 PRN=CPG*VIS/GCAY
  600 H=V21*GCAY*RE**V22*PRN**V23/(2.D0*R)
  605 HW=CW*GCAY*RE**0.83D0/DI
  610 B0=CR*(BEDTI**3)*1.712D-9
  617 HR=B0*((TW(1)+1.D0)**2+1.D0)*(TW(1)+2.D0)
      HR=HR*0.5D0
  619 G1=4.0D0*DELTAT/(ROT*CPT*(D0**2-DI**2))
  620 GA=G1*DI*HW
  621 GAR=G1*D0*HR
  630 CAYG=(H*RBAR*(TG(2,J-1)+1.D0)*BEDTI)/(P*CPG)
      CAYG=CAYG*3.0D0
  635 A2=CAY/H
  636 A=(H*AY*DELTAZ)/(EPSLON*CPG)
  650 P7=EPSLON*CPG/(H*AY*DELTAT)
  651 P8=RHOG(2,J-1)+G(1,J)/B
  652 P10=4.D0/(AY*DI*(1.D0+GA+GAR))
  653 P9=P7*P8+1.D0+P10*(GAR+1.D0)*HW/H
  654 A2P9=A2*P9
  655 DR1=P7*DELTAR/A2P9
  656 DR2=(GAR+1.D0)*HW*P10*DELTAR/(A2P9*H)
  657 DR3=P10*DELTAR/A2P9
  660 QA=1.D0/P9
  662 AP=BEDROG-RHOG(2,J-1)
  663 BR6=G(1,J)*TG(1,J)/B
  664 QB=(P7/P9)*(AP+BB6)+(P10/P9)*TW(1)*HW/H
C
C**********BED PARAMETER CALCULATIONS-END**********
C
C**********LONG TIME PERCOLATOR SOLUTION-START**********
C
  665 ITCHEK=0
  666 IF(JIF.EQ.0)GO TO 724
  667 W01=EF1*A4*D(1)
  668 WW0=W02*W01/(1.D0+W01)
  669 W05=1.D0+A4*D(1)+WW0
  670 W06=TE(1)*D(1)/(PE(2,1)*ALFA)
  671 WW1=W06*A9*(1.D0+WW0)/(W04*W05)
  672 WW2=(PC1+WW0*PD1+W06*A9*(1.D0+WW0)*TC1/W04)/W05
  673 WW3=EF*YLAMDA*W03*W06*(1.D0+WW0)*SIG/(W04*W05*ROCPS)
  674 WW4=A4*D(1)/W05
  675 W07=SIG*(A8+A9*YLAMDA*EF/W04)
  677 W0=H/W07
  681 W1=(H+A7/W04)/W07
  682 W2=(A7*IC1/W04)/W07
  683 W5=1.0D0/A5-WW3
  684 W3=(1.D0-WW4)/W5
  685 W4=WW1/W5
  686 W6=WW2/W5
  687 W7=B*RHOG(2,J-1)+G(1,J)
  688 W8=B*RHOG(2,J-1)*Y(2,J-1)+G(1,J)*Y(1,J)
  689 W9=W2+W1*BEDTI*(1.D0+QB-QA)/QA
  690 W10=W4*W9/ (W1-W0*QA)-W6-W4*BEDTI*(1.D0+QB-QA)/QA
  691 W11=W3*RBAR*(W8-W7)/(CAYG*(W1/QA-W0))
  692 W12=W4/(W1-QA*W0)
  693 W13=(W7+(P*W3+W10)*A3-W9*W11-W7*W12)/(2.D0*(W11+(1.D0-W12)*A3))
  694 W14=(W3*P*W8+W10*W7)/((W11+(1.D0-W12)*A3)*W13**2)
  699 YJST=W13*(1.D0-DSQRT(1.D0-W14))
  700 W08=EF*YLAMDA*W03*SIG*YJST
  701 TG(2,J)=(YJST+W9)/((W1/QA-W0)*BEDTI)-1.D0
  702 RHOG(2,J)=P/(RBAR*(TG(2,J)+1.D0)*BEDTI)
  703 Y(2,J)=(W8-A3*YJST)/(W7-A3*YJST)
```

Table XLVI (continued)

```
  704 G(2,J)=H*(RHOG(2,J-1)-RHOG(2,J))+G(1,J)-A3*YJST
  705 TST=BEDTI*((TG(2,J)-QB)/QA+1.D0)
  706 PST=(YJST+W6-W4*TST)/W3
  707 TC2=(TC1+A9*TST+W08/ROCPS)/W04
  708 PC2=WW4*PST-WW1*TST+WW2-WW3*YJST
  709 PD2=(PD1+W01*PC2-W06*(A9*(TST-TC2)+W08/ROCPS))/(1.D0+W01)
  718 CO=A5*(PST-PC2)
  720 UP(2,1)=(PST-BEDPI)/DP
  721 UP(2,2)=RN*(PC2-BEDPI)/(YT*DP)
  722 CGST=RHOG(2,J)*PST/P
  723 GO TO 1270
C
C*******************LONG TIME PERCOLATOR SOLUTION-END*****************************
C
C************SOLUTION OF GRANULE MASS TRANSFER EQUATION START*******************
C
  724 Q3=B*RHOG(2,J-1)+G(1,J)
  755 Q4=B*RHOG(2,J-1)*Y(2,J-1)+G(1,J)*Y(1,J)
  760 Q5=(Q3-Q4)/(CAYG*RHOG(2,J-1))+A3
  765 Q6=CF*(Q5-Q4*A3/Q3)*PE(2,1)*DP/(DELTAR*Q3)
  870 BE(1)=Q6*YT/((Q6+DP/P)*RN)
  871 GE(1)=(Q4/Q3-BEDPI/P)/(Q6+DP/P)
  872 DX=1.D0
  873 DELX2=DELTAR
  874 UP(1,N+1)=0.D0
  875 UP(2,N+1)=0.D0
  876 PE(1,N+1)=PE(1,N)
  877 PE(2,N+1)=PE(2,N)
  973 DO 1016 K=2,N
  974 KAL=N-K+1
  975 YKAL=KAL
  976 PHID=EF1*15.D0*D(K)*DELTAT/R**2
  977 PHID1=PHID/(1.D0+PHID)
  978 W06=1E(K)*D(K)/(PE(2,K)*ALFA)
  980 IF(NR*NA+1-K)988,986,981
  981 AR=(YNS-YNA)*YNR+(YKAL-YNS+YNA)
  985 GO TO 991
  986 DX=DRDS
  987 GO TO 990
  988 DX=1.D0
  989 DELX2=DELTAS
  990 AR=YKAL*DELTAS/DELX2
  991 DEN=2.D0*DELX2**2*PE(2,K)/(D(K)*DELTAT)
  992 DIN=2.D0*DELX2**2*PE(1,K)/(D1(K)*DELTAT)
  993 DO 996 JQ=1,2
  994 AAP(JQ)=(.5D0/AR+1.D0)*DX*((1.D0-.5D0*DX)*PE(JQ,K)+.5D0*DX*PE(JQ,K
     @+1))-.5D0*DX*PE(JQ,K)/AR
  995 BBP(JQ)=(.25D0/AR+.5D0)*(PE(JQ,K-1)+PE(JQ,K))+(DX-(1.D0-.5D0*DX)/A
     @R)*((1.D0-.5D0*DX)*PE(JQ,K)+.5D0*DX*PE(JQ,K+1))+(.5D0*(1.D0-DX)/AR
     @)*PE(JQ,K)
  996 CCP(JQ)=(.5D0-.25D0/AR)*(PE(JQ,K-1)+PE(JQ,K))+.5D0*PE(JQ,K)/AR
  997 DIVP=BBP(2)+DEN*(W02*PHID1+1.D0)-CCP(2)*BE(K-1)
  998 BE(K)=AAP(2)/DIVP
  999 DE=(CCP(1)*UP(1,K-1)-(BBP(1)- DIN)*UP(1,K)+AAP(1)*UP(1,K+1))/DIN-W
     @06*BEDT1*DELUTI(2,K)*(1.D0+W02*PHID1)/DP+W02*PHID1*UPD(1,K)
 1010 IF(DABS(GE(K-1)).GT.1.D-30)GO TO 1015
 1011 DEDEN=DE*DEN
 1012 WRITE(6,1013)II,J,K,GE(K-1),DEDEN,DIVP
 1013 FORMAT(5H II =,I3,2X,4H J =,I5,2X,4H K =,I4,2X,10H GE(K-1) =,D12.5
     @,2X,8H DEDEN =,D12.5,2X,7H DIVP =,D12.5)
 1014 GE(K-1)=0.D0
```

Table XLVI (continued)

```
 1015 GE(K)=(DE*DEN+GE(K-1)*CCP(2))/DIVP
 1016 CONTINUE
 1054 DO 1076 KAL=1,N
 1055 K=N-KAL+1
 1056 W06=TE(K)*D(K)/(PE(2,K)*ALFA)
 1057 UP(2,K)=GE(K)+BE(K)*UP(2,K+1)
 1058 PHID=EF1*15.0D0*D(K)*DELTAT/R**2
 1059 UPD(2,K)=(UPD(1,K)+PHID*UP(2,K)-W06*BEDTI*DELUTI(2,K)/DP)/(1.D0+PH
     @ID)
 1063 YK=K
 1064 IF(K.GE.NR*NA+1)GO TO 1067
 1065 DUM=YNS/(YNS-YNA+(YNR*YNA-YK+1.D0)/YNR)
 1066 GO TO 1068
 1067 DUM=YNS/(YN-YK+1.D0)
 1068 PP=DUM*UP(2,K)*DP+BEDPI
 1069 IF(PP.GE.0.D0)GO TO 1076
 1070 WRITE(6,1071)II,J,K,PP,UP(2,K)
 1071 FORMAT(5H II =,I3,2X,4H J =,I5,2X,4H K =,I4,2X,5H PP =,D12.5,2X,10
     @H UP(2,K) =,D12.5)
 1075 UP(2,K)=DABS(UP(2,K))
 1076 CONTINUE
 1080 YJST=PE(2,1)*DP*(UP(2,1)-YT*UP(2,2)/RN)/DELTAR
 1085 CQ=(Q4-(DP*UP(2,1)/P+BEDPI/P)*Q3)/(CF*(Q5-Q4*A3/Q3))
 1090 CF=1.D0/(1.D0-YJST*A3/Q3)
C
C*************SOLUTION OF GRANULE MASS TRANSFER EQUATION END*********************
C
C***************SOLUTION OF GRANULE HEAT TRANSFER EQUATION START*****************
C
 1124 BE(1)=1.D0/((RN/YT)*(DB1*P8+1.D0+DB2))
 1125 GE(1)=(DB1*(AP+BB6)+DB3*TW(1)*HW/H+DELTAR*A8*YJST*SIG/(CAY*BEDTI))
     @/(1.D0+DB1*P8+DB2)
 1128 UT(2,N+1)=0.D0
 1129 UT(1,N+1)=0.D0
 1130 DX=1.D0
 1131 DELX2=DELTAR
 1132 DO 1159 K=2,N
 1133 PHID=EF1*15.0D0*D(K)*DELTAT/R**2
 1135 B1=1.D0-EF*YLAMDA*TE(K)*SIG/CAY
 1136 B2=EF*YLAMDA*DP*PE(2,K)*SIG/(ROCPS*BEDTI*D(K))
 1143 IF(NR*NA+1-K)1150,1146,1152
 1146 DX=DRDS
 1147 GO TO 1152
 1150 DX=1.D0
 1151 DELX2=DELTAS
 1152 BETA=2.D0*DELX2**2/(ALFA*DELTAT)
 1154 DIVT=B1*BETA+ 1.D0+DX -BE(K-1)
 1155 BE(K)=DX/DIVT
 1156 DE=(DX*UT(1,K+1)+UT(1,K-1))/BETA-((1.D0+DX)/BETA-B1)*UT(1,K)+B2*(U
     @P(2,K)-UP(1,K)+W02*PHID*(UP(2,K)-UPD(2,K)))
 1158 GE(K)=(BETA*DE+GE(K-1))/DIVT
 1159 CONTINUE
 1176 DO 1190 KAL=1,N
 1179 K=N-KAL+1
 1185 UT(2,K)=GE(K)+BE(K)*UT(2,K+1)
 1190 CONTINUE
C
C*****************SOLUTION OF GRANULE HEAT TRANSFER EQUATION END*****************
C
C************************SOLUTION OF BED EQUATIONS START****************************
C
```

Table XLVI (continued)

```
 1200 TG(2,J)=QB+QA*UT(2,1)
 1205 TH=UT(2,1)-TG(2,J)
 1206 TJ2=TG(2,J)+1.0D0
 1210 RHOG(2,J)=BEDROG/TJ2
 1215 G(2,J)=(G(1,J)*(TG(1,J)+1.0D0)+A*TH-A3*TJ2*YJST)/TJ2
 1220 Y(2,J)=(B*RHOG(2,J-1)*Y(2,J-1)+G(1,J)*Y(1,J)-A3*YJST)/(B*RHOG(2,J)
     @+G(2,J))
 1225 CGST=RHOG(2,J-1)*Y(2,J)-(1.D0-Y(2,J))*(YJST/CAYG)
 1239 STERR=0.D0
 1240 DO 1247 K=1,N
 1241 DELUTO=UT(2,K)-UT(1,K)
 1242 UTERR=1.D0-DELUTI(2,K)/DELUTO
 1244 IF(DABS(UTERR).LE.DABS(STERR))GO TO 1246
 1245 STERR=UTERR
 1246 DELUTI(2,K)=DELUTO
 1247 CONTINUE
 1250 IF(DABS(STERR).LT.1.D-2.OR.J.GT.2)GO TO 1255
 1251 WRITE(6,1252)II,J,K,STERR
 1252 FORMAT(5H II =,I3,2X,4H J =,I5,2X,4H K =,I4,2X,8H STERR =,D12.5)
 1253 GO TO 400
 1255 PST=UP(2,1)*DP+BEDPI
 1260 PG2=YT*UP(2,2)*DP/RN+BEDPI
C
C**********SOLUTION OF BED EQUATIONS END**********
C
C**********GRANULE WRITE START**********
C
C**********GRANULE WRITE END**********
C
C**********CONTROL START**********
C
 1270 TW(2)=(TW(1)+GA*TG(2,J))/(1.D0+GA+GAR)
 1271 IF(JWRITE.LT.180)GO TO 1290
 1272 DCDP=PE(2,N)/D(N)
 1273 DCDT=TE(N)/ALFA
 1274 DXDP=PE(2,N)/(D(N)*DC1)
 1275 DXDT=TE(N)/(ALFA*DC1)
 1276 TJ2=T-460.D0
 1277 PP=PP/144.D0
 1278 WRITE(6,1279)TJ2,PP,D(N),PE(2,N),TE(N)
 1279 FORMAT(2X,6H T,F =,D12.5,2X,9H PP,PSI =,D12.5,2X,7H D(N) =,D12.5,2
     @X,10H PE(2,N) =,D12.5,2X,8H TE(N) =,D12.5)
 1280 WRITE(6,1281)DC1,DCDP,DCDT,DXDP,DXDT
 1281 FORMAT(2X,6H DC1 =,D12.5,2X,8H DC/DP =,D12.5,2X,8H DC/DT =,D12.5,2
     @X,8H DX/DP =,D12.5,2X,8H DX/DT =,D12.5)
 1282 CKFILM=CAYG*RHOG(2,J)/(P*(1.D0-Y(2,J)))
 1283 CKNORM=PE(2,1)/DELTAR
 1284 CKLONG=A5
 1285 WRITE(6,1286)J,CKFILM,CKNORM,CKLONG,X
 1286 FORMAT(1H0,9X,4H J =,I5,5X,9H CKFILM =,D12.5,5X,9H CKNORM =,D12.5,
     @5X,9H CKLONG =,D12.5,5X,4H X =,D12.5)
 1287 JWRITE=0
 1290 JWRITE=JWRITE+1
 1300 IF(TG(2,J).LE.TDUM)GO TO 1320
 1310 TDUM=TG(2,J)
 1315 JMAX=J
 1320 IF(J .EQ. 2)SJST=YJST
 1321 YJST2=YJST
 1322 SGFILM=SGFILM+AT*CAYG*(RHOG(2,J-1)*Y(2,J)-CGST)/(1.D0-Y(2,J))
 1323 SUMCQ=SUMCQ+CQ*AT
 1324 SUMJST=SUMJST+AT*YJST2
```

Table XLVI (continued)

```
 1325 SUMGAS=SUMGAS+AT*(EPSLON*((G(1,J)*Y(1,J)-G(2,J)*Y(2,J))/DELTAZ-
     @(RHOG(2,J)*Y(2,J)-RHOG(2,J-1)*Y(2,J-1))/DELTAT)/(AY*SIG))
 1331 IF(J .EQ. 2) SUP1=UP(2,1)
 1332 IF(J .EQ. 2) SUP2=UP(2,2)
 1333 VV=Y(2,J)*P
 1334 JTK=JU+J
 1335 IF(JTK.NE.KL.AND.J.GT.4)GO TO 1338
 1336 WRITE(6,1337)J,KL,YJST2,VV,PST,PC2,CF,SUMJST,SUMCQ,SUMGAS,SGFILM
 1337 FORMAT(I2,I8,9D12.5)
C
C**********************************CONTROL END*************************************
C
C*********************************BED WRITE START**********************************
C
 1338 ZII=II
 1339 Z=ZII*DELTAZ
 1340 ITSUM=IISUM+1
 1342 IF(I .LT. IPRINT)GO TO 1550
 1344 IF(J .NE. 4)GO TO 1450
 1350 WRITE(6,1360)Z
 1360 FORMAT(18H0      BED HEIGHT =,D12.5,102H FEET.   PERCOLATION CALCUL
     @ATIONS INCLUDING MASS AND HEAT TRANSFER WITH THERMAL DIFFUSION AND
     @ VARIABLE/37X,57H GAS VELOCITY AND DENSITY DUE TO HEAT EFFECTS BY
     @S.H.JURY)
 1363 WRITE(6,1366)B,AA
 1366 FORMAT(1H0,21X,16H DELTAZ/DELTAT =,D15.8,23X,21H (DELTAR**2)/DELTA
     @T =,D15.8)
 1367 WRITE (6,1368)
 1368 FORMAT(1H0,31X,69H RATIOC = (Y-BEDCGI/BEDROG)/(CFEED/ROGIN-BEDCGI/
     @BEDROG) BY DEFINITION)
 1370 WRITE(6,1380)
 1380 FORMAT(1H0,55X,22H INPUT PARAMETERS WERE)
 1390 WRITE(6,1400) ALFA,BEDTI,CPG,II ,N,TTIME,ALERR,CAYG,EL,IPRINT,P,
     @VFEED,AY,CAY,EPSLON,L,R,YLAMDA,BEDCGI,CFEED,H,M,TFEED,TIMEJU
 1400 FORMAT(9H   ALFA =,D12.5,4X,8H BEDTI =,D12.5,6X,6H CPG =,D12.5,4X,
     @6H  II =,I4,7X,4H N =,I3,14X,8H TTIME =,D12.5/9H  ALERR =,D12.5,5X
     @,7H CAYG =,D12.5,7X,5H EL =,D12.5,1X,9H IPRINT =,I4,7X,4H P =,D12.
     @5,5X,8H VFEED =,D12.5/9H      AY =,D12.5,6X,6H CAY =,D12.5,3X,9H EP
     @SLON =,D12.5,6X,4H L =,I4,7X,4H R =,D12.5,4X,9H YLAMDA =,D12.5/9H
     @BEDCGI =,D12.5,4X,8H CFEED =,D12.5,8X,4H H =,D12.5,6X,4H M =,I4,3X
     @,8H TFEED =,D12.5,4X,9H TIMEJU =,D12.5/)
 1430 WRITE(6,1440)
 1440 FORMAT(3(12H     TIME,MIN,5X,7H RATIOC,4X,11H GAS TEMP,F,2X,3H IT))
 1450 IF(J .LT. JAY) GO TO 1550
 1460 JAY=J+JPRINT
 1465 JO=JO+1
 1467 JT=J-1
 1468 TJ=JT
 1470 TIME(JO)=(UJ+TJ)*DELTAT*60.D0
 1480 RATIOC(JO)=(Y(2,J)-BEDCGI/BEDROG)/(CFEED/ROGIN-BEDCGI/BEDROG)
 1490 YTEMP(JO)=(TG(2,J)+1.0D0)*BEDTI-459.69D0
 1500 ICHEK(JO)=ITCHEK
 1510 IF(JO .LT. 3) GO TO 1550
 1520 JO=0
 1530 WRITE(6,1540)(TIME(JON),RATIOC(JON),YTEMP(JON),ICHEK(JON),JON=1,3)
 1540 FORMAT(3(2H  ,D11.4,2H  ,D11.4,2H  ,D11.4,2H  ,I3))
C
C**********************************BED WRITE END************************************
C
C************************TRANSPORT ZONE CONTROL START*******************************
C
```

Table XLVI (continued)

```
C*************************************************************************
C TRANSPORT ZONE CONTROL OMITS COMPUTATIONS WHENEVER THE BED INCREMENT UNDER
C CONSIDERATION IS IN EQUILIBRIUM WITH THE FEED STREAM.  STATEMENTS 1620 AND
C 1630 TEST THE TRAILING EDGES AND STATEMENTS 1780 AND 1790 TEST THE LEADING
C EDGES OF THE CONCENTRATION AND THERMAL WAVES FOR EQUILIBRIUM.  STATEMENTS
C 1680 THROUGH 1720 CONVERT THE OUTPUT STREAM VALUES TO INPUT VALUES FOR THE
C FOLLOWING BED INCREMENT.  STATEMENTS 1850 THROUGH 1910 SHIFT THE STREAM
C QUANTITIES IN TIME.  THE TRANSPORT ZONE EXTENDS FROM J=2 TO J=JJ.
C EQUIVALENT CLOCKTIME EXTENDS FROM JU TO JU+JJ.  TIME SAVED IS M-JJ FOR
C EACH BED INCREMENT.
C*************************************************************************
C
 1550 IF(J .GE. JV) GO TO 1660
 1590 DIFT=(TG(2,J)+1.0D0)*BEDTI-TFEED
 1600 RATC=(Y(2,J)-BEDCGI/BEDROG)/(CFEED/ROGIN-BEDCGI/BEDROG)
 1610 DIFC=1.0D0-RATC
 1620 IF(DIFC .GT. ALERR) GO TO 1940
 1630 IF(DABS(DIFT) .GT. 0.01D0) GO TO 1940
 1660 JJ=J
 1665 IF(I .LT. IPRINT)GO TO 1680
 1668 CONCI=RHOG(2,J)*(UP(2,1)*(BEDPF-BEDPI)+BEDPI)/P
 1670 WRITE(6,1671)
 1671 FORMAT(1H0,55X,23H OUTPUT PARAMETERS WERE)
 1672 WRITE(6,1673)JJ,JV,J,II,SJST,YJST2,CGST,CONCI,SUMJST,SUMCQ,SGFILM,
     @SUMGAS,SUP1,SUP2
 1673 FORMAT(1H ,2X,5H JJ =,I5,2X,5H JV =,I5,2X,4H J =,I5,2X,5H II =,I5,
     @7H SJST =,D12.5,2X,7H YJST =,D12.5,2X,7H CGST =,D12.5,2X,8H CONCI
     @=,D12.5/2X,9H SUMJST =,D12.5,2X,8H SUMCQ =,D12.5,2X,9H SGFILM =,D1
     @2.5,2X,9H SUMGAS =,D12.5,2X,10H UP(2,1) =,D12.5/2X,10H UP(2,2) =,D
     @12.5 )
 1675 TMAX=(TDUM+1.0D0)*BEDTI-459.69D0
 1677 WRITE(6,1678)KL,ITSUM,TMAX,JMAX
 1678 FORMAT(1X,5H KL =,I8,2X,8H ITSUM =,I10,2X,7H TMAX =,D12.5,1X,3H AT
     @,1X,4H J =,I5/////////////)
 1680 DO 1720 JB=2,JJ
 1690 Y(1,JB)=Y(2,JB)
 1700 TG(1,JB)=TG(2,JB)
 1710 RHOG(1,JB)=RHOG(2,JB)
 1720 G(1,JB)=G(2,JB)
 1760 DIFT=TG(1,2)*BEDTI
 1770 CRATIO=((Y(1,2)-BEDCGI/BEDROG)/(CFEED/ROGIN-BEDCGI/BEDROG))
 1775 RATERR=0.1D0*ALERR
 1780 IF(CRATIO.GT.RATERR)GO TO 3000
 1790 IF(DABS(DIFT) .GT. 0.01D0) GO TO 3000
 1850 DO 1890 JA=2,JJ
 1860 RHOG(1,JA-1)=RHOG(1,JA)
 1870 G(1,JA-1)=G(1,JA)
 1880 Y(1,JA-1)=Y(1,JA)
 1890 TG(1,JA-1)=TG(1,JA)
 1900 RHOG(1,JJ)=ROGIN
 1903 G(1,JJ)=VFEED*ROGIN
 1905 Y(1,JJ)=CFEED/ROGIN
 1907 TG(1,JJ)=(TFEED-BEDTI)/BEDTI
 1910 JJ=JJ-1
 1911 JU=JU+1
 1912 UJ=JU
 1913 TIMEJU=UJ*DELTAT
 1920 GO TO 1760
 1940 IF(JIF.EQ.1)GO TO 1970
 1941 DO 1960 K=1,N
 1945 PE(1,K)=PE(2,K)
```

Table XLVI (continued)

```
 1946 DI(K)=D(K)
 1950 UT(1,K)=UT(2,K)
 1955 UP(1,K)=UP(2,K)
 1960 UPD(1,K)=UPD(2,K)
 1970 TW(1)=TW(2)
 1980 IF(JIF.EQ.0)GO TO 2000
 1981 TC1=TC2
 1982 PC1=PC2
 1983 PD1=PD2
C
C**************************TRANSPORT ZONE CONTROL END*****************************
C
 2000 CONTINUE
 3000 CONTINUE
 4000 STOP
      END
```

Table XLVII. The Input Data and Diffusion Parameter Calculations of LMS-4A Program.

```
//LMS1   JOB (038441,054178,BINS,T-60,L-999,R-512),C,MSGLEVEL=(1,1)
//*RESOURSE INSTR360
// EXEC FORTHCLG,GOREG=512K,OPT=2,FORTREG=512K
//FORT.SYSIN DD *
      IMPLICIT REAL*8(A-H,O-Z)
      REAL*8 DEXP,DABS,DERF,DSQRT,DLOG,DMAX1
      INTEGER*4 IDINT
      DIMENSION TG(2,3000),RHOG(2,3000),G(2,3000),Y(2,3000)
      DIMENSION UI(2,31),UP(2,31),UPD(2,31),PE(2,31),DELUTI(2,31)
      DIMENSION BE(30),GE(30),D(30),TE(30),DI(30)
      DIMENSION RATIOC(3),TIME(3),YTEMP(3),ICHEK(3)
      DIMENSION TW(2),AAP(2),BBP(2),CCP(2)
C
C*************************S. H. JURY CARD DECK*********************************
C
C*********************************INPUT DATA START*****************************
C
C***********************GRANULE PARAMETERS*************************************
C
C EF IS THE FRACTION OF ADSORPTION HEAT LIBERATED IN THE GRANULE. THE FRACTION
C (1.00-EF) IS THE HEAT LIBERATED AT THE GRANULE SURFACE.
C SIG IS THE FRACTION OF CONTINUOUS PHASE IN GRANULE.
C EF1 IS A FRACTION IN THE RELATION  EF1=(DD(K)/RD**2)/(D(K)/R**2)  WHERE DD(K)
C AND RD ARE THE MICROSPHERE DIFFUSIVITY AND RADIUS.
C
    1 SIG=1.0D0
    2 EF1=1.0D0
    3 EF=0.0D0
    4 R=0.002412080600                                                    L12/14
    5 CAY=0.08400
    6 YLAMDA=26855.40794D0
      YLAMDA=YLAMDA*1.270D0
    7 EPSLON=0.464D0                                                      L12/14
    8 ROS=77.0989D0
    9 SI=0.92360
C
C***********************PERCOLATOR PARAMETERS**************************************
C
   10 DI=1.250D0/12.D0
   11 DO=1.500/12.D0
   12 ROT=1.052500*62.427D0
   13 CPT=0.320
C
C*************************FEED GAS PARAMETERS*************************************
C
   15 SCFH=11.200                                                         LMS1
   16 TFEED=537.690
   17 BEDTI=537.690
   18 UNITP=14.6960*144.0D0/760.0D0
   19 BEDPI=0.0013259793D0*UNITP                                          L12/14
   20 BEDPF=11.3568D0*UNITP                                               LMS1
   21 P=748.057D0*UNITP                                                   LMS1
C
C*************************R RUN DESIGN*********************************************
C
   28 NR=11
   29 NA=1
   30 NS=20
   31 YNR=NR
   32 YNA=NA
   33 YNS=NS
```

Table XLVII (continued)

```
   34 N=NS-NA+NA*NR
   35 YN=N
   36 NN=N-1
   37 YT=YNS*YNR
   38 RN=YT-1.D0
   39 DELTAS=R/YNS
   40 DELTAR=DELTAS/YNR
   41 DROS=DELTAR/DELTAS
C
C*****************************************************************************
C JPRINT IS THE TIME INTERVAL BETWEEN THE PRINTS FOR EACH IPRINT INCREMENTS OF
C BED. PRIOR TO A COMPUTER RUN THE USER SHOULD USE A CALCULATOR TO EXECUTE
C STATEMENTS LISTED UNDER Z- AND T- RUN DESIGN TO INSURE PROPER COMPUTER RUN
C DESIGN.
C*****************************************************************************
C
C**************************Z RUN DESIGN***************************************
C
   45 EL=2.D0/12.D0
   46 DELTAZ=4.D0*R
   47 IPRINT=1
   48 YIP=IPRINT
   49 LW=IDINT(EL/(DELTAZ*YIP)+.5D0)
   51 L=LW*IPRINT
   52 YL=L
   53 DELTAZ=EL/YL
C
C**************************T RUN DESIGN***************************************
C
   64 DELTAT=3.0D0/3600.D0
   65 TTIME=3000.D0*DELTAT
   66 JPRINT=1
   68 YJP=JPRINT
   69 MW=IDINT(TTIME/(DELTAT*YJP)+.5D0)
   70 M=MW*JPRINT
   71 YM=M
   72 DELTAT=TTIME/YM
C
C************************MISCELLANEOUS CONSTANTS**********************************
C
   73 ALERR=1.D-3
   74 VP1=0.64152D0
   76 VP2=0.67160D0
   77 VP3=0.34685D0
   78 CW=2.7017D0
   80 CR=0.61305D0
   82 RBAR=1545.33D0
C
C*********************************INPUT DATA END*********************************
C
```

Table XLVII (continued)

```
C
C*********************DIFFUSION PARAMETER CALCULATION START************************
C
C LMS-4A
C
  400 K=0
  410 K=K+1
  412 YK=K
  415 IF(K.GE.NR*NA+1)GO TO 420
  418 DUM=YNS/(YNS-YNA+(YNR*YNA-YK+1.D0)/YNR)
  419 GO TO 421
  420 DUM=YNS/(YN-YK+1.D0)
  421 T=(DUM*UT(1,K)+1.D0)*BEDTI
  427 PP=DUM*UP(1,K)*DP*BEDPI
  466 XPP=DEXP(13516.2D0/T)/DSQRT(T)
  467 X=PP*XPP
  472 Z1=1.D0+3.069699154D-9*X
  473 Z2=1.D0+1.491244527D-11*X
  475 VA=2.690515396D-11/Z1
  476 VB=3.964988329D-14/Z2
  490 C1=ROS*X*(VA+VB)
  491 C1PP=ROS*XPP*(VA+VB)
  495 DC1=ROS*(VA/Z1+VB/Z2)
  499 D(K)=(36.84667369D0*DEXP(-12589.2D0/T)*(1.D0-1.042796517D0*C1)*C1P
     &P +1.988713121D-6/DSQRT(T))/(DC1*XPP)
      D(K)=D(K)*2.40D0
  502 PE(2,K)=D(K)*DC1*XPP
  505 TE(K)=-ALFA*DC1*X*(.5D0+13516.2D0/T)/T
  506 IF(JIF.EQ.1.OR.J.NE.2)GO TO 510
  507 PE(1,K)=PE(2,K)
  508 D1(K)=D(K)
  510 IF(K.LT.N.AND.JIF.NE.1)GO TO 410
C
C*********************DIFFUSION PARAMETER CALCULATION END**************************
C
```

VITA

The author, Arnooparp Charmikorn, was born in Bangkok, Thailand on April 2, 1954. He is the second child and the only son of Vice Admiral Ophas Charmikorn, the Royal Thai Navy Associated Chief of Staff and the Senator, and Mrs. Saiyood Charmikorn.

He attended Parinyathip primary school in 1957, Saint Dominic secondary and junior high school in 1961, and Triam Udom Suksa senior high school in 1969. He graduated from Chulalongkorn University in Bangkok, Thailand with a B.S. degree in Chemical Engineering in March 1976.

The author entered The University of Tennessee, Knoxville, in September 1976 and was awarded a research assistantship supported by the National Science Foundation to participate in the graduate research activities under Dr. Jury's direction in January 1977. He will go back to Thailand after graduation in August 1979 with a M.S. degree in Chemical Engineering.